Modeling and Evaluation of Bioenergy and Agriculture System Integration

PhD Thesis

$$(EIv'')'' = q - \rho A\ddot{v}$$

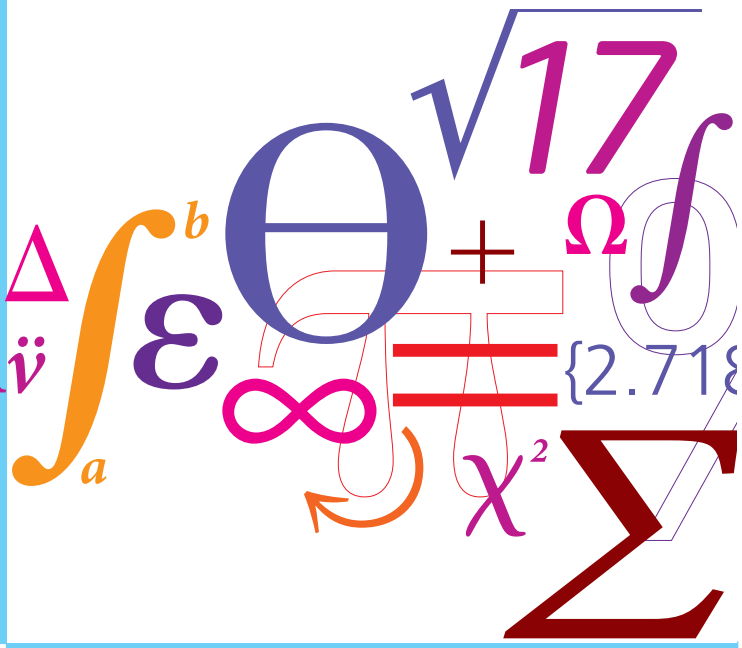

Hafthor Ægir Sigurjonsson
DCAMM Special Report No. S227
January 2016

DTU Mechanical Engineering
Department of Mechanical Engineering

Modeling and Evaluation of Bioenergy and Agriculture System Integration

Hafthor Ægir Sigurjonsson

Kongens Lyngby 2016

Technical University of Denmark
Department of Mechanical Engineering
Nils Koppels Allé, building 404,
2800 Kongens Lyngby, Denmark
Phone +45 45251960
info@mek.dtu.dk
www.mek.dtu.dk

Summary

Emphasis on effective utilization of biomass as both energy and food resources has increased as the public and policy makers become more aware of climate change, security of energy supply and fossil fuel depletion issues of energy generation. Parallel to these issues are increasing concern of land use, essential mineral depletion and soil degradation associated with agriculture, which could directly affect food supply.

This Ph.D thesis focuses on exploring the integration between agriculture and bioenergy, by developing and analysing biomass fuelled energy system concepts that can produce heat and power in the effort of replacing fossil fuelled production. Bioenergy technologies based on thermochemical and biochemical conversion have been developed to utilize residual resources from agricultural systems. Nevertheless, these technologies are more often used in systems that maximize energy generation while disregarding and destroying the "waste" products which often contain essential elements to agriculture. Those type of systems could then eventually lead to soil depletion and contribute to mineral resource scarcity. New energy system concepts are developed in this thesis that 1) maximize biomass utilization for heat and power generation 2) while maintaining soil quality and 3) decrease consumption of mineral fertilizers in the agricultural system.

It was revealed that developing bioenergy systems to maximize energy

generation, their operation will results in a net decrease in soil carbon build-up which can compromise soil quality in the agricultural system. But when decreasing energy efficiency and increasing biochar production the soil carbon build-up can be re-established and even increased beyond the potential if the residual resources are not utilized by the energy system. It was further found that by applying the analytical framework and analysing climate change impact of straw and manure utilization in the integrated bioenergy an agriculture system concepts, maximizing biochar production at the expense of energy generation proved to be the better option if theses systems would avoid energy generations from natural gas. However, the economic feasibility analysis and the non-renewable resource requirements analysis revealed that it is better to maximize energy generation. The effective utilization of residual resources from the agricultural system in the energy system is thus determined by a compromise between different criteria. This research further revealed that co-gasification of manure and/or digestate is just as relevant for heat and power production as co-digestion.

Preface

This thesis is submitted as a monograph as a partial fulfillment of the requirements for the PhD degree at the Technical University of Denmark.

The study was carried out at the Department of Mechanical Engineering, Section of Thermal Energy Systems from November 2012 to January 2016 under the supervision of Associate Professor Brian Elmegaard, and co-supervision of Associate Professor Lasse Røngaard Clausen and Senior Scientist Jesper Ahrenfeldt.

The PhD study was funded by the Technical University of Denmark and the Villum foundation.

Lyngby, 01-January-2016

Hafthor Ægir Sigurjonsson

Acknowledgements

I would like to thank my supervisors Brian Elmegaard and Lasse Røngaard Clausen for their understanding and guidance during my study. Their support throughout the project has been invaluable, especially during thesis writing. I would also like to thank co-supervisor Senior Scientist Jesper Ahrenfeldt and everybody who was a part of the two Villum funded collaboration projects.

A special thanks goes to Professor Brynhildur Davíðsdóttir and Programme Coordinator Bjargey Anna Guðbrandsdóttir for allowing me to be a part of the Environment and Natural Resources program during my stay at University of Iceland, and for interesting discussions. I hope we can continue to work together in the future.

Additionally, I would like to thank my colleagues at the Technical University of Denmark and at the University of Iceland for lively discussions and support throughout the project.

Last but not least, I wish to thank Andrea and Eiríka Ýr for their love and patience. I know that I have been very much occupied with writing the thesis in the final part of the study.

List of Publications

The PhD thesis includes two journal papers and two conference paper. The papers can be found in Appendix A.

I. ISI Journal Paper Sigurjonsson, H.Æ., Clausen L.R., Elmegaard B., Ahrenfeldt J. "Climate effect of an integrated wheat production and bioenergy system with Low Temperature Circulating Fluidized Bed gasifier." Applied Energy 160 (2015) 511–520.

II. Proceedings Paper - Peer Reviewed Manuscript Sigurjonsson, H.Æ., Clausen L.R., Elmegaard B., Ahrenfeldt J. "Climate Effect of Bioenergy and Agriculture Integration Based on Lowtar Gasification of Wood Chips." Proceedings of ECOS 2015, 2015, Presented at: 28th International Conference on Efficiency, Cost, Optimization, Simulation and Environmental Impact of Energy Systems

III. Proceedings Paper - Peer Reviewed Manuscript Sigurjonsson, H.Æ., Elmegaard B., Clausen L.R. "Integrated model of bioenergy and agriculture system." The 56th Conference on Simulation and Modelling (SIMS 56).

IV. ISI Journal Paper Sigurjonsson, H.Æ., Elmegaard B., Clausen L.R. "Multi-Criteria Analysis of an Integrated Polygeneration Energy System and Agriculture Utilizing Cereal Straw." Submitted to Applied Energy (manuscript number: APEN-D-16-06038).

Co-authorship statement

All four papers have been planned and written by the author of this thesis. The co-authors have contributed with academic discussions, as well as linguistic and academic comments to the draft of the papers.

Contents

List of Figures

List of Tables

Chapter 1

Introduction

1.1 Background and Motivation

Climate change, security of energy supply and fossil fuels depletion are issues of energy generation that need to be addressed. Increased use of biomass feedstock for heat and power production, along with biofuels production, is commonly believed to be relevant to mitigate these issues. However, in addition to these concerns of energy generation is the increasing attention on land use, essential mineral depletion and soil degradation associated with agriculture, which could directly affect food supply. For these reasons the awareness of effective biomass utilization as both an energy and food resource has increased.

Denmark's future energy plan for 2050 is to be completely independent of fossil fuels for all energy consumption in the country [1]. Parallel to this target, the goal is to decrease greenhouse gas emissions significantly in coming decades [2]. In the annual energy statistics, published by the Danish Energy Agency in 2013 the electricity production in Denmark was mostly by either combined heat and power (CHP) plants, and wind

turbines that year [3]. The share of the production from CHP plants was 61.1% of which 79% was produced in large-scale (centralized) CHP units. In Denmark about 73.3% of all district heating was also produced in CHP plants that year [3], of which 75% was produced in large-scale (centralized) CHP plants and 25% in small-scale (de-centralized) CHP plants.

There are currently 32 large-scale and 637 small-scale CHP plants in Denmark according to the Danish Energy Agency, and those plants are fuelled by various energy sources. Figure 1.1 shows the share of fuels used in CHP plants in Denmark calculated based on fuel consumption in relation to heat supply from CHP plants. It can be seen that coal

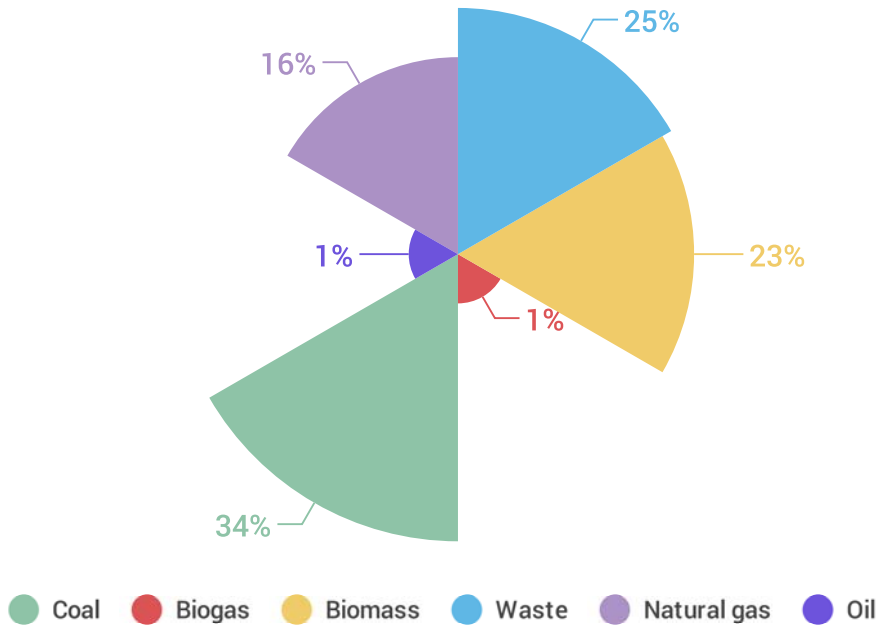

Figure 1.1: *Share of fuels used on Danish electricity and CHP plants [3].*

still accounted for 34% of the fuels used in CHP plants in Denmark in 2013 and natural gas accounted for other 16%. However, according to the Danish Energy Agency, coal, natural gas and oil gross consumption had decreased respectively by 18.2%, 28.0% and 26.2% since 2000 while renewable energy consumption increased by 130.4% [3]. Based on these statistics the Danish energy system is still heavily dependent on large scale CHP plants fuelled with fossil fuels. The most obvious way to change this is by increasing the share of biomass utilized by the large scale

CHP plants and by increasing the number of small scale biomass fuelled CHP plants, effectively substituting fossil fuels. Biomass for bioenergy can be obtained by utilizing residues or by growing dedicated energy crops [4]. Biomass residues are obtained as a results of economic activity or production of goods and not specifically produced as an energy resource [4]. By-products from agriculture, forestry and household waste can all be categorised as biomass residues [5]. Cherubini et al. [4] defines dedicated energy crops as crops grown first and foremost for energy, although the by-products can be used for non-energy purposes.

However, increased demand for residual biomass can have a negative effect on the agricultural system, e.g. soil incorporation of crop residues can increase soil organic carbon which can be essential to soil quality [6] and removing them can cause soil depletion in the long run. Focus on the changes in soil carbon and its effects have gained more attention as cultivation of land for food and energy increases. The estimated soil carbon content in the world is 2157-2293 Gt, of which 684-724 Gt is in the upper 30 cm of soils [7]. Since the industrial revolution, soil organic carbon depletion has contributed 66-90 Gt of carbon to the atmosphere, whereas during the same time-frame the contribution from fossil-fuel combustion has been 240-300 Gt of carbon [8].

Moreover, keeping the nutrients within the residues on the agricultural field is important as this can decrease the need for mineral fertilizers. Crops need nitrogen, phosphorus and potassium fertilizers to maintain yield [9]. Nitrogen mineral fertilizers are mostly supplied as different forms of ammonia, which is mainly produced by the Haber–Bosch synthesis process by using nitrogen from the atmosphere and natural gas. In addition to needing fossil fuels, the process is energy intensive and about half of the nitrogen applied as a fertilizer ends up as harmful emissions, e.g. dinitrogen monoxide to air, nitrogen oxides to air and nitrates to water. Phosphorus fertilizer is produced from phosphate rocks, which is a non-renewable resource. Steen [10] and Smil [11] estimate that the phosphate rock reserves could be exhausted within 50–100 years and as Cordell et. al [9] noted from the work of Runge-Metzger [12], Driver [13] and Smil [11], the fertilizer industry recognizes decreased resource quality and thus increased associated costs.

This Ph.D thesis focuses on exploring the integration between agriculture and bioenergy, by developing and analysing biomass fuelled energy system concepts that can produce heat and power in the effort of replacing fossil fuelled production. Bioenergy technologies based on thermochemical and biochemical conversion have been developed to utilize residual resources from agricultural systems. Nevertheless, these technologies are more often used in systems that maximize energy generation while disregarding and destroying the "waste" products which often contain essential elements to agriculture. Those type of systems could then eventually lead to soil depletion and contribute to mineral resource scarcity. New energy system concepts are thus necessary to 1) maximize biomass utilization for heat and power generation 2) while maintaining soil quality and 3) decrease consumption of mineral fertilizers in the agricultural system.

1.2 Literature Review

In this section the literature related to the objective of this work is reviewed. First it focuses on biomass conversion technologies, than knowledge on the sustainability of bioenergy systems is presented.

1.2.1 Biomass Conversion for Heat and Power

The two main process bioenergy technologies to convert biomass are thermochemical and biochemical. The main process options used for thermochemical conversion are: combustion, pyrolysis and gasification [14]. The main difference between combustion and gasification is that combustion is achieved by burning biomass in air to convert the chemical energy of the biomass to heat which is subsequently used in steam cycle power plants to produce electricity and district heat. Gasification on the other hand uses partial oxidation to convert the biomass to a combustible gas which is subsequently burnt in a gas engine, gas turbine, or combusted if utilized in a steam cycle power plant [14]. Pyrolysis involves heating the biomass in absence of air, forming liquid (bio-oil/tar), solid (char) and

gaseous factions [14]. That process can also be used as a pre-treatment for gasification where the char product of the pyrolysis is gasified [15]. Nguyen et al. [16] found that the gasification has a higher electrical efficiency and is more environmentally friendly in terms of climate change impact and non-renewable energy utilization in a life cycle perspective, when comparing electricity production from straw using either gasification or direct combustion. The gasification technology analysed in that paper is called Low Temperature - Circulating Fluidized Bed (LT-CFB) gasifier and uses pyrolysis as a pretreatment.

The LT-CFB gasifier is a promising gasification technology. It was designed to operate on biomass which had been difficult to utilize in thermochemical conversion processes, e.g. cereal straw, sewage sludge and animal manure. In a review article by Ahrenfeldt et al. [17] on state-of-the- art technology and future perspectives of biomass gasification cogeneration, the LT-CFB is noted to have operated on two types of straw, chicken manure, two types of pig manure, two types of digested manure from an anaerobic digester and one type of wood [17]. This opens the possibility of integrating thermochemical conversion and biochemical conversion of biomass. In addition, that article noted that because of the relatively low temperature and the solid residual fraction having no toxic polyaromatic hydrocarbons, char and ash from LT-CFB gasification can be applied to an agricultural field which can benefit from the nutrients of the ash and the recalcitrant carbon.

The Danish climate change mitigation potentials inter-ministerial working group report identified a few connections between the agricultural and energy industries to mitigate their respective environmental impacts, along with promoting sustainable bioenergy [18]. There the potential of gasifying straw in a low temperature gasifier is specially noted, along with the return of the biochar co-product back to the agricultural field. However, it was recognized in that report that insufficient information are available to analyse this measure at that time. That report also identified great potential in increased processing of manure for energy purposes, it is even suggested that a special tax levied on slurry that is not already utilised for biogas production [18].

Two process options are mainly considered for biochemical conversion,

i.e. fermentation and anaerobic digestion [14]. Fermentation is mainly used to produce ethanol and anaerobic digestion converts organic material (often manure) directly to biogas with about 20% - 40% energy content of the inputs. Biogas can than directly be used in a gas engine or a gas turbine. With the LT-CFB gasifier the efficiency of a bioenergy system including anaerobic digestion can be increased by gasifying the organic material that could not be converted in the anaerobic digester. Prapaspongsa et al. [19] showed that including thermochemical conversion technologies after anaerobic digestion when utilizing manure can improve the energy efficiency and decrease greenhouse gas emissions, but concluded in a following article based on life cycle impacts that anaerobic digestion without further utilization has the lowest greenhouse gas emissions [20]. However, Prapaspongsa et al. also note that further research on the economics of such technology integration is needed.

1.2.2 Sustainability of Bioenergy

In recently published work on the climate change impact from bioenergy systems, Yang et al. [21] and Parajuli et al. [22] found that the soil organic carbon loss from agricultural residue removal is a major contributor to its climate change environmental impact. Additionally, Sastre et al. [23] shows that loss of soil organic carbon from agricultural soils when utilizing wheat straw for bioenergy is the greatest contribution to climate change impact, as previously sequestered carbon is released to the atmosphere. The effect of extensive soil cultivation is that some soils have lost up to one-half to two-thirds of their organic carbon [8]. The impact of soils carbon loss was highlighted by Cherubini et al. [4, 24] where the change in carbon pools and nitrogen emissions were specifically noted as important when analysing bioenergy systems. It is also worth noting that the most influential air-born emissions from both the agricultural and energy systems in Denmark are carbon and nitrogen bound according to Danish Statistics [25].

Taheripour et al. [26] notes that the sustainability of bioenergy systems will ultimately be determined to a large degree by the possibility of by-product disposal. In a thermochemical and biochemical conver-

sion system, these by-products are mostly digestate and ashes. However, gasification ashes in general are considered to be relatively unattractive as a fertilizer in comparison to combustion ashes. The main reason is that the inert carbon matrix can lower the nutrient value of the ashes. Pels et al. [27] noted that the carbon matrix from gasification ashes can also cause hydrophobic properties and the ability to bind trace elements. But Mozaffari et al. [28] found that gasification ash from alfalfa stem to be good liming agent and source of potassium (K). Additionally, Müller-Stöwer et al. [29] further found that the solid residues from LT-CFB gasification of wheat straw, because of the relatively low process temperature, can replace mineral fertilizers while Kuligowski et al. [30] found that ash from gasified slurry in the LT-CFB gasifier has a positive phosphorus fertilizer replacement value.

Moreover, agricultural soils can be used as carbon sinks, as suggested by Mao et al. [31] and Brandão et al. [32], by applying ash containing recalcitrant carbon fraction – often referred to as biochar – to soils and thus mitigate climate change. In a recent article, Veronika et al. [33] concluded from experimental results that the biochar from LT-CFB gasifier has a good potential for long-term soil carbon sequestration. Where she additionally concluded that thermochemical conversion of biomass residues with gasification can combine production of bioenergy and biochar that can lead to positive impact on soil quality [33]. Cayuela et al. [34] concluded that the dynamics of the soil amendment of by-products from bioenergy cannot be ignored when analysing bioenergy production chains.

Buchholz et al. [35] devised an expert survey on the sustainability of bioenergy systems, to identify the most important criteria. Out of 35 criteria the most important ones were found to be related to environmental impact, e.g. greenhouse gas balance, energy balance, soil protection and natural resource efficiency. But the economic criteria (microeconomic sustainability) and social criteria (local participation) were also identified as important. It is thus recognised that the sustainability of the developed bioenergy system anlysed in this work will need to be evaluated based on multiple criteria.

1.3 Objective and Methods

This section introduces the scope of this thesis by listing the research questions under investigation. Subsequently, the main methodologies used to answer those questions are briefly summarised.

1.3.1 Research questions and objectives

The hypothesis is that technology integration and combined utilization of different resources in the bioenergy system can result in a production that is more environmentally friendly and economically feasible. The objectives are to develop, model and analyse integrated bioenergy and agricultural system concepts to facilitate increased biomass utilization as an energy source in Denmark, without adverse affects on the agricultural system.

More specifically, along with finding the optimal system concept, this study aims at answering the following research questions:

I Is it possible to reverse soil carbon loss by recycling some of the carbon in the utilized resource while still producing heat and power?

II What impact does recycling of nutrients and carbon have on the overall system?

III How will increased biochar production impact the sustainability of bioenergy systems?

IV Can the integration between bioenergy and agriculture mitigate climate change?

V Is system integration of bioenergy and agriculture through integrated bioenergy technologies economically feasible?

VI What is the optimal bioenergy system concept in terms of environmental impact, economic feasibility and non-renewable resource requirements?

1.3.2 Methodologies

As far as the overall objective is concerned, this work proposes utilization of cereal straw and pig manure along with a novel design of bioenergy and agriculture integration through the Low Temperature Circulating Fluidized bed (LT-CFB) gasifier and anaerobic digestion in polygeneration power plants. The novelty of that concept is that it is designed to produce electricity, district heat and fertiliser. The fertilizer product consists of ash and biochar from the gasifier, along with liquid fractions of manure and digestate from the anaerobic digestion, which effectively recycles the nutrients and some of the carbon originally harvested from an agricultural system.

To answer the first research question, the impact of the biomass resources (straw and manure) on the carbon content in agricultural soils needs to be found. This can be done by modelling the carbon decay in soil after application over a specific time horizon and by assuming annual application, the carbon build-up in soil over a specified time can then be estimated. This carbon build-up is lost if these resources are harvested. But carbon build-up of the recycled carbon is than found and depending on the recycling rate and state of the carbon, the mitigation potential can be found.

To find the impact of recycled nutrients and carbon, the system concepts should be modelled by including the associated direct and indirect emissions, along with the carbon sequestration potential. The change in mineral fertiliser requirements on the agricultural field also needs to be outlined, along with the added revenue stream by fertilizer production. For this purpose the work proposes an multi-criteria analysis based on climate change impact, non-renewable resource requirements and economic feasibility.

The third question can be answered for a specific bioenergy system concept by making a thermodynamic model of the thermal power plant from which the biochar is produced. Where the LT-CFB gasifier is modelled and simulated over a range of carbon conversion factors, which essentially describes how much of the char from pyrolysis will be extracted as biochar and how much will be gasified and used to fuel the power plant.

However, first the upper and lower limit of the carbon conversion for the LT-CFB gasifier needs to be identified to find the biochar production capacity.

For the fourth question, questions two and three need to be answered in terms of climate change impact and the affect of the bioenergy system needs to be elaborated on by accounting for emissions and material consumption. The impact of energy efficiency can be approach in different ways, here the avoided energy generation as a consequence of the proposed system integration is accounted for. In addition the consequential impact of harvesting the residual resources from the agricultural system is also included.

Economic feasibility of electricity generation from the system integration is found by a techno-economic analysis of the required investment and operation. This includes placing a value on the fertilizer product of the bioenergy system, along with adding cost of transportation. The resulting levelized cost of electricity is then compared with the premium feed-in tariff for bioenergy systems in Denmark.

The trade-off between environmental impact, renewable energy generation and profitability is found by using a multi-criteria analysis method. Technique for Order Preference by Similarity is proposed to identify the best bioenergy system concepts and product mix, based on multiple criteria, representing climate change impact, non-renewable resource requirements and economic feasibility.

References

[1] D. M. of Climate. Energy and Buildings. *Our Future Energy*. Tech. rep. Copenhagen: Danish Ministry of Climate. Energy and Buildings.

[2] *The Danish Climate Policy Plan Towards a low carbon society*. Tech. rep. Copenhagen: Inter-ministerial, 2013.

[3] *Energy Statistics 2013: Data, tables, statistics and maps*. Tech. rep. Copenhagen: Danish Energy Agency, 2015.

[4] F. Cherubini et al. "Energy-and greenhouse gas-based LCA of biofuel and bioenergy systems: Key issues, ranges and recommendations". In: *Resources, conservation and recycling* 53.8 (2009), pp. 434–447.

[5] M. Hoogwijk et al. "Exploration of the ranges of the global potential of biomass for energy". In: *Biomass and Bioenergy* 25.2 (2003), pp. 119 –133. DOI: http://dx.doi.org/10.1016/S0961-9534(02)00191-5.

[6] D. S. Powlson et al. "Implications for Soil Properties of Removing Cereal Straw: Results from Long-Term Studies". en. In: *Agronomy Journal* 103.1 (Jan. 2011), p. 279. DOI: 10.2134/agronj2010.0146s.

[7] N. H. Batjes. "Total carbon and nitrogen in the soils of the world". In: *European Journal of Soil Science* 65.1 (Jan. 2014), pp. 10–21. DOI: 10.1111/ejss.12114_2.

[8] R. Lal. "Soil carbon sequestration to mitigate climate change". In: *Geoderma* 123.1-2 (Nov. 2004), pp. 1–22. DOI: 10.1016/j.geoderma.2004.01.032.

[9] D. Cordell, J.-O. Drangert, and S. White. "The story of phosphorus: Global food security and food for thought". In: *Global Environmental Change* 19.2 (May 2009), pp. 292–305. DOI: 10.1016/j.gloenvcha.2008.10.009.

[10] I. Steen. "Phosphorus availability in the 21st Century: Management of a non-renewable resource | Global Phosphorus Network". In: *Phosphorus and Potassium* 217 (1998), pp. 25–31.

[11] V. Smil. "P HOSPHORUS IN THE E NVIRONMENT : Natural Flows and Human Interferences". en. In: *Annual Review of Energy and the Environment* 25.1 (Nov. 2000), pp. 53–88. DOI: 10.1146/annurev.energy.25.1.53.

[12] A Runge-Metzger. "Closing the cycle: obstacles to efficient P management for improved global food security". In: *Scope-Scientific Committee on Problems of the Environment International Council of Scientific Unions* 54 (1995), pp. 27–42.

[13] J. Driver. "Phosphates recovery for recyling from sewage and animal wastes". eng. In: *Phosphorus and potassium* 216 (), pp. 17–21.

[14] P. McKendry. "Energy production from biomass (part 2): conversion technologies". In: *Bioresource technology* 83.1 (2002), pp. 47–54.

[15] B. Digman, H. S. Joo, and D.-S. Kim. "Recent progress in gasification/pyrolysis technologies for biomass conversion to energy". In: *Environmental Progress and Sustainable Energy* 28.1 (2009), pp. 47–51. DOI: 10.1002/ep.10336.

[16] T. L. T. Nguyen, J. E. Hermansen, and R. G. Nielsen. "Environmental assessment of gasification technology for biomass conversion to energy in comparison with other alternatives: the case of wheat straw". In: *Journal of Cleaner Production* 53.0 (2013), pp. 138 –148. DOI: http://dx.doi.org/10.1016/j.jclepro.2013.04.004.

[17] J. Ahrenfeldt et al. "Biomass gasification cogeneration – A review of state of the art technology and near future perspectives". In: *Applied Thermal Engineering* 50.2 (2013), pp. 1407 –1417. DOI: http://dx.doi.org/10.1016/j.applthermaleng.2011.12.040.

[18] *Catalogue of Danish Climate Change Mitigation Measures*. Tech. rep. Copenhagen: Inter-ministerial, 2013.

[19] T Prapaspongsa et al. "Energy production, nutrient recovery and greenhouse gas emission potentials from integrated pig manure management systems." In: *Waste management & research : the journal of the International Solid Wastes and Public Cleansing Association, ISWA* 28.5 (2010), pp. 411–22. DOI: 10.1177/0734242X09338728.

[20] T. Prapaspongsa et al. “LCA of comprehensive pig manure management incorporating integrated technology systems”. In: *Journal of Cleaner Production* 18.14 (2010), pp. 1413 –1422. DOI: http://dx.doi.org/10.1016/j.jclepro.2010.05.015.

[21] J. Yang and B. Chen. “Global warming impact assessment of a crop residue gasification project—A dynamic LCA perspective”. In: *Applied Energy* 122 (2014), pp. 269 –279. DOI: http://dx.doi.org/10.1016/j.apenergy.2014.02.034.

[22] R. Parajuli et al. “Life Cycle Assessment of district heat production in a straw fired {CHP} plant”. In: *Biomass and Bioenergy* 68 (2014), pp. 115 –134. DOI: http://dx.doi.org/10.1016/j.biombioe.2014.06.005.

[23] C. Sastre, Y. González-Arechavala, and A. Santos. “Global warming and energy yield evaluation of Spanish wheat straw electricity generation – A LCA that takes into account parameter uncertainty and variability”. In: *Applied Energy* 154 (2015), pp. 900 –911. DOI: http://dx.doi.org/10.1016/j.apenergy.2015.05.108.

[24] F. Cherubini and A. H. Stromman. “Life cycle assessment of bioenergy systems: State of the art and future challenges”. English. In: *BIORESOURCE TECHNOLOGY* 102.2 (2011), pp. 437–451. DOI: 10.1016/j.biortech.2010.08.010.

[25] *Statistics Denmark, https://www.dst.dk/en, accessed: 2016-01-31.*

[26] F. Taheripour et al. “Biofuels and their by-products: Global economic and environmental implications”. In: *Biomass and Bioenergy* 34.3 (2010), pp. 278 –289. DOI: http://dx.doi.org/10.1016/j.biombioe.2009.10.017.

[27] J. R. Pels, D. S. de Nie, and J. H. Kiel. “Utilization of ashes from biomass combustion and gasification”. In: *14th European Biomass Conference & Exhibition*. 2005.

[28] M. Mozaffari et al. “Nutrient supply and neutralizing value of alfalfa stem gasification ash”. In: *Soil Science Society of America Journal* 66.1 (2002), pp. 171–178.

[29] D. Muller-Stover et al. “Soil application of ash produced by low-temperature fluidized bed gasification: effects on soil nutrient dynamics and crop response”. English. In: *Nutrient Cycling in Agroecosystems* 94.2-3 (2012), pp. 193–207. DOI: 10.1007/s10705-012-9533-x.

[30] K. Kuligowski et al. “Plant-availability to barley of phosphorus in ash from thermally treated animal manure in comparison to other manure based materials and commercial fertilizer”. In: *European Journal of Agronomy* 33.4 (2010), pp. 293 –303. DOI: http://dx.doi.org/10.1016/j.eja.2010.08.003.

[31] J.-D. Mao et al. “Abundant and stable char residues in soils: implications for soil fertility and carbon sequestration”. In: *Environmental science & technology* 46.17 (2012), pp. 9571–9576.

[32] M. Brandão et al. “Key issues and options in accounting for carbon sequestration and temporary storage in life cycle assessment and carbon footprinting”. In: *The International Journal of Life Cycle Assessment* 18.1 (June 2012), pp. 230–240. DOI: 10.1007/s11367-012-0451-6.

[33] V. Hansen et al. “Gasification biochar as a valuable by-product for carbon sequestration and soil amendment”. In: *Biomass and Bioenergy* 72 (2015), pp. 300 –308. DOI: http://dx.doi.org/10.1016/j.biombioe.2014.10.013.

[34] M. L. CAYUELA et al. “Bioenergy by-products as soil amendments? Implications for carbon sequestration and greenhouse gas emissions”. In: *GCB Bioenergy* 2.4 (2010), pp. 201–213. DOI: 10.1111/j.1757-1707.2010.01055.x.

[35] T. Buchholz, V. A. Luzadis, and T. A. Volk. “Sustainability criteria for bioenergy systems: results from an expert survey”. In: *Journal of Cleaner Production* 17, Supplement 1 (2009). International Trade in Biofuels, S86 –S98. DOI: http://dx.doi.org/10.1016/j.jclepro.2009.04.015.

Chapter 2

System Integration Concepts

This chapter describes the main characteristics of the integration between bioenergy and agriculture as approached in this work. The resource availability from agricultural residues is outlined and the bioenergy system concepts are defined based on combined utilization of resources.

2.1 Integration of Bioenergy and Agriculture

Biomass for bioenergy can be obtained from various sources, one of which are residues from the agricultural industry. According to data from the World Bank, agricultural land covered about 61.5% of the total area of Denmark in 2013, which results in abundance of residual biomass from food production. The main criteria for the agricultural system is that the main production and use of land does not change. This criteria sets a boundary on the bioenergy potential from agriculture analysed in this work around residual products. Additionally, based on the background information of this thesis it is essential for future sustainability

of the agricultural system that removed nutrients while harvesting residual product are recycled and that soil quality is not compromised by continued decrease in soil carbon content.

The total agricultural area in Denmark is mostly divided between cereals, rape, pulses, root crops, and grass and green fodder production. Where cereal crops have the largest share according to Statistics Denmark, i.e. 55-60% of the whole area from 2006 to 2014. All of this production generates considerable residues in the form of straw. Figure 2.1 displays the share of residual straw from the agricultural sector. From the figure it

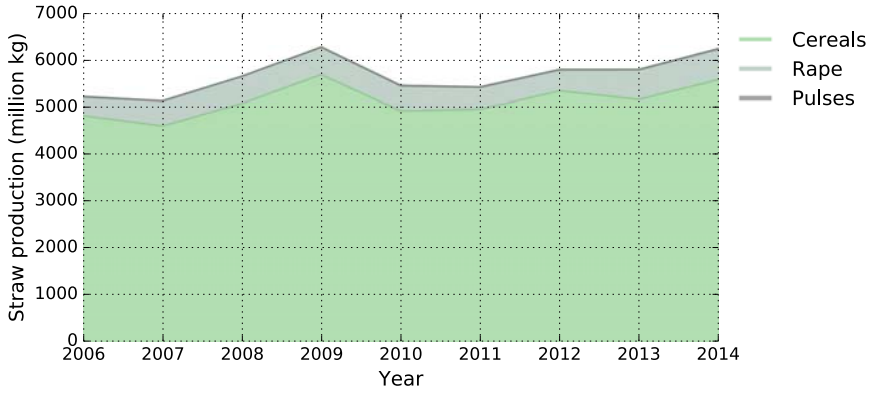

Figure 2.1: *Straw production in Denmark [25].*

can be seen that cereals dominate the generated straw share in Denmark. However, these resides are considered as products and the utilization of cereal straw in Denmark is divided between energy, fodder, bedding, etc., with the rest incorporated into soil. Figure 2.2 shows graphically how the utilization of straw is distributed in Denmark. It can be seen that utilization of straw from 2006 to 2014 ranges from 61% - 84% for both energy generation and soil incorporation. The estimated availability of straw for bioenergy utilization in Denmark is based on the amount of cereal straw left on the field and used for energy, according to Statistics Denmark [25]. By assuming 80% feasible extraction limit on the straw left on the field as estimated by Elsgaard et al. [36] the theoretical maximum is 2464.78 million kg. Using the estimated lower heating value of straw at 15.0% moisture content, based on the reference chemical composition of straw (14.434 MJ/kg), the energy content of those residues is about 35.6 PJ. Over the last 5 years an average of 21.30 PJ was used in the energy system and 14.28 PJ was left on the field, which is about 13% and

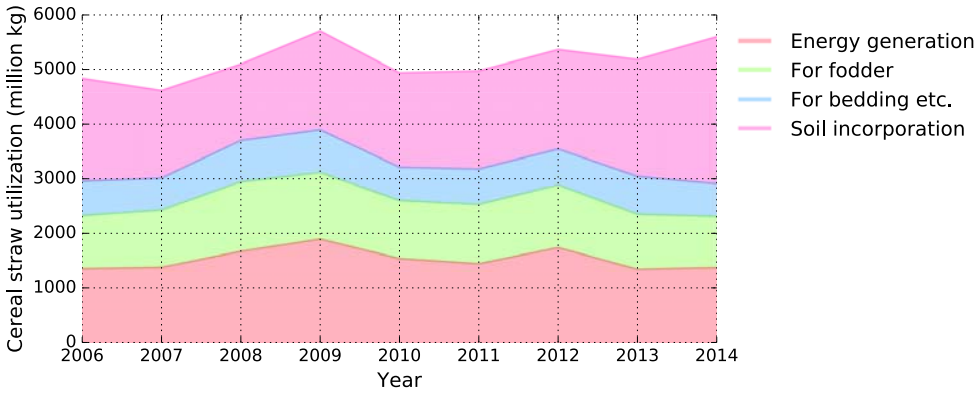

Figure 2.2: *Overall cereal straw utilization in Denmark [25].*

15% of the final electricity and district heating consumption in Denmark (2014) [**ens_2014**], respectively.

According to Statistics Denmark, on average about 70% of cereal grains were used as animal feed [25] from 1995 to 2014. Manure from the livestock industry is about 89% slurry. Most of the manure produced is from pigs and cattle. Their respective share is 49% and 46% of all manure production [37]. This manure can be and is utilized as an organic fertilizer for the agricultural system and re-circulates some of the nutrients contained in the grain, which is consumed by the animal, back to the agricultural field. This process reduces the demand for mineral fertilizers, which are produced by utilizing non-renewable resources.

In the Danish report "Biomass to Biogas Plants in Denmark, a Short and Long View" by Birkmose et al. [37], it is estimated that pig manure generation for the whole of Denmark for one year is 17.657 million tonnes. The annual pig manure generation was estimated to be a little less by the Baltic Forum of Innovative Technologies for Sustainable Manure Management [38]. There, pig manure generation was estimated to be 14,676 thousand tonnes per year. However, the feasible amount of manure to be used for bioenergy is about 2/3 of the total amount, as reported by Birkmose et al. [37], which gives a theoretical maximum potential for bioenergy use of 10.778 million tonnes per year using the average value between the two estimations above. If the calculated lower heating value of straw at 92.2% moisture content is used, based on the reference chemical composition of manure (1.42 MJ/kg), the energy con-

tent of those residues is 15.32 PJ or about 14% and 16% of the respective final electricity and district heating consumption in Denmark.

According to these estimates the availability of energy from the main residual resources in agriculture is 50.9 PJ, or about 46.2 of the final electricity- and 53.2% of the district heating consumption in Denmark in 2014. However, those residues contain about 96,600, 13,700, 2,150 and 28,800 tonnes of carbon, nitrogen, phosphorus and potassium respectively[1]. The objective is to develop bioenergy system concepts that can utilize the energy available in cereal straw and pig manure to substitute fossil fuels while recycling the nutrients and carbon for an overall system that is environmentally friendly and economically feasible. Figure 2.3 displays a simple schematic of the general concept of the integration between agriculture and bioenergy. Where the energy content of the

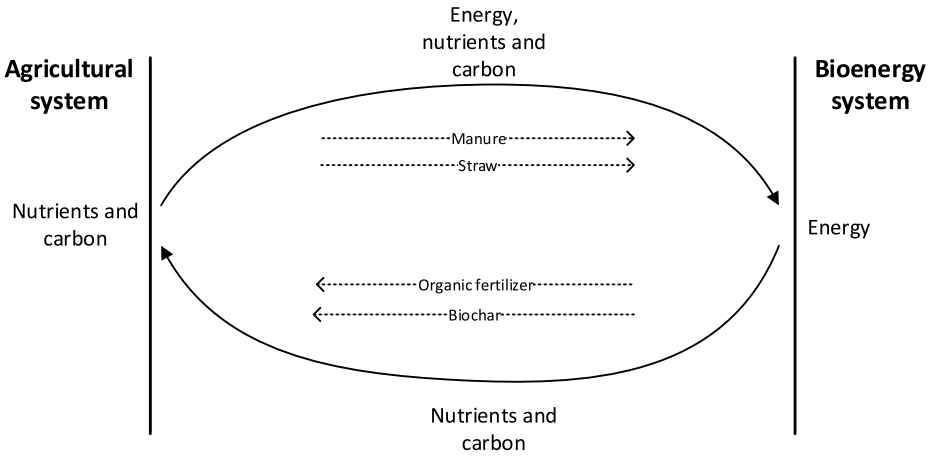

Figure 2.3: *Schematic showing the general concept of the integration between agriculture and bioenergy.*

agricultural residues is used to produce heat and power, while returning organic fertilizers and biochar. Organic fertilizer includes all flows recycled which due to de-watering of manure or manure sourced "waste" flows from the biochemical conversion process, biochar includes ash and char after thermochemical conversion process.

[1]Note that those numbers are based on the chemical composition of straw and manure reported respectively by Vassilev et. al [39] and Phyllis2 database [40], and may not reflect the average composition of cereal straw in Denmark.

2.2 Bioenergy System Concepts

A bioenergy system in this project would essentially need to be a poly-generating system producing electricity, district heat, and fertiliser. Based on the literature review, the bioenergy system concepts were developed by combining a decentralized biogas power plant using anaerobic digestion for biochemical conversion and a centralized thermal power plant using gasification for thermochemical conversion.

The biogas power plants and the thermal power plant are not assumed to be located at the same place, the physical location of the biogas plant is located in close proximity to the pig farm while the thermal plant is located in a more centralized location to increase the capacity of the power plant and benefit from economies of scale. A simple schematic showing the distance between the agricultural fields, biogas power plant and thermal power plants is given in Figure 2.4. It is assumed that within

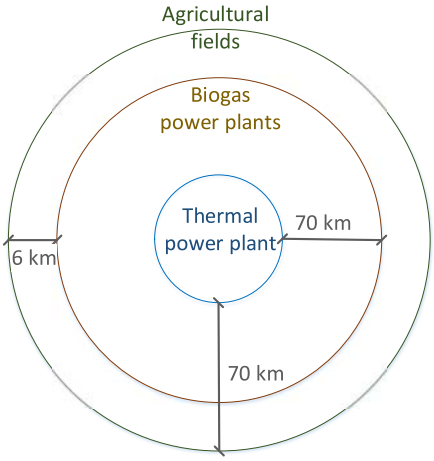

Figure 2.4: *Schematic showing the average transportation distances between the thermal power plant, biogas power plant, and agricultural fields.*

a 70 km average radius 100MW of cereal straw can be collected and used to fuel the thermal power plant. In the thermal power plant the Low Temperature - Circulating Fluidized Bed gasifier is then used to convert the inputs to product gas which is subsequently utilized in a power plant for heat and power production. The biogas power plant is assumed to be able to process 600-1000 tonnes daily depending on a concept. Where

the inputs are converted in a anaerobic digester which produces biogas. The biogas is then utilized in a power plant to generate heat and power. The ration of manure to straw is determined based process optimisation in the bioenergy system concept process modelling in reference to the 100MW capacity decided for straw. If manure utilization is beyond 1000 tonnes daily per 100MW straw, biogas power plants are added.

Figure 2.5 shows the schematic of four system concepts that are analysed in this work. It should be noted that the de-watering processes are all located at the site of the biogas power plant.

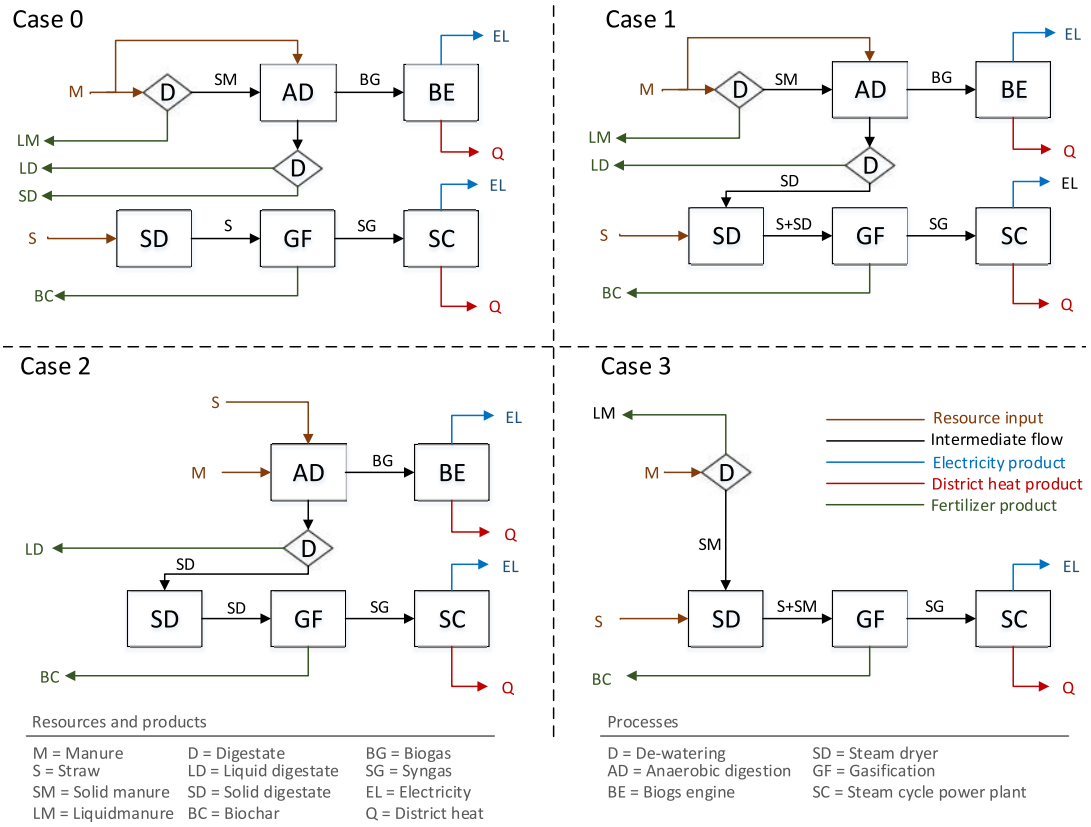

Figure 2.5: *Schematic of the system concepts and their main components and resource flows.*

Case 0: Separate utilization of straw and manure.
In this case part of the raw manure is sent to the anaerobic digester where it is digested with the solid fractions after de-watering the other part. The ratio of manure directly sent to the digestion process to manure sent to de-watering is found by optimization. The produced biogas is then combusted in a gas engine for heat and power. The digestates which contain most of the nutrients and part of the carbon are recycled as organic fertilizer. Straw is utilized in a thermal power plant, where it is dried before gasification in a Low Temperature Circulating Fluidized Bed (LT-CFB) gasifier. The product gas is then combusted in a steam cycle power plant for heat and power. Biochar is a co-product of the gasification process which contains most of the nutrients of the straw and some of the carbon.

Case 1: Co-gasification of straw and solid digestate.
This case study is similar to Case 0, except that instead of applying the solid fractions of digestate after de-watering to an agricultural field as an organic fertilizer it is sent to the thermal power plant to be co-gasified with straw. This increases the heat, power and biochar production, while decreasing the organic fertilizer production in comparison with Case 0. So the capacity of the thermal power plant increase beyond 100MW.

Case 2: Co-digestion of straw and manure
Here the manure is directly co-digested with straw and the biogas is combusted in the biogas engine like in Case 0 and Case 1. The digestate is dewatered from which the solid fractions are gasified in the LT-CFB gasifier and the product gas is combusted in the steam cycle power plant. The liquid fraction of the digestate and biochar from the gasifier are returned back to the agricultural system. This case defines the straw to manure ratio of all the cases as the ratio is found based on the optimum mix of straw and manure for co-digestion. In this case the biogas power plant capacity increases, but the capacity of the thermal power plant will be lower than 100MW.

Case 3: Co-gasification of straw and solid manure
In this case the biogas power plants are avoided and the raw manure is de-watered before being sent to the thermal power plant where it is co-gasified with straw. Product gas is then combusted in the steam cycle power plant for heat and power production. Compared with the other cases, the biochar poduction will increase but there will be less organic fertilizer production will be produced. Additionally, the capacity of the thermal power plant will be higher in this case compared with other cases as most of the resources utilized are utilized there.

Modes of Operation In all system concepts the thermal power plant is analysed based on two mode of operation, one where heat and power production is maximized and another where the biochar production is maximized. The analysis will be made for each mode of operation assuming that the thermal power plant has been designed specifically to operate at one or the other, which will effect the size of some components in the thermal power plant. The two operation mode are decided based on the carbon conversion in the LT-CFB gasifier, where maximum carbon conversion results in maximum heat and power production and minimum carbon conversion results in maximum biochar production. The upper and lower limit on the carbon conversion is found during the process modelling process.

References

[25] *Statistics Denmark, https://www.dst.dk/en, accessed: 2016-01-31.*

[36] L. Elsgaard et al. *Anvendelsesmuligheder for halm til energiformål.* Mar. 2011.

[37] T. Birkmose, K. Hjort-Gregersen, and K. Stefanek. *Biomasse til biogasanlæg i Danmark - på kort og langt sigt.* Tech. rep. AgroTech: Institute for Jordbrugs- og FødevareInnovation, 2013.

[38] S. Luostarinen. *Energy Potential of Manure in the Baltic Sea Region: Biogas Potential and Incentives and Barriers for Implementation.* Tech. rep. Baltic Forum for Innovative Technologies for Sustainable Manure Management, 2013.

[39] S. V. Vassilev et al. "An overview of the chemical composition of biomass". In: *Fuel* 89 (2010), pp. 913–933.

[40] E. research Centre of the Netherlands. *Phyllis2, database for biomass and waste,*

Chapter 3

Methods

This chapter describes the methods used to answer the research question of this thesis. First the analytical framework and the modelling tools are described. Then the methods needed to model and simulate the thermal power plant and the biogas power plant are outlined. Finally, the agricultural system process models are presented which includes the approaches used to model and simulate resource removal and recycling along with soil carbon build-up.

3.1 Analytical Framework

The analysis of the system concepts was based on environmental impact, non-renewable resource requirements and economic feasibility. All of the system concepts have different attributes and it was expected that the optimum concept would not necessarily be found to be the same for each criteria. To account for that the analytical framework includes a multi-criteria decision analysis (MCDA) which collects the results of the environmental impact assessment, along with the non-renewable resource

requirements and the economic feasibility of each concept and mode of operation. The optimum concept is then found at all possible weight points between each criteria.

For this analysis, the TOPSIS method was chosen as the only judgement required is the weighting of the criteria [41]. The method is described in Behzadian et al. [42] as a method that identifies the alternative (case or specific system operation) that is closest to the ideal solution (best) in a multi-dimensional computing space [42], based on specific criteria (environmental impact, non-renewable resource required and economic feasibility). It involves defining a normalized decision matrix with values and weights assigned to each criteria [43].

$$r_{ij} = \frac{x_{ij}}{\sum_{J}^{j=1} x_{ij}^2}, j = 1, 2, 3, ...J; i = 1, 2, 3...., n \tag{3.1}$$

Next the weighted normalized decision matrix is constructed by multiplying weights w_i of each evaluation criteria with r_{ij}.

$$v_{ij} = w_i \cdot r_{ij}, j = 1, 2, 3, ..., J; i = 1, 2, 3...., n \tag{3.2}$$

The positive A^+ and negative A^- ideal solutions are then calculated.

$$A^+ = v_1^+, v_2^+, v_3^+, ..., v_n^+ \tag{3.3}$$

Here, $v_i^+ = max(v_{ij})\ if\ j \varepsilon J$; or $v_i^+ = min(v_{ij})\ if\ j \varepsilon J^-$.

$$A^- = v_1^-, v_2^-, v_3^-, ..., v_n^- \tag{3.4}$$

Next, the separation measures for each alternative are calculated and the relative closeness to the ideal solution is found as a ratio.

$$d_i^+ = \sqrt{\sum_{n}^{j=1} (v_{ij} - v_j^+)^2}, i = 1, 2, 3...., j \tag{3.5}$$

$$d_i^- = \sqrt{\sum_{n}^{j=1} (v_{ij} - v_j^-)^2}, i = 1, 2, 3...., j \tag{3.6}$$

Finally, the relative closeness to the to the ideal solution is found by the RC_i ratio.

$$RC_i = \frac{d_i^-}{d_i^+ + d_i^-}, i = 1, 2, 3...., j \tag{3.7}$$

Ranking of the operation scenarios can then be determined by the highest value of RC_i ratio for the best solution. Using TOPSIS is very beneficial to this project because no attempt was been made to compare the relative importance of the criteria to each other and the results will be presented in a ternary graph showing all possible weighting options between them, i.e. RC_i is found for all possible w_i. This is done in order to show how much compromise, e.g. on the economic objective compared to the environmental impact objective, is needed for the optimum concept to be different. The results of this analysis are given in a Ternary graph where all weights of the different criteria are represented in the grid. Figure 3.1 shows an example of the ternary graph.

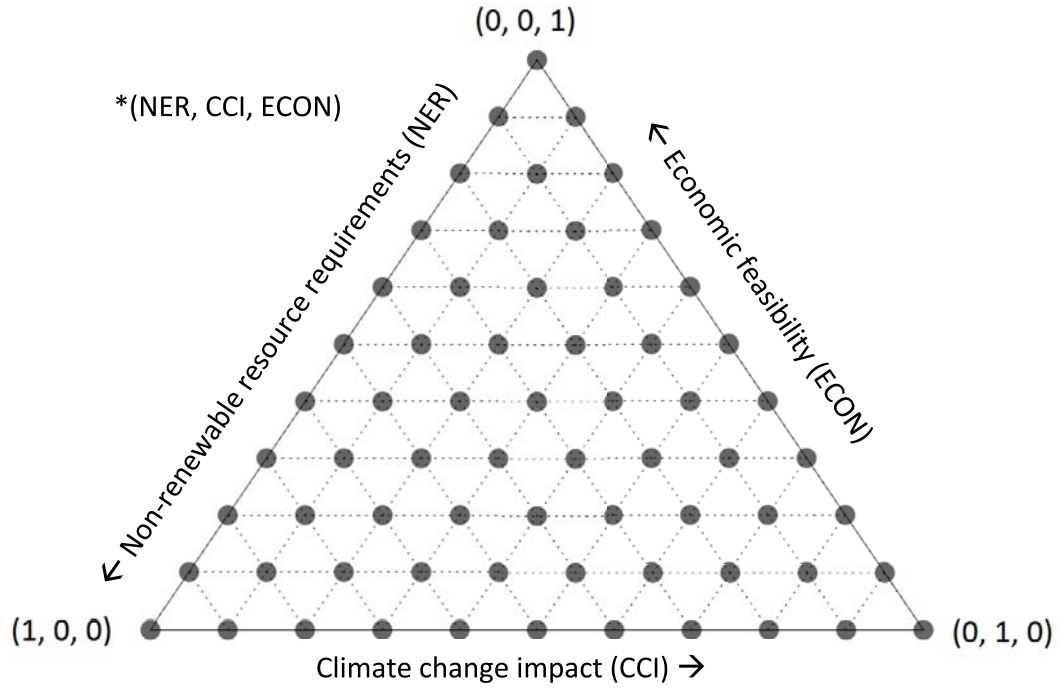

Figure 3.1: *Descriptive ternary graph for the multi-criteria analysis.*

At each point on the grid (representing w_i), the optimum system concept and operation mode is found. The weight of each criteria is increased on each point in Figure 3.1 as it gets closer to the corner pointed to by its label.

3.1.1 Climate Change Impact

As the climate change impact from fossil fuel utilization is driving the changes towards increased biomass utilization instead of fossil fuels, the environmental impact was measured to reflect affect on climate change using the Global Warming Potential (GWP) [44]. The GWP was developed by the Intergovernmental Panel on Climate Change (IPCC) and is the most common impact method for climate change and recommended by the International Reference Life Cycle Data System (ILCD) [45, 46] to represent impact on climate change.

However, to adequately report the climate change impact due to changes in the radiative forcing of carbon emissions from bioenergy systems, the biogenic carbon cycle needed to be accounted for. This was done by multiplying the GWP of carbon emissions with a correction factor. Effectively accounting for the difference between the atmospheric carbon dioxide concentration over a specific time horizon as a result of carbon emissions from systems that capture carbon from the atmosphere by photosynthesis within the same time horizon, and the atmospheric carbon dioxide concentration as a result of pulse carbon emissions from a system that does not capture carbon (e.g. fossil fuels combustion or from primary forest not regrown after harvest). This factor is represented by the following equation.

$$GWP_{biogenic} = \frac{B(t)}{F(t)} \tag{3.8}$$

Here, $B(t)$ represents atmospheric carbon dioxide concentration related to biogenic carbon emission and $F(t)$ represents atmospheric carbon dioxide concentration related to fossil carbon emission. This ratio was found for each biomass resource to create a unique GWP correction factor for each resource as the biogenic carbon cycle of biomass is effected by its growth via photosynthesis and decay if it is not combusted. The calculation method for the biogenic GWP correction factor follows the approach of Cherubini and colleagues [47, 48, 49, 50, 51], and Petersen et al. [52]. However, as bioenergy systems using manure usually include considerable amount of methane emissions the biogenic GWP was calculated in this work at the emission source, which gives a unique factor depending on the emission profile (one pulse or continuous release over time) and

types of carbon emissions (e.g. carbon dioxide, carbon monoxide and methane).

The report by the IPCC, "Climate Change 2013: The Physical Science Basis. Contribution of Working Group I to the Fifth Assessment Report of the Intergovernmental Panel on Climate Change", noted the work of Cherubini and colleagues as a new emission metric concept that takes on the common assumption that neglects the radiative forcing imposed by the time lag between combustion and regrowth of biomass [44]. In Guest et al. [51] and Petersen et al. [52], this is extended by including the time-integrated carbon mission profile from decaying biomass. The function ($B(t)$) representing the atmospheric carbon dioxide concentration related to biogenic carbon utilized (C_0) is calculated as follows:

$$B(t) = C_0 \cdot [E(t) - G(t)] \tag{3.9}$$

Here, $E(t)$ represents the atmospheric concentration profile over time from biomass emission (one pulse when combusted or gradual release when decomposing in agricultural soil) and $G(t)$ represents the decrease in atmospheric concentration from biomass regrowth over time. These functions are calculated by a convulsion operation between the respective emission and regrowth rates, and the impulse response function (IRF) [47, 53],

$$E(t) = \int_0^t \delta(t') \cdot y(t - t')dt' \tag{3.10}$$

$$G(t) = \int_0^t g(t') \cdot y(t - t')dt' \tag{3.11}$$

where t is time within the 100-year time horizon, δ is the emission rate, g is the regrowth rate and y is the IRF from the global carbon cycle climate model by Joos et al. [54, 55].

$$y(t) = k_0 + \sum_{i=1}^{3} k_i e^{-t/\tau_i} \tag{3.12}$$

$$F(t) = C_0 \cdot \int_0^t y(t)dt \tag{3.13}$$

Here, k represents the relative capacity of natural sinks to capture atmospheric carbon dioxide and τ is a relaxation time scale representing

the rate of atmospheric carbon dioxide capture by the natural sinks; the values for k and τ are given in Cherubini et el. [48] and Petersen et al. [52]. The correction factor calculation is thus split into two parts carbon emission and carbon capture. The emissions from combustion and other pulses in the bioenergy system were modelled in Section 3.3, and emission during decomposition of biomass in agricultural soil was modelled in Section 3.4 for cereal straw, pig manure and biochar.

The carbon capture part $G(t)$ of the Equation 3.10 is further elaborated on here. As noted in Cherubini et al. [47], the rate of biomass growth is commonly modelled as a normal distribution [56, 57], where C captured by photosynthesis during regrowth is shown as a function of the rotation period and where the mean and variance are assumed to be half and one quarter of the rotation period respectively [47, 50]. Figure 3.2 graphically displays the normalized growth rate and normalized cumulative growth function, generalized for all biomass types.

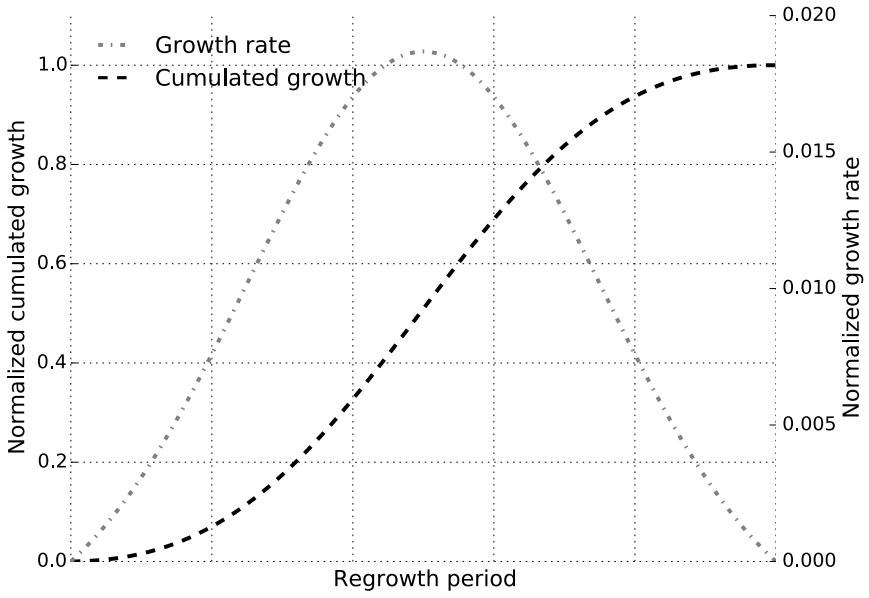

Figure 3.2: *Normalized growth rate and normalized cumulative growth during biomass regrowth.*

The atmospheric carbon concentration associated with the regrowth for all regrowth periods can then be calculated by Equation 3.10. The results of Equation 3.10 for regrowth periods (1, 5, 10 , 25, 50, 75, 100 and ∞)

and a time horizon from 0 - 100 years are plotted in Figure 3.3.

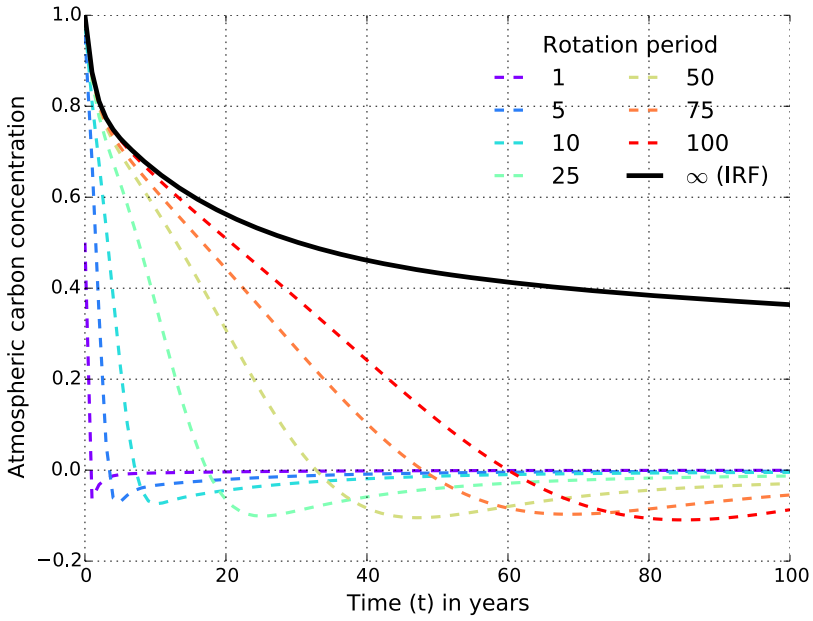

Figure 3.3: *Atmospheric concentration associated with regrowth over 0 - 100 year time horizon.*

It can be seen in Figure 3.3 that an infinite rotation period is equal to the IRF function and represents the case of biomass harvested without subsequent regrowth. These results are verified with the results from Cherubini et al. [47]; however, there the growth rate was not normalized to one which explains the moderately different results reported there, where the atmospheric concentration is slightly overestimated. Crop cultivated on the field and all organic fertilizer inputs are assumed to have an annual rotation period. Additionally, biochar from gasification of straw and solid or digested manure can also be assumed to have an annual rotation period.

The main functional unit of the environmental impact analysis and to which the impact of each system concept was normalized to is weight of the biomass resources utilized by the bionergy system in *tonnes*. This was done to find the impact independent from the conversion process to effectively compare alternative utilization of the same biomass. As such the normalization to unit input was considered the right approach, as recommended for Life Cycle Impact Assessment (LCA) of residual

biomass in bioenergy system [4].

This analysis is consequential, as such the impact of removing resources from the agricultural system was accounted for by assuming that their reference state is to applied to an agricultural field. By apply straw and manure on an agricultural field, they nutrients and carbon within them are incorporated into the soil. Because of this when they are removed mineral fertilizers are assumed to be needed to compensate for the removed nutrients. The impact of those resources was found by using the econivent 3.3 database [58]. Carbon removal from soil with the resources is modelled to effect the climate change impact by calculating the carbon sequestration impact of straw and manure, which is then lost when removed.

Additionally, the electricity and district heat products of the bioenergy system were assumed to avoid emissions from a substituted production To account for that a scenario analysis was made where Combined Heat and Power (CHP) plant, fuelled with different types of fuels is substituted. Included are scenarios where the substituted production is fuelled with coal, natural gas or biomass (wood chips). In addition to these scenario, two other scenarios were made that represent the marginal electricity technology and fuel in Denmark based on Lund et al. [**rae**]. It is assumed that the new electricity produced with the system concepts will substitute the marginal electricity on the grid in Denmark which was found to be 51% coal and 48% natural gas fuelled, with 1% from wind. Two district heating scenarios accompany the marginal electricity scenario, one where the avoided district heating is fuelled with wood chips and the other with natural gas. The climate change impact by these alternative CHP processes were found by using the ecoinvent 3.3 database [58].

3.1.2 Non-renewable Resource Requirements

The non-renewable resource requirements of each system concepts was found by calculating the Exergy Return on Investment (ExROI) for each

system concept. ExROI is defined as the ratio of the non-renewable exergy required (or demanded) by the analysed system over its life cycle, to the exergetic value of its products [59]. It is an extension of the Energy Return on Investment (EROI) concept defined by Cleveland et al. [60] as the ratio of the energy required to obtain a particular resource to the usable energy acquired by its expenditure.

EROI utilizes thermodynamics to indicate the sustainability of a system purely from an energy perspective. However, the EROI concept is constrained by its utilization of the first law of thermodynamics which states that energy is always conserved and cannot be created or destroyed but only transformed. By its definition, a first law concept cannot take the quality of energy into account, which can lead to misleading conclusions [61]. The second law of thermodynamics, on the other hand, captures the irreversibility of processes and states that energy is always wasted once transformed. Exergy is a second law concept that expresses the quantity of energy that is available to be converted to work. The exergy of a product can be defined as the minimum amount of work needed for its production [62].

Exergy analysis that aims at reducing exergy lost/destroyed when designing, retrofitting or operating equipment or processes is well established and its utilization has been thoroughly documented. However, although exergy utilization in a life cycle scope is less established, numerous concepts have been defined in recent decades that deal with the life cycle perspective of exergy analysis. Those methods generally use either cumulative exergy consumed/extracted/required or cumulative exergy losses to indicate the life cycle impact on natural resources of a product [63, 64, 65, 66]. This is also the case for the Cumulative Exergy Demand (CExD), which quantifies demand for both energy and material resources in terms of exergy [67]. The CExD method has been fully coupled with ecoinvent database by Bösch et al. [67]. It can then be used to include all upstream data and to calculate the cumulated sum of all exergy demanded for the production.

The product exergy is found by an exergy analysis, where the final product was defined to be the net electricity and district heat, as biochar and the organic fertilizer products are utilized within the system boundary.

The net electricity produced is assumed to be equivalent to exergy while the exergy of the district heating produced is based on heat transfer which is assumed to occur at the thermodynamic average temperature and at constant pressure between the defined upper and lower temperature levels of the district heating system [62].

$$\dot{E}_q = 1 - \frac{T_0}{T_a} \cdot \dot{Q} \tag{3.14}$$

Here, $\dot{E}_q$, T_0, T_a, $\dot{Q}$ are the exergy rate transferred to district heating, the temperature of the exergy reference environment (15°C), the thermodynamics average temperature of the district heating network and the heat rate transferred to district heating respectively. The thermodynamic average temperature at the district heating network is calculated by assuming constant pressure by the specific enthalpy (h) and specific entropy (s) for water at the forward (e) (80°C) and return (i) (40°C) temperatures of the district heating grid.

$$T_a = \frac{h_e - h_i}{s_e - s_i} \tag{3.15}$$

The specific enthalpies and entropies were gathered from the C++ library Coolprop, which can implement pure and pseudo-pure fluid equations of state and transport properties [68]. ExRIO is thus the sum of the exergetic values of electricity and district heat, divided by the sum of CExD values for non-renewable material and energy resources.

$$ExROI = \frac{E_p}{nCExD_p} \tag{3.16}$$

Here, E_p is the product exergy (electricity and district heat) and $nCExD_p$ is the cumulative sum of exergy of all non-renewable resources required to obtain the products. Mora et al. [69] considers that the system is renewable from an exergy perspective if the ratio is above 1, as the exergy required from non-renewable resources is less then the products' exergy content. In addition, greater ExROI means that even less non-renewable resources are required and the system produces its products more effectively from a renewable energy point of view.

The advantage of using ExROI is that it combines the life cycle perspective by including CExD and process efficiency by including the exergy

product. It can then be found whether the non-renewable resources required indicator (ExROI) is more effected by the cumulative demand of non-renewable resources or the inefficiency of the production process. The inefficiency of the production process in exergy terms was found by analysing the components of each system concept for exergy lost or destroyed. The results are given by the inefficiency ratio y_I.

$$y_{I,i} = \frac{\dot{E}_{l,i} + \dot{E}_{d,i}}{\dot{E}_f, total} \tag{3.17}$$

Where, $\dot{E}_l$ and $\dot{E}_d$ represent the exergy lost and destroyed in the $i-th$ component, respectively. $\dot{E}_f, total$ is the total exergy value of the fuel used by the system concept, i.e. straw and manure. The physical exergy at process level is based on the state properties of flow between each component and the chemical exergy is based on model II in Bejan et al. [62] which uses Szargut's definition [63].

3.1.3 Economics

The economic analysis of the integrated bioenergy and agriculture cases is based on finding the real payback period and the levelized annual average revenues required for electricity production using the methods described by Bejan et al. [62] in the book "Thermal Design and Optimization". The annual revenues required were found by calculating, over the expected lifetime of the investment, the total capital recovery (TCR), the minimum return on investment (ROI) for common equity and debt, income taxes and other taxes and insurance, along with operation and maintenance costs (O&M) and fuel costs.

The carrying charges are defined for the annual payments required to cover the cost related to the investment cost and taxes. Table 3.1 gives the evaluation assumptions for the carrying charges calculation made for each component in the system concepts.

Table 3.1: *Economic evaluation assumptions, for the carrying charges.*

Plant availability	85%
Equity share	25%
Discount rate for equity[a]	13%
Loan interest rate[a]	5.0%
Tax rate	23.5%
Insurance and other tax	2.0%
Expected lifetime	25 years
Working capital	5% of TCR
Green electricity	110 Euro/MWh[b]

[a] The overall discount rate is 7%.
[b] Premium feed-in tariff.

The investement cost for each component of the bioenergy system is given in Section 3.3, along with the O&M costs. The fuel cost is based on straw and manure prices, along with transportation costs. Additionally, the revenues of fertilizer sales are included in the fuel cost. The fuel cost (F_c) was calculate by the following equation.

$$F_c = S_c + M_c - O_r - B_r + T_c \tag{3.18}$$

Where, S_c, M_c, O_r, B_r and T_c represent the straw cost, manure cost, revenues from organic fertilizers, revenues from biochar and transportation costs. The transportation cost includes both the transport of fuel to the bionenergy system and the transportation of organic fertilizers and biochar to the agricultural system. The fuel cost components are given in Section 3.4. Where the revenues from the organic fertilizer sales depend on the nutrients that are within them and the carbon sequestration potential. The value of the nutrients was based on the price of nitrogen, phosphorus and potassium fertilizers and the value of carbon sequestration was accounted for by using the price of carbon emission quotas (see Section 3.4).

The district heating product was accounted for by allocating a certain percentage of the carrying charges and expenses to it. Revenues of district heating sales in Denmark should always be equal to the cost of producing; in this project, the allocation of costs to district heating production was done using energy. The sum of these cost/benefit categories represent the expenses part of the total revenue required. The equation used to

calculate the total revenues required of electricity sales from the total revenues required is as follows.

$$E_{trr} = T_{trr} - T_{trr} \cdot \alpha_{dh} \tag{3.19}$$

Where T_{trr} is the total revenues required and α_{dh} is the allocation factor to the district heating product. But an upper limit was place on α_{dh} of 0.6 to ensure that most of the costs are just not allocated to the district heating product. The levelized value of the annual total revenues required to produce electricity is then found by summing the present values of the total revenues required for each year and then converting that sum to an equivalent annuity using the uniform series present worth factor (U_f) [62].

$$U_f = \frac{(1+i)^T - 1}{i \cdot (1+i)^T} \tag{3.20}$$

Where, T is the lifetime of the unit and i is the discount rate. The real payback period (τ_{pb}) is then found by assuming electricity sales at a certain price. According to the Danish Promotion of Renewable Energy Act §44 par. 2 VE-Lov, the premium feed-in tariff subsidy scheme (bonus plus market price) is DKK 0.793 (approx. 11 Euro-cents) per kWh electricity generated through biogas, gasification gas produced from biomass, Stirling engines and other specialized electricity production plants that use biomass as an energy source.

$$N_0 = -F_{e,0} + Y_T \tag{3.21}$$

$$Y_T = \sum_{t=0}^{T} Y \cdot (1+i)^{-t} \tag{3.22}$$

$$Y = F_{c_t} - F_{b_t} - F_{i_t} \tag{3.23}$$

$$\tau_{pb} = -\frac{ln(1 + i \cdot F_{e,0} / \frac{\sum Y}{T}}{ln(1+i))} \tag{3.24}$$

Here, $F_{e,0}$ is the initial investment cost, N_0 is the net present value, t is a specific year in its lifetime, F_b, F_c and F_i are the annual benefits, costs and income,

3.2 Modelling Tools

Modelling the system integration of bioenergy and agriculture was assisted with various freeware tools, such as C-TOOL [70, 71, 72], Dynamic Network Analysis (DNA) [73] and Brightway2 for Life Cycle Inventory (LCI) analysis and Life Cycle Impact Assessment (LCIA). These tool were bundled together in Python to form a tool specifically made to analyse bioenergy system concepts based on the requirements of the analytical framework as described above. Figure 3.4 shows a schematic describing the main components of the tool. As shown in the schematic, the tool

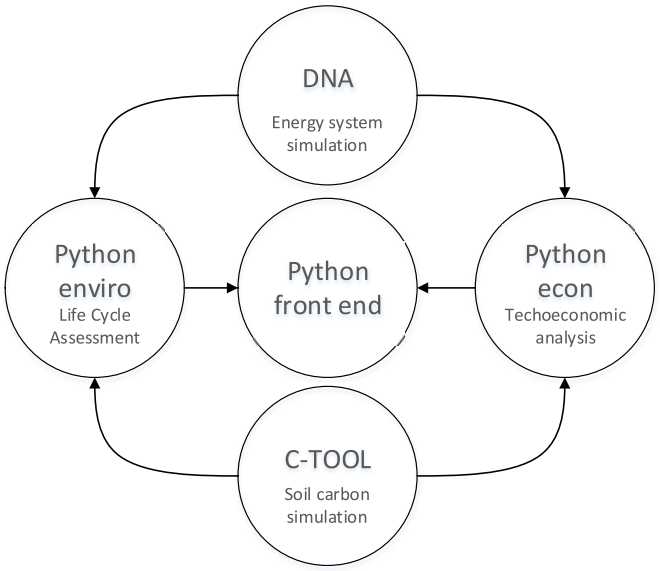

Figure 3.4: *A scematic of a multi-level tool for bioenergy system analysis.*

can be thought of as five parts. The energy system process models are developed in DNA, there the thermal power plant and part of the biogas power plant is modelled (see Section 3.3). In C-TOOL the decomposition of carbon in soil is modelled for straw, manure and biochar (see Section 3.4). Both the techno-econmic analysis for the economic feasibility calculation and Life Cycle Assessment for the climate change impact and part of the non-renewable resource requirements are modelled in Python. Both Python models are based on mass and energy balances. But the LCA requires data from a database to cover the upstream processes not physically modelled by the tool.

DNA (Dynamic Network Analysis) is an open-source component based thermodynamic modelling and simulation tool [73]. DNA was developed at the Thermal Energy Section of the mechanical engineering department of the Technical University of Denmark. A bridge to DNA was made through its text interface in Python, but the program is compiled in FORTRAN code. From Python the information about the resources used by the thermal power plant and the biogas engine was feed into DNA, where the state properties are defined and calculated for each component, effectively simulating the power plants and calculating the electricity, district heating, along with the biochar production for further analysis.

C-TOOL is a carbon storage in soil simulation tool [70, 74, 75, 72, 76]. With C-TOOL the decay of biomass in soil could be simulated over a chosen time horizon. The seven carbon pool model in C-TOOL was used, where two carbon pools represent added organic matter, another two soil microbial biomass and further three C pools represent soil organic matter. The flow of carbon from organic input through the seven carbon pools is described by Petersen et al. [74, 72] and graphically illustrated in Figure 3.5, which was adopted from Petersen et al. [74]. The model considers

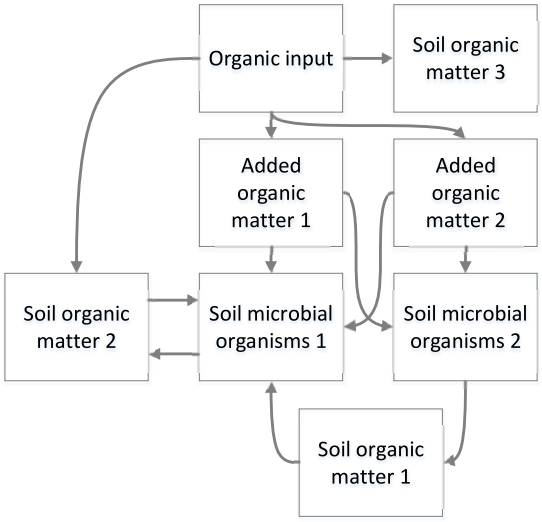

Figure 3.5: *Flow of carbon input to soil as simulated by C-TOOL.*

the top-soil, where each carbon pool has a defined decay rate and that decay is either directed towards other pools or emitted as carbon dioxide according to a specific utilization efficiency [74]. A detailed description

of the calculation methods used in C-TOOL can be found in the user manual [71] and more detail on the specific seven carbon pool model can be found in Petersen et al. [74, 72].

The upstream Life Cycle Inventory (LCI) data is found using the ecoinvent 3.3 cut-off allocation database [58]. To communicate with that database, the Brightway2 advanced life cycle assessment framework was used [77]. Brightway2 is an open source framework that is primarily written in Python and is split into several packages, one of which – Brightway2-data – is used in the LCI modelling of this work and handles the storage and searching of all data sources, including ecoinvent 3.3 database and a biosphere database that contains all available elementary flows that can be modelled in this project. An advantage of Brightway2-data is that it is possible to write and store unlimited databases with links to each other. The LCI modelling of this work takes advantage of this by writing and storing databases for each component of a system integration case where the unit processes are linked with ecoinvent 3.3 and elementary flows are linked with the biosphere database. This makes dynamic LCI calculation both easy and fast by normalizing each component to a specific reference flow. Figure 3.6 displays a schematic of the links between the components and the utilized databases. As shown in

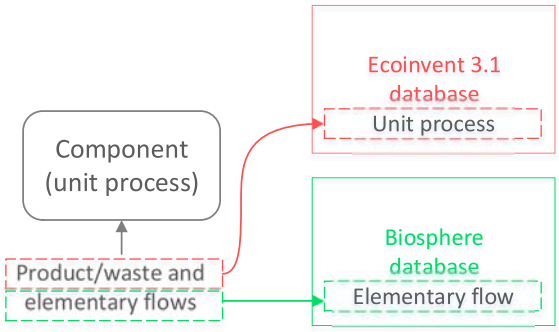

Figure 3.6: *Schematic of components links with the ecoinvent 3.3 and biosphere databases.*

the figure, all unit processes are linked with the ecoinvent 3.3 database which stores all of the upstream processes, while the elementary flows are linked with the biosphere database which can then be used in a Life Cycle Impact Assessment (LCIA) by the chosen impact methods.

3.3 Bioenergy System Process Models

In this section the bioenergy system process models developed for this work are described. It outlines the methods used to model and simulate the polygeneration system concepts producing heat, power and fertilizer as introduced in Section 2.2 and is divided into manure processing, biogas power plant and thermal power plant.

Each process model was based on modelling the mass and energy balance, along with the infrastructure which took into account the energy and material required by each process. In the infrastructure model the investment and O&M costs was also found.

3.3.1 Manure Processing

The manure processing was divided into storage and de-watering of manure. The storage system includes both indoor and outdoor storage units, and the de-watering process model includes both decanter a screw-press which are used to separate the inputs to solid and liquid fractions.

The process model of the storage units was constructed to minimize emissions by using favourable storage types and time of storage. For wet biomass, the indoor storage of manure was assumed to be less than one month in pit storage under animal confinements, but according to the IPCC guidelines it is estimated that for longer storage time the emission factor could increase from 3% for methane to about 17% and up to 80% depending on the temperature inside the storage [78]. Raw slurry, along with liquid manure and liquid digestate, was assumed to be stored outside in a concrete tank with natural crust after removal from the animal housing. Using natural crust can decrease the methane emissions from the outdoor storage units by 7% - 30%, but could increase dinitrogen monoxide emissions, depending on temperature [78]. However, although the dinitrogen monoxide emissions could increase while the methane emissions decrease it was not expected to have a net negative impact on in terms of climate change. The solid manure and digestate were assumed to be stored in a covered heap on a concrete slab with an additional tent

canvas and Pumping and stirring associated with the storage units are powered by electrical motors.

Macro-nutrients and carbon substance balances were compiled for storage units. Where the difference between the inputs and outputs are governed by emissions. Emissions of phosphorus and potassium are neglected, as such the only macro-nutrient emitted from storage is nitrogen. The nitrogen balance calculation can be described by the following equation

$$N_{out} = N_{in} - \sum N_{in} \cdot \eta_i \tag{3.25}$$

Here N represents nitrogen and the in/out subscripts refer to the input and output of the storage units, η_i is the emission factor for i emission. The emission factors modelled in this process model were based on the factors reported by Hamelin et al. [79]. The fate of nitrogen inputs to storage are displayed in Figure 3.7 for each wet biomass input source included in the model, where the total nitrogen emissions are divided into dinitrogen monoxide, ammonia, nitrogen oxides and nitrogen gas.

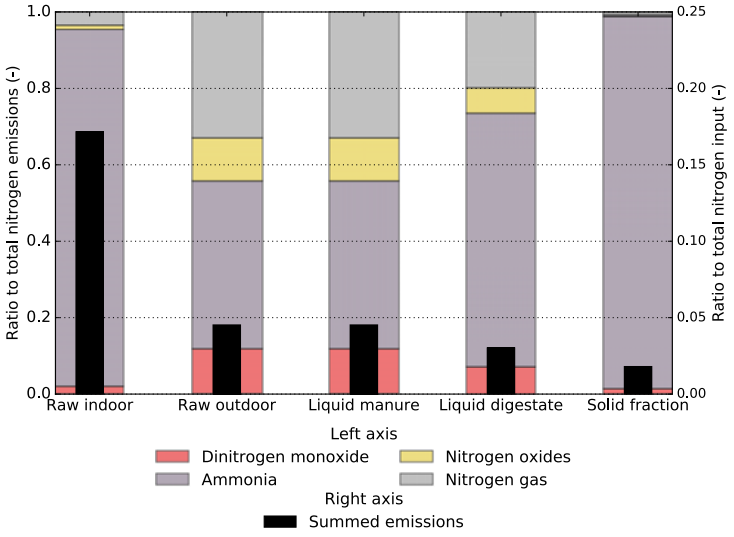

Figure 3.7: *Nitrogen emissions in the storage units.*

Most of the emitted nitrogen is in the form of ammonia from the indoor and outdoor storage, followed by dinitrogen monoxide and nitrous oxide from outdoor storage. Additionally, it can be seen that the total nitrogen lost during storage is almost 18% in the indoor storage input but will be

less then 5% for all outdoor storage inputs, with the lowest loss when storing solid fractions in an outdoor storage unit.

The carbon balance in the storage system is governed by the emissions of methane and carbon dioxide. The maximum methane conversion capacity was assumed to be 0.45 m^3 CH_4 per volatile solids in manure [79]. The volatile solids were given by the proximate chemical composition and methane density is 0.65 kg/m^3. The following equations describe the carbon balance of the storage units.

$$C_{out} = C_{in} - CH_{4,c} - CO_{2,c} \tag{3.26}$$

$$CH_4 = 0.45 \cdot 0.65 \cdot VS_{in} \cdot \eta_{emi} \tag{3.27}$$

Here VS_{in} is the content of volatile solids at inlet. For every carbon emitted in the storage unit the capture of carbon as CO_2 by photosynthesis was accounted for and allocated to the source of emission, i.e. in this case the storage unit. The CO_2 emission was found based on either the carbon input or the emitted CH_4. Figure 3.8 displays the fate of carbon inputs to storage for each modelled wet biomass. But included in Figure 3.8 is the carbon capture during subsequent regrowth of the biomass. It can be

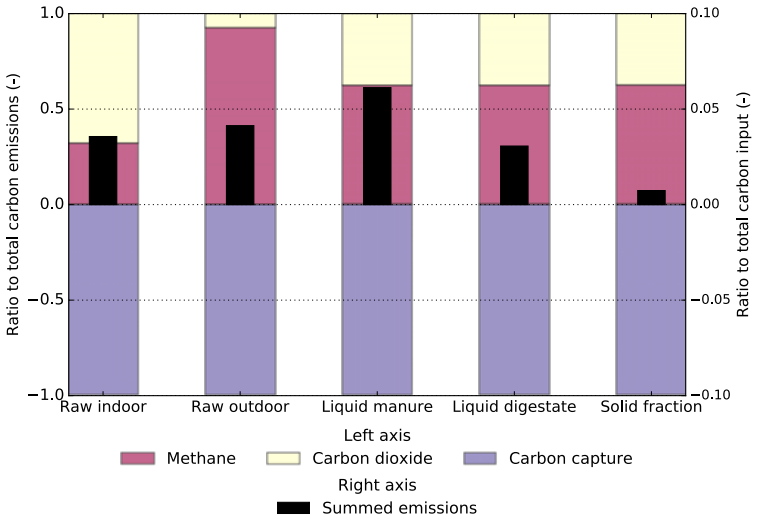

Figure 3.8: *Carbon emissions and regrowth in the storage units.*

seen in Figure 3.8 that for the indoor storage input, the carbon emission

is mostly carbon dioxide. However, for the outdoor storage inputs most of emitted carbon is in the form of methane. Furthermore, it can be seen that the amount emitted and the amount captured by regrowth of the biomass source are almost equal, as the manure biomass source was assumed to be regrown within one year as the animal feed was assumed to consists only of annual rotation crops.

The energy and material consumption of the storage unit over its lifetime were estimated using the ecoinvent LCI (Life Cycle Inventory) database, [58] exploiting values for the operation of a liquid manure storage and processing facility which include the energy and auxiliary material for the operation of a marine screw agitator, along with a covered and an underfloor rectangular concrete storage container [80]. The investment along with the O&M cost for storage units were estimated based on the cost of electricity in Denmark and the cost of components, i.e. the storage unit itself. Electricity costs are 0.091 $euro/kWh$ and the cost of the liquid manure storage and processing facility is assumed to be 43 $euro/m^3$ stored for solid fractions of manure and digestate in the bioenergy system [81]. The investment in liquid manure and liquid digestate storage was assumed to be unnecessary as enough storage is assumed to be available in the agricultural system.

3.3.1.1 De-watering

Modelling the mass and energy balance of de-watering process of manure or digestate is difficult as the efficiencies of different techniques vary for dry matter and specific substances [82]. There were two separation processes modelled, i.e. one decanter process and one screw press process. The decanter was based on the GEA Westfalia separation processes and the UCD 305 decanter centrifuge [83]. And the screw press process model was based on the Samson Bimatech mechanical separation plant as defined by Hamelin, Wesnæs and colleagues [84, 85].

The input to the separation process is split into a liquid fraction and a solid fraction at the outlet. The properties profile of the outputs after separation needs to be equal to the profile at inlet. Distribution of other substances not reported in the reference articles were found by using the

fraction of dry matter (DM) and nitrogen (N) for the remaining elements ash free ultimate chemical composition and the average of phosphorus (P) and potassium (K) for the distribution of the remaining ash compounds, as shown in Equations 3.28 and 3.29 respectively.

$$\eta_A = \frac{P_{in} \cdot \eta_P + K_{in} \cdot \eta_K}{P_{in} + K_{in}} \tag{3.28}$$

$$\Psi_{i,solid} = \Psi_{i,in} - (\sum \Psi_{in} - \Delta N - \Delta A - DM_{solid}) \cdot \frac{\Psi_{i,in}}{\sum \Psi_{in}} \tag{3.29}$$

Here, η refers to the separation efficiency efficiency of the input to the solid fraction, Ψ is a substance and i refers to a specific substance. Δ is the difference between the input and solid fraction. Table 3.2 shows the separation to solid fraction efficiency of the de-watering units for dry matter, fixed carbon, volatile solids, potassium and phosphorus pentoxide, along with components of the ultimate chemical composition.

Table 3.2: *Separation efficiency (%) of input to the solid fraction of the de-watering outlet.*

	Decanter	Screw press
Mass	24.2	5.2
Moisture	21.1	3.2
Fixed carbon	69.2	35.3
Volatile solids	66.5	33.7
Carbon	69.2	35.3
Oxygen	69.2	35.3
Hydrogen	69.2	35.3
Nitrogen	21.2	6.8
Sulphur	69.2	35.3
Ash	26.3	4.7
Potassium	90.3	97.1
Phosphorus pentoxide	33.8	90.9

The electrical consumption of the decanter and screw press was gathered from data made available respectively by Frandsen [83] and Hamelin, Wesnæs and colleagues [84, 85]. The material consumption of all of the equipment is assumed to be the same, based on the estimation made by Wesnæs et al. [85]. The main trade-off between the decanter and

the screw-press as modelled are in the electricity consumption and the distribution of substances between liquid and solid outlets. From Table 3.2 it can be seen that although the mass, dry matter and carbon is more effectively separated to the solid fraction of the outlet when decanter is used, the macro-nutrients are more effectively separated to the liquid fraction of the outlet of the separation unit if screw-press is used. Both characteristics of the decanter and screw-press are desired as the solid fraction is generally assumed to be an energy resource and the liquid fraction a fertilizer resource.

After separation the solid fraction is modelled to enter either the thermal or biogas power plant, whereas the liquid fraction is used as af fertilizer. Thus it can be important how the distribution of energy is between the liquid and solid fractions at the outlet of the separation processes. Using Equation 3.32 and the mass and substance balance results from Table 3.2 the distribution of energy content was found as displayed in Table 3.3.

Table 3.3: *Distribution of energy between the solid and liquid fraction at the outlet of the separator units (%).*

	Decanter	Screw press
Liquid fraction	29.2	52.6
Solid fraction	70.8	36.3

It can be seen that the decanter units more effectively distribution the energy contents to the solid fraction for further use to generate heat and power. However, the distribution of energy is not the only factor affecting heat and power generation in downstream processes. The carbon to nitrogen (CN) ratio has an effect on the biogas production.

The cost of the separation techniques are given by the environmental protection agency [86, 87] and reported by Sommer et al. [88]. Accounting for the exchange rate of $ to *euro* and the current year index, the investment cost of the screw press is estimated to be 0.071 million $euro/tonne$ input and the annual capital cost is 0.010 million $euro/yr$ for each tonne processed. The operation and maintenance (O&M) cost for the screw press is 3.06 $euro/h$. For the decanter unit the investment cost is 0.148 million $euro/tonne - hour$ input, capital cost is 0.018 $euro/yr$ and the O&M is 6.79 $euro/h$ of each tonne processed.

3.3.2 Biogas Power Plant

The biogas power plant consists of biochemical conversion and a power generation unit. The biochemical conversion is done by anaerobic digestion producing biogas and digestate, and the power generation by a biogas engine which produces heat and power.

3.3.2.1 Biomass Conversion

The anaerobic digester biochemical conversion process can be either mesophilic or thermophilic. The mesophilic process is assumed to operate at 32 °C and the thermophilic process operates at 52 °C. The names of these processes refer to the type of micro-organisms used in the digester, as mesophiles and thermophiles grow best at moderate and warmer temperatures respectively. The biochemical conversion process model was modelled to choose between these two processes depending on the ratio between carbon and nitrogen of the input. As that ratio is the main indicator for the methane yield achieved by the digestion process of specific inputs. Wang et al. [89] devised a regression model for predicting the methane yield based on the carbon to nitrogen ratio of the input. Equations 3.30 and 3.31 displays the regression equations for methane yield (mL/g VS) based on C/N ratio of the input.

$$CH4_{meso} = -0.8475 \cdot \left(\frac{C}{N}\right)^2 + 45.36 \cdot \frac{C}{N} - 345.3 \tag{3.30}$$

$$CH4_{thermo} = -1.160 \cdot \left(\frac{C}{N}\right)^2 + 71.16 \cdot \frac{C}{N} - 781.4 \tag{3.31}$$

Using these equations it could be found that the maximum methane yield in a mesophilic processes is when inputs have around 26 CN ratio but about 32 CN ratio for a thermophilic process, resulting in about 260- and 310 mL/g volatile solids (VS) respectively. Moreover, it can be seen that the mesophilic process works better at CN ratios lower than 23, after which the thermophilic process has a superior yield. The biochemical conversion model takes advantage of that information and chooses the

mesophilic process if the CN ratio of the system is lower than 23, but chooses the thermophilic process if it is above that number. This regression model is based on experiments on dairy manure, poultry manure and rice straw [89]. Although the resources used in that research differ from the ones modelled, they were assumed to have similar characterization at the same CN ratio. However, the estimation given by the regression model was considered reasonable as similar methane yield could be modelled as has been found in other projects. Cuetos et al. [90] observed a methane yield of 260-340 mL/g VS when analysing the co-digestion productivity of swine manure and energy crop residues [90]. In a study by Zhang et al. [91], the methane yield of a mixture of co-digested chicken manure and wheat straw was found to range from 243-345 mL/g VS, depending on the manure to straw ratio, while Fischer et al. [92] experienced a yield of 220-240 mL/g VS when co-digesting swine manure and wheat straw [92], for relatively low CN ratios (10-14). Furthermore, Hamelin, Wesnæs and colleagues assumed a methane yield of 319 mL/g VS for pig manure flocculated with polymer and 187 mL/g for solid manure without polymer flocculation [79, 84, 85].

To close the carbon balance of the digester, the carbon dioxide produced also needed to be identified. In Fischer et al. [92] the carbon dioxide fraction of the biogas was found to be 38% for pig manure digestion and 42%,for pig manure and wheat straw co-digestion. Wu et al. found that the carbon dioxide fraction ranged from 32-53% of the biogas produced by co-digestion of swine manure and three types of crop residues [93], whereas the same fraction was found to range from 42-50% in a study by Risberg et al. [94]. Cuetos et al. found the carbon dioxide fraction to range from 28-37% in their study on co-digestion of swine manure and energy crop residues [90], while Hamelin, Wesnæs and colleagues assumed a fixed carbon dioxide ratio of 35% for pig manure flocculated with polymer and solid manure without polymer flocculation [79, 84, 85]. Based on this the carbon dioxide ratio was assumed to be 38% in this work.

The only emission assumed in the anaerobic digestion process was biogas loss to the atmosphere, which was assumed to be 1% of the biogas produced [79, 84, 85]. The biogenic GWP for the carbon dioxide emission from the digestion process was modelled in the same way as for the

carbon dioxide emissions from product gas combustion. The biochemical conversion process demands both heat and electricity, along with material for the infrastructure of the anaerobic digester. Heat requirement (supplied by the waste heat from the biogas engine) was calculated based on raising the temperature of the biomass in the mesophilic or thermophilic process. The electricity requirements, also supplied by the biogas engine, was assumed to be 5% of the gross energy production from the biogas engine [79]. Based on data from the Danish national energy agency [95], the specific investment cost (50 euro/tonne input) and operation and maintenance cost (5.68 euro/tonne input) of the anaerobic digester based on 1000 tonne daily input are estimated. The investment cost given in that report includes all physical equipment and infrastructure, i.e. the engineering, procurement and construction (EPC) price and the overnight cost. but the cost of land, pre-development costs and interest during construction are excluded. This results in 1.355 installation factor multiplied with the specific investment cost, giving the total investment cost.

3.3.2.2 Heat and Power Production

A biogas engine was modelled to represent the power generation of the biogas power plant. The biogas engine is modelled in DNA as a simple gas engine where the chamber gas is burned under perfect combustion and the electric and "cooling" efficiencies are predefined, along with pressure and heat loss. The air input is defined by the air to fuel ratio which is also prefixed as a default. The biogas composition is fixed at 62% methane and 38% which results in 40% and 52% electric and district heat efficiencies when combusted. It was assumed that there is a 5% heat loss and 2% pressure drop, and the lambda value is fixed to 2 and all the required electricity and heat internal demand are supplied by its own production.

The emissions for the gas engine were based on data from ecoinvent 3.3 for a biogas combustion in a gas engine. However, like in the anaerobic digester model and steam cycle model the carbon dioxide emissions were adjusted according to the biogenic GWP factor.

Resource use and infrastructure unit processes of the biogas engine was estimated based on a unit process from the ecoinvent database. The infrastructure and resource use was collected from the Heat and power co-generation, biogas, gas engine, in DK, unit process. However, to represent the system modelled in this project the upstream biogas unit process in the ecoinvent dataset was replaced with the biogas generated from the biochemical process above. In a report on technology data for energy plants [95], data from the Danish national energy agency gives the specific investment cost (1.4 million euro/MW electric) and operation and maintenance cost (17.2 Euro/MWh electricity) for a biogas engine. the cost excluded from the data is assumed to be the non-depreciable investment and the investment cost data from the Danish national energy agency is assumed to represent TDI. To account for this the installation factor was assumed to be 1.355.

3.3.2.3 Process Model Simulation

The biogas power plant process could then be simulated and optimized based on digestion of manure and co-digestion of straw and manure. Based on data from the simulation, production levels for heat, power and digestate could be found based on a specific capacity. Those information for each case could then be used to find the climate change impact, non-renewable resource requirements and economic feasibility of the biogas power plant in each system concept.

As the performance of the anaerobic digestion is based on the ratio of carbon to nitrogen of the inputs, the raw manure needs to be divided in two and one part needs de-watered by either decanter or screw press to raise the CN content. This process is simulated by varying the ratio of total manure that is diverted to the de-watering process. Another way to increase CN ratio is to mix a low CN ratio source with a high CN ratio source. This is done when co-digesting straw and manure. That process is simulated by varying the ratio of straw to the total input. Figures 3.9a and 3.9b show a schematic of the simulation process for manure digestion and co-digestion of straw and manure.

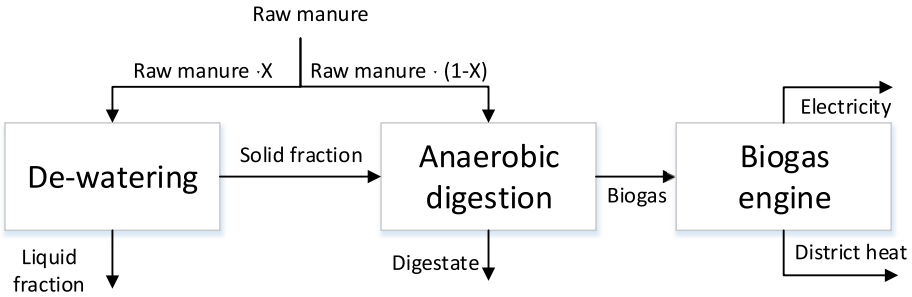

(a) Manure digestion

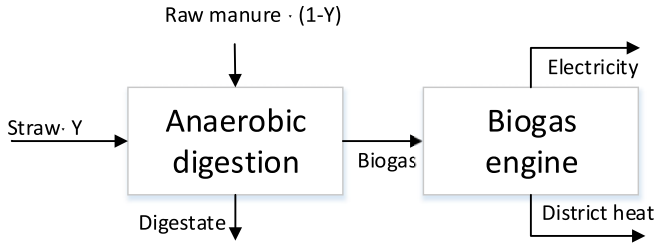

(b) Co-digestion

Figure 3.9: *A simple flow diagram showing the simulated manure digestion and straw co-digestion processes in the biogas power plant.*

Manure digestion The manure digestion process was simulated to find the optimum mixture of raw manure and solid fraction after de-watering with a decanter or a screw-press. The process was optimized for maximum heat and power production. Figures 3.10a and 3.10b show the energy efficiency of the biogas power plant when utilizing a mix of raw manure and solid fractions from decanter and screw-press de-watering, respectively. The efficiency is given as a function of raw manure directly to the digester and raw manure that enters the de-watering process from which the solid fractions are utilized. It can be seen when comparing the energy content of the raw manure that the energy efficiency of liquid manure production is much higher when de-watering using a screw press compared with a decanter. It can also be seen that the optimum mass to mass ratio in terms of heat and power production is at a mass ratio of 0.8, which means that about 80% of the total raw manure needs to be de-watered to maximize the performance of the biogas production based on the chemical composition of the raw manure and the separation efficiency of the de-watering process.

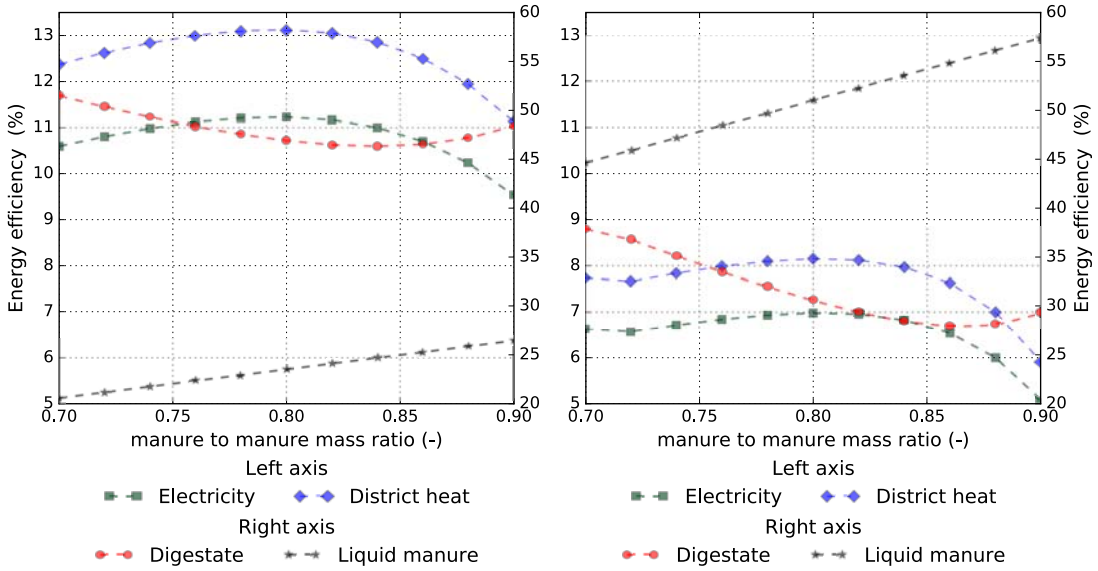

(a) Decanter **(b)** Screw press

Figure 3.10: *Energy efficiency of the biogas power plant when co-digesting raw manure and solid fraction from two de-watering process over a range of raw manure to digester and raw manure to de-watering ratio.*

Manure and straw co-digestion The manure and straw co-digestion was simulated to find the optimum ratio of straw to manure. Like in the manure digestion optimization, the co-digestion process was optimized for maximum heat and power production. Figure 3.11 gives the energy efficiency of the biogas power plant when co-digesting raw manure and straw as a function of straw to manure mass ratio. It can be seen that the biogas power plant heat and power production are optimized at mass ratio of 0.155. It can also be seen that there is plentiful energy available in the digestate output which could be further utilized in the thermal power plant.

The optimum straw ratio was used to find the total mass of straw and manure analysed in the four cases that have been defined. The reference case is when straw and manure are utilized separately and the capacity of the thermal power plant has been set to 100 MW fuel input. That requires an input of 218.2 thousand tonnes of straw yearly. This means that the daily mass input to co-digestion of 3.85 thousand tonnes which are assumed to be divided between 3 plants 1000 tonne/daily capacity plants and one 800 tonne/daily capacity plant. Similarly, the daily input

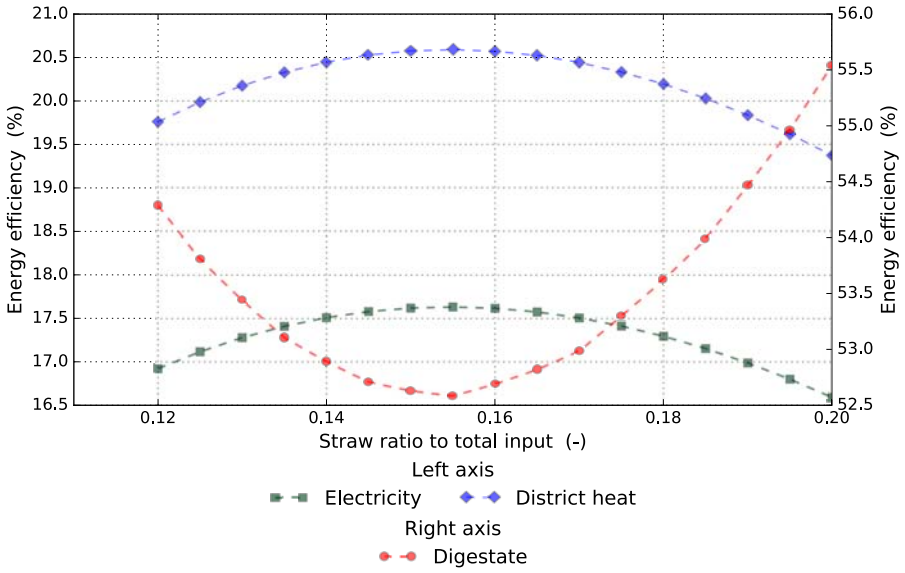

Figure 3.11: *Energy efficiency of the biogas power plant when co-digesting manure and straw as a function of straw to manure mass ratio.*

for the manure digestion was found to be 1.28 thousand tonnes divided between 2 plants 600 tonne/daily capacity plants. Table 3.4 summarizes the information needed for further analysis of this case in the results chapter.

Table 3.4: *Summary of the data found by simulation for further analysis of the biogas power plant based on manure digestion.*

	Manure digestion	Straw and manure co-digestion
Anaerobic digester		
Mass input (t/h)	53.4	160.7
Mass output (t/h)	50.5	147.4
Electricity demand (MW_e)	0.60	2.02
Heating demand (MW_{th})	0.45	2.79
Biogas engine		
Electricity (MW_e)	5.22	24.1
District heat (MW_{th})	6.84	31.6

3.3.3 Thermal Power Plant

The thermal power plant consists of pre-processing, thermochemical conversion, and heat and power generation. Within the pre-processing, the biomass handling (inc. storage, conveyors, feeding system, grinding) and steam drying were modelled. Thermochemical conversion is done by the Low Temperature - Circulating Fluidized Bed (LT-CFB) gasifier which produces product gas and biochar, and a steam cycle was modelled representing the heat and power generation

3.3.3.1 Pre-processing

The pre-processing process has three inputs (wet biomass, process heat and electricity) and three outputs (dry biomass, district heat and cooled condensate). The biomass handling part was modelled as electrical consumption per weight of inputs. But the thermodynamic process of steam drying was modelled mathematically.

The steam dryer operates between 120°C and 200 °C, where the moisture in the biomass is vaporized until a desired final moisture content is achieved at 115°C for the gasification process. The vapour is captured and condensed in a heat exchanger (HEX) connected to the district heating grid to provide extra heating. Heat required by the steam dryer is supplied by the flue-gas from product gas combustion for low heating demand, but for hight heating demand, steam was modelled to be extracted from the steam cycle in the power generation unit at 205°C to supply the remaining heat demand.

This process was modelled with the thermochemical conversion and power production process in DNA where mass and energy balances are conserved. Figure 3.12 displays the process flow diagram of the steam dryer including the main parameters of the process. The energy required to dry the input biomass is based on the sensible heat required to increase the temperature of the biomass to the predefined output temperature at the defined moisture content at inlet and the latent heat of vaporization of the amount evaporated which was defined by the moisture content at

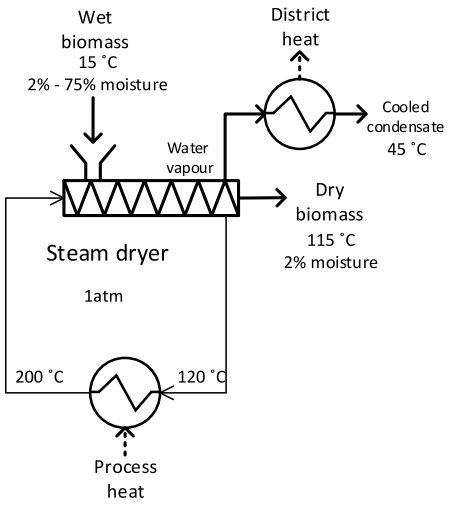

Figure 3.12: *Process flow diagram of the steam dryer.*

inlet and outlet of the dryer.

There are no emissions from the steam dryer, but the material consumption of the infrastructure was estimated by the drying of bread grain, seed and legumes LCI data from ecoinvent [58], but subtracting the heat and electricity demand as it is supplied by on-site processes. Dry biomass storage is estimated by the building hall, LCI data from ecoinvent [58] where the size is estimated to be 0.47 $m^2/tonne$ input, along with land occupation of 0.21 and 3.47 $m^2/kg-year$ for the construction and industrial area, transforming 1.39 $m^2/tonne$ from pasture to industrial area.

The steam dryer unit was assumed to have a total base cost of 9.91 million Euro (ave. 2016) per 33.5 tonnes biomass as received (base scale) where the scale factor is 0.8 and the overall installation factor is 2.0 [96]. As the heat and electricity demand are supplied internally by the power generation unit it serves as a factor in the net production of both heat and electricity. Additionally, the grinder and feeding system are assumed to cost 0.48 million euro per 33.5 tonnes/h of biomass as received each, but the scale factor is 0.56 for the grinder and 1.35 for the feeding system and the overall installation factor is assumed to be 2.0 [96].

3.3.3.2 Biomass Conversion

The LT-CFB gasifier [97, 98, 99] was modelled to represent the biomass thermochemical conversion process to product gas which subsequently is combusted in a steam cycle power plant. That gasifier was chosen as it was designed to be able to gasify biomass resources which contain low melting ash compounds in relatively high quantities [17]. This is achieved by keeping the process temperature below the melting point of the ash compounds, therefore allowing them to leave the process in solid form and hence resolving the problems of fouling and corrosion caused by sintered ash compounds [99]. As the ash can be extracted in solid form, it can be applied back to an agricultural field as a source of fertilizer [30, 29]. In addition, unconverted carbon is collected with the ash in a quantity established by the carbon conversion in the gasifier. The ash and unconverted carbon are together called biochar, which is the third product of the thermal power plant together with electricity and district heat.

The gasifier model calculates the product gas composition and energy content based on the conditions of the converted biomass at inlet and the operational specifications. The gasifier is split into a pyrolysis chamber, a char reactor and two cyclones. In the pyrolysis chamber the biomass is pyrolysed before most of the residual char and ash are separated from the pyrolysis gas with the primary cyclone. In the primary cyclone residual char and ash along with sand and directed to the char reactor where the char is gasified using air before it is circulated through the pyrolysis chamber providing fuel for the pyrolysis process. The char gas ultimately mixes with the pyrolysis gas to form the final product gas from which ash and unconverted carbon are cleaned out by the secondary cyclone before exiting the gasifier. Figure 3.13 displays the process flow diagram of the LT-CFB gasifier. It can be seen in the figure that the process produces two main products, i.e. product gas and biochar from two inputs (dry biomass and air). The process is operated at atmospheric pressure where the temperature inside of the pyrolysis chamber is assumed to be 630 °C and 730 °C in the char gasification chamber.

The gasifier is modelled in the Dynamic Network Analysis (DNA) software [73]. In DNA the composition and energy content were calculated

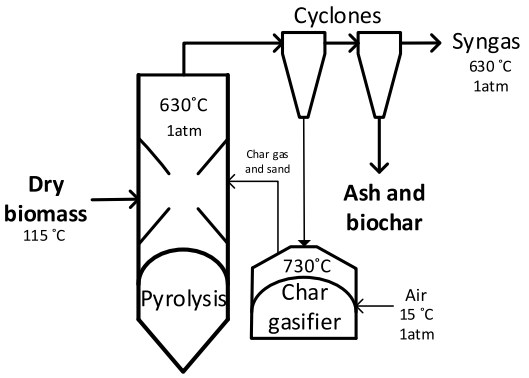

Figure 3.13: *Process flow diagram of the LT-CFB gasifier.*

for both the product gas and biochar based on the biomass inlet conditions and the operational definition. The inlet conditions depend on the operation of the steam dryer, along with the ultimate chemical composition, energy content and specific heat. For the Higher Heating Value (HHV) of a dry biomass the equation based on biomass ultimate chemical composition by Friedl et al. [100] was used.

$$HHV_{dry} = 341.7 \cdot C + 1322.1 \cdot H + 119.8 \cdot (O+N) - 123.2 \cdot S/10000 - 15.3 \cdot A \tag{3.32}$$

Here, C, H, O, N, S, A are the carbon, hydrogen, oxygen, nitrogen, sulphur and ash content of the biomass. The specific heat can be found based on an equation developed by Dupont et al. [101] as a result measurements on 21 different biomasses.

$$cp = (5.340 \cdot T(K) - 299)/1000 \tag{3.33}$$

To simulate the gasification process, Gibbs minimization was used to calculate the outlet gas composition at chemical equilibrium for the operation parameters defined for this conversion process. However, as the gas produced from the gasifier is a mix from biomass pyrolysis and char gasification processes the equilibrium assumption was used as a first estimate and the process was then calibrated based on experimental results and expected performance to get a realistic operation. According to Nielsen [102] and Stoholm [103] the hot gas efficiency (chemical energy of the dry product gas with sensible heat of the hot gas per energy input to the gasifier) is expected to be 95% for a large scale commercial solution. It should be noted that as the gas will be combusted the impurities like tar are included in the chemical energy.

To establish the hot gas efficiency the heat losses from the process were assumed to be 1.5% of the energy input (this was considered reasonable as the highest temperate inside the gasification process is relatively low). Additionally, the pyrolysis gas contains some out of equilibrium substances such as methane and tars as a result of the pyrolysis process. To account for this, Nielsen modelled the process by fixing the composition of methane and higher hydrocarbon (tars) at the outlet of the pyrolysis process which resulted in 1.8%vol on a wet basis and 10.1%vol on a dry basis combined for the final product gas. As the outlet of the steam dryer is expected to be relatively dry, the outlet composition of methane and tars were fixed based on the estimation by Nielsen on a dry basis. This results in a 95.1% hot gas efficiency based on cereal straw gasification and 94.3% based on pig manure utilization assuming maximum carbon conversion.

The unconverted carbon is established by the carbon conversion factor which represents the ratio of carbon in the biomass input that is converted to gas and thus the inverse of that factor defines the amount of unconverted carbon in the biochar co-product. Higher carbon conversion means more carbon in the product gas which ultimately results in more heat and power production, and more carbon in the biochar can ultimately result in more carbon sequestration. Figure 3.14 displays a simplified schematic of the main biomass thermochemical mechanisms of the LT-CFB gasifier.

In the figure, the thought process behind the idea of increased biochar production in the LT-CFB gasifier can be seen more clearly as the flow of substances between processes within the gasifier can be seen. The calculation of the amount and composition of the biochar can be understood by this equation.

$$\dot{m}_{biochar,out} = \dot{m}_{biomass,in} \cdot (\chi_{A,in} \cdot \eta_A + \chi_{C,in} \cdot (1 - CC)) \tag{3.34}$$

The amount of ash at input that is retained in the biochar output is described by the ash retention efficiency (η_A) which is assumed to be 95% [97, 104]. Carbon conversion (CC) in the gasifier is specially analysed in this project as this parameter controls the amount of carbon recycled back to the agricultural system. The practical CC range is considered

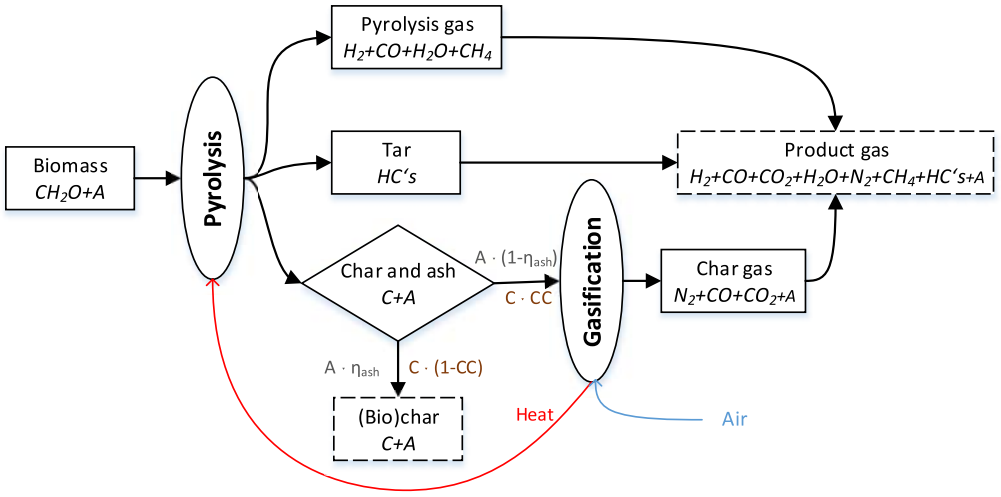

Figure 3.14: *Schematic of the main mechanisms of the LT-CFB gasification process.*

to be 98% CC for maximum energy generation and the lower limit represents maximum biochar production. The lower limit was estimated by finding the amount of fixed carbon in the biomass at inlet and accounting for the energy required to sustain the pyrolysis process, which is fuelled by the gasification of char. To make sure that enough energy in the char available for gasification, the Char Sufficiency Ratio (CSR) was calculated which describes the energy content in the char relative to the energy requirements in the pyrolysis reactor [105]. As different mixes of straw, manure and digestate are utilized by the process, the CSR was calculated for straw and manure by using generalized assumptions and the result was used to find a common benchmark for the lower limit of CC. According to the proximate chemical composition of straw [39] and manure [40] their fixed carbon contents are 15.4% and 1.5% of mass as received, respectively. Knowing that the heat of vaporization at 115C is 2.3 kJ/kg, and assuming that the energy required to heat dry matter and to achieve endothermic reaction is 800 kJ/kg [106], the energy required for straw pyrolysis was assumed to be 680.3 kJ/kg straw with 15% moisture content and 64.0 kJ/kg manure with 92.3% moisture content. By assuming that the higher heating value of fixed carbon is 35 MJ/kg, the energy available in the fixed carbon can then be estimated to be 5394.0 kJ/kg and 514.5 kJ/kg for straw and manure, respectively. Figure 3.15 displays the CSR as a function of CC in the gasifier based on utilization of straw and manure to find the lower limit for the CC factor.

As shown in the figure there is a dotted line drawn at CSR = 2, that

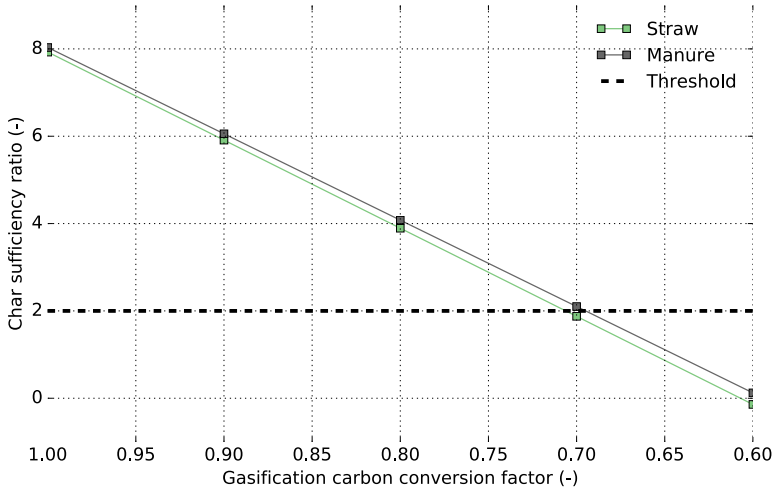

Figure 3.15: *Char sufficiency ratio as a function of carbon conversion based on LT-CFB gasification of straw and manure.*

number was assumed to be the threshold for CC lower limit for CSR as below 2 the energy content of the char available to gasify would be too close for realistic operation, also if CC is even lower then the energy of the syngas could be to low to utilize for heat and power production along with fuelling the steam dryer. This results in lower limit of CC = 0.7, representing the maximum biochar production operation mode.

It has been established that no emission occur from the gasifier. However, to complete the model all resources required by its production an operation were needed to be established. The only resources required for its operation are electricity, heat and bed material. Both electricity and heat are supplied by the thermal power plant's own production and the bed material is assumed to be 0.0126 kg silica sand per cubic metre product gas produced. This value was found by modifying the Life Cycle Inventory (LCI) information for a synthetic gas production, from wood, at a fluidized bed gasifier in the ecoinvent database [58], leaving out the wood, zeolite, dolomite, sodium hydroxide and sulphuric acid inputs, along with electricity as it is supplied by the on-site power production. By doing this the infrastructure production of a fluidized bed gasifier is included for life cycle perspective.

In a report on technology data for energy plants [95], data from the

Danish national energy agency gives the specific investment cost (0.40 million euro/MW fuel) and operation and maintenance cost (2.15 euro/MWh fuel) of the LT-CFB gasifier based on 100MW biomass input. The investment cost given in that report includes all physical equipment and infrastructure, i.e. the engineering, procurement and construction (EPC) price and the overnight cost. However, it excludes the cost of land, pre-development costs and interest during construction. The cost excluded from the data is assumed to be the non-depreciable investment and the investment cost data from the Danish national energy agency is assumed to represent TDI. To account for this the installation factor was assumed to be 1.355.

For the modelling of the energy and material requirements of the the infrastructure, along with the investment and O&M costs the change in size of the components when lowering CC needed to be estimated. Knowing the internal process of the LT-CFB gasifier the sizing estimation is that the pyrolysis part of the gasifier remains the same although the CC is changed and product gas production is decreased. However, the gasification part is changed as less char is gasified and less air is used and knowing that these two vessels are the largest part of the overall LT-CFB gasifier the average difference in the flow of biomass input (unchanged as carbon conversion is varied) and product gas output. As the data from ecoinvent is based on volume of product gas this factor is applied to account for less decrease in the consumption of materials by change in CC than if only the change in volume product gas produced would. The investment and O&M costs are baaed on fuel input which is constant with changed CC, then this factor accounts to increase the investment cost per fuel input by using assumptions for economy of scale.

3.3.3.3 Heat and Power Production

The amount of tar in the gas produced from the LT-CFB gasifier is too high, rendering it unsuitable for synthesis and combustion in a gas engine or a gas turbine without treatment [17], because of that the thermochemical conversion process is succeeded by a steam cycle power plant. The product gas from the gasifier is combusted using lambda value of 1.7 (ratio of actual air to fuel ratio to stoichiometric air to fuel ratio) and

the flue gas from the combustion fuels the steam cycle through a heat recovery steam generator (HRSG), it is also used to fuel the steam dryer (fully or partly) and supply the district heating grid if enough energy is still available. Figure 3.16 displays the process flow diagram of the steam cycle showing the main parameters of the model.

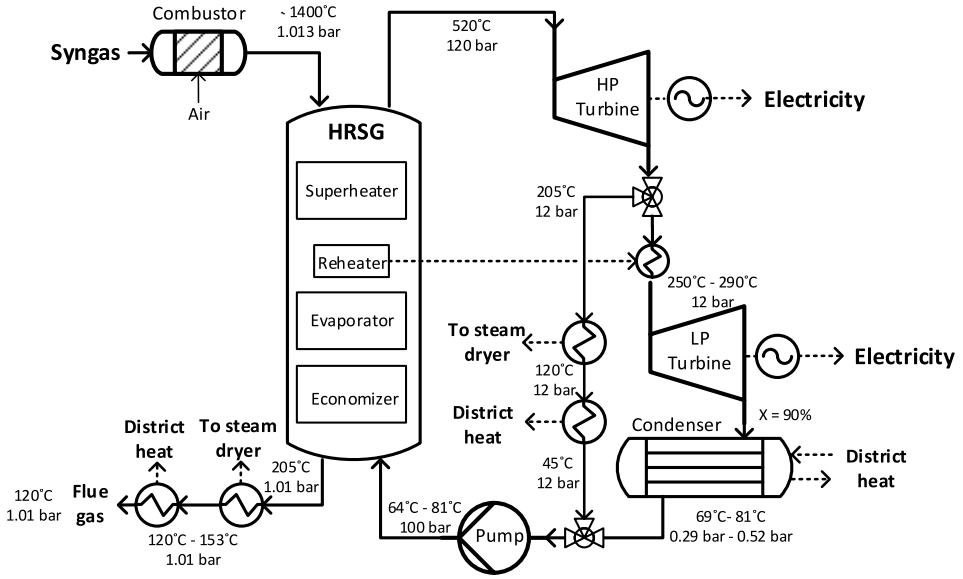

Figure 3.16: *Process flow diagram of the steam cycle power generation.*

It can be seen in the figure that the combustion temperature is about 1400 °C depending in the operation of the gasifier, as noted in Section 3.3.3.1 the temperature of the product gas and combustion air ranges respectively from 453°C - 485°C and 20°C - 36°C depending on the CC operation scenario. The live temperature and pressure in the steam cycle are 520 °C and 120 bar, respectively. These operation parameters are estimated in reference to a specific steam turbine from Siemens (SST-300) which has an output range of 10 MW - 50MW electric and can have controlled steam extraction and back pressure up to 72 bar [107]. Depending on the energy requirements of the steam dryer, steam is extracted at 205°C and 12 bar to help the flue gas fuel the drying process. The extracted steam is cooled to 120°C by the steam dryer return flow and then down to 45°C by the district heat return flow (supplying heat) before mixing again with the condensate before the feed pump. The temperature difference in the district heating system is 40 °C with maximum and minimum temperature set to 80 °C and 40 °C respectively.

It should also be noticed that the district heating units in the steam cycle and the steam dryer work together to provide heat at the temperatures required by the district heating grid, i.e. if a wet biomass is utilized the steam dryer could supply heat at about 115°C allowing the condensation temperature (back pressure) to decrease. The extracted steam going to the low pressure turbine is reheated to a temperature calculated by fixing the outlet steam quality to 90% and assuming a isentropic efficiency of 95%. Figure 3.17 shows the temperature-entropy property diagram of the steam cycle when the thermal power plant utilizes biomass with 70%, 50% and 30% dry matter content.

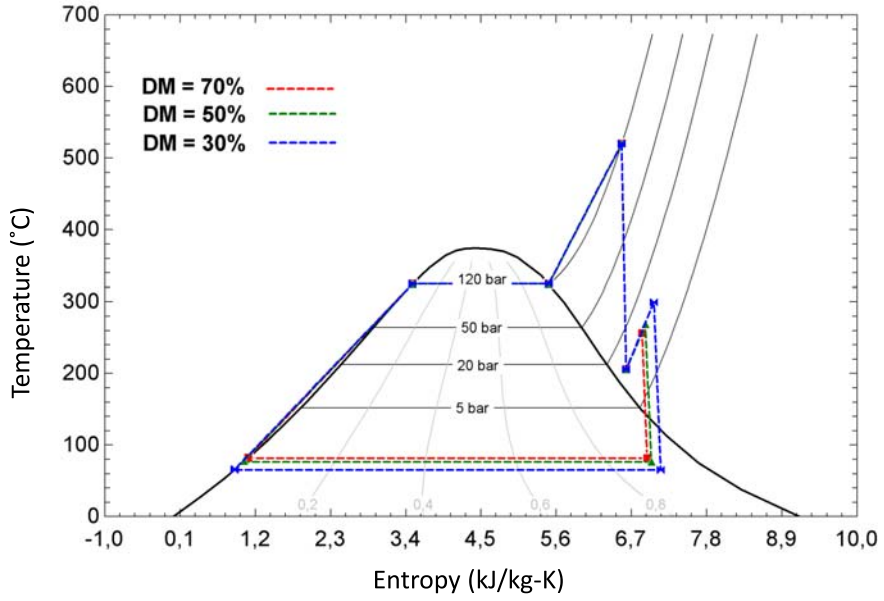

Figure 3.17: *Temperature-Entropy diagram of the steam cycle.*

It can be seen in the figure, that the condensation temperature decreases as the moisture content increases. This is a result of the calculated condensation temperature required for the district heating to have a forward temperature of 80°C as the other sources for district heating increase with decreased dry matter and they are supplied at 115°C.

The steam cycle is modelled in DNA like the steam dryer and gasifier but the emissions during combustion of the product gas are estimated using assumptions made by Nguyen et al. [16] based on combustion of product gas from wheat straw gasification. These emission factors per weight

of biomass input were applied in a computational model by normalizing based on electrical production to account for changes in emission as CC is changed as the electrical production is directly connect with the product gas product this was considered reasonable to account for decreased product gas production as CC is decreased.

In addition to this the biogenic GWP was calculated based on the carbon dioxide emissions from combustion by using Equation 3.8. The carbon emitted as carbon dioxide was found by the carbon content of the product gas minus the carbon emitted as methane and carbon monoxide. This is a pulse emission which represents E(t) of Equation 3.9. However, the regrowth part of that equation G(t) is found by using the total amount of carbon emitted, i.e. carbon dioxide, carbon monoxide and methane, as all of the carbon of the product gas is from the biomass input. To include all resources required to operate and produce the steam cycle power plant, the infrastructure material and energy consumption needed to be estimated. Like most coal power plants, the power plant is a steam-generated Rankine cycle. The ecoinvent unit process used That was done by using the LCI data for a hard coal power plant construction [58] as it is also a steam cycle power plant.

The steam cycle unit was assumed to have a base cost of 1.05 million euro (ave. 2016) per 10.3 MW electricity produced (base scale) where the scale factor is 0.7 and the overall installation factor is 2.0 [96]. The high and low pressure part of the turbine are calculated separately, each based on 5.83 million euro (ave. 2016) per 10.5 MW electricity produced as a base scale and including a scale factor of 0.7 and an installation factor of 2. The heat recovery steam generator is estimated to cost 9.45 million euro (ave. 2016) per 138.1 MW heat transferred including reheat with a scale factor of 0.6 and an installation factor of 2.0[96]. Additionally, the district heating heat exchangers were estimated to cost 4.5 million euro (ave. 2016) 50 MW heat transferred including reheat with a scale factor of 0.6 and an installation factor of 2.0[96].

3.3.3.4 Process Model Simulation

Based on the biogas power plant process model simulation and optimization the flow of resources to the thermal power plant could be found. The thermal power plant could then be simulated utilizing four different inputs and two modes of operation. Based on data from the simulation, production levels for heat, power and biochar could be found based on a specific capacity. Those information for each input could then be used to find the climate change impact, non-renewable resource requirements and economic feasibility of the thermal power plant for each system concept and each mode of operation.

Case 0 In the separate utilization case the cereal straw is gasified alone in the thermal power plant. Figures 3.18a and 3.18b display the process flow diagrams with flow sheets of simulations at maximum energy and maximum biochar operation, respectively.

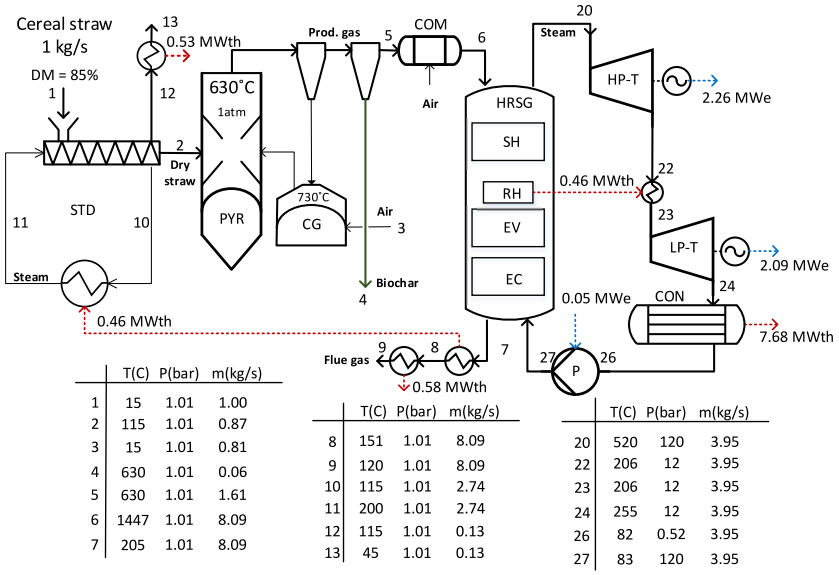

	T(C)	P(bar)	m(kg/s)
1	15	1.01	1.00
2	115	1.01	0.87
3	15	1.01	0.81
4	630	1.01	0.06
5	630	1.01	1.61
6	1447	1.01	8.09
7	205	1.01	8.09

	T(C)	P(bar)	m(kg/s)
8	151	1.01	8.09
9	120	1.01	8.09
10	115	1.01	2.74
11	200	1.01	2.74
12	115	1.01	0.13
13	45	1.01	0.13

	T(C)	P(bar)	m(kg/s)
20	520	120	3.95
22	206	12	3.95
23	206	12	3.95
24	255	12	3.95
26	82	0.52	3.95
27	83	120	3.95

(a) Maximum energy

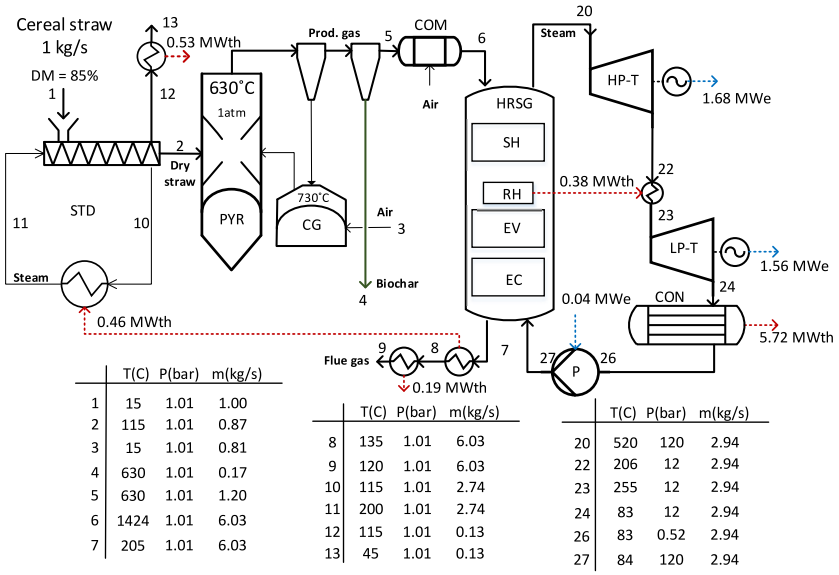

	T(C)	P(bar)	m(kg/s)
1	15	1.01	1.00
2	115	1.01	0.87
3	15	1.01	0.81
4	630	1.01	0.17
5	630	1.01	1.20
6	1424	1.01	6.03
7	205	1.01	6.03

	T(C)	P(bar)	m(kg/s)
8	135	1.01	6.03
9	120	1.01	6.03
10	115	1.01	2.74
11	200	1.01	2.74
12	115	1.01	0.13
13	45	1.01	0.13

	T(C)	P(bar)	m(kg/s)
20	520	120	2.94
22	206	12	2.94
23	255	12	2.94
24	83	12	2.94
26	83	0.52	2.94
27	84	120	2.94

(b) Maximum biochar

Figure 3.18: *Flow sheet of the thermal power plant model utilizing cereal straw in max energy and max biochar mode.*

Based on the chemical composition of straw and using Equation 3.32 the energy content was found to be 14.45 MJ/kg. The desired capacity of the straw fuelled thermal power plant is 100 MW fuel. Table 3.5 summarizes the information needed for further analysis of this case in the results chapter.

Table 3.5: *Summary of the data found by simulation for further analysis of the thermal power plant in Case 0.*

	Maximum energy	Maximum biochar
Pre-processing		
Mass input (t/h)	24.9	24.9
Mass output (t/h)	21.6	21.6
Electricity demand (MW_e)	1.74	1.74
Biomass conversion		
Energy input (MW)	100	100
Size adjustment (-)	1.00	0.866
Cold gas efficiency (%)	89.5	64.3
Biochar output (t/t-fuel)	0.117	0.388
Heat and power production		
Electricity (MW_e)	30.3	22.1
District heat - total (MW_{th})	62.0	45.1

Based on the chemical composition of the straw input and the ash retention efficiency the biochar contain 7.1 kg of phosphorus and 114.0 kg of potassium per tonne at maximum energy operation mode. Additionally, the carbon content of the biochar is 0.0 kg/tonne and 303.5 kg/tonne at maximum energy and maximum biochar operation modes, respectively.

Case 1 In case 1 cereal straw and solid fraction of digested manure are co-gasified in the thermal power plant. Figures 3.19a and 3.19b display the process flow diagrams with flow sheets of simulations at maximum energy and maximum biochar operation, respectively. Base on the flow from the biogas power plant and the efficiency of the de-watering process, the mixture was found to be 71% cereal straw and 29% solid digestate.

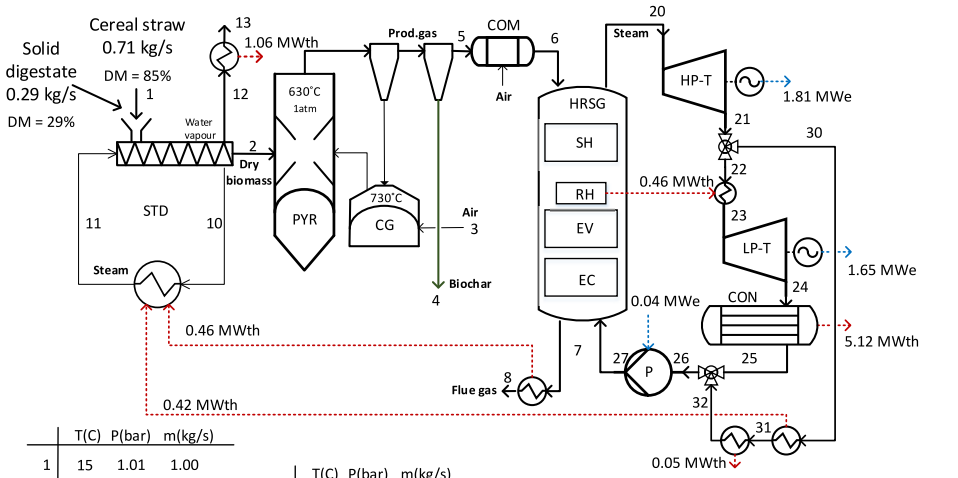

	T(C)	P(bar)	m(kg/s)
1	15	1.01	1.00
2	115	1.01	0.70
3	15	1.01	0.66
4	630	1.01	0.05
5	630	1.01	1.30
6	1439	1.01	6.54
7	205	1.01	6.54

	T(C)	P(bar)	m(kg/s)
8	120	1.01	6.54
10	115	1.01	5.23
11	200	1.01	5.23
12	115	1.01	0.30
13	45	1.01	0.30

	T(C)	P(bar)	m(kg/s)
20	520	120	3.17
21	206	12	3.17
22	206	12	3.05
23	259	12	3.05
24	81	0.49	3.05
25	81	0.49	3.05

	T(C)	P(bar)	m(kg/s)
26	79	12	3.17
27	80	12	3.17
30	206	12	0.12
31	120	12	0.12
32	45	12	0.12

(a) Maximum energy

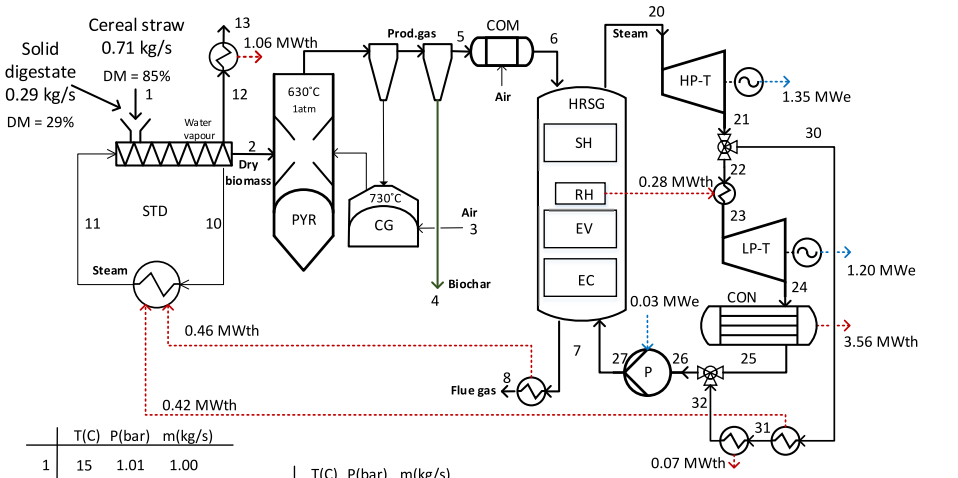

	T(C)	P(bar)	m(kg/s)
1	15	1.01	1.00
2	115	1.01	0.70
3	15	1.01	0.42
4	630	1.01	0.14
5	630	1.01	0.98
6	1416	1.01	4.91
7	205	1.01	4.91

	T(C)	P(bar)	m(kg/s)
8	120	1.01	4.91
10	115	1.01	5.23
11	200	1.01	5.23
12	115	1.01	0.30
13	45	1.01	0.30

	T(C)	P(bar)	m(kg/s)
20	520	120	2.36
21	206	12	2.36
22	206	12	2.18
23	262	12	2.18
24	79	0.49	2.18
25	79	0.49	2.18

	T(C)	P(bar)	m(kg/s)
26	77	12	2.36
27	78	12	2.36
30	206	12	0.18
31	120	12	0.18
32	45	12	0.18

(b) Maximum biochar

Figure 3.19: *Flow sheet of the thermal power plant model utilizing cereal straw and the solid fraction of the digestate from manure digestion in max energy and max biochar mode.*

Based on the chemical composition of the straw and solid digestate mixture and using Equation 3.32 the energy content was found to be 11.25 MJ/kg. However, the mass input increases by a factor of 1.49 resulting in 116 MW input to the thermal power plant. Table 3.6 summarizes the information needed for further analysis of this thermal power plant case.

Table 3.6: *Summary of the data found by simulation for further analysis of the thermal power plant in Case 1.*

	Maximum energy	Maximum biochar
Pre-processing		
Mass input (t/h)	37.1	37.1
Mass output (t/h)	25.0	25.0
Electricity demand (MW_e)	2.01	2.01
Biomass conversion		
Energy input (MW)	116	116
Size adjustment (-)	0.99	0.866
Cold gas efficiency (%)	89.4	64.4
Biochar output (t/t-fuel)	0.093	0.298
Heat and power production		
Electricity (MW_e)	34.3	24.8
District heat - total (MW_{th})	63.0	46.6

Based on the chemical composition of the mixture at input and the ash retention efficiency the biochar contain 24.4 kg of phosphorus and 82.7 kg of potassium per tonne at maximum energy operation mode. Additionally, the carbon content of the biochar is 0.0 and 299.2 kg/tonne at maximum energy and maximum biochar operation modes, respectively.

Case 2 In case 2 the solid fractions of the digestate from manure and straw co-digestion are utilized the thermal power plant. Figures 3.19a and 3.19b display the process flow diagrams with flow sheets of simulations at maximum energy and maximum biochar operation, respectively.

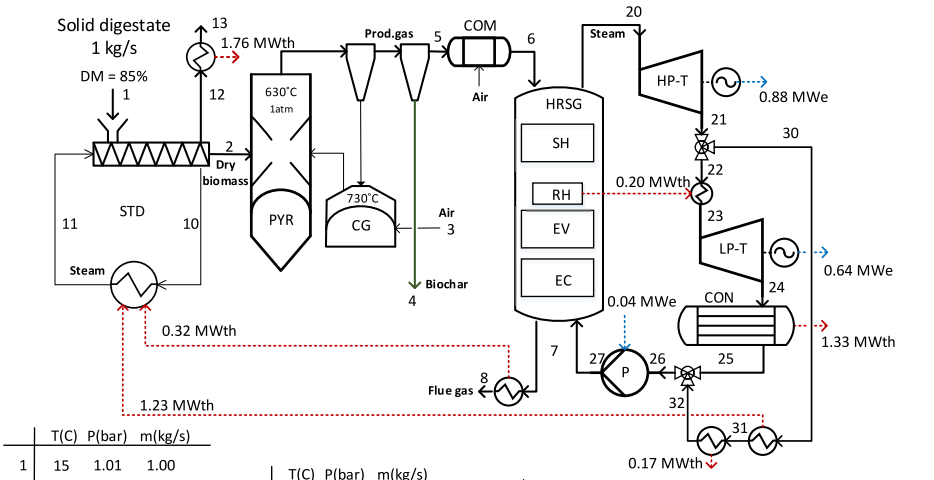

	T(C)	P(bar)	m(kg/s)
1	15	1.01	1.00
2	115	1.01	0.44
3	15	1.01	0.24
4	630	1.01	0.02
5	630	1.01	0.66
6	1383	1.01	3.32
7	205	1.01	3.32

	T(C)	P(bar)	m(kg/s)
8	120	1.01	3.32
10	115	1.01	9.15
11	200	1.01	9.15
12	115	1.01	0.56
13	45	1.01	0.56

	T(C)	P(bar)	m(kg/s)
20	520	120	1.54
21	206	12	1.54
22	206	12	1.01
23	290	12	1.01
24	69	0.29	1.01
25	69	0.29	1.01

	T(C)	P(bar)	m(kg/s)
26	60	12	1.54
27	61	12	1.54
30	206	12	0.53
31	120	12	0.53
32	45	12	0.53

(a) Maximum energy

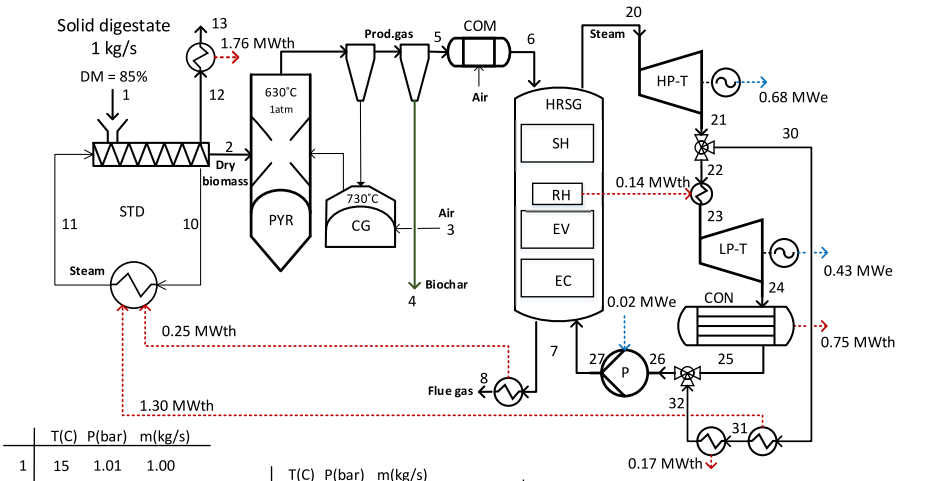

	T(C)	P(bar)	m(kg/s)
1	15	1.01	1.00
2	115	1.01	0.44
3	15	1.01	0.14
4	630	1.01	0.06
5	630	1.01	0.52
6	1383	1.01	2.59
7	205	1.01	2.59

	T(C)	P(bar)	m(kg/s)
8	120	1.01	2.59
10	115	1.01	9.15
11	200	1.01	9.15
12	115	1.01	0.56
13	45	1.01	0.56

	T(C)	P(bar)	m(kg/s)
20	520	120	1.19
21	206	12	1.19
22	206	12	0.63
23	290	12	0.24
24	64	0.29	0.24
25	64	0.29	0.24

	T(C)	P(bar)	m(kg/s)
26	55	12	1.19
27	56	12	1.19
30	206	12	0.52
31	120	12	0.52
32	45	12	0.52

(b) Maximum biochar

Figure 3.20: *Flow sheet of the thermal power plant model utilizing solid fraction of the digestate from straw and manure co-digestion in max energy and max biochar mode.*

Based on the chemical composition of the solid digestate at input and using Equation 3.32 the energy content was found to be 5.62 MJ/kg, However, the mass input increases by a factor of 1.43 in reference to the straw input in Case 0 resulting in 55.7 MW input to the thermal power plant. Table 3.7 summarizes the information needed for further analysis of this thermal power plant case.

Table 3.7: *Summary of the data found by simulation for further analysis of the thermal power plant in Case 2.*

	Maximum energy	Maximum biochar
Pre-processing		
Mass input (t/h)	35.6	35.6
Mass output (t/h)	14.9	14.9
Electricity demand (MW_e)	1.21	1.21
Biomass conversion		
Energy input (MW)	55.7	55.7
Size adjustment (-)	0.98	0.873
Cold gas efficiency (%)	87.4	65.7
Biochar output (t/t-fuel)	0.037	0.128
Heat and power production		
Electricity (MW_e)	14.3	10.1
District heat (MW_{th})	31.6	24.7

Based on the chemical composition of the solid digestate input and the ash retention efficiency the biochar contain 76.2 kg of phosphorus and 43.5 kg of potassium per tonne at maximum energy operation mode. Additionally, the carbon content of the biochar is 0.0 and 308.8 kg/tonne at maximum energy and maximum biochar operation modes, respectively.

Case 3 In case 3 cereal straw and solid fraction of manure are co-gasified in the thermal power plant. Figures 3.19a and 3.19b display the process flow diagrams with flow sheets of simulations at maximum energy and maximum biochar operation, respectively. Base on the flow from the biogas power plant and the efficiency of the de-watering the mixture was found to be 43.2% cereal straw and 56.8% solid digestate.

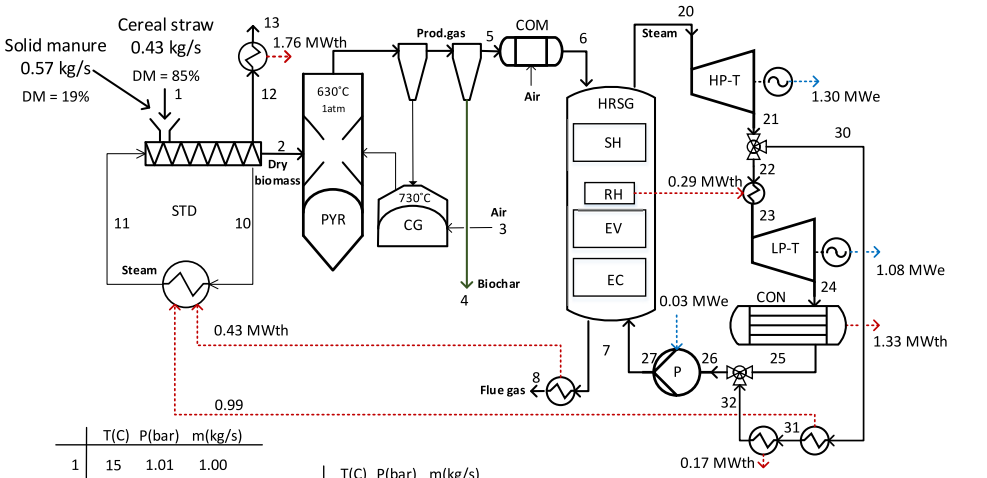

	T(C)	P(bar)	m(kg/s)
1	15	1.01	1.00
2	115	1.01	0.48
3	15	1.01	0.49
4	630	1.01	0.04
5	630	1.01	0.94
6	1448	1.01	4.75
7	205	1.01	4.75

	T(C)	P(bar)	m(kg/s)
8	120	1.01	4.75
10	115	1.01	8.43
11	200	1.01	8.43
12	115	1.01	0.52
13	45	1.01	0.52

	T(C)	P(bar)	m(kg/s)
20	520	120	2.27
21	206	12	2.27
22	206	12	1.84
23	274	12	1.84
24	75	0.38	1.84
25	75	0.38	1.84

	T(C)	P(bar)	m(kg/s)
26	69	12	2.27
27	69	12	2.27
30	206	12	0.43
31	120	12	0.43
32	45	12	0.43

(a) Maximum energy

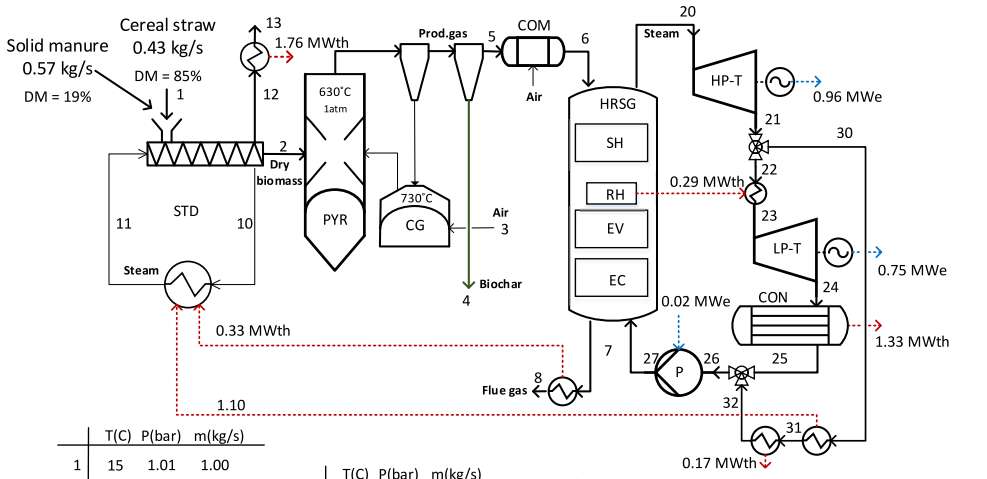

	T(C)	P(bar)	m(kg/s)
1	15	1.01	1.00
2	115	1.01	0.48
3	15	1.01	0.32
4	630	1.01	0.10
5	630	1.01	0.71
6	1426	1.01	3.56
7	205	1.01	3.56

	T(C)	P(bar)	m(kg/s)
8	120	1.01	3.56
10	115	1.01	8.43
11	200	1.01	8.43
12	115	1.01	0.52
13	45	1.01	0.52

	T(C)	P(bar)	m(kg/s)
20	520	120	1.69
21	206	12	1.69
22	206	12	1.22
23	274	12	1.22
24	71	0.33	1.22
25	71	0.33	1.22

	T(C)	P(bar)	m(kg/s)
26	64	12	1.69
27	64	12	1.69
30	206	12	0.47
31	120	12	0.47
32	45	12	0.47

(b) Maximum biochar

Figure 3.21: *Flow sheet of the thermal power plant model utilizing cereal straw and solid fraction of manure in max energy and max biochar mode.*

Based on the chemical composition of the straw and solid digestate mixture and using Equation 3.32 the energy content was found to be 8.52 MJ/kg. However, the mass input increases by a factor of 2.32 compared with the straw input in Case 0 resulting in 136.6 MW input to the thermal power plant. Table 3.8 summarizes the information needed for further analysis of this thermal power plant case.

Table 3.8: *Summary of the data found by simulation for further analysis of the thermal power plant in Case 3.*

	Maximum energy	Maximum biochar
Pre-processing		
Mass input (t/h)	57.7	57.7
Mass output (t/h)	28.0	28.0
Electricity demand (MW_e)	2.28	2.28
Biomass conversion		
Energy input (MW)	136.6	136.6
Size adjustment (-)	0.99	0.867
Cold gas efficiency (%)	89.1	64.5
Biochar output (t/t-fuel)	0.066	0.221
Heat and power production		
Electricity (MW_e)	38.4	27.1
District heat (MW_{th})	75.5	56.2

Based on the chemical composition of the straw input and the ash retention efficiency the biochar contain 28.5 kg of phosphorus and 81.2 kg of potassium per tonne at maximum energy operation mode. Additionally, the carbon content of the biochar is 0.0 and 305.9 kg/tonne at maximum energy and maximum biochar operation modes, respectively.

3.4 Agricultural System Process Models

In this section the methods used to model and simulate residual resource removal. Along with thee subsequent recycling of major elements from the removed resource after utilization. The agricultural system section is divided into three parts; carbon removal and recycling, nutrients removal and recycling, and field work and transportation.

3.4.1 Carbon Removal and Recycling

In order to find out if it is possible to mitigate soil carbon loss by recycling some of the carbon back from the bioenergy system when resources removed from the agricultural system have been utilized. The carbon build-up which otherwise would have been gained by repeated annual incorporation of the these resources to agricultural soil needed to be simulated over time. Carbon build-up can be calculated if the emission rate over time during decomposition of the incorporated resource is known. However, the emission rate is both resource and site specific. The modelled soil was made to represent sandy clayey soil (JB-6), which is the most common soil type in Zealand according the Danish soil classification [108] and with 70 tonne/hectare of carbon in the topsoil (0-30cm), based on the average carbon content in Denmark [109].

The carbon emission rate functions were found using C-TOOL. In reference to Figure 3.5, the general definition of soil organic matter 2 and soil organic matter 3 carbon pools in the software needs to be further elaborated for the development of the biochar emission rate function as described below. Carbon input to soil organic matter 2 is simulated to represent relatively slow decay and carbon input to soil organic matter 3 is simulated to be inert. There are two organic inputs pre-defined in C-TOOL, i.e. plant residues and manure, the plant residue definition was used to estimate the emission rate during decomposition of straw when left on the field, and manure was used to estimate the decay of carbon in raw manure, liquid manure and digested manure when applied as organic fertilizers. The plant residue carbon input was defined in C-TOOL to enter added organic matter 1 and 2 with a specific decay rate, though

about 20% of manure carbon inputs were defined to enter the soil organic matter 2 carbon pool [71, 74, 72] where it decays more slowly. But a new model was needed for the biochar decomposition.

The stability of carbon in biochar on an agricultural field was modelled to estimate the results found in a study done by Veronika et al. [33] based on biochar input to soil from straw gasifier with the same gasifier as used in this work. In that study only 1 - 3% of the biochar carbon was respired in the first few months after input to soil, while 41 - 78% of carbon input in straw was respired within the same time frame. Based on this information, a biochar organic input was created in C-TOOL, where 85% ($\alpha - ratio$) of carbon in biochar enters the soil organic matter 3 and considered inert, 100% ($\beta - ratio$) of the rest enters soil organic matter 3 carbon pool for slow decay. This can also be compared with the assumption made by Nguyen et al. [110], where 85% of carbon input with biochar is assumed to be stable in soil. Nguyen et al. refers to a study made by Laired et al. [111] where it is noted that only 17% of the carbon in biochar is mineralized. This can be further supported by referencing to Song and Guo [112] where 86.4% of carbon in biochar was found to be stable in soil after high temperature poultry litter pyrolysis. Figure 3.22 displays the emission rate and accumulation profiles for the simulation of straw and manure incorporation in soil after application in year 0, as well as that of biochar over 100-year time horizon.

The emission rate functions visualized in figure 3.22 represent the δ component in Equation 3.10 for each input. The difference between the emission rates for decaying biomass type is apparent when Figure 3.22 is analysed. It can be seen that the straw have the fastest emission rates, followed closely by manure. For these biomass types the majority of carbon is emitted within the first 30 years, but the highest emission rate is within the first three years. Biochar decay is very slow, as displayed in Figure 3.22, as its rate is almost continual from the first year to the last year of the time horizon.

The reverse of the accumulated emission profile can be viewed as a carbon sequestration profile, as carbon not emitted stays in the soil. If these resources are continually applied to an agricultural field, carbon soil content will increase. Figure 3.23 displays the carbon build-up potential for

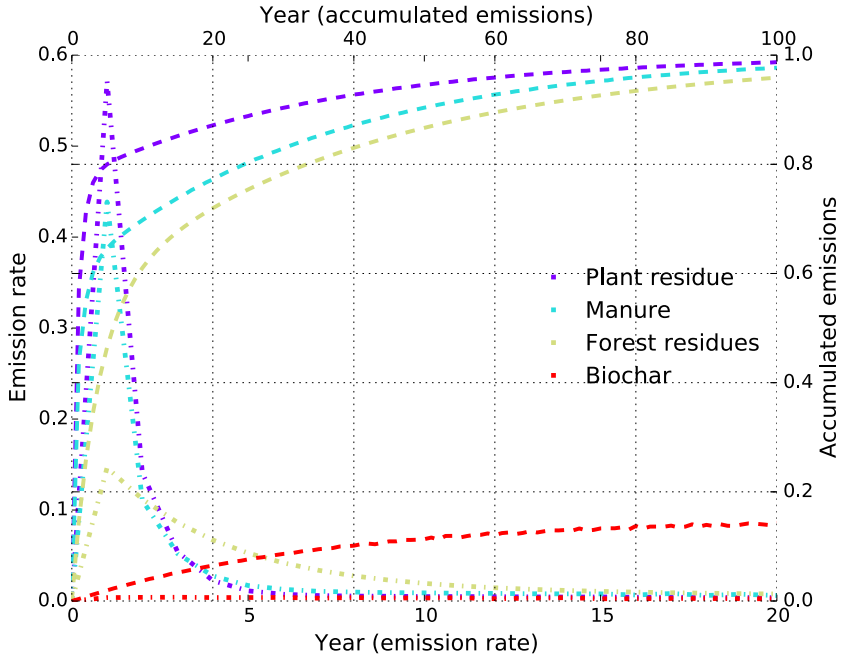

Figure 3.22: *Organic input accumulated emission profiles normalized to unit input.*

straw, manure and biochar repeated annual application to an agricultural field over a 100 year time horizon.

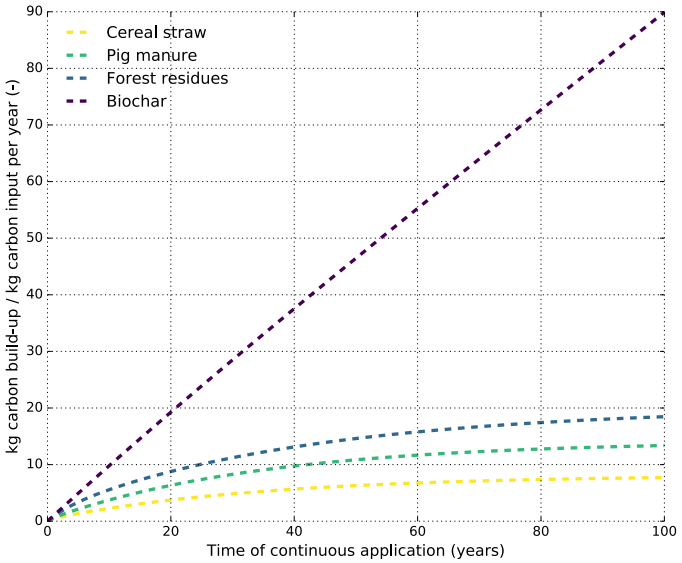

Figure 3.23: *Soil carbon build-up over time based on annual application of straw, manure, forest residue or biochar to the field.*

It can be seen that the biochar incorporation has the greatest potential for carbon build-up as 90 kg of carbon could be sequestered by applying 1 kg of carbon in biochar every year for 100 years. But only 8 kg if 1 kg of carbon in straw is applied. However, when answering the question if it is possible to mitigate soil carbon loss when removing a certain resource, i.e. straw or manure, from the agricultural system by recycling some of the carbon with biochar production, the amount of recycled carbon (in biochar and/or digestate) per straw or manure removed from agriculture is possible to produce while still generating energy needs to be found. The functions given visually in Figure 3.23 were used to answer research question I, along with the carbon flow to and from the bioenergy system.

However, although soil carbon build-up or loss can be simulated more information and other methods are needed to find the impact of carbon removal from agricultural system and subsequent recycling with biochar and/or digestate from the bioenergy system. To enable that, the biogenic GWP correction factor needed to be found for the resources modelled in this work. With the emission rate given for straw, manure and biochar in Figure 3.22, all components of the $E(t)$ function in Equation 3.10 had been found and the atmospheric carbon concentration as a result of emission during decomposition of biomass in soil could be estimated over time. Figure 3.24 display those results graphically over 0 - 100 years for each resource. It can be seen that the atmospheric concentration of carbon due to biochar decomposition is very low compared with the other. It can be also be seen that although about 98% and 97% of the carbon is emitted 100 years after application respectively for straw and manure, there is a difference in the atmospheric concentration between emission during decomposition in soil and a one pulse emission (represented by IRF) from e.g. combustion.

Using the atmospheric concentration function for a pulse emission F(t) and accounting for regrowth G(t) for the biogenic emission as represented in Figure 3.3. The biogenic GWP to be used with the IPCC GWP environmental impact method for each resource could then be found with Equation 3.8. Figure 3.25 displays the biogenic GWP of the resources over a range of reference years.

Usually when using IPCC GWP impact method the reference year 100 is

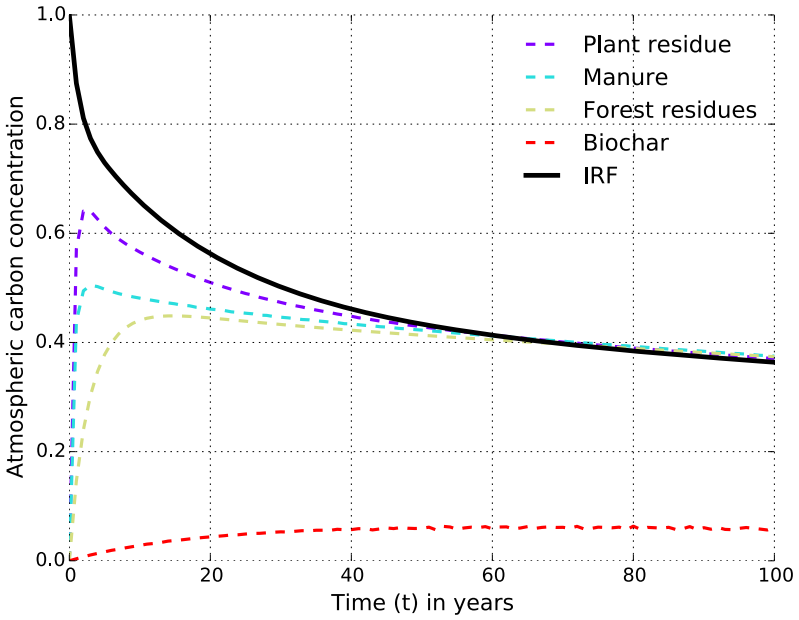

Figure 3.24: *Atmospheric carbon concentration $E(t)$ from biomass decay emissions, with the impulse response function (IRF) $y(t)$ as a reference.*

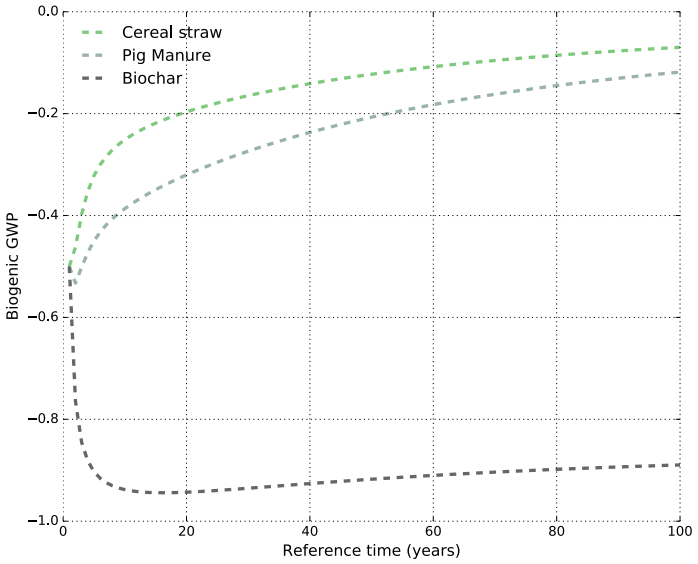

Figure 3.25: *Biogenic Global Warming Potential for the resources effecting the carbon balance of the agricultural system.*

used. Using 100 years as a reference the biogenic GWP for leaving cereal straw on the agricultural field was found to be -0.07, which means that

for every carbon in straw left on the field 7% of that carbon accounts to carbon sequestration. The carbon sequestration potential of applying pig manure on an agricultural field as an organic fertilizer was found to be 12% of every carbon input. Consequently, if those resources are removed from the agricultural system the impact will be loss of carbon sequestration (or soil carbon build-up). However, the biogenic GWP of biochar incorporation to agricultural field was found to be -0.89 as shown in Figure 3.25.

Moreover, for the biochar input to agricultural field, the stable carbon has an effect on the nitrogen balance model as it raises the C:N ratio of the overall inputs, this was assumed to increases immobilization of nitrogen. A large part of the carbon input is sequestered as noted above and the build-up of nitrogen follows the build-up of carbon in a 0.1:1 ratio [84, 85, 110, 16]. The increased immobilization is modelled to affect the distribution of surplus nitrogen between immobilization and mineralization causing less leaching, which also has an effect on indirect nitrogen emissions to air. Based on resource carbon flow from the agricultural system and carbon flow back to the agricultural system from the bioenergy system the impact from carbon removal and recycling could be found.

3.4.2 Nutrients removal and recycling

To be able to find the impact of resource removal and recycling in relation to nutrients, the nutrient value of resources needed to be found. This required the difference between the uptake of nutrients by the main product on the field (assumed to be cereal grain) if mineral fertilizers are used to supply the nutrients, to be compared with with nutrients supplied with organic resources like cereal straw, manure or biochar. Usually, the phosphorus and potassium nutrients value in straw and manure are assumed to be equivalent to mineral fertilizer and according to experiments by Müller-Stöwer et al. [29] and Kuligowski et al. [30], ash from LT-CFB gasification of wheat straw and slurry could replace mineral fertilizers. The impact of phosphorus and potassium removal could then be estimated to be equal to the impact of producing and adding the same quantity of phosphorus and potassium mineral fertilizers to the field. And thus the recycling impact depends on the efficiency of the bioenergy

system to recycle phosphorus and potassium and the avoided mineral fertilizer inputs.

However, the nitrogen value in straw or manure does not have the same value as nitrogen in mineral fertilizer. To account for that the grain nitrogen uptake from mineral fertilizers was calculated by this balance equations including both mineral fertilizer input and residual resource inputs not harvested with straw.

$$N_{grain} + N_{straw} = N_{mineral} - N_{emission} - N_{immobilized} \tag{3.35}$$

The methods used by Nemecek and Schnetzer [113] were used as a foundation to estimate the emissions for mineral nitrogen fertilizers by adding some missing emissions to it (closing the nitrogen balance) and the effect of uptake by residues not harvested, but left on the field. Nemecek and Schnetzer assume that 2% of the nitrogen input to be emitted as ammonia [114, 85], direct emission of diammonium monixide is assumed to be 1% of nitrogen inputs. Added to their method is that nitrogen gas is emitted in a 4.5:1 ratio to direct diammonium monoxide [85, 115]. Indirect diammonium monoxide emissions were then estimated to be 1% of nitrogen emitted as ammonia and 0.75% of the leached nitrogen. The SQCB-NO_3 model was used to estimate nitrogen leaching. It is a regression model developed by de Willigen [116], based on 43 different measurements.

$$NO_3 - N = 21.37 + (0.0037 \cdot \frac{\Gamma}{\Omega \cdot Z}) \cdot (\Theta - N_{upt}) \tag{3.36}$$

Here, Γ is the annual precipitation (mm), Ω is the clay content (%), Z is the crop rooting depth (m), Θ is the mineral nitrogen fertilizer and N_{upt} is the total nitrogen uptake by the crop ($\frac{kg-N}{ha}$). However, to solve this equation the nitrogen uptake by the crop was first estimated.

The nitrogen uptake by harvest is assumed to be 39.6% for cereal crops (grain and harvested straw), which was found by taking the average nitrogen wheat grain and barley uptake between JB-3 and JB-6 from Wesnæs and Wenzel [85] to estimate the uptake in JB-4 soil. Using then the production values of wheat and barley to estimate the uptake for cereal in general (as those are the most commonly produced cereals in Denmark). The consequence of removing straw was analysed by assuming that all available straw is harvested, which is about 55% of the grain (dry weight)

as assumed by Gyldenkærne et al. [117] and the ratio of nitrogen uptake by straw to grain is 0.29 and 0.37 for wheat and barley [118], respectively. The remaining surplus nitrogen is either taken up by the whole plant or immobilized in soil, where the uptake value is 69% [119] of the remaining 50%.

Having estimated the nitrogen uptake value of mineral fertilizer inputs along with the associated emissions the value of straw needed to be elaborated on. According to Nguyen et al. [110, 16] 70% of the nitrogen in straw is immobilized and 30% is mineralized when left on the field. From which the grain uptake value of the mineralized nitrogen was assumed to be 69% [120, 84, 85]. The mineralized nitrogen was assumed to be emitted according to the emission profile of mineral fertilizer as noted above.

For raw manure nitrogen inputs, the grain uptake value was assumed to be 25% lower than for the mineral fertilizer nitrogen input that is estimated in Danish legislation about manure management [121], whereas digested manure is assumed to have 11% greater grain uptake value then directly applied manure. Figure 3.26 displays the fate of the nitrogen input for each input source.

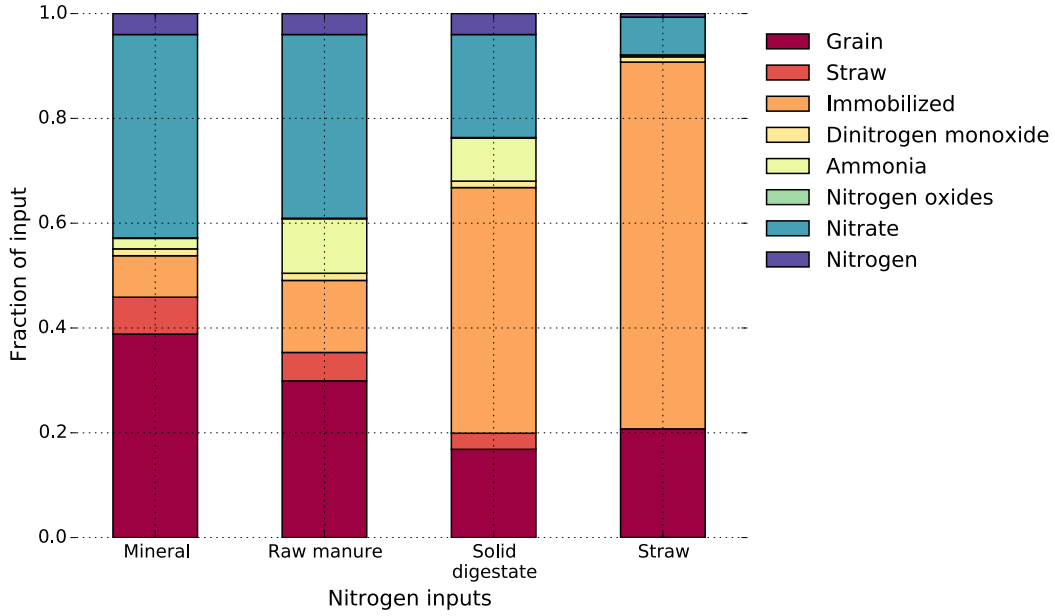

Figure 3.26: *Fate of nitrogen inputs to agriculture.*

The resulting fate of nitrogen inputs in the nitrogen balance model corresponds well with the calculated fate of nitrogen inputs by Hamelin, Wesnæs and colleagues [79, 84, 85] for mineral fertilizer, manure and solid digestate inputs. The fate of nitrogen in incorporated straw is in agreement with the calculated fate of nitrogen in straw by Nguyen et al. [110, 16], except that the crop uptake value of the mineralized nitrogen is adjusted according to Petersen et al [120].

As shown in Figure 3.26, the agronomic fertilizer value of the different inputs is varied: this can be observed by the fraction of the input that is taken up by the grain. Mineral fertilizer has the highest fertilizer value, fallowed by raw manure, straw and solid digestate. However, the agronomic value of liquid manure and liquid digestate is found in both the mineral fertilizer and raw manure, because the C:N ratio in liquid manure and liquid digestate is usually less than that in raw manure [84, 85]. The proportion of liquid manure and liquid digestate was modelled as mineral or raw manure depends on the difference between their C:N ratio and the C:N ratio of raw manure.

As noted in Section 3.1.3 the fuel costs was based on the price of straw, manure and by accounting for the revenues of organic fertilizer and biochar sales, along with the cost of transportation (see Section 3.4.3). The report "Analysis of biomass prices, future Danish prices for straw, wood chips and wood pellets" by Ea Energy Analyses for the Danish Energy Agency provides data for current and projected fuel prices [122] while the technical report on the cost of producing electricity in Denmark reports historic prices to 1984 [123, 124]. Figure 3.27 displays the historic, current and future projection of straw prices in Denmark, including transportation costs. As seen in Figure 3.27, the price of straw is assumed to be steadily increasing again after a few years of relatively low prices. However, as shown by the historic prices there have been sharp fluctuations in the pricing of straw between 1984 and 2011.

The price of manure was calculated by the assumed cost of utilization in the energy system instead of the agricultural system, along with transportation costs. The cost of utilization in the energy system depends on the price of fertilizers used instead of the manure. However, these costs and the cost of straw are partly mitigated by the value of the co-products

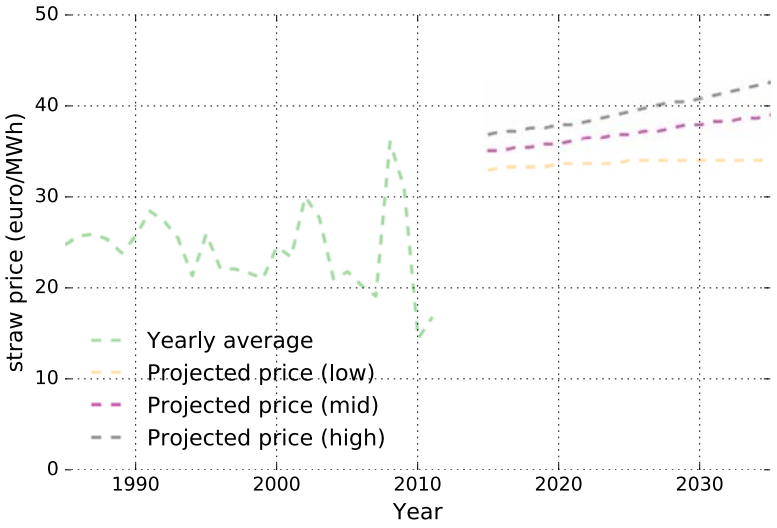

Figure 3.27: *Current and projected straw prices in Denmark.*

of the energy system, i.e. ash, biochar and digestate. The price of the fertilizers was estimated based on Import/Export data from the United Nations Statistics Database (also used by the ecoinvent database) [58].

The same report that was used to find the current and projected straw prices provides cost of emissions, where current and projected carbon pricing scenarios are given. These scenarios can be seen in Figure 3.28. Those pricing scenarios were used to estimate the benefits of sequestered carbon with biochar on an agricultural field, which determines the value of the carbon in biochar.

3.4.3 Field Work and Transportation

The agricultural system also includes machinery operation on the field associated with collecting, processing the resources before transportation to the energy system, along with incorporating of these residual resources and the residues from the energy system to agricultural soils. The life cycle inventory database ecoinvent 3.3 [58] was used to gather the upstream processes and emissions associated with the production of the mineral fertilizers used in the system, along with all mechanical field work required, as noted in Section 3.2.

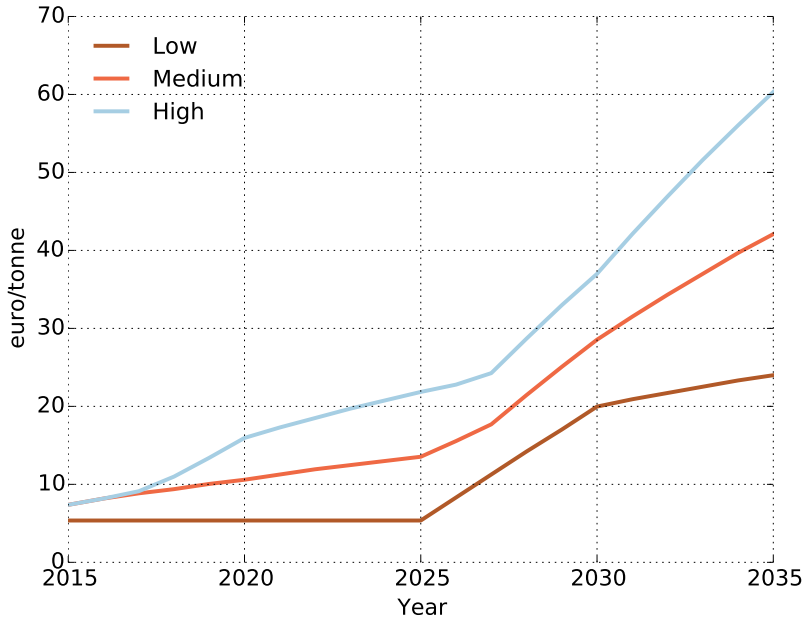

Figure 3.28: *Current and projected future cost of carbon in Denmark.*

Field work is different for organic fertilizers than for mineral fertilizers. Mineral fertilizers are assumed to be spread on the field by a broadcaster. The ecoinvent unit process 'fertilising, by broadcaster' was used to get all upstream impacts of that process. The unit for that unit process in ecoinvent is given by hectares of fertilizer. This process was thus normalized to the weight of mineral fertilizers used on the field for a reference agricultural system. The weight of the avoided mineral fertilizers could then be used to account for the decreased work required by the broadcaster. Baling and loading of bales when straw is harvested was accounted for. The ecoinvent baling unit process assumes round bales of 1.4 m3 for a silage bale with wrapping foil, weighing 700 kg. The loading ecoinvent process used assumes that straw bales are loaded with a bale gripper onto a trailer. The units used by these processes are units of bales and loading units, where 4.35 bales are loaded per unit, those units were normalized to kg of straw. The mechanical work of drilling down the straw when it is left on the field was estimated by the ecoinvent unit process 'tillage, harrowing by rotary harrow', where the unit of hectare is normalized to kg of straw, based on straw generated by a reference system per hectare. Application of raw manure, liquid manure and liquid digestate was assumed to be spread using a vacuum tank with 5000 l carrying capacity, where

the unit is cubic metre of product spread. Application of solid manure, solid digestate and biochar to the agricultural field was assumed to be by hydraulic loader (power take-off driven); its unit in ecoinvent database is kg applied to the field. Nitrogen, phosphorus and potassium mineral fertilizer unit processes are estimated by the market for nitrogen fertilizer, market for phosphate fertiliser and market for potassium fertiliser respectively. The units of these fertilizer inputs is defined by ecoinvent as kg nitrogen, kg phosphorus pentoxide (P_2O_5) and kg potassium oxide (K_2O) applied.

The transportation process involves transport of straw and manure-sourced resources from the agricultural system to the energy system. The ecoinvent 3.1 database [58] was used to gather the LCI data on the assumed vehicle. All resources were assumed to be transported in a truck larger than 32 tonnes with the EURO-5 emission technology standard [58]. Transportation cost was assumed to be 0.08 Euro/tonnes-km [125].

References

[4] F. Cherubini et al. “Energy-and greenhouse gas-based LCA of biofuel and bioenergy systems: Key issues, ranges and recommendations”. In: *Resources, conservation and recycling* 53.8 (2009), pp. 434–447.

[16] T. L. T. Nguyen, J. E. Hermansen, and R. G. Nielsen. “Environmental assessment of gasification technology for biomass conversion to energy in comparison with other alternatives: the case of wheat straw”. In: *Journal of Cleaner Production* 53.0 (2013), pp. 138 –148. DOI: http://dx.doi.org/10.1016/j.jclepro.2013.04.004.

[17] J. Ahrenfeldt et al. “Biomass gasification cogeneration – A review of state of the art technology and near future perspectives”. In: *Applied Thermal Engineering* 50.2 (2013), pp. 1407 –1417. DOI: http://dx.doi.org/10.1016/j.applthermaleng.2011.12.040.

[29] D. Muller-Stover et al. “Soil application of ash produced by low-temperature fluidized bed gasification: effects on soil nutrient dynamics and crop response”. English. In: *Nutrient Cycling in Agroecosystems* 94.2-3 (2012), pp. 193–207. DOI: 10.1007/s10705-012-9533-x.

[30] K. Kuligowski et al. “Plant-availability to barley of phosphorus in ash from thermally treated animal manure in comparison to other manure based materials and commercial fertilizer”. In: *European Journal of Agronomy* 33.4 (2010), pp. 293 –303. DOI: http://dx.doi.org/10.1016/j.eja.2010.08.003.

[33] V. Hansen et al. “Gasification biochar as a valuable by-product for carbon sequestration and soil amendment”. In: *Biomass and Bioenergy* 72 (2015), pp. 300 –308. DOI: http://dx.doi.org/10.1016/j.biombioe.2014.10.013.

[39] S. V. Vassilev et al. “An overview of the chemical composition of biomass”. In: *Fuel* 89 (2010), pp. 913–933.

[40] E. research Centre of the Netherlands. *Phyllis2, database for biomass and waste,*

[41] I. B. Huang, J. Keisler, and I. Linkov. "Multi-criteria decision analysis in environmental sciences: ten years of applications and trends". In: *Science of the total environment* 409.19 (2011), pp. 3578–3594.

[42] M. Behzadian et al. "A state-of the-art survey of TOPSIS applications". In: *Expert Systems with Applications* 39.17 (Dec. 2012), pp. 13051–13069. DOI: 10.1016/j.eswa.2012.05.056.

[43] C.-L. Hwang and K. Yoon. *Multiple attribute decision making: methods and applications a state-of-the-art survey*. Vol. 186. Springer Science & Business Media, 2012.

[44] G Myhre et al. "Anthropogenic and Natural Radiative Forcing. In: Climate Change 2013: The Physical Science Basis. Contribution of Working Group 1 to the Fifth Assessment Report of the Intergovernmental Panel on Climate Change". In: *Table* 8 (2013), p. 714.

[45] H. Michael et al. *Recommendations for Life Cycle Impact Assessment in the European context - based on existing environmental impact assessment models and factors (International Reference Life Cycle Data System - ILCD handbook)*. ENG. Oct. 2010. DOI: 10.2788/33030.

[46] M. Z. Hauschild et al. "Identifying best existing practice for characterization modeling in life cycle impact assessment". In: *The International Journal of Life Cycle Assessment* 18.3 (Sept. 2012), pp. 683–697. DOI: 10.1007/s11367-012-0489-5.

[47] F. Cherubini et al. "CO2 emissions from biomass combustion for bioenergy: atmospheric decay and contribution to global warming". In: *GCB Bioenergy* 3.5 (Oct. 2011), pp. 413–426. DOI: 10.1111/j.1757-1707.2011.01102.x.

[48] F. Cherubini, A. H. Stromman, and E. Hertwich. "Effects of boreal forest management practices on the climate impact of CO2 emissions from bioenergy". In: *Ecological Modelling* 223.1 (Dec. 2011), pp. 59–66. DOI: 10.1016/j.ecolmodel.2011.06.021.

[49] F. Cherubini, G. Guest, and A. H. Stromman. "Application of probability distributions to the modeling of biogenic CO 2 fluxes in life cycle assessment". In: *GCB Bioenergy* 4.6 (Nov. 2012), pp. 784–798. DOI: 10.1111/j.1757-1707.2011.01156.x.

[50] G. Guest, F. Cherubini, and A. H. Stromman. "Global Warming Potential of Carbon Dioxide Emissions from Biomass Stored in the Anthroposphere and Used for Bioenergy at End of Life". In: *Journal of Industrial Ecology* 17.1 (Feb. 2013), pp. 20–30. DOI: 10.1111/j.1530-9290.2012.00507.x.

[51] G. Guest, F. Cherubini, and A. H. Stromman. "The role of forest residues in the accounting for the global warming potential of bioenergy". In: *GCB Bioenergy* 5.4 (July 2013), pp. 459–466. DOI: 10.1111/gcbb.12014.

[52] B. M. Petersen et al. "An approach to include soil carbon changes in life cycle assessments". In: *Journal of Cleaner Production* 52.0 (2013), pp. 217 –224. DOI: http://dx.doi.org/10.1016/j.jclepro.2013.03.007.

[53] U Siegenthaler and H Oeschger. "Predicting Future Atmospheric Carbon-Dioxide Levels". In: *Science* 199.4327 (1978), pp. 388 – 395.

[54] F. Joos et al. "An efficient and accurate representation of complex oceanic and biospheric models of anthropogenic carbon uptake". In: *Tellus B* 48.3 (July 1996), pp. 397–417. DOI: 10.1034/j.1600-0889.1996.t01-2-00006.x.

[55] F. Joos et al. "Global warming feedbacks on terrestrial carbon uptake under the Intergovernmental Panel on Climate Change (IPCC) Emission Scenarios". In: *Global Biogeochemical Cycles* 15.4 (Dec. 2001), pp. 891–907. DOI: 10.1029/2000GB001375.

[56] S. K. Swallow, P. J. Parks, and D. N. Wear. "Policy-relevant nonconvexities in the production of multiple forest benefits". In: *Journal of Environmental Economics and Management* 19.3 (Nov. 1990), pp. 264–280. DOI: 10.1016/0095-0696(90)90073-8.

[57] S. Rossi et al. "Growth and productivity of black spruce in even- and uneven-aged stands at the limit of the closed boreal forest". In: *Forest Ecology and Management* 258.9 (Oct. 2009), pp. 2153–2161. DOI: 10.1016/j.foreco.2009.08.023.

[58] B. Weidema et al. *The ecoinvent database: Overview and methodology, Data quality guideline for the database version 3.* 2013.

[59] E. Font de Mora, C. Torres, and A. Valero. "Assessment of biodiesel energy sustainability using the exergy return on investment concept". In: *Energy* 45.1 (Sept. 2012), pp. 474–480. DOI: 10.1016/j.energy.2012.02.072.

[60] C. J. Cleveland et al. "Energy and the u.s. Economy: a biophysical perspective." en. In: *Science (New York, N.Y.)* 225.4665 (Aug. 1984), pp. 890–7. DOI: 10.1126/science.225.4665.890.

[61] M. U.C.f. E. Cleveland C.J. (Boston Univ., E. Studies), and U. I. U. Herendeen R. (Illinois Natural History Survey. "Solar parabolic collectors; Successive generations are better net energy and exergy producers". English. In: *Energy Systems and Policy; (USA)* 13:1 (Jan. 1989).

[62] *Thermal Design and Optimization*. John Wiley & Sons, 1996, p. 542.

[63] J. Szargut, D. Morris, and F. Steward. "Exergy analysis of thermal, chemical, and metallurgical processes". English. In: (Jan. 1987).

[64] M.-A. Lozano, A. Valero, and L. Serra. "Theory of exergetic cost and thermoeconomic optimization". In: *Proceedings of the International Symposium ENSEC'93*. 1993.

[65] "The value of the exergetic life cycle assessment besides the LCA". In: *Energy Conversion and Management* 43.9-12 (June 2002), pp. 1417–1424. DOI: 10.1016/S0196-8904(02)00025-0.

[66] J. Dewulf et al. "Cumulative Exergy Extraction from the Natural Environment (CEENE): a comprehensive Life Cycle Impact Assessment method for resource accounting". In: *Environmental Science & Technology* 41.24 (Dec. 2007), pp. 8477–8483. DOI: 10.1021/es0711415.

[67] M. E. Bösch et al. "Applying cumulative exergy demand (CExD) indicators to the ecoinvent database". In: *The International Journal of Life Cycle Assessment* 12.3 (Nov. 2006), pp. 181–190. DOI: 10.1065/lca2006.11.282.

[68] I. H. Bell et al. “Pure and Pseudo-pure Fluid Thermophysical Property Evaluation and the Open-Source Thermophysical Property Library CoolProp”. In: *Industrial & Engineering Chemistry Research* 53.6 (2014), pp. 2498–2508. DOI: 10.1021/ie4033999. eprint: http://pubs.acs.org/doi/pdf/10.1021/ie4033999.

[69] E. F. de Mora, C. Torres, and A. Valero. “Thermoeconomic Analysis of Biodiesel Production from Used Cooking Oils”. In: *Sustainability* 7.5 (2015), pp. 6321–6335.

[70] B. M. Petersen, J. E. Olesen, and T. Heidmann. “A flexible tool for simulation of soil carbon turnover”. In: *Ecological Modelling* 151.1 (2002), pp. 1 –14. DOI: http://dx.doi.org/10.1016/S0304-3800(02)00034-0.

[71] B. M. Petersen. *C-TOOL version 1.1 a Tool for Simulation of Soil Carbon Turnover : Description and users guide*. Tech. rep. Danish Institute of Agricultural Sciences: Department of Agroecology, 2003.

[72] B. M. Petersen et al. “CN-SIM: a model for the turnover of soil organic matter. II. Short-term carbon and nitrogen development”. In: *Soil Biology and Biochemistry* 37.2 (Feb. 2005), pp. 375–393. DOI: 10.1016/j.soilbio.2004.08.007.

[73] B. Elmegaard, N. Houbak, et al. “DNA - a general energy system simulation tool”. In: *Proceedings of SIMS*. Citeseer. 2005, pp. 1–10.

[74] B. M. Petersen et al. “CN-SIM- a model for the turnover of soil organic matter. I. Long-term carbon and radiocarbon development”. In: *Soil Biology and Biochemistry* 37.2 (2005), pp. 359 –374. DOI: http://dx.doi.org/10.1016/j.soilbio.2004.08.006.

[75] B. M. Petersen and J. Berntsen. *Ther turnover of soil organic matter on different farm types*. DARCOFenews. 2003.

[76] A. Taghizadeh-Toosi et al. “C-TOOL: A simple model for simulating whole-profile carbon storage in temperate agricultural soils”. In: *Ecological Modelling* 292 (Nov. 2014), pp. 11–25. DOI: 10.1016/j.ecolmodel.2014.08.016.

[77] C. Mutel. *Brightway2 life cycle assessment framework*. 2015.

[78] S. Eggleston, L. Buendia, and K. Miwa. *2006 IPCC guidelines for national greenhouse gas inventories [recurso electrónico]: industrial processes and product use.* Kanagawa, JP: Institute for Global Environmental Strategies, 2006.

[79] L. Hamelin et al. "Environmental Consequences of Future Biogas Technologies Based on Separated Slurry". In: *Environmental Science & Technology* 45.13 (2011). PMID: 21671646, pp. 5869–5877. DOI: 10.1021/es200273j. eprint: http://dx.doi.org/10.1021/es200273j.

[80] T. Nemecek et al. "Life cycle inventories of agricultural production systems". In: *Data v2. 0, Ecoinvent report* 15 (2007).

[81] K. Pellervo et al. *Economics of manure logistics, separation and land application.* 2013.

[82] M. Hjorth et al. "Solid–liquid separation of animal slurry in theory and practice. A review". In: *Agronomy for sustainable development* 30.1 (2010), pp. 153–180.

[83] T. Q. Frandsen. *Separering af svinegylle med GEA Westfalia UCD 305.* Tech. rep. Aarhus: Dansk Landbrugsrådgivning, Landscentret, 2009.

[84] L. Hamelin et al. *Life cycle assessment of biogas from separated slurry.* Tech. rep. Danish Ministry of the Environment/Danish Environmental Protection Agency, 2010.

[85] M. Wesnæs, H. Wenzel, and B. M. Petersen. *Life cycle assessment of slurry management technologies.* Miljøstyrelsen, 2009.

[86] Environmental Protection Agency. *Separering af gylle med dekantercentrifuge (Separation of Slurry using Decanter Centrifuge).* Tech. rep. Copenhagen: The Environmental Protection Agency, 2010.

[87] Environmental Protection Agency. *Separering af gylle med skruepresse (Separation of Slurry using Screw Press).* Tech. rep. Copenhagen: The Environmental Protection Agency, 2010.

[88] S. Sommer et al. "Pig slurry characteristics, nutrient balance and biogas production as affected by separation and acidification". In: *The Journal of Agricultural Science* 153.01 (2015), pp. 177–191.

[89] X. Wang et al. "Effects of temperature and carbon-nitrogen (C/N) ratio on the performance of anaerobic co-digestion of dairy manure, chicken manure and rice straw: focusing on ammonia inhibition." In: *PloS one* 9.5 (Jan. 2014), e97265. DOI: 10.1371/journal.pone.0097265.

[90] M. J. Cuetos et al. "Anaerobic co-digestion of swine manure with energy crop residues". In: *Biotechnology and Bioprocess Engineering* 16.5 (Sept. 2011), pp. 1044–1052. DOI: 10.1007/s12257-011-0117-4.

[91] T. Zhang et al. "Improved Biogas Production from Chicken Manure Anaerobic Digestion Using Cereal Residues as Co-substrates". In: *Energy & Fuels* 28.4 (Apr. 2014), pp. 2490–2495. DOI: 10.1021/ef500262m.

[92] J. R. Fischer, E. Iannotti, C. Fulhage, et al. "Production of methane gas from combinations of wheat straw and swine manure." In: *Transactions of the ASAE (American Society of Agricultural Engineers)* 26.2 (1983), pp. 546–548.

[93] X. Wu et al. "Biogas and CH(4) productivity by co-digesting swine manure with three crop residues as an external carbon source." In: *Bioresource technology* 101.11 (June 2010), pp. 4042–7. DOI: 10.1016/j.biortech.2010.01.052.

[94] K. Risberg et al. "Biogas production from wheat straw and manure–impact of pretreatment and process operating parameters." In: *Bioresource technology* 149 (Dec. 2013), pp. 232–7. DOI: 10.1016/j.biortech.2013.09.054.

[95] *Technology data for energy plants - Generation of Electricity and District Heating, Energy Storage and Energy Carrier Generation and Conversion.* Tech. rep. The Danish Energy Agency and Energinet.dk.

[96] C. N. Hamelinck et al. "Production of {FT} transportation fuels from biomass; technical options, process analysis and optimisation, and development potential". In: *Energy* 29.11 (2004), pp. 1743 –1771. DOI: http://dx.doi.org/10.1016/j.energy.2004.01.002.

[97] P. Stoholm et al. “The Low temperature CFB gasifier: Latest 50 kW test results and new 500 kW test plant”. In: *Proceedings of The 16t. International Conference of Efficiency, Cost, Optimization, Simulation, and Environmental Impact of Energy Systems, ECOS 2003*. Technical University of Denmark, 2003, pp. 1113–1120.

[98] P. Stoholm et al. “The Low Temperature CFB Gasifier - Further Test Results and Possible Applications”. In: *Proceedings of the 12. European Biomass Conference*. ETA-Florence & WIP-Munich, 2002, pp. 706–709.

[99] R. Nielsen et al. “Optimering af Lav Temperatur Cirkulerende Fluid Bed forgasningsprocessen til biomasse med højt askeindhold”. PhD thesis. 2007.

[100] A. Friedl et al. “Prediction of heating values of biomass fuel from elemental composition”. In: *Analytica Chimica Acta* 544.1-2 (July 2005), pp. 191–198. DOI: 10.1016/j.aca.2005.01.041.

[101] C. Dupont et al. “Heat capacity measurements of various biomass types and pyrolysis residues”. In: *Fuel* 115 (Jan. 2014), pp. 644–651. DOI: 10.1016/j.fuel.2013.07.086.

[102] R. G. Nielsen. “Optimering af Lav Temperatur Cirkulerende Fluid Bed forgasningsprocessen til biomasse med højt askeindhold”. PhD thesis. PhD Thesis, DTU Mechanical Engineering, Technical University of Denmark, Denmark, 2007.

[103] R. G. Nielsen et al. “The LT-CFB gasifier: First test results from the 500 kW test plant”. In: *14th European Biomass Conference*. 2005.

[104] P. Stoholm et al. “The low temperature CFB gasifier—100 kWth tests on straw and new 6 MWth demonstration plant”. In: *Proceedings of the European biomass conference, Lyon*. 2010.

[105] T. P. Thomsen et al. “Screening of various low-grade biomass materials for low temperature gasification: Method development and application”. In: *biomass and bioenergy* 79 (2015), pp. 128–144.

[106] H.-S. Ding and H. Jiang. “Self-heating co-pyrolysis of excessive activated sludge with waste biomass: Energy balance and sludge reduction”. In: *Bioresource Technology* 133 (2013), pp. 16 –22. DOI: http://dx.doi.org/10.1016/j.biortech.2013.01.090.

[107] *Industrial Steam Turbines: A Full Range of World-class Industrial Steam Turbines.* Tech. rep. Erlangen, Germany: Siemens AG, 2013.

[108] H. B. Madsen, A. H. Nørr, and K. A. Holst. *Atlas of Denmark, Series 1, Volume 3: The Danish soil classification.* Ed. by N. K. Jakobsen. Copenhagen: The Royal Danish Geographical Society, 1992.

[109] K. Adhikari et al. "Digital mapping of soil organic carbon contents and stocks in Denmark". In: *PloS one* 9.8 (2014), e105519.

[110] T. L. T. Nguyen, J. E. Hermansen, and L. Mogensen. "Environmental performance of crop residues as an energy source for electricity production: The case of wheat straw in Denmark". In: *Applied Energy* 104.0 (2013), pp. 633 –641. DOI: http://dx.doi.org/10.1016/j.apenergy.2012.11.057.

[111] D. A. Laird et al. "Review of the pyrolysis platform for coproducing bio-oil and biochar". In: *Biofuels, Bioproducts and Biorefining* 3.5 (Sept. 2009), pp. 547–562. DOI: 10.1002/bbb.169.

[112] W. Song and M. Guo. "Quality variations of poultry litter biochar generated at different pyrolysis temperatures". In: *Journal of Analytical and Applied Pyrolysis* 94 (Mar. 2012), pp. 138–145. DOI: 10.1016/j.jaap.2011.11.018.

[113] T. Nemecek and J. Schnetzer. "Methods of assessment of direct field emissions for LCIs of agricultural production systems". In: *Agroscope Reckenholz-TlniNRn Research Station ART* (2011).

[114] W. A. Asman. *Ammonia emission in Europe: updated emission and emission variations.* National Institute of Public Health and Environmental Protection Bilthoven, the Netherlands, 1992.

[115] F. P. Vinther and S. Hansen. *SimDen - en simpel model til kvantificering af N2O-emission og denitrifikation.* May 2004.

[116] P. d. Willigen. "An analysis of the calculation of leaching and denitrification losses as practised in the NUTMON approach." In: *Rapport-Plant Research International* 18 (2000).

[117] S. Gyldenkærne et al. *Konsekvenser og muligheder ved Danmarks deltagelse i Kyoto-protokollens artikel 3.4 på landbrugsområdet.* Arbejdsrapport fra Miljøstyrelsen. Miljøstyrelsen, 2011.

[118] J Møller et al. “Sammensætning og foderværdi af fodermidler til kvæg”. In: *Møller, J* 112 (2005).

[119] J Petersen et al. *Beregning af nitratudvaskning: Forslag til metode, der sikrer ensartethed i sagsbehandlingen i forbindelse med fremtidig miljøgodkendelse af husdyrbrugsudvidelser*. Tech. rep. Danmarks JordbrugsForskning; Danm arks Miljøundersøgelser; Danm arks og Grønlands Geologiske Undersøgelse, 2006.

[120] J. Petersen and P. Sørensen. “Fertilizer value of nitrogen in animal manures - basis for determination of a legal substitution rate.” Danish. In: (2008).

[121] Gødskningsbekendtgørelsen. *Plantedirektoratets bekendtgørelse nr. 786 af 22. juli 2008 om jordbrugets anvendelse af gødning og om plantedække i planperioden 2008/2009*. 2008.

[122] C. Bang et al. *Analysis of biomass prices - Future Danish prices for straw, wood chips and wood pellets*. Tech. rep. Ea Energy Analyses, 2013.

[123] C. J. Levitt and A. Sørensen. *The Cost of Producing Electricity in Denmark*. Tech. rep. Rockwool Fondens Forskningsenhed, 2014.

[124] C. J. Levitt and A. Sørensen. *The Cost of Producing Electricity in Denmark: A Technical Companion*. Tech. rep. Rockwool Fondens Forskningsenhed, 2014.

[125] L Bína et al. “Comparative model of unit costs of road and rail freight transport for selected European countries”. In: *European Journal of Business and Social Sciences* 3.4 (2014), pp. 127–136.

Chapter 4

Results

This chapter contains the results of this thesis. It is divided into three main section. The first deals with the results of bioenergy systems simulation, including both energy and exergy analysis. Then the results of the agricultural system are given, including the resource removal and recycling analysis, along with the soil carbon simulation. Finally the overall results of each system concept are presented in terms of climate change impact, non-renewable resource requirements and economic feasibility.

4.1 Bioenergy System

In this section the results related to the bioenergy system are given for all system concepts by applying the analytical framework from section 3.1 on the simulation data from Section 3.3. The section is divided into energy analysis and environmental impact, and exergy analysis and resource utilization.

4.1.1 Energy Analysis and Environmental Impact

Figures 4.1a - 4.1d display the energy efficiency of electricity, district heat and fertilizer production for the bioenergy system concepts introduced in Section 2.2 as a function of carbon conversion in the gasifier. It can be seen in the graphs, that combined utilization of straw and ma-

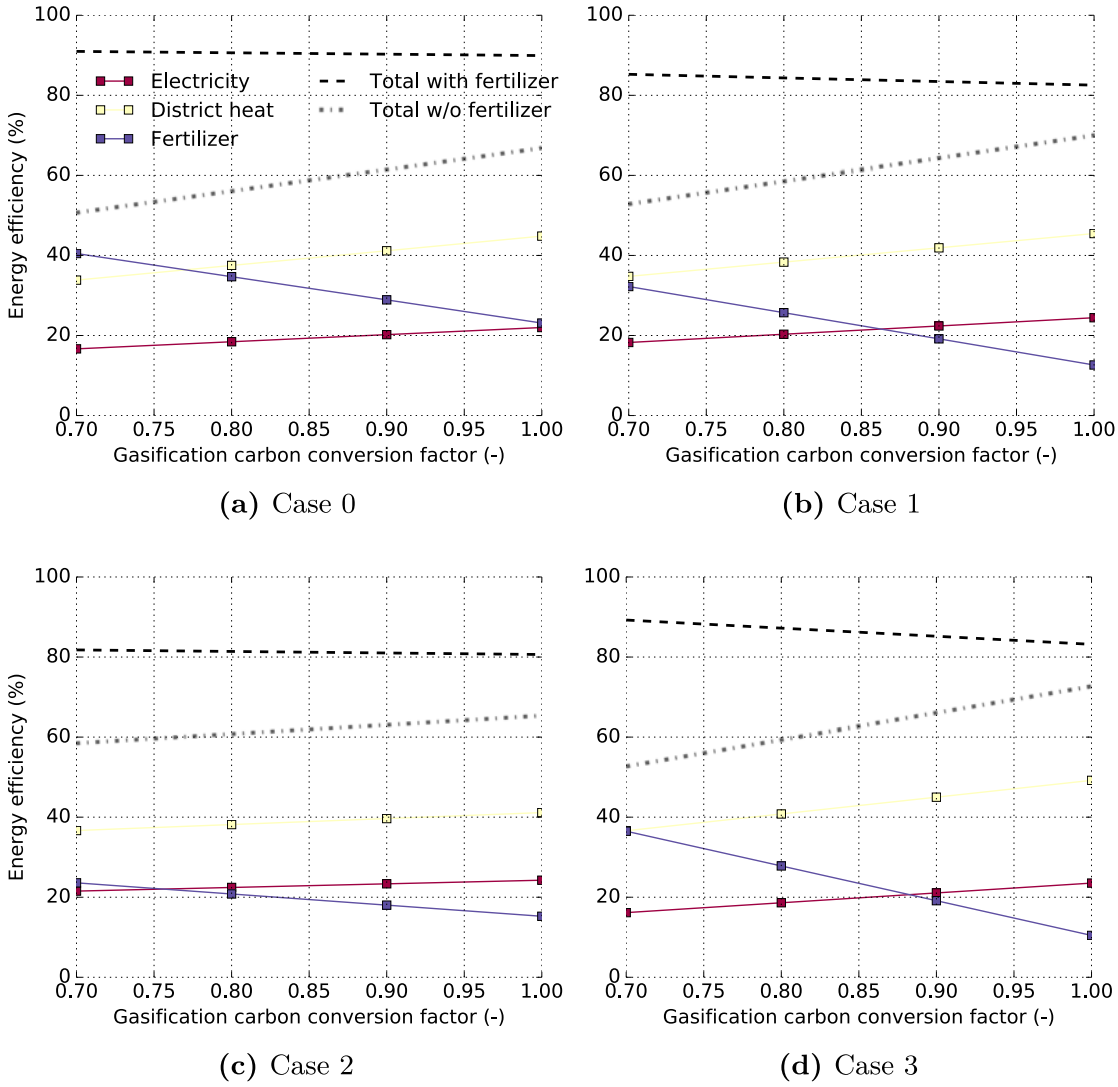

(a) Case 0 **(b)** Case 1

(c) Case 2 **(d)** Case 3

Figure 4.1: *Energy efficiency of the system concepts over as a function of carbon conversion in the gasifier.*

nure (Cases 1-3) results in more efficient heat and power production than separate utilization (Case 0). System integration Case 1 has the highest

electrical efficiency (24.4%) and Case 3 the highest district heat efficiency (49.2%). The highest energy efficiency in all cases is found when carbon conversion is maximized, but efficiencies linearly decrease with decreased carbon conversion and increased biochar production. Maximum carbon conversion operation is referred to as *maximum energy mode* and operation at minimum carbon conversion is referred to as *maximum biochar mode*. Looking at the results of bioenergy system simulation at maximum energy mode the potential increase in produced electricity when combining utilization of straw and manure is 11.1% (Case 1), and 9.7% increase in district heat production (Case 3), compared with separate utilization (Case 0). Maximum increase in fuel utilization is 8.8% (Case 3).

In Figures 4.1a - 4.1d, the energy efficiency of the fertilizer production is also shown. With more biochar production its energy efficiency increases. However, although it is desired to recycle the nutrients and some of the carbon according to the overall concept, most of the energy should be extracted in the bioenergy system and higher energy content of the fertilizer production is considered a side effect of increased biochar production. It was found that for every kg of carbon that is unconverted and recycled with biochar, the decrease in energy content of the syngas is 31 MJ, which results in about 10.5 MJ and 17.7 MJ decrease in electrical and district heat production in the thermal power plant, respectively.

The difference in heat and power production between the system concepts can have a significant impact on the environmental impact of the overall system. As other heat and power production is assumed to be avoided as a consequence of that production (see Section 3.1.1). Table 4.1 shows the avoided climate change impact estimated as a result of substituted production fuelled with coal, natural gas or biomass (wood chips). Additionally, two scenarios representing Denmark with the marginal electricity production avoided and either natural gas (Denmark (high)) or biomass (Denmark (low)) fuelled district heating is avoided.

Table 4.1: *Avoided climate change impact (kg-CO_2/tonne biomass utilized) as a result of heat and power production from the analysed system concepts.*

	Case 0	Case 1	Case 2	Case 3
Coal				
Maximum energy	-304.4	-330.2	-320.3	-328.0
Maximum biochar	-230.4	-248.1	-284.6	-230.4
Natural gas				
Maximum energy	-147.2	-159.7	-154.9	-158.6
Maximum biochar	-111.4	-120.0	-137.6	-111.4
Biomass				
Maximum energy	-17.0	-18.5	-18.0	-18.3
Maximum biochar	-12.9	-13.9	-16.0	-12.9
Denmark (high)				
Maximum energy	-204.5	-223.3	-218.0	-219.9
Maximum biochar	-154.8	-167.5	-193.7	-153.5
Denmark (low)				
Maximum energy	-171.3	-189.7	-187.6	-183.4
Maximum biochar	-129.7	-141.8	-166.5	-126.4

It can be seen that at maximum energy operation mode, the Case 1 has the potential to avoid more greenhouse gas emissions than the other cases and about 26 kg-CO_2/tonne-biomass-utilized more than Case 0, if coal fuelled production is substituted. The potential to avoid greenhouse gas emission becomes less when the substituting production fuelled with more environmentally friendly fuels. However, at maximum biochar operation Case 2 avoids the most impact.

The impact of decreasing carbon conversion can then be estimated by knowing the greenhouse gas emissions per MJ of heat and power production by the avoided production. It was found that for every kg of carbon unconverted and returned to the agricultural system, the loss of avoided climate change impact is -4.03 kg-CO_2, -1.95 kg-CO_2 and -0.23 kg-CO_2 if the substituted production is fuelled with coal, natural gas or biomass, respectively. However, utilization of the fertilizer products within the agricultural system boundary (shown in Section 4.2) could also have a significant influence on the overall impact.

Moreover, the avoided production is not the only factor impacting climate change within the bioenergy system boundary. Figures 4.2a and 4.2b give the climate change impact of the processes in each system concepts per tonne biomass utilized. Figure 4.2a gives the impact for maximum energy mode and Figure 4.2b gives the impact for maximum biochar mode of operation. There it can be seen that all cases have similar climate change

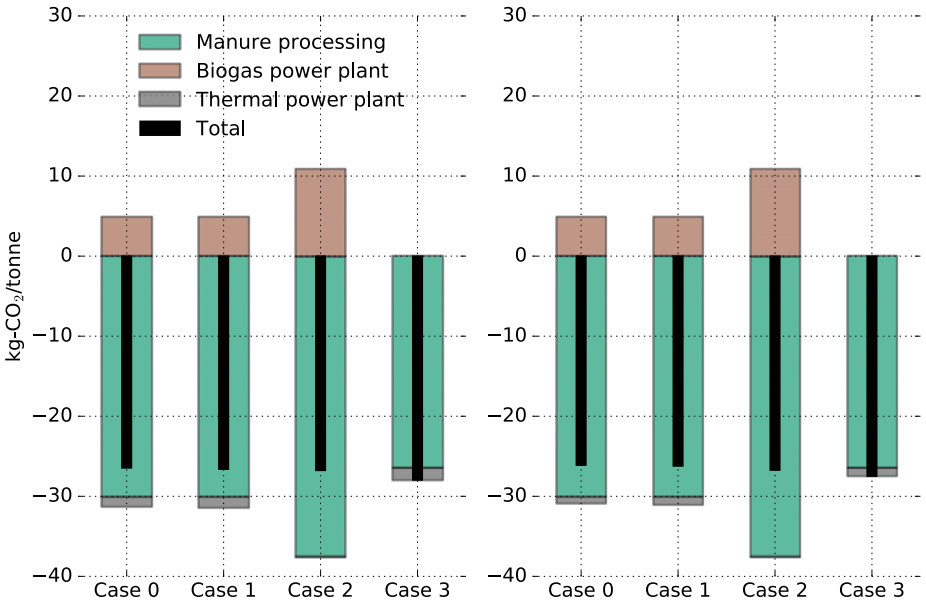

(a) Maximum energy **(b)** Maximum biochar

Figure 4.2: *Climate change impact (kg-CO_2/tonne biomass utilized) of the processes defined in the bioenergy system for the analysed system concepts.*

impact which is mostly influenced by the mitigating impact of the manure processing processes. The reason for that mitigating impact is found in the difference between the impact from raw manure storage if utilized as an organic fertilizer and storage of liquid and solid fractions after dewatering before further utilization in the bioenergy system. Figures 3.7 and 3.8 show the difference in emission from storage units depending on input.

Case 2 has the largest mitigation potential of the system cases in manure processing, but that is lessened by increased impact in the biogas power plant. The thermal power plant has a small mitigating impact on

climate change as the carbon emissions are mostly carbon dioxide which are recaptured by photosynthesis, and both the nitrous oxide and sulphur dioxide emission have a "cooling" impact in IPCC GWP 2013 method.

When comparing the result of the climate change impact by processes within the bioenergy system boundary and the avoided impact. It is clear that the impact from substituted production is potentially considerably greater than the impact of the processes within the bioenergy system. As the difference is greater between each system concept.

4.1.2 Exergy Analysis and Non-renewable Resource Requirements

Figures 4.3a - 4.3d display the exergy efficiency of electricity, district heat and fertilizer production for the system concepts as a function of carbon conversion in the gasifier. As shown in the figures, the integration of bioenergy technologies results in a higher overall exergy efficiency like in the energy analysis above. The overall exergy efficiency is highest in Case 3 (31.0%) at maximum energy operation mode which result in about 15.5% increase in product exergy compared with separate utilized in Case 0. When exergy from only electricity production is analysed the highest efficiency is found in Case 1, followed by Case 3. But Case 3 has higher exergy product from district heating production. At maximum biochar mode the highest overall exergy efficiency was found in Case 2, followed by Case 1.

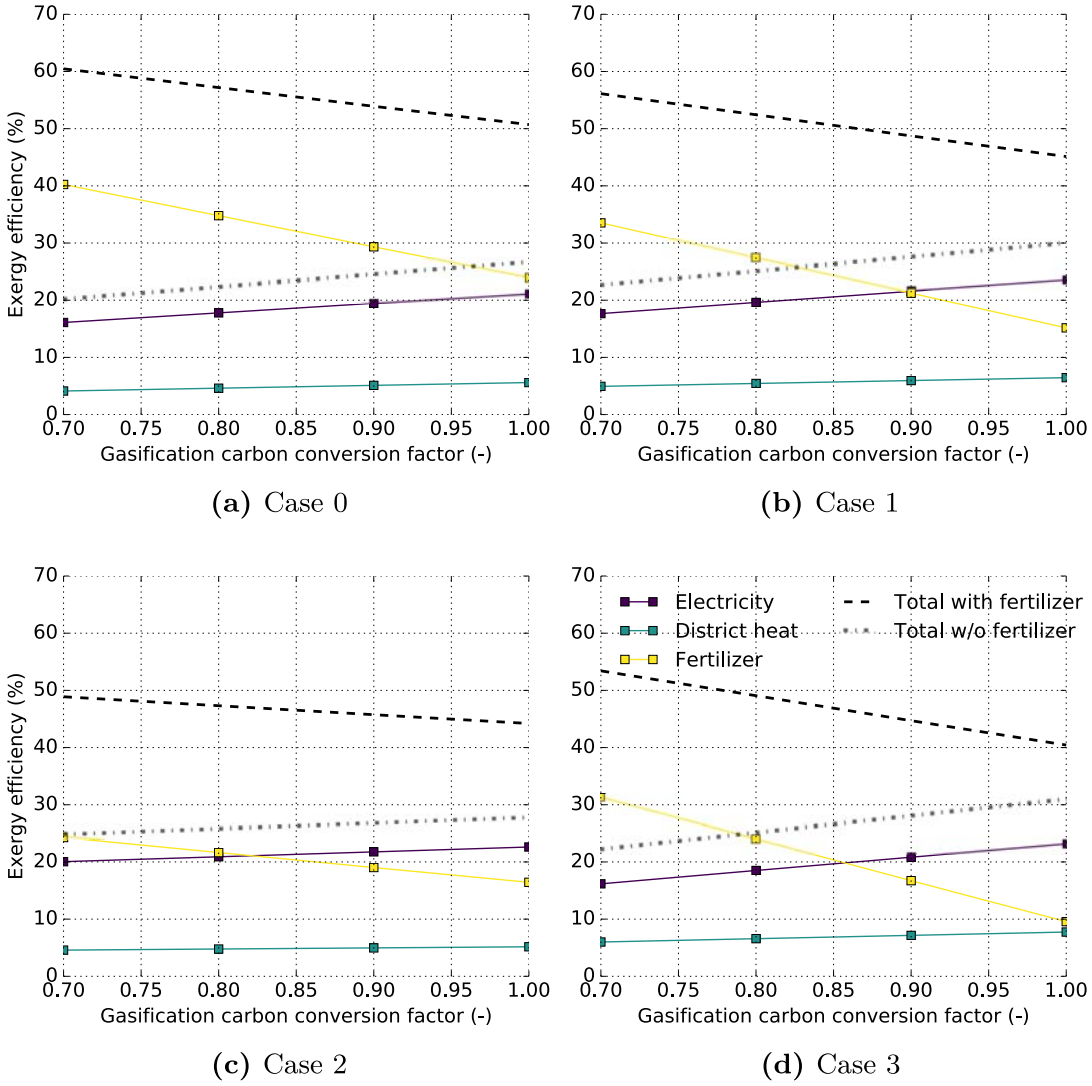

(a) Case 0 **(b)** Case 1

(c) Case 2 **(d)** Case 3

Figure 4.3: *Exergy efficiency of the system concepts over as a function of carbon conversion in the gasifier.*

Table 4.2 displays the exergy losses and destruction in all major components of each system concept and based on maximum energy generation and maximum biochar production.

Table 4.2: *Total exergy losses and destruction (% of total exergy inputs) in the components of the bioenergy system for each system concept.*

	Case 0	Case 1	Case 2	Case 3
Manure processing	%	%	%	%
Solid manure storage	-	-	-	0.134
Decanter (manure)	0.040	0.040	-	0.050
Liquid manure storage	0.534	0.534	-	0.667
Solid manure storage	-	-	-	0.134
Biogas power plant	%	%	%	%
Anaerobic digester	1.149	1.149	3.618	-
Biogas engine	5.177	5.177	23.934	-
Digestate processing	%	%	%	%
Decanter (digestate)	0.019	0.019	0.054	-
Liquid digestate storage	0.178	0.178	0.771	-
Solid digestate storage	0.070	0.070	0.296	-
Thermal power plant	%	%	%	%
Steam dryer	0.004	0.013	0.024	0.029
Maximum energy				
LT-CFB gasifier	7.457	9.391	6.317	10.562
Steam boil power plant	34.412	40.889	21.842	50.223
Maximum biochar				
LT-CFB gasifier	6.898	8.783	6.028	9.832
Steam boil power plant	25.186	30.465	17.442	37.937

As the combined exergy content of straw and manure is 3.69 MJ/kg. It can be seen in the table that the inefficiency of the manure and digestate processing processes result in about 28.4 MJ - 36.3 MJ per tonne biomass utilized, with Cases 0 and 1 having the lowest loss and Case 3 the highest. The exergy lost or destroyed in the biogas power plant is 233 MJ and 1016 MJ respectively for Cases 0 and 1, and Case 2. In the thermal power plant, the difference between the maximum energy and maximum biochar operation modes range from 480 MJ - 173 MJ per tonne biomass utilized. Where the maximum biochar production results in lower losses. In table 4.3 all the product exergy flows out of the bioenergy system are given for each system concept as a % of the total exergy input in reference to straw and manure fuel input.

Table 4.3: *Exergy flows (% of total exergy inputs) out of the bioenergy system for each system concept.*

	Case 0	Case 1	Case 2	Case 3
Fuel input	%	%	%	%
Straw	65.18	65.18	65.18	65.18
Manure	34.82	34.82	34.82	34.82
Manure processing	%	%	%	%
Liquid manure	7.499	7.499	-	9.374
Biogas power plant	%	%	%	%
Electricity	3.558	3.558	16.448	-
District heat	0.558	0.558	2.580	-
Digestate processing	%	%	%	%
Liquid digestate	5.440	5.440	16.371	-
Solid digestate	10.885	-	-	-
Thermal power plant	%	%	%	%
Maximum energy				
Biochar	0.147	0.169	0.066	0.185
Electricity	18.642	21.124	8.811	23.636
District heat	4.956	4.968	1.539	4.906
Maximum biochar				
Biochar	16.414	18.525	7.892	21.874
Electricity	13.606	15.286	6.245	16.666
District heat	3.476	3.446	0.956	3.164

Here the exergy flow out of the system as fertilizer in the form of liquid fraction of de-watered manure, liquid fraction of de-watered digestate and the solid fraction of digestate (Case 0), along with biochar can be seen. These fertilizer products will be further used within the agricultural system boundary as they will be applied on agricultural fields and the impact of recycling the nutrients and some of the carbon on the exergy demand is found. Nevertheless, when comparing Case 0 and Case 1 about 10.9% of the exergy input leaves as fertilizer in Case 0, but that same exergy flow (solid digestate) is utilized in the thermal power plant, effectively increasing the exergy product from 23.6% - 26.1% of the overall exergy utilized from straw and manure in the thermal power plant. It can also be seen that the increase in exergy efficiency of the thermal power plant between maximum energy generation and maximum biochar production is because of the biochar production which results in a higher overall

efficiency, but the biochar will be further utilized within the agricultural system where it will effect the CExD of that system.

Figures 4.4a and 4.4b display the Cumulative Exergy Demand (CExD) of the processes defined in the bioenergy system boundary for the system concepts per tonne biomass. Figure 4.4a gives the results for the maximum energy mode and Figure 4.4b shows the results of the maximum biochar mode. The difference between the two modes of operation is not

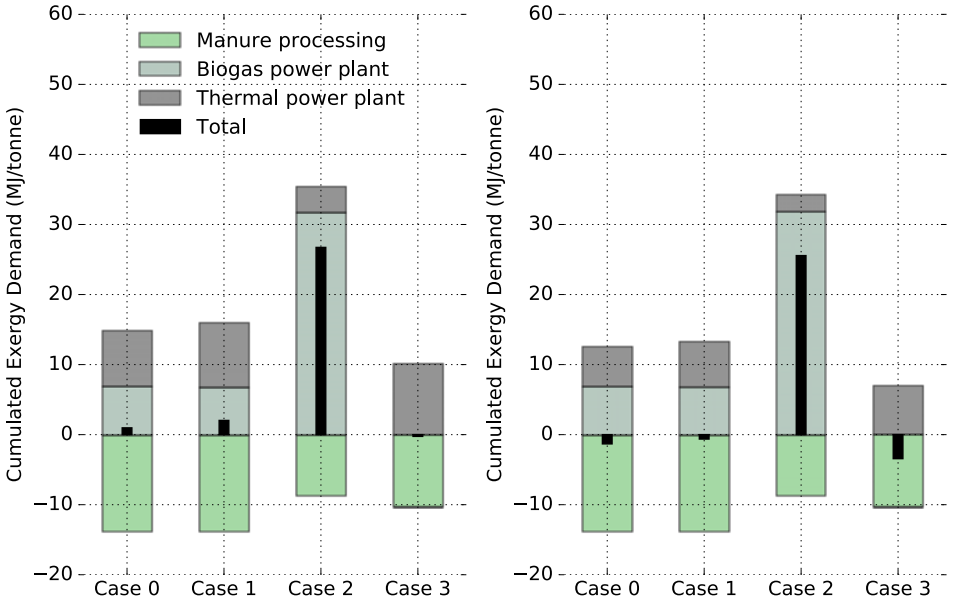

(a) Maximum energy **(b)** Maximum biochar

Figure 4.4: *Cumulative Exergy Demand (MJ/tonne biomass utilized) of the processes defined in the bioenergy system for the analysed system concepts per tonne biomass.*

great. But manure processing part of the bioenergy system has the most incluence on cumulated exergy demand in Cases 0,1 and 3. However, in Case 2 the biogas power plant has the greatest demand. Nevertheless, the CExD in the bioenergy system is much lower in comparison with the product exergy and the difference in product exergy is considerably greater than the CExD of the processes within the bioenergy system. The Exergy Return on Investment (ExROI) is found by dividing the exergy product of the overall system with non-renewable CExD by the overall system. The exergy value of the straw and manure mix is 3.69 MJ/kg of

which 65.2% is from the straw and 34.8% is from the manure. If just 1% is lost then that would amount to more exergy than all of the CExD by the processes within the bioenergy system boundary for cases 0,1 and 3.

Depending on case and operation mode the fertilizers leave the bioenergy system with 9.6% - 40% of the exergy value of the biomass. However, these fertilizers will have an impact on the CExD by the agricultural system as by recycling the nutrients less mineral fertilizers are need. It was found that for every kg of carbon that is unconverted and recycled with biochar, the decrease in product exergy of the syngas is 32 MJ, which results in about 10.5 MJ and 2.7 MJ decrease respectively in electrical and district heat product exergy in the thermal power plant, and about 13.2 MJ in total exergy product. This will have to be abated by utilization in the agricultural system for the production of biochar to result in an overall decrease in non-renewable resources.

4.1.3 Investment and Operation Costs

Figures 4.5a and 4.5b display the investment cost build-up of the bioenergy system, disaggregated to manure processing, biogas power plant and thermal power plant, for each system concept. Figure 4.5a gives the results for the maximum energy mode and Figure 4.5b shows the results of the maximum biochar mode. According to the graph, Case 2 has the highest investment cost and Case 3 has the lowest. It can also be seen that the cost of the thermal power plant is similar between the concepts but the major difference is in the cost of the biogas power plant and manure processing units. Where the difference between the highest and lowest investment cost is significant.

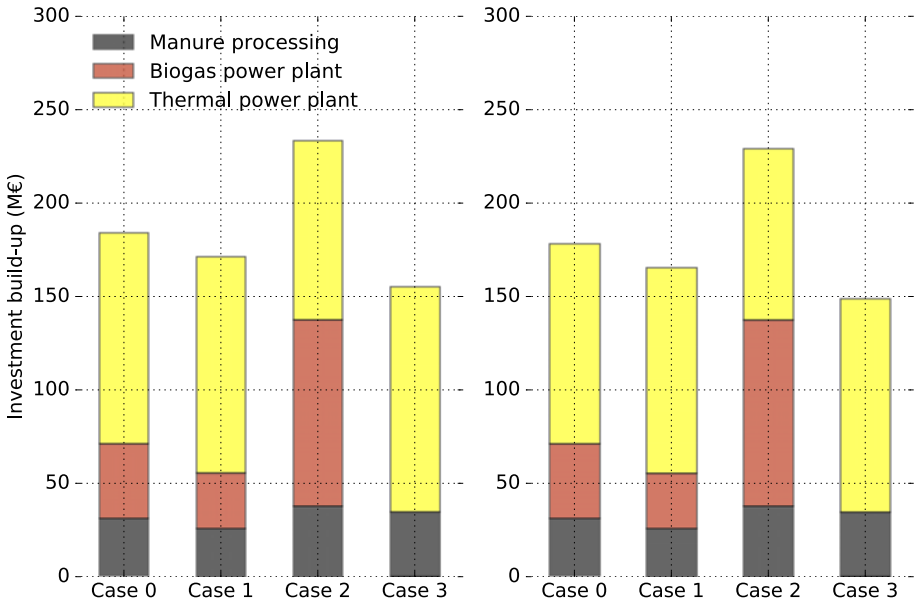

(a) Maximum energy **(b)** Maximum biochar

Figure 4.5: *Investment cost build-up (M Euro) of the bioenergy system for the analysed cases.*

Table 4.4 displays the investment cost breakdown to all major components of the bioenergy system for each system concept in million Euro.

Table 4.4: *Investment costs breakdown to all major components of the bioenergy system (million Euro) for each analysed system concept.*

	Case 0	Case 1	Case 2	Case 3
Biogas power plant				
Anaerobic digester	22.13	22.13	64.57	-
Biogas engine	7.64	7.64	35.30	-
Manure processing				
Solid manure storage	-	-	-	14.40
Solid digestate storage	10.75	5.37	15.67	-
Decanter	20.10	20.10	21.82	20.10
Thermal power plant				
Pre-processing	24.02	23.82	23.49	23.59
Maximum energy				
Gasifier	54.45	56.88	45.53	59.75
Steam cycle	34.12	35.48	26.83	37.28

... continued				
Maximum biochar				
Gasifier	52.28	54.67	43.96	57.42
Steam cycle	30.49	31.71	24.02	33.16

As shown in the table the single greatest cost is for the gasifier in all system concepts except Case 2 where the highest cost is the anaerobic digester. It can also be seen that the difference in investment cost in the thermal power plant is not much between the two operation scenarios. The total decrease is just 4.4 - 6.5 Million Euro, where the biggest difference is in Case 3 and the smallest in Case 2.

Figures 4.6a and 4.6b display the O&M cost build-up of the bioenergy system, disaggrigated to manure processing, biogas power plant and thermal power plant, for the analysed system concepts. Figure 4.6a gives the results for the maximum energy generation mode and Figure 4.6b shows the results of the maximum biochar mode.

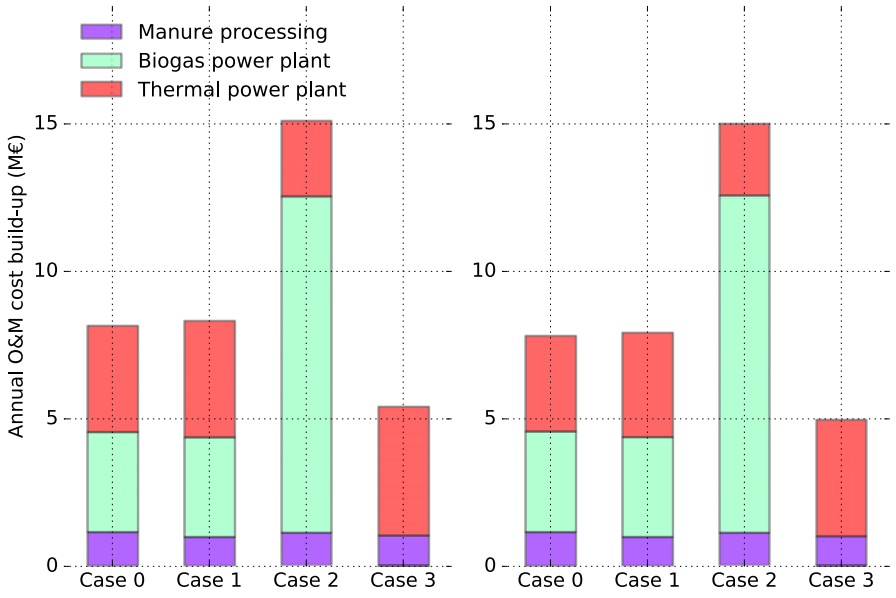

(a) Maximum energy **(b)** Maximum biochar

Figure 4.6: *O&M cost build-up (M Euro) of the bioenergy system for the analysed cases.*

As shown in the graph, the annual O&M costs are similar in the thermal and biogas power plants for Cases 0 and 1. But the cost is greatest in Case 2 where the O&M cost of biogas power plant is significant, without much decrease in thermal power plant O&M cost. The lowest cost is found in Case 3 as the costs of running a biogas power plant are avoided.

Table 4.4 displays the O&M costs breakdown to major components of the bioenergy system for each case in million Euro.

Table 4.5: *O&M costs breakdown to all major components of the bioenergy system (million Euro) for each analysed case.*

	Case 0	Case 1	Case 2	Case 3
Biogas power plant				
Anaerobic digester	2.51	2.51	7.34	-
Biogas engine	0.88	0.88	4.08	-
Manure processing				
Solid manure storage	-	-	-	0.43
Solid digestate storage	0.32	0.16	0.47	-
Decanter	0.83	0.83	0.65	0.60
Thermal power plant				
Pre-processing	0.72	0.71	0.70	0.71
Maximum energy				
Gasifier	1.88	2.18	1.05	2.57
Steam cycle	1.02	1.06	0.81	1.12
Maximum biochar				
Gasifier	1.88	2.18	1.05	2.57
Steam cycle	0.91	0.95	0.72	0.99

It can be seen in the table that the operation of the anaerobic digester is the single highest cost, followed by the gasifier for cases 0, 1 and 3. But the cost of running the biogas engine is considerably higher than running the gasifier in Case 2.

By including the return on equity and debt, along with taxes and insurance costs, the carrying charges for the system concepts of the bioenergy system can be found. Figures 4.7a and 4.7b gives the average annual carrying charges along with the annual O&M cost of the system concepts. As shown in the figures, the annual carrying charges and O&M cost of the system concepts are highest for Case 2 and lowest for Case 3. The

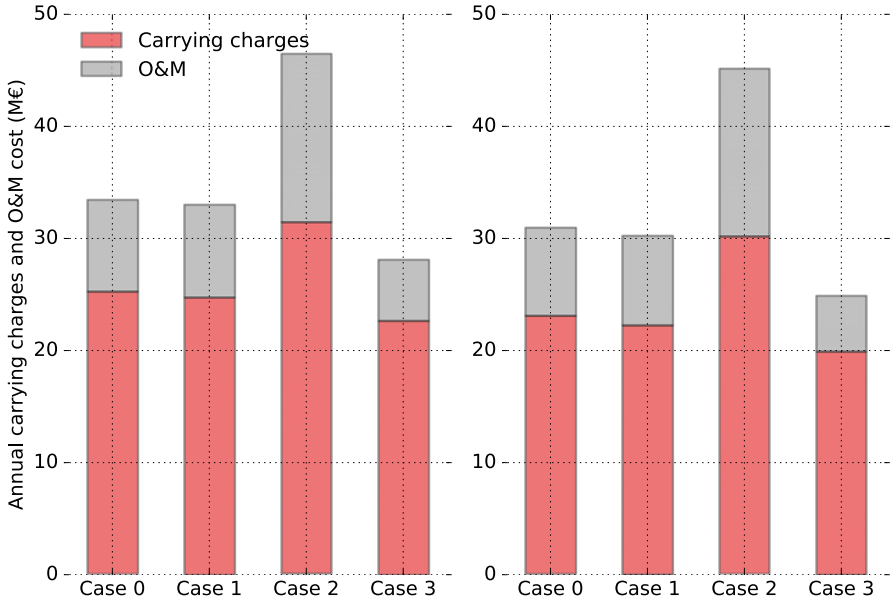

(a) Maximum energy **(b)** Maximum biochar

Figure 4.7: *Annual carrying charges and O&M cost (M Euro) of the bioenergy system for the analysed cases.*

difference between the lowest and highest is more than double or 22.6 M Euro. The difference between the maximum energy and maximum biochar modes of operation differs for each case. In Case 3 maximizing biochar production could lower the annual carrying charges and O&M cost by 2.9 M Euro annually. For Cases 0 and 1 the decrease is about 2.55 M Euro, but the lowest decrease is found for Case 2 or 1.3 M Euro.

However, decreasing the carbon conversion in the gasifier will result in lower electrical production and thus lower revenues from electricity sales. The premium feed-in tariff for bioenergy system is about 107 Euro/MWh electricity and the loss in revenues from electricity sales after tax are then found to be 6.9 M Euro in Case 3, 2.5 M Euro in Case 2, 5.8 M Euro in Case 1 and 5.0 M Euro in Case 0. It was found that the loss of revenues for every carbon unconverted in the gasifier is 0.20 Euro/kg-C, but the decrease in carrying charges and O&M cost is about 0.095 Euro/kg-C.

4.2 Agricultural System

In this section, the results related to the agricultural system are given based on applying the process models introduced in Section 3.4 and the analytical framework, to the resource flows to and from the bioenergy system. It is divided into soil carbon build-up, and resource removal and recycling.

4.2.1 Soil Carbon Build-up

There will be a carbon build-up deficit when removing resources from the agricultural system which otherwise are applied to fields, but this deficit can be mitigated or even turned into a surplus by fertilizer production in the bioenergy systems. The carbon build-up potential depends on biochar production (controlled by carbon conversion in the gasifier) as the thermal treatment of carbon will make it more stable in soil as shown in Section 3.4.1. Figures 4.8a - 4.8d show the net carbon build-up as a function of carbon conversion in the gasifier for the system concepts analysed in this work.

It can be seen in the figure, that the greatest carbon build-up potential is when the straw and manure are utilized in Case 3 and operated at maximum biochar production mode. Utilizing the resources in that system concept could result in 16 kg net carbon build-up per 1 kg carbon harvested compared with leaving the straw on the field and using the raw manure as an organic fertilizer (based on 100 years of application). The 100th year net carbon build-up potential in Case 1 is 12.2 kg carbon, in the separate utilization Case 0 it is 11.1 kg carbon and only 1.5 kg carbon in Case 2. It can also be seen that there is a net carbon build-up deficit when maximizing carbon conversion for all system concepts, as the soil carbon build-up would have been greater if the resource are not harvested and utilized for bioenergy.

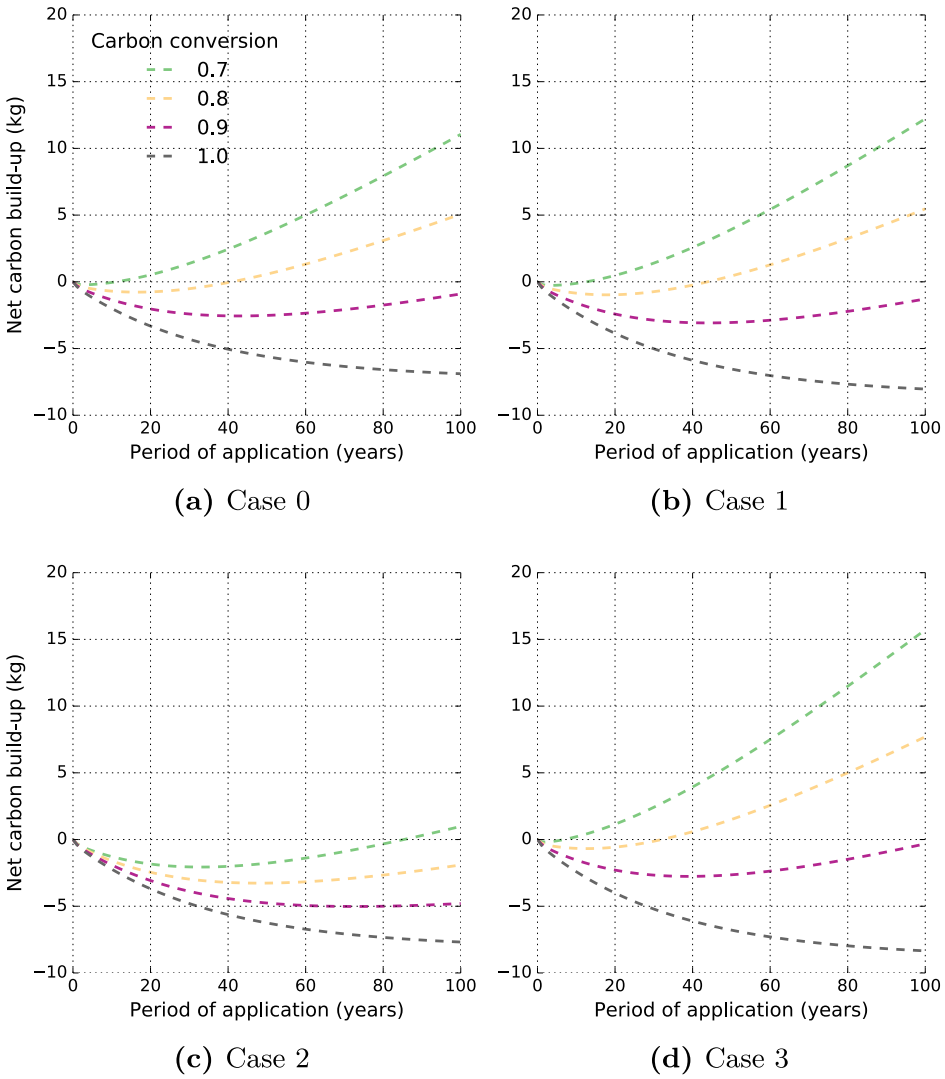

(a) Case 0 **(b)** Case 1

(c) Case 2 **(d)** Case 3

Figure 4.8: *Net carbon build-up in the agricultural system for a range of carbon conversion factors in the bioenergy systems over years of application.*

The results above are then used to find the break even point when carbon build-up by applying the produced fertilizers is equal to the carbon build-up that would have been if the straw and manure resources were applied on the field instead of being harvested as an energy source. Here it can be seen that carbon build-up break even point for Case 2 is only reached after 100 years of application and at an operating mode close to maximum biochar production in the thermal power plant. It can be seen that in order to mitigate carbon build-up deficit over a 100 year horizon

the carbon conversion needs to be close to 90% for for Cases 0, 1 and 3, but will need to be about 74% in Case 2.

Table 4.6: *Carbon conversion factor (-) break even point for carbon build-up potential.*

Years of application	Case 0	Case 1	Case 2	Case 3
100	0.885	0.882	0.738	0.896
80	0.863	0.860	-	0.877
60	0.836	0.830	-	0.852
40	0.798	0.791	-	0.818
20	0.740	0.733	-	0.767
10	-	-	-	0.724

In the economic analysis, the technical lifetime of the bioenergy system is assumed to be 25 years. If the soil carbon build-up should be equivalent to leaving the straw and applying the manure in soil, the carbon conversion factor in the gasifier would need to be about, 75.0%, 74.5%, 78% in Cases 0, 1, 3, but Case 2 is not able to return equivalent soil carbon build-up after 25 years.

If only the gasifier is analysed and assume to gasify either straw or raw manure, the carbon conversion factor (or the biochar production) required to have the same soil carbon build-up as applying straw and manure on field, can be found as a function of time of continuous resource removal and biochar application. Figure 4.9 gives the required carbon conversion factor as a function of time (of continuous resource removal and biochar application). As shown in the figure, the carbon conversion would need to be about 82% to have an equivalent carbon build-up after 25 years and about 91% after 100 years. For manure gasification, the carbon conversion would need to be about 68% to ahve an equivalent carbon build-up after 25 year and 85% after 100 years.

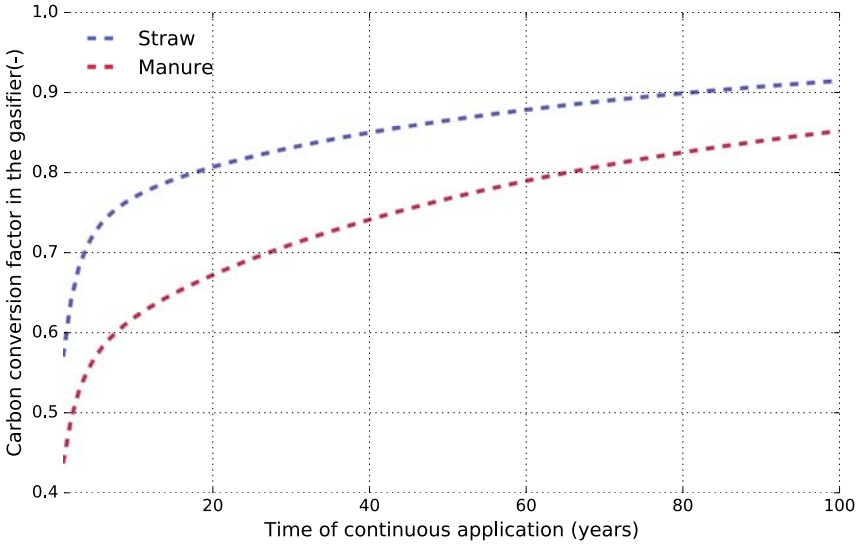

Figure 4.9: *Required carbon conversion factor (-) as a function of time of continuous resource removal and biochar application (year) for straw and manure.*

4.2.2 Resource Removal and Recycling

Figures 4.10a and 4.10b give the climate change impact of straw and manure removal from the agricultural system, along with the affect of applying organic fertilizers and biochar produced in the bioenergy system to an agricultural field. The organic fertilizer production (liquid manure, liquid digestate and solid digestate) is aggregated. Figure 4.10a shows the results at maximum energy mode and Figure 4.10b gives the results for maximum biochar mode. First it can be seen that there is a significant difference between the two operation modes for all system concepts, as the maximum biochar mode has a greater climate change mitigation potential than maximum energy mode. This difference is the increase in carbon sequestration between the scenarios. It can also be seen that the impact of removing straw and manure is 62 kg-CO_2/tonne and recycling of nutrients and carbon through organic fertilizers is not enough to fully mitigate that impact. To enable that, the biochar production will need to increase operating the gasifier using carbon conversion at 82.7%, 78.9% and 83.9% respectively for Cases 0, 1 and 3. However, at maximum biochar production mode the carbon build-up achieved in Case 2 is not enough to mitigate the impact of harvesting the resources.

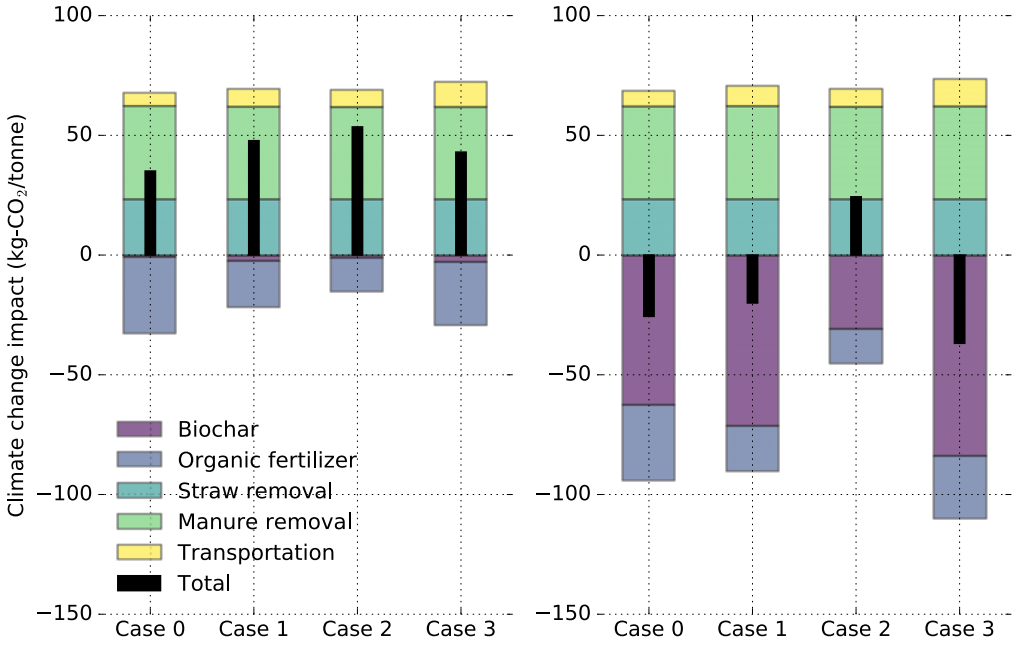

(a) Maximum energy **(b)** Maximum biochar

Figure 4.10: *Climate change impact of resource removal and recycling in the agricultural system for the analysed system concepts per tonne biomass.*

It was found that for every kg of carbon left unconverted in the bioenergy system and returned with biochar back to the agricultural system the mitigation impact by carbon sequestration is -3.26 kg-CO_2, which can be compared with the loss of avoided impact by substitution of heat and power production fuelled with coal, natural gas and biomass from Section 4.1.

Figures 4.11a and 4.11b give the CExD of resource transportation, and straw and manure removal from the agricultural system, along with the affect of applying organic fertilizers and biochar produced in the bioenergy system to an agricultural. Figure 4.11a shows the results at maximum energy mode and Figure 4.11b gives the results for maximum biochar mode. As shown in the graphs, the impact of transportation is significantly greater in terms of CExD than in terms of climate change impact. Case 3 demands more exergy than the other cases and the reason is mostly because of its impact from the transportation processes. It can

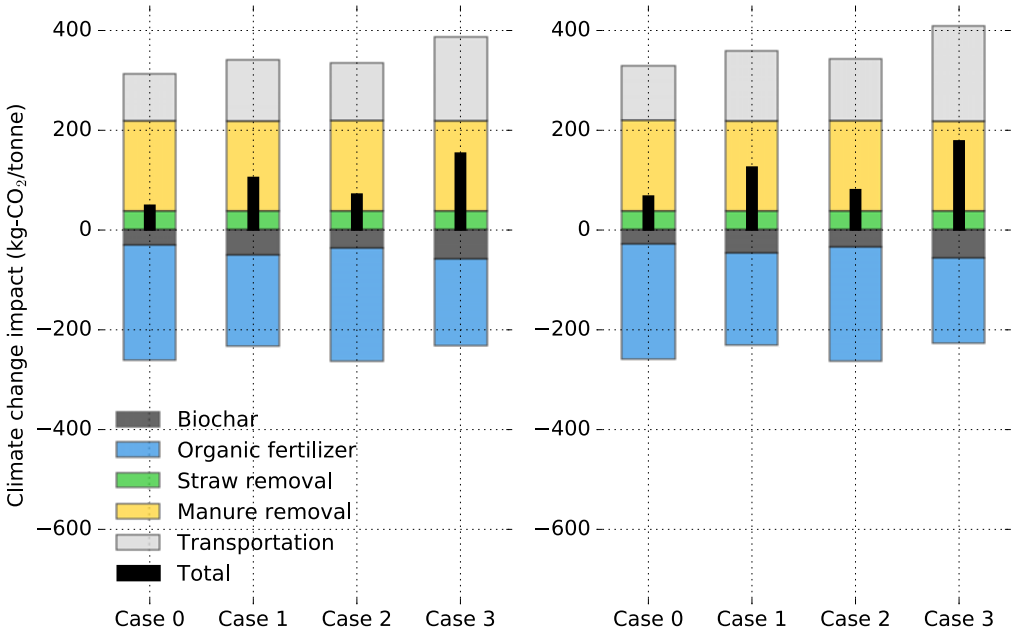

(a) Maximum energy **(b)** Maximum biochar

Figure 4.11: *Cumulative Exergy Demand of resource removal and recycling in the agricultural system for the analysed system concepts per tonne biomass.*

also be seen that the mitigating potential of biochar production is significantly less than the mitigating potential of the organic fertilizers and there is not much difference between the two modes of operation. The lowest non-renewable exergy demand is found for Case 0 which has the lowest transportation distance and highest organic fertilizer production. The second lowest exergy demand is found in Case 2 which has more organic fertilizer production than the other combined utilisation concepts. Additionally, for every kg carbon unconverted in the gasifier and recycled with biochar the CExD is increased by 0.878 MJ/kg-C. From Section 4.2 it was found that the biochar input in agriculture would need to abate the loss of exergy from heat and power production. These results show that it does not and the overall system will need more non-renewable exergy input if biochar production is increased.

Figures 4.12a and 4.12b display the annual fuel cost build-up for each system concept. Figure 4.12a gives the results for the maximum energy generation mode and Figure 4.12b shows the results of the maximum

biochar production mode.

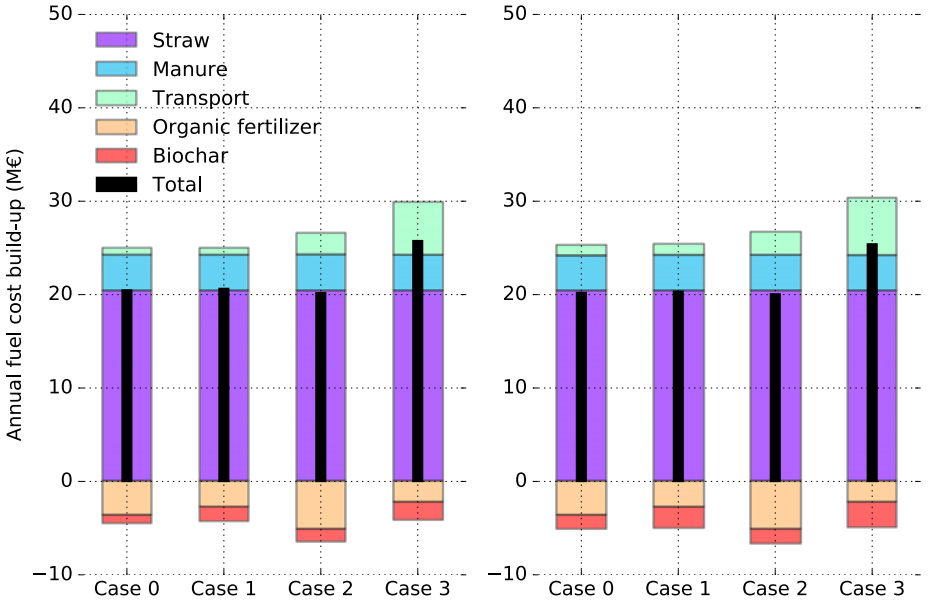

(a) Maximum energy **(b)** Maximum biochar

Figure 4.12: *Annual fuel cost build-up (M Euro) for the analysed system concepts.*

According to the graph, the fuel cost is highest for Case 3 and lowest for Case 2. The main difference between the cases are in the cost of fuel transportation and benefits of organic fertilizer sales revenues. The cost impact of transporting the solid manure is about 5.7 Million Euro annually. In the other cases this cost ranges from 2.3 Million Euro to 0.7 Million Euro. It can also be seen in the figure that the benefit of carbon sequestration is minimal. The benefits of increased biochar production by lowering the carbon conversion is valued economically by raising the value of the biochar by the current and projected cost of carbon quota as shown in Figure 3.28. Based on that assumption the increased revenues for every carbon unconverted are at most 0.06 Euro/kg-C and at least 0.005 Euro/kg-C before sales tax on biochar.

4.3 Multi-criteria Analysis

This section gives the results of the overall system integration between agriculture and bioenergy for the analysed system concepts. First climate change impact results are outlined, followed by the non-renewable resource requirements and economic feasibility. Finally the result represented by these criteria are used in a multi-criteria analysis.

4.3.1 Climate Change Impact

Figures 4.13a and 4.13b give the total climate change impact (g-CO_2 / kg-input) of the bioenergy and agricultural integration for each system concept, by combining the impact found within the bioenergy system boundary (Section 4.1) and agricultural system boundary (Section 4.2). Figure 4.13a shows the results at maximum energy mode and Figure 4.13b gives the results at maximum biochar mode. As shown in the graphs, there is a large difference between the impacts if operation is maximized for energy generation or biochar production. The reason is the impact from carbon sequestration associated with biochar application in agricultural soils. It can also be seen that the optimum system concept is Case 3 at maximum biochar mode. At maximum energy generation mode the optimum is separate utilization Case 0, and the optimum combined utilization concept is Case 3. The reason for the lower impact by Case 0 compared with the other cases is less transportation and more nutrients and carbon recycled with the organic fertilizers.

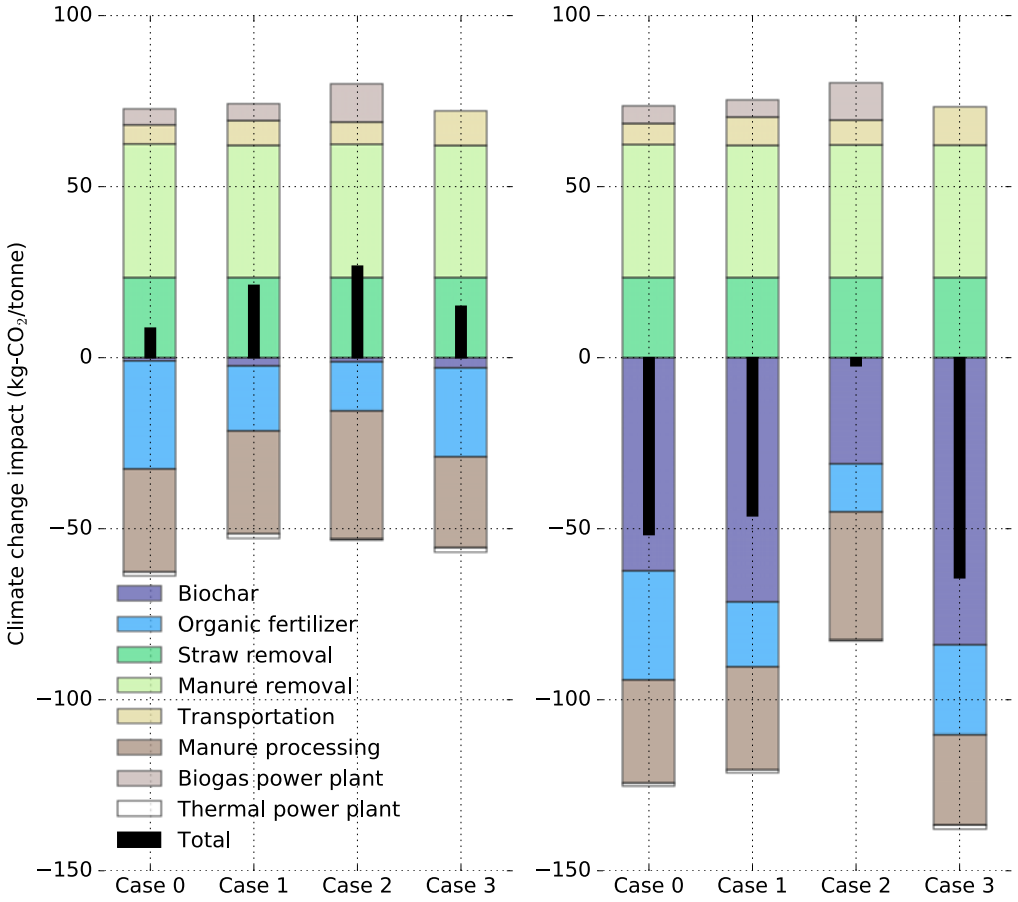

(a) Maximum energy **(b)** Maximum biochar

Figure 4.13: *Total climate change impact (kg-CO_2 / tonne-input) of the bioenergy and agricultural system integration concepts.*

However, those results do not account for avoided CHP production fuelled with alternatives, i.e coal, natural gas or biomass. Table 4.7 displays the total climate change impact (kg-CO_2 / tonne-input) of the bioenergy and agricultural system integration concepts including avoided CHP production for both modes of operation.

Table 4.7: *Total climate change impact (kg-CO_2 / tonne-input) of the bioenergy and agricultural system integration concepts including avoided CHP production for both modes of operation.*

	Case 0	Case 1	Case 2	Case 3
Maximum energy				
Total kg-CO_2	8.63	21.15	26.76	15.03
Inc. avoided production				
Coal	-295.80	-309.10	-293.57	-312.93
Natural gas	-138.57	-138.53	-128.13	-143.55
Biomass	-8.40	2.64	8.78	-3.31
Denmark (high)	-195.84	-202.18	-191.28	-204.82
Denmark (low)	-162.64	-168.50	-160.81	-168.39
Maximum biochar				
Total kg-CO_2	-51.72	-46.24	-2.37	-64.35
Inc. avoided production				
Coal	-282.12	-294.39	-286.99	-294.75
Natural gas	-163.12	-166.23	-139.99	-175.75
Biomass	-64.62	-60.14	-18.35	-77.22
Denmark (high)	-206.51	-213.76	-196.05	-217.81
Denmark (low)	-181.45	-188.02	-168.90	-190.70

Here it can be seen, at maximum energy mode, that if the system concept substitutes heat and power production fuelled with alternative fuels Case 3 is optimal, except when biomass fuelled production is avoided and in the Denmark (low) scenario. If more environmentally friendly production is substituted Case 0 is optimal in terms of climate change impact as maximum energy mode. At maximum biochar mode, it can be seen that Case 3 is optimal for all avoided alternative production scenarios, because of greater carbon sequestration

Nevertheless, if the results at maximum energy mode and maximum biochar mode are compared it can be seen that if coal fuelled production is avoided it is optimal to maximise heat and power production by maximising carbon conversion in the gasifier in all cases. But if natural gas fuelled production or more environmentally friendly production is avoided it is optimal in all cases to maximise biochar production.

To be able to compare with alternative production from other resources, the functional unit is changed to per kWh electricity production and the district heat co-product is assumed to avoid heat production fuelled with biomass. Figure 4.14 gives the climate change impact of the system concepts at both maximum energy and maximum biochar modes of operation in comparison with alternative electricity production. As the figure

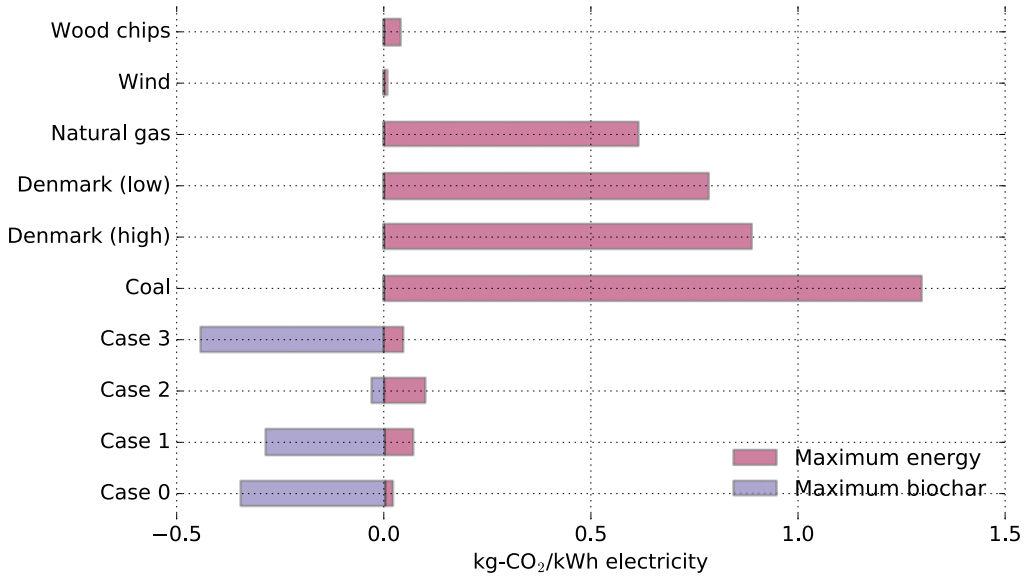

Figure 4.14: *Total climate change impact (kg-CO_2 / kWh-electricity) of the bioenergy and agricultural system integration concepts compared with alternatives.*

shows, the electricity production from the system concepts are climate friendly compared with fossil fuels and the marginal Danish production. At maximum energy operation mode they are comparable with electricity production from wind and wood chips based on data from the ecoinvent 3.3 database. But the maximum biochar production operation the impact per electricity produced is negative and can be considered climate change mitigating.

4.3.2 Non-renewable Resource Requirements

Figures 4.15a and 4.15b give the total Cumulative Exergy Demand of the bioenergy and agricultural system integration concepts. Figure 4.15a shows the results of maximum energy mode and Figure 4.15b gives the results for maximum biochar mode. As shown in the graph, the lowest ex-

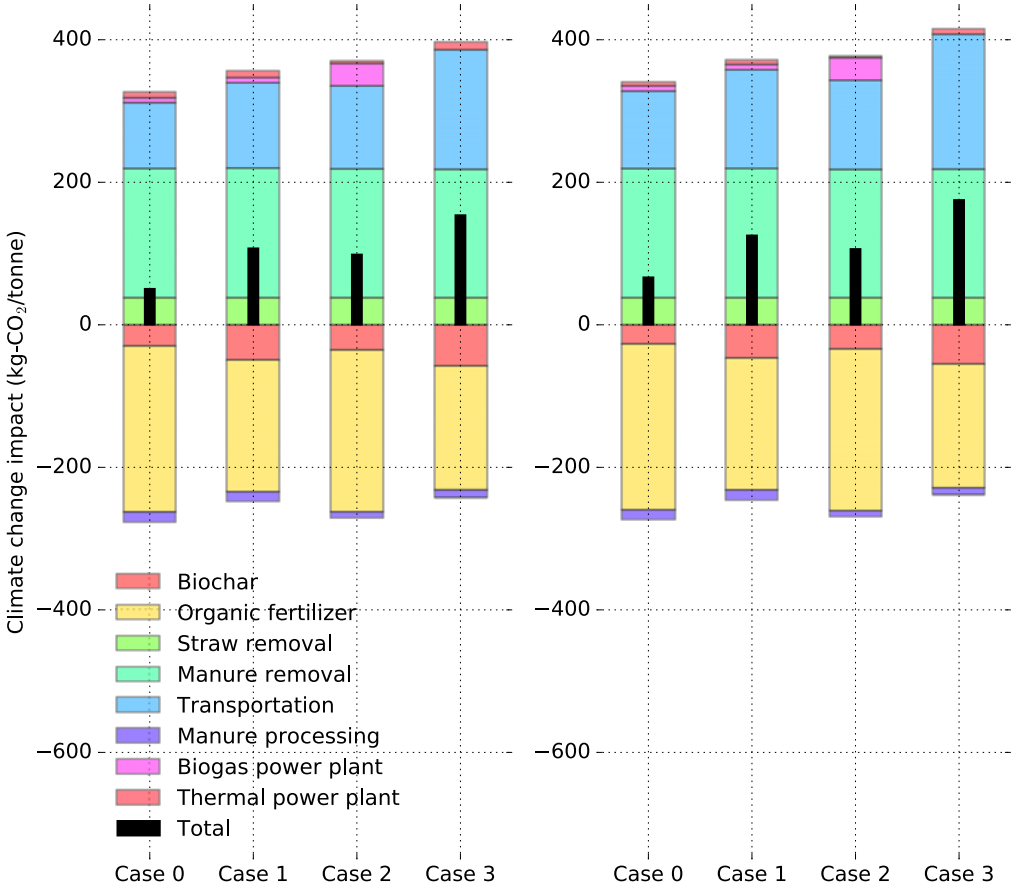

(a) Maximum energy **(b)** Maximum biochar

Figure 4.15: *Total Cumulative Exergy Demand (MJ/tonne-utilized) of the bioenergy and agricultural system integration concepts.*

ergy demanded is in Case 0 and the highest demand is in Case 3, followed by Case 1. It can also be seen that there is just a small difference between the two operation scenarios, where the maximum biochar production demands more exergy. It can also be seen that the processes within the bioenergy system boundary contribute little to the CExD result com-

pared with the processes within the agricultural system boundary.

However, the final Exergy Return on Investment indicator is found by including the product exergy. The product exergy is found by all heat and power production in the bionergy system. Table 4.8 gives the total Cumulative Exergy demand together with the product exergy and the resulting Exergy Return on Investment of the bioenergy and agricultural system integration concepts for both modes of operation.

Table 4.8: *Total Cumulative Exergy demand (MJ) together with the product exergy (MJ) and the resulting Exergy Return on Investment (-) of the bioenergy and agricultural system integration concepts.*

	Case 0	Case 1	Case 2	Case 3
Maximum energy				
Total CExD (MJ)	50.7	107.5	98.8	154.0
Product exergy (MJ)	1033.6	1156.7	1156.3	1157.0
ExROI (-)	20.39	10.76	11.70	7.51
Maximum biochar				
Total CExD (MJ)	66.8	125.6	106.5	175.3
Product exergy (MJ)	793.3	885.2	1040.1	835.7
ExROI (-)	15.65	8.23	10.53	5.43

Here it can be seen for the maximum energy operation mode that although Case 3 has the highest product exergy, the higher ExROI factor is found for Case 0, followed by Case 2 and the lowest factor is found for Case 3. The results of the maximum biochar operation scenario follows the same trend as the maximum energy operation scenario as described above, where the optimum system concept is Case 0 in terms of ExROI results, followed by Case 2 and the lowest ExROI is found for Case 3.

For both operation scenarios, the Case0 has the highest ExROI but the lowest product exergy. The reason for this can be seen when observing Figures 4.15a and 4.15b, there it can be seen that the major difference between the system concepts are in the exergy demanded by transportation and exergy demand avoided by nutrients recycling from organic fertilizer production. It can also be seen that the ExROI factor decreases for each system concept at maximum biochar production operation, and the main reason as can be seen in the table is decrease in product exergy which is not compensated by CExD decrease.

These results can be compared with ExROI from alternative heat and power production by finding the non-renewable CExD using ecoinvent 3.3 and assuming 40% electrical effienciency and 55% district heating efficiency for alternatives, except wind fuelled production, there the electricity is produced with wind turbines and a district heating product has been added which is fuelled with biomass. It can be seen in the figure

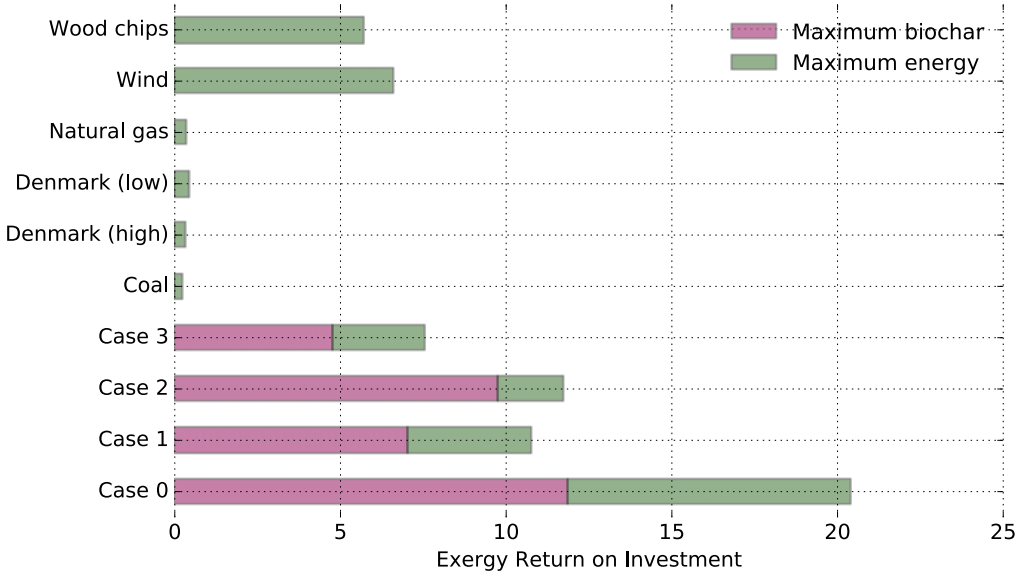

Figure 4.16: *Exergy Return on Investment of the bioenergy and agricultural system integration concepts compared with alternatives.*

that the ExROI of production fuelled with fossil fuels and the scenarios representing marginal production in Denmark is below 1, which is the benchmark for renewable energy generation. When comparing the ExROI of the system concepts it can be seen that at maximum energy operation mode the result is better than for wood chips and wind fuelled production, but at maximum biochar operation mode the ExROI value is lower than both wind and wood chips fuelled production in Case 3, but higher or equal in Cases 0-2.

4.3.3 Economic Feasibility

Figures 4.17a and 4.17b give the annual cost of the bioenergy and agricultural system integration concepts. Figure 4.17a shows the results of maximum energy mode and Figure 4.17b gives the results for maximum biochar mode. As shown in the graph, the annual cost is lowest for Cases

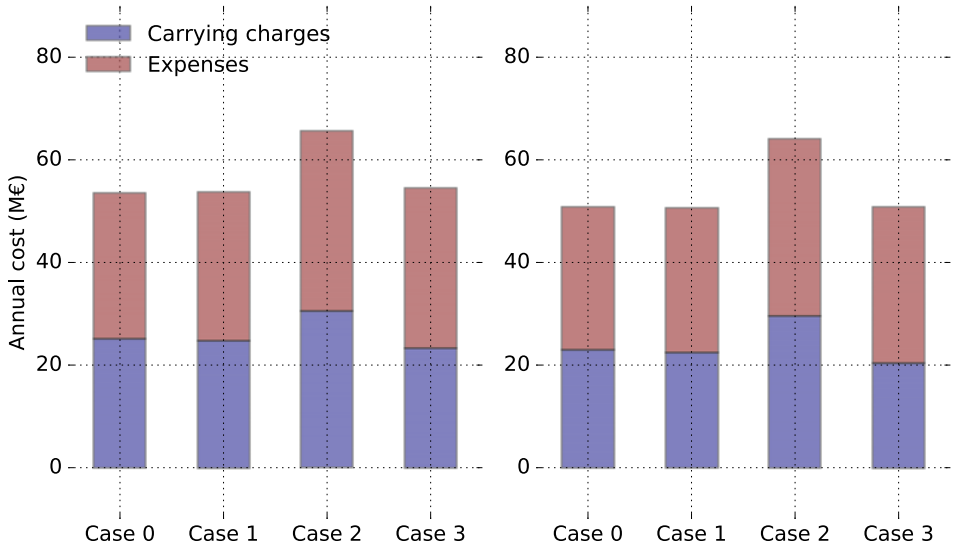

(a) Maximum energy **(b)** Maximum biochar

Figure 4.17: *Total annual cost (M Euro) of the bioenergy andz agricultural system integration concepts.*

0, 2 and 3, where the biggest difference compared with Case 2 is the carrying charges related to biogas power plant. Case 1 has a marginally lower annual cost than Case 0, mainly because of slightly lower investment cost due to economies of scale. It can also be seen that the impact of decreased carbon conversion is small decrease in annual cost. Mostly because of decreased carrying charges and revenues of biochar sales (although quite small).

Table 4.9 displays the levelized cost of electricity production, payback period and net present values of the system concepts analysed for an integrated bioenergy and agriculture, including maximum energy generation and maximum biochar production operation scenarios.

Table 4.9: *Levelized cost of electricity, payback period and net present value of the system concepts for integrated bioenergy and agriculture.*

	Case 0	Case 1	Case 2	Case 3
Maximum energy				
Levelized cost of electricity	85.8	76.9	91.2	81.2
Payback period	12.9	9.8	15.0	10.4
Net present value	72.9	111.5	65.7	90.8
Maximum biochar				
Levelized cost of electricity	107.2	96.8	99.7	110.9
Payback period	23.5	17.1	18.9	27.0
Net present value	4.7	31.8	31.1	-4.7

As shown in the table, all concepts are economically feasible at maximum energy generation mode and Case 1 is optimal. That case has the lowest levelized cost of electricity production and highest net present value in both operation scenarios. It can also be seen that the feasibility of the concepts at maximum biochar production mode is significantly less and Case 3 becomes infeasible. For perspective, these results can be compared with the Elspot system price (2011-2016) and the aggregated levelized cost of electricity production in Denmark (2006-2011). It can be seen

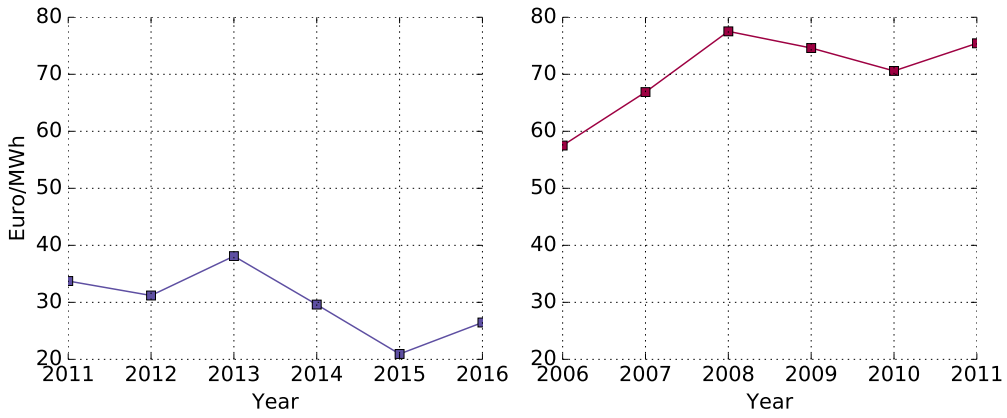

(a) ELspot system price (ave) **(b)** LCOE in Denmark

Figure 4.18: *Total Cumulative Exergy Demand (MJ/tonne-utilized) of the bioenergy and agricultural system integration concepts.*

when comparing the annual expenses of running the power plants is just under or equivalent to the average Elspot system price and the levelized

cost of electricity production is bit above the aggregated levelized cost of electricity production in Denmark from 2008 - 2011.

4.3.4 Optimal System Concept

As shown by the preceding results, the optimum system concept depends on the criteria among other factors. In terms of climate change impact the optimum system concept also depends on the mode of operation and avoided production. The optimum system concept in terms of non-renewable resource required is the separate utilization Case 0, while the most economically feasible concept is Case 1 as it has the lowest levelized cost of electricity production and thus the fasted investment payback period. Figures 4.19a - 4.19e display the results of the multi-criteria analysis of the system concepts, where each criteria is weighted against another giving only one optimum system concept at each point in the ternary graph. Note that the carbon conversion range between maximum energy mode and maximum biochar mode is given by the brightness of the colour for each system concept, where the brightest represents maximum energy mode and the lightest the maximum biochar mode.

It can be seen in the figure, that the separate utilization Case 0 dominates a large part of the area in the pyramid. The reason is that by comparison, Case 0 is optimal by a larger margin in terms of non-renewable resource requirements than the optimum concept based on climate change impact and economic feasibility are to the other concepts. However, this does not necessarily indicate that Case 0 is optimal as when more weight is given to economic feasibility Case 1 could be found to be optimal (depending on the weight given to economic feasibility compared to other criteria) and if more weight is given to climate change impact either Case 1 or Case 3 become optimal. Additionally, if more weigh is given to the climate change criteria and environmentally feasible production is substituted Case 3 at maximum biochar production operation becomes optimal.

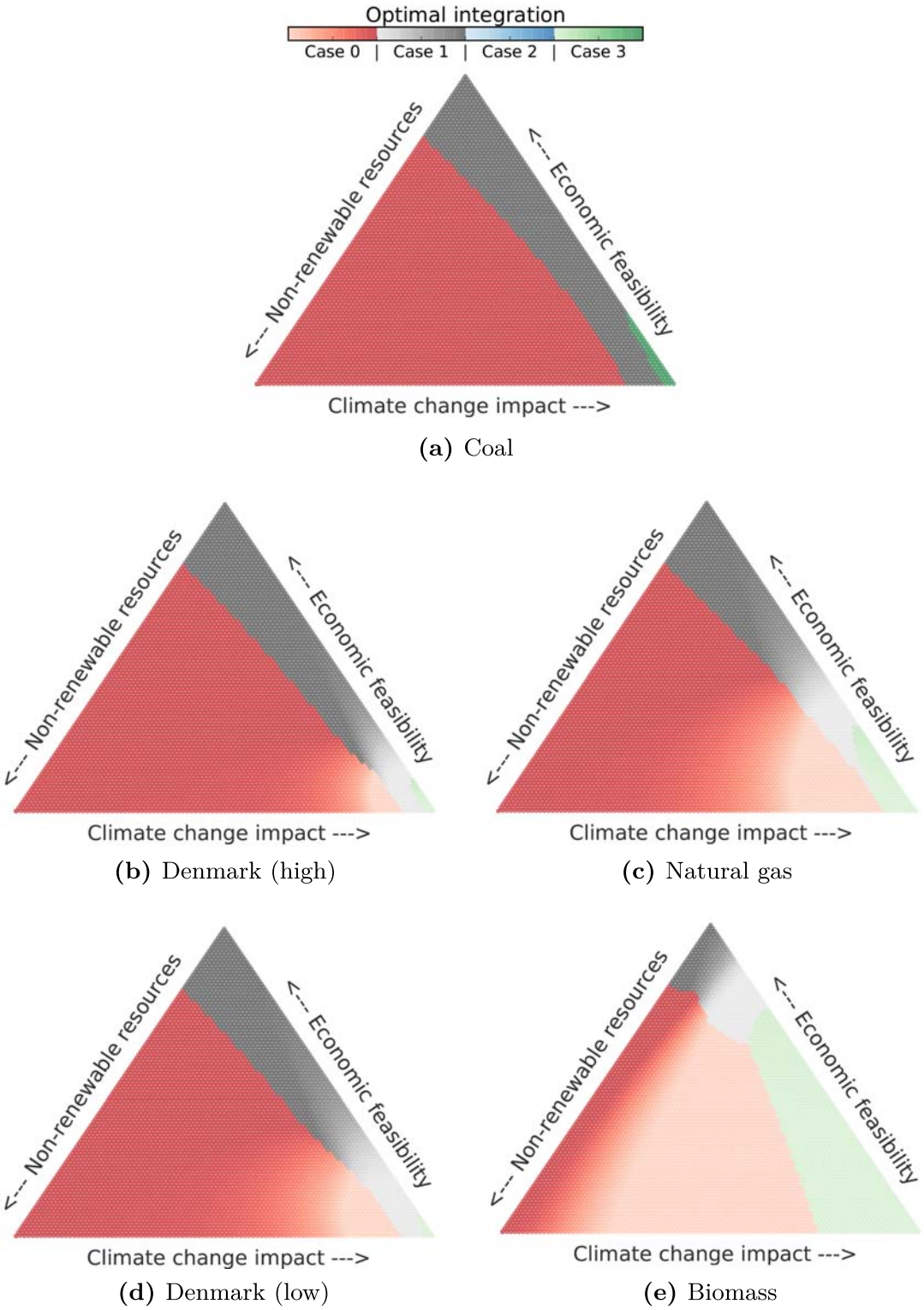

Figure 4.19: *Ternary graphs showing the optimum system concept and operation mode by weight of each criteria to another.*

Chapter 5

Discussion

This chapter discusses the main findings of the thesis. First the results from the energy analysis and climate change impact assessment are reviewed, followed by the findings of the soil carbon build-up analysis. Then the results of the exergy analysis and non-renewable resource requirements assessment are studied. After which the findings of the economic feasibility analysis are assessed, and finally the optimal bioenergy system concept is discussed.

5.1 Energy Analysis and Climate Change Impact

In the energy analysis of the bioenergy system concepts it was found that combined utilization of straw and manure results in increased heat and power production compared with separate utilization. The greatest increase in electrical production was found when the manure is digested alone in the biogas power plant and the solid fractions of the digestate

are then co-gasified with straw in the thermal power plant (Case 1). The greatest increase in district heat and overall fuel utilization was found when the biogas power plant is skipped and the solid fractions of raw manure are co-gasified with straw (Case 3). In addition, it was found that the energy efficiency of the system concepts impacted significantly the final climate change impact results, but not as much as the carbon sequestration by biochar production and nutrient recovery from organic fertilzer production. From Figure 1.1 based on data from the Danish Energy Agency [3], it is shown there that significant amount of coal and natural gas are still used in combined heat and power (CHP) plants in Denmark and according to the goal set by the government to be independent on fossil fuels in year 2050 [1], ideally either coal or natural gas fuelled production would be substituted. If coal or natural gas fuelled production is substituted the optimum bioenergy system concept is Case 3, in terms of climate change impact.

As in the article by Sastre [23], it was found that the loss of soil organic carbon from agricultural soils when utilizing residual resources from agriculture for bioenergy is the greatest contribution to climate change impact. However, as indicated by Mao [31] and Brandao [32], that impact was shown to be abated by biochar production at a certain production level. Nevertheless, the analysis of the biochar production in the LT-CFB gasifier found that for every additional kg of carbon in biochar, the electrical and district heat production decrease respectively by about 10.5 MJ and 17.7 MJ. Which resulted in -4.03 kg-CO_2, -1.95 kg-CO_2 and -0.23 kg-CO_2 loss of avoided emissions when substituting coal, natural gas or biomass fuelled CHP production, respectively. But this is counterweighted by carbon sequestration potential of the carbon in biochar, which was found to be 3.26 kg-CO_2/kg-C. This resulted in an overall benefit by lowering carbon conversion in the gasifier when the substituted production is not fuelled with coals, using impact data from the ecoinvent 3.3 database [58]. The mitigating impact of carbon sequestration per kg unconverted carbon can also be compared with the data on greenhouse gas emissions from Cherubini at al. [4] which are taken from the GEMIS 4.42 database and gives upper and lower limit of climate change impact from a range of energy technologies using various fuels. Figure 5.1 displays the loss of avoided impact per kg carbon unconverted using data from GEMIS 4.42 in reference to the mitigation potential of carbon

in biochar by carbon sequestration in agricultural soils. If the avoided

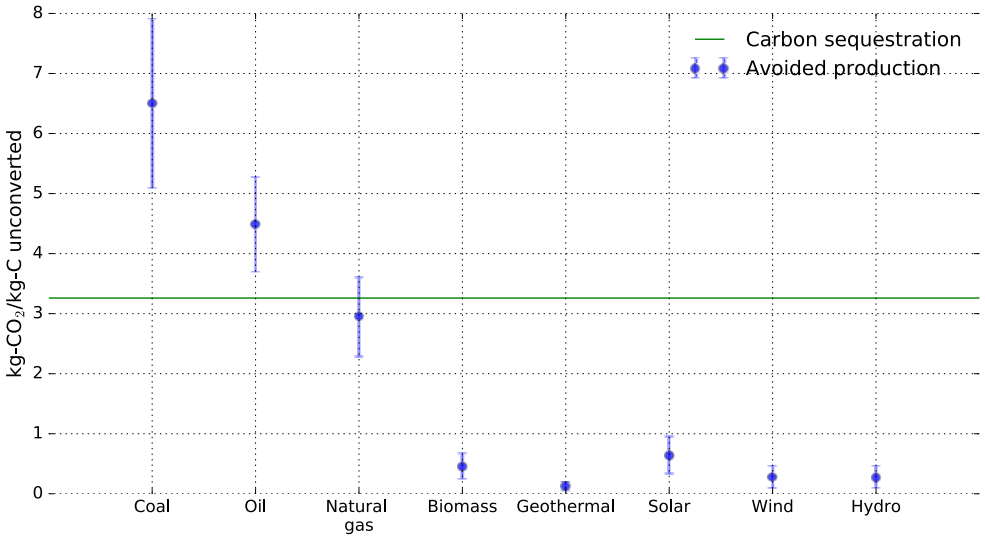

Figure 5.1: *Carbon sequestration mitigation impact per unconverted carbon vs loss of avoided production per unconverted carbon.*

production is above the green line it is better in terms of climate change impact to maximize the carbon conversion, but if it falls below the green line it is better to minimize carbon conversion. Basically, according to this it is better to maximize heat and power production if coal or oil fuelled CHP is substituted, but for natural gas fuelled and climate friendly production, it is better to maximize biochar production.

The uncertainty of the carbon sequestration potential was analysed by a sensitivity analysis of the assumptions made when modelling the decomposition of biochar in agricultural soils in Section 4.2. There the ratio of carbon input to the inert carbon pool was assumed to be 85% (α-ratio) and 100% (β-ratio) of the remaining 15% were assumed to enter a slow decay carbon pool. The resulting carbon sequestration was analysed by varying the α-ratio and β-ratio where more of the 85% enters the slow decay pool instead of the inert pool and instead of entering the slow decay pool more of the carbon enters the fast decay pool, respectively.

As the graph shows, the α ratio is more sensitive to change and that the β-ratio has a very small impact on the carbon sequestration potential. When comparing these results with Figure 5.1, it can be seen that if the α-ratio is decreased by 20% the carbon sequestration potential will be less

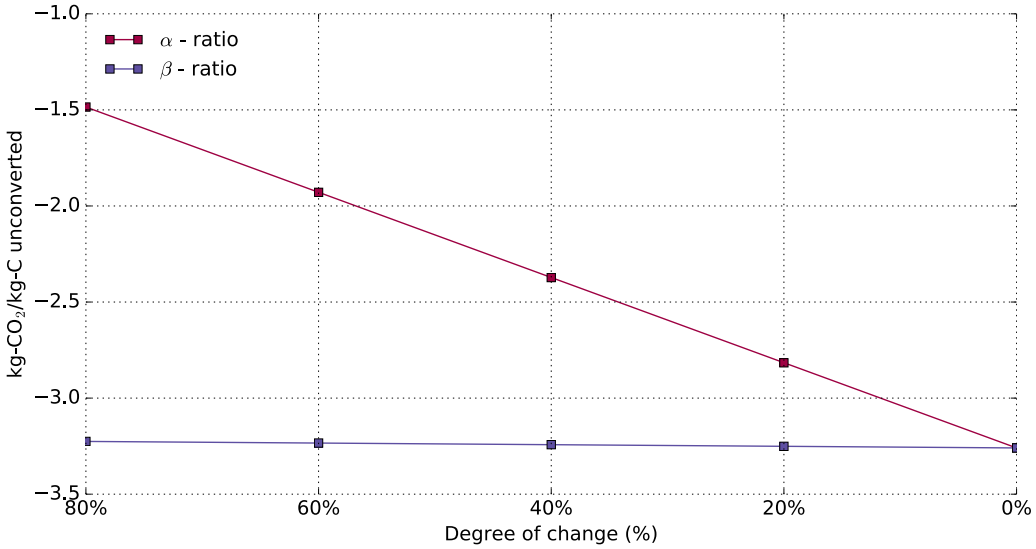

Figure 5.2: *Sensitivity analysis of the carbon sequestration potential of carbon in biochar per kg unconverted carbon.*

than the average climate change impact avoided if a production fuelled with natural gas is substituted. It can also be seen that although the α-ratio is decreased by 80% it is still better to minimize carbon conversion if the substituted production is environmentally friendly (hydro, solar, wind, biomass or geothermal).

Using the Low Temperature Circulating Fluidized Bed (LT-CFB) opens up new pathways for bioenergy production, as gasification of fuels commonly disregarded for such utilization become available. These results show that co-gasifying straw with manure or digestate is just as relevant in terms of energy efficiency as co-digestion and utilization of straw and manure should be analysed together to achieve greater heat and power production from biomass. Additionally, these results show that biochar production is very relevant if the goal is to mitigate climate change and the correct balance between energy generation and biochar production could result in a zero net emission irrespective of avoided fossil fuel utilization while still achieving decent energy efficiency. Moreover, these results underline the importance of considering the whole carbon flow when analysing climate change impact from bioenergy systems.

5.2 Soil Carbon Build-up

When the gasifier was analysed in isolation for straw and manure input, it was found that for every carbon in straw about 9% and 18% would need to be unconverted for equivalent soil carbon build-up as leaving straw on the field after 100 years and 25 years, respectively. For manure this % was found to be 15% and 22%, respectively. The reason for the time required to reach equivalent soil carbon build-up is a result of the difference in emission profiles of decaying straw and manure to biochar. The soil carbon build-up when leaving straw on field and applying manure as fertilizer is rapid in the first 10-20 years, but will then stabilize and reach equilibrium some 100 years later. Biochar soil carbon build-up on the other hand is more steady and will continually increase soil carbon content within a reasonable time-frame, this can be seen in Figure 3.23. The reason for lower carbon conversion requirements to balance the manure removal from agriculture compared with straw is that the carbon in manure decays more slowly than carbon in straw and thus builds-up more soil carbon. The biochar production per carbon input will then need to be increased to compensate for the added loss compared with straw utilization.

The sensitivity of these results are analysed by the same method as above for the carbon sequestration potential of unconverted carbon in biochar. Figure 5.3 shows the carbon conversion factor required in the gasifier to achieve equivalent soil carbon build-up after 100 and 25 years as incorporating straw and manure in soil, while varying the α-ratio. The sensitivity analysis shows that significant change in the α-ratio assumption is required for the straw utilization to not achieve equivalent carbon build-up when operating the gasifier at 80% carbon conversion or lower. For manure utilization, the change in α-ratio has more influence, but at the 100th year the change will also need to be significant and at the 25th year reference, the increase in α-ratio will need to be about 20% higher to achieve the same carbon build-up. However, a 20% decrease in α-ratio leads to 70% carbon stability in soil 100 years after application which is considerably lower than the 85% as assumed by Laired et al. [111], and 83% as assumed by Song and Guo [112].

Moreover, in the analysis of the system concepts, it was found that Case

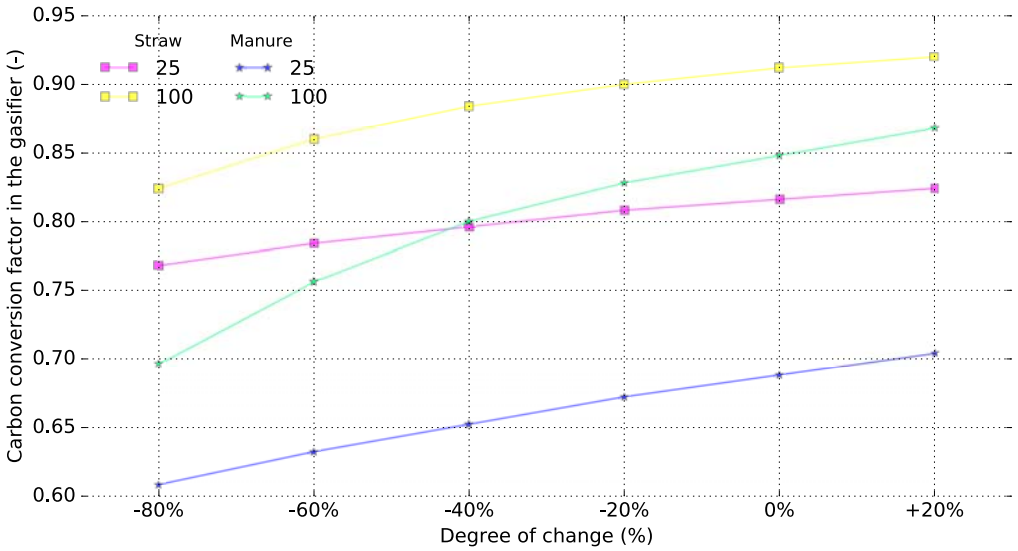

Figure 5.3: *Sensitivity analysis of the carbon soil build-up potential of carbon in biochar per kg unconverted carbon.*

3 has the best build-up potential, followed by Case 1 and Case 2 has a lowest potential for build-up. When comparing the 100th year soil carbon build-up for the system concepts to that of not harvesting the straw and applying the raw manure to agricultural field as fertilizer, a surplus carbon build-up of 11.1, 12.2, 1.5 and 16.0 kg carbon in soil per kg carbon utilized yearly was found, if production of biochar is maximized, for Cases 0-3, respectively. To have an equivalent soil carbon build-up after 25 years it was found that the carbon conversion in the gasifier would need to be about 75% for cases 0 and 1, and 78% for Case 3. However, Case 2 does not reach the equivalent soil carbon build-up at maximum biochar production mode within the expected lifetime.

As one of the main concerns regarding intensive biomass utilization is loss of soil carbon content and soil depletion [6, 7], these results could give an estimate to the required biochar production in order to compensate for carbon loss in soils when utilizing straw and manure. However, although the stability of biochar in soil is significantly higher, leaving straw incorporation in soil still improves several soil quality parameters as it increases microbial activity [126] which should not be overlooked. This could mean that a balance of straw and biochar input to soil could be the best solution to maintain and even increase soil quality while increasing biomass utilization for bioenergy.

5.3 Exergy Analysis and Non-renewable Resource Requirements

Like in the energy analysis, the exergy efficiency of the bioenergy system increased when straw and manure were utilized together, resulting in about 15.5% increase in product exergy when comparing Case 3 with separate utilization in Case 0. However, it was found that the exergy product (heat and power) is similar for Cases 1-3 (30%, 28% and 31% of the utilized fuel). Because of that, the Exergy Return on Investment (ExROI) was found to be determined by the non-renewable Cumulative Exergy Demand (CExD). As a result, the optimum system concept in terms of non-renewable resource requirements was found to be Case 0. The reason is mainly due to lower impact from transportation and more avoided mineral fertilization.

Because of lower exergy product when maximizing biochar production, the ExROI factor of that mode of operation is smaller than at maximum energy mode. Increasing the biochar production results in a small increase in CExD as its input to soil was not assumed to replace any other product. However, it should be noted that although not included in the modelling of this work, the long term effect on the soil could be significant and impact the CExD of the agricultural system. As it was modelled, the nitrogen balance was only effected by the biochar input with decreased dinitrogen monoxide emission (indirectly because of less leaching). Decreased dinitrogen monoxide emissions was identified as

important benefit of biochar application in a review article by Blanco-Canqui [127] about how to offset carbon losses from agriculture due to residual resource utilization for bioenergy. However, he also noted that change in yield showed mixed results between articles. Nevertheless, in a study by Vaccari et al [128] biochar application to an agricultural field did show improvements in yield, as did Peng et al. [129].

To test the assumption made in this work regarding biochar effect on yield, the required decrease in nitrogen mineral fertilizers was analysed. According to ecoinvent 3.3 [58], using the market for mineral nitrogen fertilizer unit process, to fully mitigate the loss of exergy and non-renewable CExD of transport and application, the biochar production impact on the fertilizer requirements would need to result in about 0.16 kg nitrogen per kg carbon in biochar decrease. To only abate the non-renewable CExD of biochar application and transportation the decrease would need to be about 0.01 kg nitrogen per kg carbon in biochar. The nitrogen build-up per carbon build-up is commonly modelled [110, 16] by a 0.1:1 ratio. Assuming that, the nitrogen bound per kg carbon is 0.1 kg. This was modelled in this work by assuming that this nitrogen is immobilised (not available to the plant) and causes decrease in leaching. To have the same impact on yield as a mineral fertilizer that nitrogen would have to be mineralized. But even if all is mineralized it is not enough to abate the loss of exergy , but if 10% of the immobilized nitrogen is quickly mineralized it can mitigate the impact of transporting and applying the biochar on an agricultural field. It is thus thought to be unrealistic to assume that biochar production could offset exergy loss, but the benefits in agricultural soils could possibly be enough to compensate for the non-renewable CExD required to transport and application. But this will need to be analysed further.

These results highlight the faults of transportation using fossil fuels to increased utilization of biomass for heat and power production. Additionally, these results underline the importance of nitrogen flow in a life cycle perspective. Non-renewable resources are mostly required by transportation and fertilization. While the recycling efficiency of phosphorous and potassium is high and accessible to the crop [29], the drawback of gasification is that the nitrogen entering the thermal power plant is lost to the atmosphere as it is combusted in the steam cycle power plant with

the product gas. For the system to be free of non-renewable resources of transportation and fertilization, the system should include production of biofuels and nitrogen fertilizer. Or use fuel transportation and nitrogen fertilizers made from renewable resources.

5.4 Economic Feasibility

In the economic analysis, it was found that the economic feasibility of combined straw and manure utilization, compared with separate utilization (Case 0) was greater for Cases 1 and 3. This is a result of increased production and lower investment cost of the thermal power plant, as a result of economies of scale. However, the economic feasibility of the combined utilization concept represented by Case 2 is less feasible than Case 0. The main reason is the relatively high investment and O&M cost of the biogas power plant in that case. The lowest annual carrying charges were found in Case 3, mostly because of the avoided biogas power plant. However, in that case the fuel costs are highest because of the transportation cost of the solid manure fraction to the thermal power plant and low value of the fertilizer products. As a result the annual cost for Cases 0, 1 and 3 are similar.

Figures 5.4a - 5.4d show the results of a sensitivity analysis of the economic feasibility for each system concept. As shown in the figures, the capacity factor and cost allocation to the district heat product are most sensitive to change and affect the economic feasibility of the system concepts almost equally. For each system concept based on maximum energy generation the maximum increase in levelized cost of electricity (LCOE) production while still being under the premium feed-in tariff varies. The LCOE of the system concepts can only increase by 25%, 40%, 18% and 32% in cases 0-3, respectively. To be economically feasible the capacity factor can only decrease by about 20%-25% and the allocation of cost to electricity product can only increase by 20%-30%. For other changes, only the increase in fuel cost beyond about 40%-60% can result in economic infeasibility. However, at maximum biochar operation Case 0 is almost infeasible and Case 3 is economically infeasible. And for Cases 1 and 2 the LCOE can only increase by 11% and 8%, which gives very

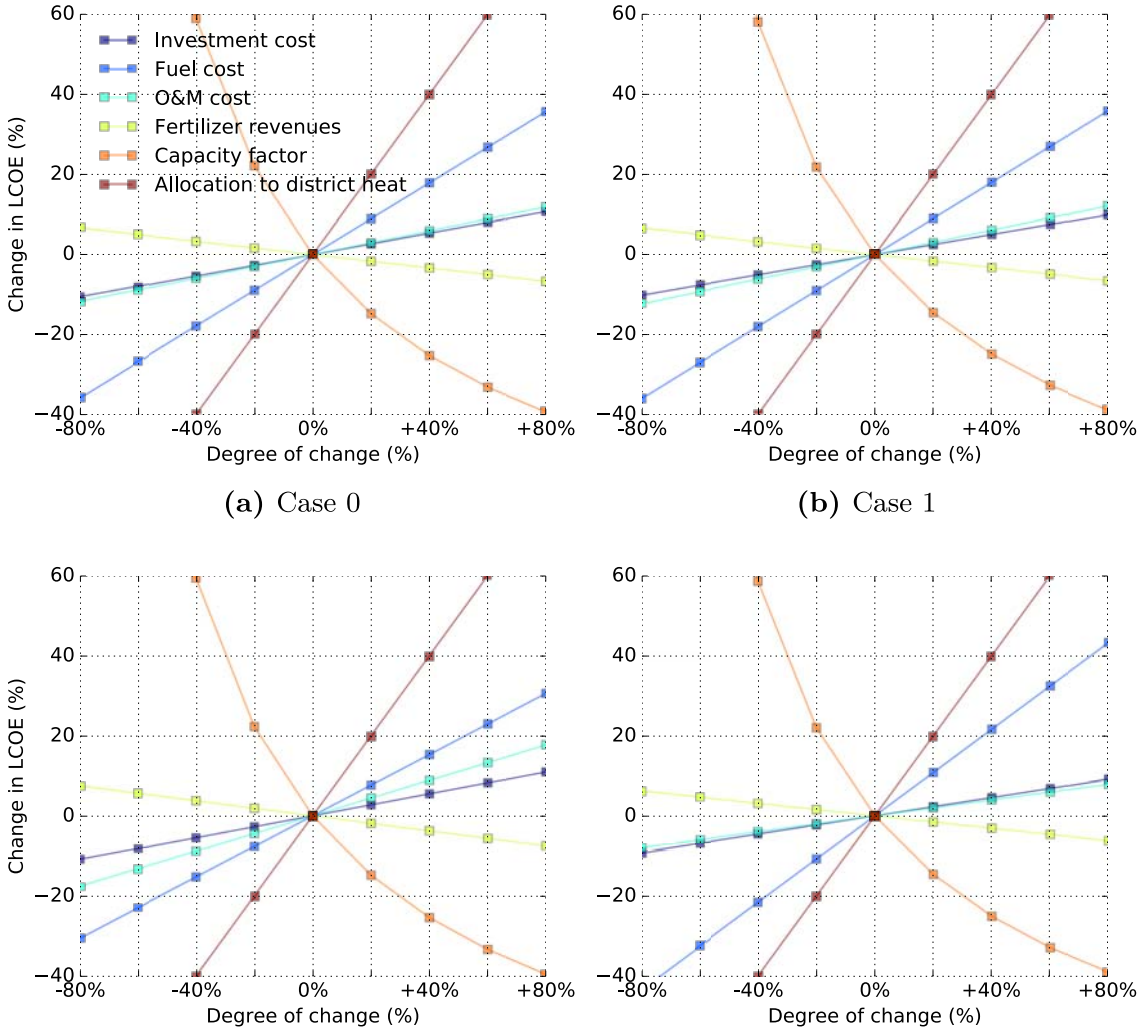

(a) Case 0 **(b)** Case 1

(c) Case 2 **(d)** Case 3

Figure 5.4: *Sensitivity analysis of the levelized cost of electricity production for each system concept.*

small room for changes that contribute to increased LCOE.

Further it was found that the revenues from fertilizer sales did not increase enough to compensate for lost revenues because of less electricity production, despite lower carrying charges and O&M cost. The biochar product was assumed to be sold at the same cost as the cost of fertilizers needed to deliver equal amount of nutrients and carbon was valued by the current and future carbon emission quotas. It is relevant to find out what the value of carbon would need to be for the decrease in carbon conversion to be economical. To be able to offset the loss of electricity sales revenues, the increase in revenues from biochar sale per kg unconverted carbon will need to be about 0.105 Euro after tax. This would require the price of carbon to increase significantly beyond the price of carbon quotas.

The comparison between the Elspot system price on the free Nordic electricity market with the expense of running the power plants in the system concepts shows that the expense of running is close to the average system price. Which could mean that these system concepts can participate in the market. However, the levelized cost of the production is considerably higher when including the carrying charges. To be economically feasible the system concepts need the premium feed-in tariffs subsidies. But it is also interesting to compare the levelized cost of electricity production with the aggregated levelized cost of producing electricity in Denmark based on research by Levitt and Sørensen [123, 124], to put the system concepts in perspective. It was found that the cost of the system concepts is a bit higher than the aggregated cost in Denmark. This could indicate that by adding production using the system concepts analysed in this thesis in Denmark would increase the aggregated cost and possibly lead to increase in electricity prices. But that also depends on what production is replaced and its levelized cost. However, to know that will require further research.

5.5 Optimal System Concept

The results showed that the optimum system concept depends on the criteria. The multiple criteria analysis was done by plotting the optimum system concept based on all possible weight options between each criteria.

That analysis showed that if all is equal, the non-renewable resource requirements criteria decides the optimum and Case 0 is then found to be optimal, but the optimum mode of operation depends on the avoided production. Nevertheless, this does not necessarily proof that Case 0 is optimal as when more weight is given to economic feasibility or climate change impact either Case 1 or Case 3 could be found to be optimal. As noted by Buchholz et al. [35] the most important criteria for sustainable bioenergy system is climate change impact. However, Case 2 where straw and manure are co-digested was not found to be optimal at any point in the ternary graphs. These results show that co-gasification of straw with manure or digestate production should be considered as a relevant option in current and future bioenergy systems.

It should be noted here that the system concepts analysed in this work assume a certain mass ration of straw to manure. That ratio was found based on the optimum mix for the co-digestion process in Case 2 (see Section 3.3.2). However, it is unlikely that this will be the ratio in a specific region where such a system would operate. Despite that, the analysis on the optimum concept is relevant as it is assumed that the optimum concepts for each criteria would not change as, e.g. if the amount of straw relative to manure is more than what is assumed, the extra straw will be gasified in the thermal power plant. The reason is that the co-digestion in Case 2 would always be done using the optimum mix and the rest is gasified and in the other cases this would only add straw to the thermal power plant. Also if there is more manure available, part of the raw manure would be de-watered to increase the C/N ratio when co-digesting with straw in Case 2, in the same way as was done in Cases 0 and 1.

References

[1] D. M. of Climate. Energy and Buildings. *Our Future Energy*. Tech. rep. Copenhagen: Danish Ministry of Climate. Energy and Buildings.

[3] *Energy Statistics 2013: Data, tables, statistics and maps*. Tech. rep. Copenhagen: Danish Energy Agency, 2015.

[4] F. Cherubini et al. "Energy-and greenhouse gas-based LCA of biofuel and bioenergy systems: Key issues, ranges and recommendations". In: *Resources, conservation and recycling* 53.8 (2009), pp. 434–447.

[6] D. S. Powlson et al. "Implications for Soil Properties of Removing Cereal Straw: Results from Long-Term Studies". en. In: *Agronomy Journal* 103.1 (Jan. 2011), p. 279. DOI: 10.2134/agronj2010.0146s.

[7] N. H. Batjes. "Total carbon and nitrogen in the soils of the world". In: *European Journal of Soil Science* 65.1 (Jan. 2014), pp. 10–21. DOI: 10.1111/ejss.12114_2.

[16] T. L. T. Nguyen, J. E. Hermansen, and R. G. Nielsen. "Environmental assessment of gasification technology for biomass conversion to energy in comparison with other alternatives: the case of wheat straw". In: *Journal of Cleaner Production* 53.0 (2013), pp. 138 –148. DOI: http://dx.doi.org/10.1016/j.jclepro.2013.04.004.

[23] C. Sastre, Y. González-Arechavala, and A. Santos. "Global warming and energy yield evaluation of Spanish wheat straw electricity generation – A LCA that takes into account parameter uncertainty and variability". In: *Applied Energy* 154 (2015), pp. 900 –911. DOI: http://dx.doi.org/10.1016/j.apenergy.2015.05.108.

[29] D. Muller-Stover et al. "Soil application of ash produced by low-temperature fluidized bed gasification: effects on soil nutrient dynamics and crop response". English. In: *Nutrient Cycling in Agroecosystems* 94.2-3 (2012), pp. 193–207. DOI: 10.1007/s10705-012-9533-x.

[31] J.-D. Mao et al. “Abundant and stable char residues in soils: implications for soil fertility and carbon sequestration”. In: *Environmental science & technology* 46.17 (2012), pp. 9571–9576.

[32] M. Brandão et al. “Key issues and options in accounting for carbon sequestration and temporary storage in life cycle assessment and carbon footprinting”. In: *The International Journal of Life Cycle Assessment* 18.1 (June 2012), pp. 230–240. DOI: 10.1007/s11367-012-0451-6.

[35] T. Buchholz, V. A. Luzadis, and T. A. Volk. “Sustainability criteria for bioenergy systems: results from an expert survey”. In: *Journal of Cleaner Production* 17, Supplement 1 (2009). International Trade in Biofuels, S86 –S98. DOI: http://dx.doi.org/10.1016/j.jclepro.2009.04.015.

[58] B. Weidema et al. *The ecoinvent database: Overview and methodology, Data quality guideline for the database version 3.* 2013.

[110] T. L. T. Nguyen, J. E. Hermansen, and L. Mogensen. “Environmental performance of crop residues as an energy source for electricity production: The case of wheat straw in Denmark”. In: *Applied Energy* 104.0 (2013), pp. 633 –641. DOI: http://dx.doi.org/10.1016/j.apenergy.2012.11.057.

[111] D. A. Laird et al. “Review of the pyrolysis platform for coproducing bio-oil and biochar”. In: *Biofuels, Bioproducts and Biorefining* 3.5 (Sept. 2009), pp. 547–562. DOI: 10.1002/bbb.169.

[112] W. Song and M. Guo. “Quality variations of poultry litter biochar generated at different pyrolysis temperatures”. In: *Journal of Analytical and Applied Pyrolysis* 94 (Mar. 2012), pp. 138–145. DOI: 10.1016/j.jaap.2011.11.018.

[123] C. J. Levitt and A. Sørensen. *The Cost of Producing Electricity in Denmark.* Tech. rep. Rockwool Fondens Forskningsenhed, 2014.

[124] C. J. Levitt and A. Sørensen. *The Cost of Producing Electricity in Denmark: A Technical Companion.* Tech. rep. Rockwool Fondens Forskningsenhed, 2014.

[126] V. Hansen et al. “The effect of straw and wood gasification biochar on carbon sequestration, selected soil fertility indicators and functional groups in soil: An incubation study”. In: *Geoderma* 269 (2016), pp. 99–107.

[127] H. Blanco-Canqui. "Crop Residue Removal for Bioenergy Reduces Soil Carbon Pools: How Can We Offset Carbon Losses?" In: *BioEnergy Research* 6.1 (2013), pp. 358–371. DOI: 10.1007/s12155-012-9221-3.

[128] F. Vaccari et al. "Biochar as a strategy to sequester carbon and increase yield in durum wheat". In: *European journal of agronomy* 34.4 (2011), pp. 231–238.

[129] X. Peng et al. "Temperature-and duration-dependent rice straw-derived biochar: Characteristics and its effects on soil properties of an Ultisol in southern China". In: *Soil and Tillage Research* 112.2 (2011), pp. 159–166.

Chapter 6

Conclusion

This chapter gives the final conclusions of the research activities disclosed in this thesis. First the answers to research questions I-VI are provided. Then the recommendation for future work in integration of bioenergy and agriculture are given, along with a final statement for conclusion of this work.

6.1 Summary of Findings

This study aims at to developing, modelling and analysing integrated bioenergy and agricultural system concepts to facilitate increased biomass utilization as an energy source in Denmark without adverse affects on the agricultural system. The author accomplishes this task by elaborating on four system concepts with varied biochar production using multiple assessment methods.

Research question I: Mitigation of soil carbon loss.
The results demonstrated that choosing the right carbon conversion in the Low Temperature - Circulating Fluidized Bed (LT-CFB) gasifier, the soil carbon loss when removing the straw and manure from the agricultural system could be mitigated. It was further found that production of biochar and application on agricultural fields could even result in soil carbon surplus. To have the equivalent soil carbon build-up as leaving straw on the field at the end of the technical life of the gasifier (25 years), the straw need to be gasified leaving about 18% of the carbon unconverted. For manure gasification 32% of the carbon input needs to go into biochar production, which results in a carbon conversion lower than the defined lower limit for the system. The bioenergy system concepts analysed in this work could all mitigate soil carbon loss within a 100 year time-frame by decreasing carbon conversion from maximum to about 90% - 75%, depending on concept. The co-gasification of solid manure fraction and straw showed the best potential, and all but one concept could mitigate soil carbon loss within 25 years by decreasing the carbon conversion to about 78% - 75%. The system concept where manure and straw are first co-digested with the subsequent gasification of the solid fraction from the digestate was found to be unable to mitigate soil carbon loss within the technical lifetime of the gasifier.

Research question II: Impact of recycling nutrients and carbon.
Returning nutrients and carbon after using the resource for energy generation, has a positive affect on the climate change impact, decreased demand for non-renewable resources and increased revenues. It was found that returning the liquid fractions after de-watering manure and digestate almost fully abated the impact of removing raw manure from the agricultural system. The biochar is able to returns most of the phosphorus and potassium back to agriculture, but the carbon conversion in the gasifier needs to be about 79% - 84% to fully abate the climate change impact of the carbon sequestration loss. However, increased biochar production showed adverse results based on non-renewable resource requirements and economic feasibility.

Research question III: Biochar production impact on efficiency.
Increasing biochar production in the LT-CFB gasifier has an impact on heat and power production in the thermal power plant. The gasification process requires energy from char gasification to sustain its pyrolysis process. It was found that the lowest feasible carbon conversion (resulting in maximum biochar production) was 70% to sustain the pyrolysis process and generate enough energy for the steam dryer while still producing heat and power. Simulation of the thermal power plant showed that with every kg of carbon unconverted by lowered carbon conversion, the decrease in product gas energy and exergy content is 31 and 32 MJ, respectively. Which results in about 28.2% and 13.2% decrease in fuel utilization in energy and exergy terms, receptively.

Research question IV: Climate change mitigation by integration.
There is a net gain in climate change impact in the agricultural system if straw and manure resources are removed, if they are used in a bioenergy system which maximises energy generation. This results in a net climate change impact of the overall system. However, if the bioenergy system is designed to produce both biochar (and organic fertilizers), the right mix of energy generation and biochar production will mitigate those adverse impacts. Nevertheless, as found in the answers to research questions II and III, increased biochar production will increase carbon sequestration while decreasing energy efficiency. By taking into account the loss of avoided impact by substituted energy generation as energy efficiency decreases, it was found that as long as the avoided production is not fuelled with coal or oil for both heat and power products, the overall climate change impact will decrease with increased biochar production.

Research question V: Economic feasibility of the bioenergy system.
All system concepts analysed in this work were found to be economically feasible when operated for maximum heat and power production, based on revenues from electricity sales at premium feed-in tariff prices. For all concepts the operation would need to be relatively steady year-round as the minimum capacity factor to ensure economic feasibility was found to be about 63.5%. At maximum biochar production operation, all system concepts except co-gasification of straw and solid manure fraction (Case 3) are feasible. However, the sensitivity analysis showed that a small increase in cost or revenue loss will lead to infeasibility.

Research question VI: Optimal bioenergy system concept.
Based on the results of the climate change impact, the optimal system concept is solid fraction of manure after de-watering are co-gasified with straw in the thermal power plant for at maximum heat and power production, if coal fuelled production is substituted. But if natural gas or even more environmentally friendly production is substituted the optimum system concept is still Case 3 but operated for maximum biochar production. Based on results of the non-renewable resource requirements, the optimal system concept is separate utilization of straw and manure in respectively the thermal and biogas power plants, operated at maximum carbon conversion. And based on economic feasibility the optimal system concept is digestion of manure and co-gasification of solid digestate fraction with straw, operated for maximum heat and power production. Based on the multi-criteria analysis, the non-renewable resource requirements results decides the optimum if all weights are equal between each criteria. However, if more weight is put on economic feasibility or climate change impact, the optimum concept is likely to be digestion of manure with subsequent co-gasification of solid manure fractions and straw.

6.2 Recommendations for Further Work

The modelling in this work is focused on residual biomass utilization by including carbon and macro-nutrient balances over the life cycle of the resource utilization in a few bioenergy system concepts. Doing similar research by including dedicated energy crops would be the logical next step. This would then not necessarily include only low temperature gasification for thermochemical conversion as more woody energy crops can easily be utilized in other types of gasifiers, e.g. TwoStage gasifier [17] which is more efficient at lower capacities. It is expected that recycling of nutrients and carbon could be just as interesting for those types of systems. Additionally, the energy simulation model of the low temperature gasifier should be further developed with increased access to the technology. During the largest part of this project the LT-CFB gasification technology owned by Dong Energy AS was undergoing sales process which restricted the information.

This study was graced by being in close collaboration with the study on carbon sequestration potential of biochar and its impact on agriculture soils from the LT-CFB gasifier [33, 126]. This collaboration aided in the simulation of the soil carbon build-up and carbon sequestration of biochar in this work. However, that research could only analyse the impact over the time of one PhD and the simulation in this work covered up to 100 years after application. Further research on the stability of biochar from gasification is needed to strengthen the estimations made in this work.

Expanding the multi-criteria decision analysis with fuzzy-TOPSIS [130], which will account for the imprecision of the collected data in the decision analysis. It would be interesting to enable utilization of the confidence interval from Monte Carlo simulation in the analysis as boundaries of vagueness in the data in this way. However, it is also important that efforts are made to weigh the criteria to each other by an analysis of the relative importance of each criteria to the stakeholders. This could be done by the Delphi technique which is often used to find the most important criteria to a certain group [131].

6.3 Final Statement

It was revealed that developing bioenergy systems to maximize energy generation, their operation will results in a net decrease in soil carbon build-up which can compromise soil quality in the agricultural system. But when decreasing energy efficiency and increasing biochar production the soil carbon build-up can be re-established and even increased beyond the potential if the residual resources are not utilized by the energy system. It was further found that by applying the analytical framework and analysing climate change impact of straw and manure utilization in the integrated bioenergy an agriculture system concepts, maximizing biochar production at the expense of energy generation proved to be the better option if theses systems would avoid energy generations from natural gas. However, the economic feasibility analysis and the non-renewable resource requirements analysis revealed that it is better to maximize energy generation. The effective utilization of residual resources from the agricultural system in the energy system is thus determined by a compromise between different criteria. This research further revealed that co-gasification of manure and/or digestate is just as relevant for heat and power production as co-digestion.

References

[17] J. Ahrenfeldt et al. “Biomass gasification cogeneration – A review of state of the art technology and near future perspectives”. In: *Applied Thermal Engineering* 50.2 (2013), pp. 1407 –1417. DOI: http://dx.doi.org/10.1016/j.applthermaleng.2011.12.040.

[33] V. Hansen et al. “Gasification biochar as a valuable by-product for carbon sequestration and soil amendment”. In: *Biomass and Bioenergy* 72 (2015), pp. 300 –308. DOI: http://dx.doi.org/10.1016/j.biombioe.2014.10.013.

[126] V. Hansen et al. “The effect of straw and wood gasification biochar on carbon sequestration, selected soil fertility indicators and functional groups in soil: An incubation study”. In: *Geoderma* 269 (2016), pp. 99–107.

[130] “Fuzzy TOPSIS method based on alpha level sets with an application to bridge risk assessment”. In: *Expert Systems with Applications* 31.2 (Aug. 2006), pp. 309–319. DOI: 10.1016/j.eswa.2005.09.040.

[131] F. Hasson, S. Keeney, and H. McKenna. “Research guidelines for the Delphi survey technique”. In: *Journal of advanced nursing* 32.4 (2000), pp. 1008–1015.

Appendix

A. Peer Review Articles

During the work on this thesis two journal papers and two conference paper were made.

Paper I includes the modelling and simulation of the Low Temperature Circulating Fluidized Bed gasifier in a polygeneration power plant producing heat, power and biochar. The evaluation and results underline the importance of the biochar as a product.

Paper II uses the same methods as Paper I, but on another polygeneration thermal power plant using the TwoStage gasifier and the fuel is wood chips from forest residues. The biochar is applied on an agricultural field and the results of this paper further underlines the importance of biochar as a product of bioenergy systems.

Paper III introduces the modelling framework of this thesis, which combines energy system simulation, soil carbon simulation and Life Cycle Assessment.

Paper IV applies the multi-criteria framework on the system analysed on paper I, by including non-renewable resource utilization and economic

feasibility. That paper shows that the optimum operation of the gasifier depends on the chosen criteria and a compromise between their goals are necessary for a truly optimum operation.

Applied Energy 160 (2015) 511–520

Contents lists available at ScienceDirect

Applied Energy

journal homepage: www.elsevier.com/locate/apenergy

Climate effect of an integrated wheat production and bioenergy system with Low Temperature Circulating Fluidized Bed gasifier

Hafthor Ægir Sigurjonsson [a,*], Brian Elmegaard [a], Lasse Røngaard Clausen [a], Jesper Ahrenfeldt [b]

[a] Department of Mechanical Engineering, Technical University of Denmark, Nils Koppels Alle 403, 2800 Kongens Lyngby, Denmark
[b] Department of Chemical Engineering, Technical University of Denmark, Frederiksborgvej 399, 4000 Roskilde, Denmark

HIGHLIGHTS

- Wheat straw removal from agricultural system has considerable GWP effect.
- Changing the carbon conv. in the gasifier to 0.8–0.86 mitigates those effects.
- Considerable difference is between sequestration potential of straw and biochar.
- Lowering the carbon conversion improves GWP, but depends on subst. technology.

ARTICLE INFO

Article history:
Received 12 June 2015
Received in revised form 22 August 2015
Accepted 24 August 2015

Keywords:
Life Cycle Assessment
Wheat production
Straw utilization
Thermal gasification
Carbon soil sequestration

ABSTRACT

When removing biomass residues from the agriculture for bioenergy utilization, the nutrients and carbon stored within these "residual resources" are removed as-well. To mitigate these issues the energy industry must try to conserve and not destroy the nutrients. The paper analyses a novel integration between the agricultural system and the energy system through the Low Temperature Circulating Fluidized Bed (LT-CFB) gasifier from the perspective of wheat grain production and electricity generation using wheat straw, where the effects of removing the straw from the agricultural system are assessed along with the effects of recycling the nutrients and carbon back to the agricultural system. The methods used to assess the integration was Life Cycle Assessment (LCA) with IPCC's 2013 100 year global warming potential (GWP) as impact assessment method. The boundary was set from cradle to gate with two different functional units, kg grain and kW h electricity produced in Zealand, Denmark. Two cases were used in the analysis: 1. nutrient balances are regulated by mineral fertilization and 2. the nutrient balances are regulated by yield. The analysis compare three scenarios of gasifier operation based on carbon conversion to two references, no straw removal and straw combustion. The results show that the climate effect of removing the straws are mitigated by the carbon soil sequestration with biochar, and electricity and district heat substitution. Maximum biochar production outperforms maximum heat and power generation for most substituted electricity and district heating scenarios. Irrespective of the substituted technologies, the carbon conversion needs to be 80–86% to fully mitigate the effects of removing the straws from the agricultural system. This concludes that compromising on energy efficiency for biochar production can be beneficial in terms of climate change effect of an integrated wheat production and bioenergy system.

1. Introduction

Climate change, security of supply and depletion of fossil fuels have become increasingly well-known issues, and the combination of the three has instigated a worldwide attention on finding pathways for sustainable energy supply [1,2]. Increased use of biomass feedstock for transport, power and heat generation are generally perceived as relevant methods to mitigate these concerns. However parallel to these before-mentioned issues are problems associated with food supply, population growth, land use, essential mineral depletion and soil degradation. All of which contribute to the increasing awareness of biomass as both an energy and food resource.

Moving from a fossil fueled energy system towards greater reliance on renewables, requires cautiously designed allocation of

* Corresponding author.
E-mail address: hafsig@mek.dtu.dk (HÆgir Sigurjonsson).

http://dx.doi.org/10.1016/j.apenergy.2015.08.114
0306-2619/

the obtainable resources and a highly flexible system [3]. In this perspective, gasification of biomass has proven its potential. A Low Temperature Circulating Fluidized Bed gasifier (LT-CFB), currently termed *Pyroneer*, was developed to be able to operate on biomass feedstock with high ash content that has proven difficult to use in other systems, e.g. straw, manure fibers, sewage sludge, organic waste etc. [3].

Biomass residues from the agricultural industry are normally taken to be readily available to the energy sector, and obvious to exploit for producing power, heat and fuels. However, what is not so obviously seen from the energy system's perspective is the fact that together with the removal of biomass residues from the agricultural sector, the nutrients and carbon within them are also removed. This entails the need to add nutrients and possibly carbon to the agricultural fields in order to maintain soil fertility and soil carbon content. This has been highlighted with recent environmental impacts studies on bioenergy. Djomo et al. [4] report the change in soil organic carbon for perennial energy crops to be climate change mitigating, conversely Sastre et al. [5] show that loss of carbon of soil carbon is the greatest contributor to the climate change effect of a bioenergy system utilizing wheat straw. It is also one of the conclusions of Yang et al. [6] and Parajuli et al. [7] that carbon loss from agricultural residue removal is an important contributor to climate change in a bioenergy system. Two latter papers discuss the impact of atmospheric carbon load due to biogenic carbon emissions, Parajuli et al. [7] uses the approach of Petersen et al. [8], which is very similar to the work of Guest et al. [9,10] for forestry systems.

Kuligowski et al. [11] concluded from a field study that ash derived from a low-temperature gasification of the fiber fraction from anaerobically digested pig slurry has the potential to be used to maintain phosphorus levels in agricultural soils. Müller-Stöwer et al. [12] further concluded that ash from low temperature gasification of biomass can replace mineral fertilizer. Moreover, in addition to the recycling of valuable nutrients, the use of ash containing recalcitrant carbon fractions could maintain or even increase soil organic carbon stocks and thus contribute to carbon sequestration as suggested by Brandao et al. [13]. Recently Veronika et al. [14] contributed to this discussion by experimental results indicate that gasification biochar is very stable in soil and has good potential for a longterm carbon sequestration in soil.

Realizing this, and integrating it into a bioenergy concept, can create the foundation of a flexible and sustainable use of biomass resources, and make such a bioenergy system a genuinely climate neutral or even climate mitigating source of energy. Nguyen et al. [15,16] used Life Cycle Assessment (LCA) to assess the environmental concerns of using wheat straw in the energy system and applying the ash back to the field using both combustion and gasification technologies. However, it was noted that more research was required on the issue to conclude on those results. This article is meant to shine a light on those issue and by further analyzing the carbon conversion (CC) in a polygeneration energy system producing; electricity, district heat and carbon rich "fertilizer" (named GBC in the article or gasification biochar). The system will be analyzed for three operational scenarios in the gasifier, i.e. maximum product gas production, maximum biochar production and a climate neutral scenario. These scenarios are compared with two reference scenarios, one where the straws are not harvested and thus no heat or power are generated, another with straw removal and combustion instead of gasification in the energy system.

Moreover, it is of interest to include in the analysis the total wheat production at a specific location in Denmark and to analyze more closely the consequences of the changes in soil nitrogen dynamics. This is done by computing a novel inter-connected model of the agricultural system and the energy system. Which combines carbon in soil simulation in C-TOOL [17,18], energy system simulation with Dynamic Network Analysis (DNA) [19], Life Cycle Inventory and Impact Assessment processing with Brightway2 [20], along with substance flow calculations and atmospheric carbon decay simulation.

2. Methods

2.1. System description

Energy system utilizing wheat straw for heat and power generation is analyzed. Ashes and biochar (GBC) are recycled back to the agricultural system, GBC is considered the third product of the energy system. Three scenarios (S1–S3) and two reference cases (RA and RB) are modeled.

2.1.1. Scenarios

- *RA: Straw not harvested.* Straws are not removed from the field and thus no electricity and heat production.
- *RB: Straw direct combustion.* Straws are removed from the field and combusted. Bottom ash is recycled back to the field and fly ash is landfilled.
- *S1: Maximum heat and power generation.* Straws are removed from the field and gasified with carbon conversion[1] (CC) of 95%, gas produced is combusted in an conventional combined heat and power (CHP) steam cycle and the GBC is returned to the field.
- *S2: Climate neutral.* Like High CC, but with a carbon conversion adjusted to make the mitigating effect of carbon soil sequestration equal to the impact of removing and utilizing the straw in the energy system.
- *S3: Maximum biochar production.* Like High CC, but the lowest possible carbon conversion is found from system simulation.

A simple schematic of the complete system including the agriculture and energy conversion is presented in Fig. 1. Grain yield per hectare is an input to the model and was assumed to be 8.0 tonnes.The harvestable residues, i.e., *straw* are calculated based on the residue harvest index (0.42), i.e. ratio between total residues and total harvest, while the straw part of the total residues was estimated to be 65%. The residues left on the field (referred to as *residues*) are equal to the total residues for RA, and equal to the difference between the total residues and the straw for RB and S1–S3. Ultimate analysis of the residues and straw was taken from Vassilev et al. [21] and the lower heating value (LHV) from Nguyen et al. [15]. Straw is then transported 20 km to the energy system where it is either directly combusted for heat and power generation or gasified at specific carbon conversion before the product gas can be combusted, the GBC or bottom ash is transported back to the same agricultural field 20 km away from the energy system.

2.2. Analytical approach

The analysis follows the framework of consequential LCA. The fertilization and field emissions were modeled by a nutrient balance based on inputs, what is harvested and the emissions that occur as a consequence. Other factors in the LCA, except for transportation between the field and the gasifier, were modeled with the aid of the Ecoinvent 3.1 database [22], i.e. the work processes, pesticides input, farm transport and seeds input. The Ecoinvent database was also used for all upstream processes. The analysis was made from cradle to gate for two functional units.

[1] Carbon conversion in the gasifier is the carbon ratio between fuel input and product gas out of the gasifier, the rest leaves the gasifier as biochar.

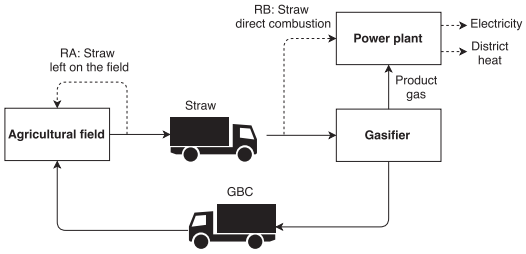

Fig. 1. Integrated bioenergy and agriculture system schematic.

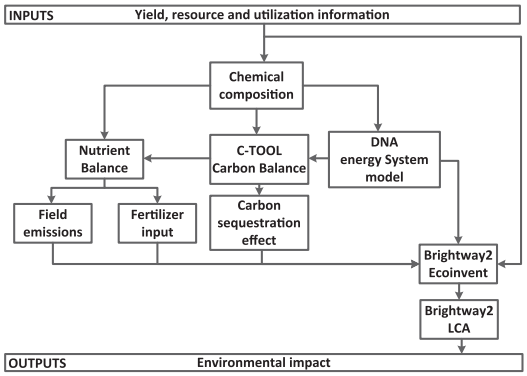

Fig. 2. Python system model.

2.2.1. Functional units

(1) kg of grain produced, to show the effect of wheat straw utilization in reference to the primary product of agricultural field.
(2) kW h of electricity produced, to show the effect of using wheat straw as a fuel in an energy system in reference to alternative resources.

The amount of carbon and the state of it is expected to have a significant effect on the nitrogen dynamics, as noted in Nguyen et al. [16]. Most changes are expected in the nitrogen build-up which affects the nitrogen leaching potential. The change in nitrogen balance was modeled for two cases. Case 1 regulates the nitrogen changes with the mineral fertilizer and constant yield, and Case 2 regulates the changes with the mineral fertilizer increase per decrease in nitrate leaching and vice versa. Which subsequently effects the yield, guidelines from the agricultural and fisheries ministry of Denmark were followed for yield impact from increase or decease in nitrogen fertilization [23]. Carbon soil sequestration potential was calculated by detail simulation of the atmospheric load of carbon emission from organic inputs to the agricultural soil, following the principles from Petersen et al. [8].

A computer model was made to calculate the LCA of the combined agricultural and bioenergy system. The model consists of blocks where the first one is a definition of the chemical composition of the residual and main product. This then connects to interconnected blocks of nutrient balance, soil carbon simulation, energy system model and the Ecoinvent 3.1 database [22]. The resulting Life Cycle Inventory (LCI) is passed to the LCA with the 2013 IPCC 100 year global warming potential [24] life cycle impact assessment (LCIA) method. The basic flow of the model is displayed in Fig. 2. The model is implemented in Python and is built on top of three freewares, i.e. Dynamic Network Analysis (DNA) for energy system modeling [19], C-TOOL for soil carbon simulation [17,18] and Brightway2 for Ecoinvent 3.1 database communication and LCA processing [20].

2.3. Agricultural system

The production is assumed to take place in Zealand Denmark, where the average high temperature during summer is 15.7 °C and the average low temperature during winter is 0.1 °C [25]. The rain fall is estimated to be 760 mm/year [25] and the soil is assumed to have a clay content of 12% and 2% soil organic carbon in the top soil. Nitrogen in organic matter is then calculated based on: 1. the soil organic carbon value, 2. the total soil nitrogen, 3. soil carbon and nitrogen ratio, 4. the ratio between nitrogen in organic matter and total soil nitrogen and 5. the soil volume and bulk density [26].

2.3.1. Nutrient balance

The average nutrient ratio between grain and straw from the Phyllis2 database [27] was used to calculate the macro nutrients, i.e. nitrogen, phosphorus and potassium (NPK), of the grain for the nutrient balance. In the Phyllis2 database the NPK of the grain is on average 70%, 75% and 25% of the whole crop (grain + straw) for nitrogen, phosphorus and potassium, respectively.

The nutrient balance model is based on conservation of mass and is restricted to the major macro nutrients, i.e. nitrogen, phosphorus and potassium. The model has the assumption that the net annual change of mass contained within the system is assumed zero for phosphorus (P) and potassium (K). This means that the inputs, i.e. P and K mineral fertilizer, are set to match the outputs. However nitrogen is modeled to both mineralize and accumulate in the soil, which affects the required input of nitrogen fertilizer in Case 1 and the yield in Case 2.

The phosphorus and potassium balances in the model are based on the uptake by the harvested products, i.e. grains and straws (if harvested), and the amount of emissions associated with these macro-nutrients. Phosphorus outputs through emissions were assumed based on a factor estimating the combined leaching and surface run-off of the nutrient according to Hauschild and Potting [28]. The potassium emissions are calculated based on a method recommended by Food and Agriculture Organization (FAO) in their Assessment of nutrient balance: Approaches and Methodologies [29]. Which estimates leaching by a regression model from an extensive literature research, valid for a wide range of soils and climates, adopted from DeWilligen [30] and his developed nitrogen leaching regression model. That model is based on annual precipitation, fertilizer input and the soil's cation exchange capacity.

The nitrogen balance includes deposition, precipitation, and biological fixation based on Nielsen et al. [31]. Moreover, mineralization and accumulation of nitrogen are included in the model, where the build-up is modeled to follow the build-up of soil organic carbon, given in Section 2.3.2. Nitrous oxide emissions were estimated based on IPCC recommendations and include both direct and indirect emissions [32]. The direct emissions are calculated as a percentage of the total nitrogen, i.e. mineral and biological fertilizer, and crop residues, added to the field from the harvest of the preceding crop to the harvest of the present crop. Indirect emissions include a certain percentage of emissions originally emitted as NH_3 and NO_3^-, which soon thereafter converts to N_2O. The NH_3 emission was estimated based on Asman [33] for the nitrogen fertilizer assumed and the nitrate leaching NO_3^- was calculated using the SQCB-N_2O model [34] with the appropriate parameters for the considered area.

The nutrients within the straw are assumed to be 100% utilized with respect to phosphorous and potassium, and 30% for nitrogen. This is in line with the assumptions of Nguyen et al. [15] and Parajuli er al. [7]. The marginal mineral fertilizer used in this assessment are based on the market of fertilizer for NPK in Ecoinvent 3.1 [22].

2.3.2. Carbon soil sequestration effect

The carbon captured by the crop which will eventually be released to the atmosphere, i.e. from carbon decay in soil and/or combustion in the power plant. The carbon soil sequestration effect is the GWP effect of introducing the soil as a carbon sink for atmospheric carbon through carbon capture by the total residues and subsequent sequestration in the soil with the residues and GBC.

Radiative forcing (RF) is a measure of the capacity of a substance, e.g. a gas, to affect the energy balance controlling the Earth's surface temperature, expressed in W/m^2. Integrated RF is thus a measure of the energy that is added to the system during a chosen time horizon due to release of the substance. The global warming potential (GWP) is an environmental indicator that uses integrated RF to predict the effects of releasing a substance to the atmosphere on global warming, and benchmarks all substances to carbon dioxide. It is thus well suited to use the method of Petersen et al. [8] to calculate the effect of storing the carbon in the soil instead of in the atmosphere as CO_2. This is in line with the biogenic GWP calculation of Cherubini et al. [35,9] for wood sourced bioenergy.

The method is based on using the Bern carbon cycle model [36,37] to describe the decay of carbon in the atmosphere over a specific time horizon. The carbon in the atmosphere decays as it is absorbed by the many sinks in Earth's system, e.g. oceans, forests.

$$y(t) = A_0 + \sum_{i=1}^{3} A_i e^{-t/\tau_i} \quad (1)$$

$$A_T = \int_1^T y(t) \quad (2)$$

where $A_0 = 0.217$, $A_1 = 0.259$, $A_2 = 0.338$, $A_3 = 0.186$, $\tau_1 = 172.9$, $\tau_2 = 18.51$, $\tau_3 = 1.186$, t = specific time and T = time horizon. Moreover A_T is the time-integrated mass load of CO_2 in the atmosphere in a specific time perspective. Further, the method includes the decay of carbon input in soil, simulated by C-TOOL, which simulates the development of soil carbon content, and can track specific carbon inputs at any desired time span. This enables the atmospheric decay of the released CO_2 from carbon decay in the soil (S_T) to be calculated.

$$S_T = \sum_{i=1}^{T} \left(a(i) \sum_{j=1}^{T-i} y(j) \right) \quad (3)$$

$$R_T = \frac{A_T - S_T}{A_T} \quad (4)$$

R_T is the ratio between the carbon stored in the natural sinks, i.e. soil, oceans, forests, etc., and carbon stored in the atmosphere as CO_2. The time horizon used is set to match the impact indicator, i.e. 100 years. The carbon in the residues and the GBC have very different characteristics, making the decay in soil very different as well, as the carbon in the residues decays much more rapidly than the carbon in the GBC after thermal treatment in the gasifier.

2.3.3. Ecoinvent processes

The Life Cycle Inventory (LCI) data of the inputs and upstream processes connected to the wheat grain production are based on average values from seven wheat grain production LCA's given in the Ecoinvent database [22].

The seeds were assumed to be botanic and cultivated in the same way as the wheat grain with some additional processes, such as transportation to processing, the processing itself, storage and finally transportation to a regional storehouse [38].

For the impact of the pesticides, the active ingredient is found and paired with the classification of a pesticide substance specified in Green [39] and Bhat et al. [40] according to Hartley and Kidd [41] and Tomlin [42], as adopted by Ecoinvent.

The work processes includes all operations, except transportation on the wheat field, during one year of wheat production. The inclusion of baling and loading of the bales is accounted for where appropriate. The machinery and their fuel usage are included in the field operations.

2.4. Transportation

For every input to the agricultural field where LCI data was collected from Ecoinvent, it was assumed that it would be transported from a regional storehouse. It was further assumed that the average distance between the wheat field and the regional storehouse is 20 km. The same assumption was applied for transportation of residues and GBC between the field and gasifier. Moreover, the large volume/weight ratio of the straw bales were accounted for by increasing the number of trips required based on the volume available in the lorries.

2.5. Energy system

The LT-CFB is a Low Temperature Circulating Fluidized Bed (LT-CFB) gasifier, designed to handle biomass with high ash content like wheat straw. The low operating temperature of the gasifier alleviates the problems caused by sintering of the ash, such as fouling from potassium and corrosion from chlorine, as the ash leaves the gasifier in solid form [3].

However, a drawback of the gasifier is that the gas produced has very high content of tar and particles, rendering it presently unsuitable for direct use in a gas engine for electricity production and for synthesis to biofuels [3]. Nevertheless, it can be combusted and used to fuel a steam power plant.

Most of the nutrients that were removed with the straw are contained in the straw ash after gasification and because the ash is in solid form, the nutrients and carbon can be returned back to the field.

The carbon content of the ash or GBC can be changed by changing the design or the operation of the gasifier. In this way more carbon can be kept in the GBC, which increases the carbon soil sequestration and thus has a significant effect on the GWP of the system. The distribution of carbon to biochar and product gas is controlled by the carbon conversion factor (CC). CC describes the ratio of carbon in the energy resource that is gasified to product gas, the rest of the carbon is biochar. To find the lowest CC the energy system was simulated by varying the CC towards zero or when no heat or power could be produced.

The energy system assumed in this analysis consists of a LT-CFB gasifier which is connected to a conventional steam power plant. In the power plant the product gas is burned to produce electricity and heat. The efficiencies of the gasifier and the subsequent conversion to electricity and heat is taken from primary data of a pilot plant [16].

For the power and heat generation in the total system, the analysis accounts for substituted technologies and accredits the impacts that are avoided by the substitution to the system. The produced electricity is assumed to replace the marginal electricity technology in Denmark, which is a composition of coal,

natural gas and wind, with the ratios, 0.48, 0.51 and 0.01, respectively [13]. The heat produced is assumed to substitute the heat production of a specific technology, which is assumed to be a decentral biomass based combined heat and power plant. The reason for the difference in the substituted technologies is that the electricity produced will be connected to the national grid, and thus affect the marginal of that grid, but the heat produced is connected to the local district heating network which in this case is assumed to be a biomass CHP plant. In the sensitivity analysis in Section 2.6 the effects of the substituted technology choices are analyzed.

2.6. Sensitivity analysis

To test the results a sensitivity analysis was performed. The most uncertain aspects of the analysis connected to its objective, are the biochar carbon decay in soil and its soil sequestration effect. and nitrogen build-up with carbon sequestration. Although there are indications that the assumptions made for the decay of GBC carbon are reasonable [14], modeling the system with different decay end states can indicate how strong the results of the carbon soil sequestration effect are. A question raised by Nguyen et al. [16], is whether or not the stability of the carbon in the GBC changes by changing the carbon conversion factor of the gasifier. Connected to the carbon decay in soil is the nitrogen build-up, where the longterm nitrogen build-up is assumed 1:10 of the carbon build-up [43]. These parameters were analyzed for their effect on the final results.

It is also interesting to take closer look at the change in energy efficiency and increase in carbon soil sequestration by changing the CC. Decreased energy efficiency of the gasifier will decrease the electricity and heat produced and thus decrease the substituted marginal electricity and district heating by the system. The difference between what is gained by the carbon soil sequestration increase and what is lost by the gasifier energy efficiency decrease can be observed in the LCA results. However, what if the marginal electricity is different then what was assumed or what if a specific energy resource is substituted rather than the marginal, and what if the energy resource used in the distric heating system is different then what is assumed. How will that change the results with respect to the best CC practice. To find that out other electricity and district heating sources are substituted and the change in GWP per change in CC is compared to the GWP per CC change or the carbon soil sequestration.

3. Results

Below the carbon soil sequestration effect for the scenarios is presented, and the LCA results of the integrated bioenergy and agriculture system scenarios for the different cases is given and explained in detail.

3.1. Gasifier carbon conversion

The energy system was simulated in DNA, to get the lowest possible CC for S3. Fig. 3 displays the result of this simulation in terms of the efficiency of the electricity and district heat production, and fuel utilization. It can be seen in Fig. 3 that no heat or power generation is beyond 20% carbon conversion, making the CC for the low CC scenario equal to 0.2. Further carbon conversion reduction could possibly be achieved in a dedicated pyrolyzer operating at lower temperatures. However, carbon emission can be expected that will decrease the carbon content of the GBC.

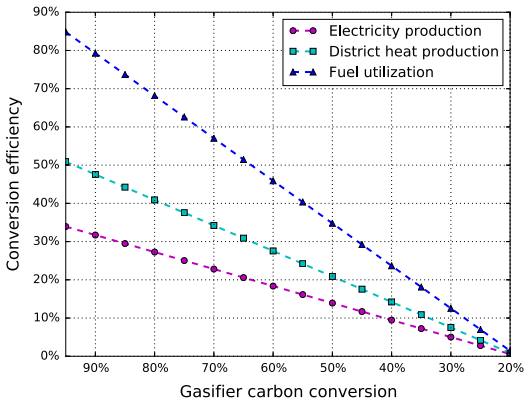

Fig. 3. Change in conversion efficiency by carbon conversion decrease in the gasifier.

3.2. Carbon soil sequestration effect

The decay of carbon which is added to the soil is displayed over a 100 year horizon in Fig. 4 for the different scenarios and normalized to the carbon input. In the legend of the figure, numerical values of carbon still retained in the soil at the 100th year end state is given for all scenarios. Additionally as a reference, GBC input to soil is included.

It can be seen that for the residues that there is much faster decay in the first years and that 1.2% of the original carbon remains in the soil when 100 years have passed. However, the High and Low CC scenarios show as expected that more carbon in the GBC increases the carbon sequestered over a 100 year horizon, 3.2 and 44.9% for S1 and S3, respectively. This is because carbon in GBC after thermal treatment in the gasifier is much more stable in soil then before the treatment, i.e. does not decay to the same extent, which is displayed in the figure by the difference between residue and carbon in GBC decay curves in the figure.

Fig. 5 displays the distribution of the carbon between atmosphere and sinks over a 100 year period. The carbon soil sequestration effect of a specific scenario is equal to the area between the curve of the scenario and the curve of the Bern carbon cycle[2] (representing the decay of carbon in the atmosphere), which is equal to the difference in the integrated radiative forcing between a pulse emission and the scenarios analyzed for the fate of carbon. In the legend of the figure, numerical values for the percentage carbon bound in sinks are given.

3.3. Life Cycle Inventory analysis

For Case 1 the results of the LCI are given in Table 1. Only resulting inventory data that were not acquired as averages from the Ecoinvent database are shown. These results correspond to the parts of the system that are of the most importance and interest, i.e. fertilization, field emissions, carbon soil sequestration, transportation and energy generation. When comparing S1–S3 it can be seen that transportation and the carbon soil input increase with decreased CC in the gasifier. This was to be expected as more carbon is in the GBC and thus more weight and amount transported back to the field and incorporated into the soil. What is also worth noting is the change in fertilization.

[2] The Bern Carbon Cycle CO_2 decay in the atmosphere can be observed in the figure, this would be the decay of the CO_2 in the atmosphere if it was never captured by the total residues.

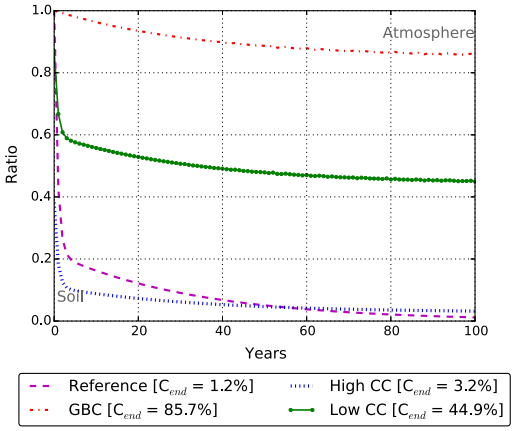

Fig. 4. Carbon decay.

Nitrogen fertilization increases when straws are removed, but is mitigated by retuning the GBC. The reason for this is that by practicing straw removal, the nitrogen in the straws cannot be mineralized in the soil and used by the plants on the field with time, and by gasifying the straws the nitrogen within them will end up in the gas phase and not be available in the GBC on their return to the soil. However, by increasing the carbon in the GBC, i.e. lowering the CC in the gasifier, and returning to the field, carbon will build up in the soil which was modeled to effect the build up of nitrogen in the soil, see Section 2.3.1. With more nitrogen in the soil, less fertilizer is required for the same yield with time as nitrogen becomes available to the plant as it is mineralized.

This is different for phosphorus and potassium fertilization. However, like for nitrogen above, phosphorus and potassium are removed with the straws, but unlike nitrogen, phosphorus and potassium are concentrated in the GBC after gasification and are modeled to return to the field with 95% efficiency and 100% mineral fertilizer substitution value, see Section 2.3.1.

The Life Cycle Inventory for Case 2 is given in Table 2 in the same way as above for Case 1. From Table 2 it can be seen that the yield increases with more carbon inputs to the soil as more nitrogen fertilization is allowed with lowered nitrate leaching. The greater the yield, the greater the electricity and heat production, transportation and carbon soil sequestration effect, as more straws are available. This is different from what was seen in the results for Case 1. When comparing the LCI results for the two cases, differences are visible in all categories. All of which are effected by the yield difference between the cases.

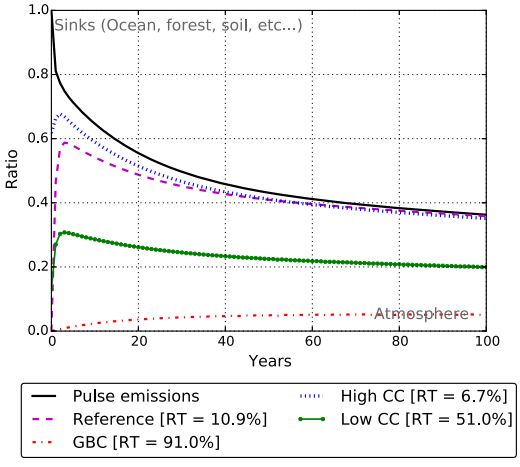

Fig. 5. Distribution of carbon in the atmosphere and sinks.

3.4. Life cycle impact assessment

Fig. 6a and b displays the result of the consequential LCIA analysis with kg grains produced as its functional unit for Cases 1 and 2, respectively. The system expansion covers the conversion of the straws in the energy system through the Pyroneer and a CHP plant for electricity and heat production, along with return of the GBC with varying carbon content with different CC values. Reference is given to wheat grain production with no straw removal and thus no heat and power production.

It can be seen in the figures that removing the straws and using them in an energy system, substituting the marginal energy sources gives better result in terms of IPCC 2013 GWP 100 than leaving them on the field. Also visible in the figures are the changes between the S1 and S3, the effects of carbon soil sequestration is greater than substituting marginal electricity and district heating. Comparing the results of the two cases it can be seen that Case 2 performs batter than Case 1, as it is accredited the substitution of another wheat grain production. As with increased yield more heat and power can be produced, and more carbon can be incorporated to the soil with the GBC.

Fig. 7a and b displays the results of the consequential LCIA analysis with kW h electricity produced as its functional unit, i.e. independent of the substituted electricity production, for Cases 1 and 2, respectively. The input of the straws to the energy system is modeled using the cut-off allocation from the grains, i.e. only the direct and indirect impacts of removing the straws are allocated to them. The system expansion includes the retuning of the GBC with varying carbon content to the field.

It can be seen in the figures that lowering the CC give better results, like we observed in Fig. 6a and b. Moreover, like above we can see that the changes are greatest for the carbon soil input effect, while other changes between the scenarios are less. From Table 2 it can be seen that the increase in yield is about more for S3 but compared to RA and S1 has less yield but less mineral fertilization. This has a negative effect on the environmental impact for

Table 1
Life Cycle Inventory, Case 1.

	RA	RB	S1	S2	S3
Grain yield [kg]	8000.0	8000.0	8000.0	8000.0	8000.0
Straw harvested [kg]	6103.8	6103.8	6103.8	6103.8	6103.8
Straw harvested [GJ (LHV)]	88.5	88.5	88.5	88.5	88.5
Transportation off field [tonne km]	0.0	164.1	167.9	173.1	210.1
N fertilizer [kg nitrogen]	148.1	164.4	162.5	158.7	131.9
P fertilizer [kg diphosphorus pentaoxide]	31.0	31.7	31.4	31.4	31.4
K fertilizer [kg potassium oxide]	55.9	65.8	61.4	61.4	61.4
N_2O emission [kg dinitrogen monoxide]	3.9	4.0	4.0	3.9	3.6
Carbon sequestration effect [kg carbon]	498.3	184.6	302.5	541.1	2224.7
Electricity production [MW h]	0.0	5.5	8.3	7.3	0.1
Heat production [GJ]	0.0	52.9	45.1	39.6	0.8

Table 2
Life Cycle Inventory, Case 2.

	RA	RB	S1	S2	S3
Grain yield [kg]	9452.2	8200.3	8344.8	8806.5	10699.1
Straw harvested [kg]	7211.8	6256.7	6366.9	6719.2	8163.1
Straw harvested [GJ (LHV)]	104.6	90.7	92.3	97.4	118.4
Transportation off field [tonne · km]	0.0	167.3	177.7	204.6	324.6
N fertilizer [kg nitrogen]	181.0	172.2	176.0	188.0	237.2
P fertilizer [kg diphosphorus pentaoxide]	31.2	31.8	31.5	31.5	31.8
K fertilizer [kg potassium oxide]	55.9	66.1	61.6	61.9	63.2
N_2O emission [kg dinitrogen monoxide]	4.7	4.2	4.3	4.6	6.0
Carbon sequestration effect [kg carbon]	588.7	189.6	315.6	748.0	2975.2
Electricity production [MW h]	0.0	5.6	8.7	7.4	0.2
Heat production [GJ]	0.0	54.2	47.0	40.0	1.0

both scenarios as the lower fertilization in S1 has less effect than lower yield.

Fig. 8 gives the results displayed in Fig. 7a and b by comparison to the total LCA score of utilization of alternative energy resources.

It can be seen in the figure that using wheat straws in an integrated bioenergy and agriculture system can outperform all other major energy sources in terms of GWP if the right CC is used. To be climate neutral or even climate friendly, the CC will need to be below 0.86 and 0.81 for Cases 1 and 2, respectively.

3.5. Sensitivity analysis

The carbon sequestration effect and nitrogen build-up were varied to test the robustness of the results. As found in the results above maximum biochar production is better then maximum heat and power production in terms of climate change impact. The carbon sequestration effect can decrease by 18% (Case 1) or 19% (Case 2) for that results to hold. However, for both Cases 1 and 2 a change in nitrogen build-up cannot effect the outcome of that result.

In Fig. 9 the results of the analysis on the effect of changing the substituted electricity and district heating, is displayed. On the *y*-axis different district heating system are substituted by the CHP plant heating part of the integrated bioenergy and agricultural system. Electricity substituted corresponding to the components of the marginal electricity composition in the Danish energy system, i.e. coal based, natural gas base and wind electricity generation. If the scatter dot is in the left side of the red line (representing the GBC carbon GWP change per CC change), that indicates that it is better to maximize biochar production. However, of the bars end at the right side of the red line, it is better to maximize CC.

It can be seen in the figures above that if the district heating substituted is by any of the systems analyzed here, it always better to maximize biochar production for Case 2. In Case 1, for the two biomass fueled district heating it is better maximize biochar production, except when coal fueled electricity system is substituted. However if the district heating substitutes fossil fuel based production, maximum energy generation should be the preferred option except when both district heating and electricity technologies substituted are fueled with natural gas.

4. Discussion

In this type of analysis a 100 year time horizon is the most common, second to that is the 20 year horizon. However, according to IPCC the current global emissions from the energy and industrial sectors have the largest contribution to warming for a 100 year horizon. Conversely the agricultural sector is said to have the largest contribution to warming for 20 year horizon. The reason for that is the CH_4 part of the emissions as its lifetime in the atmosphere is relatively short. Despite that, the main gas contributors

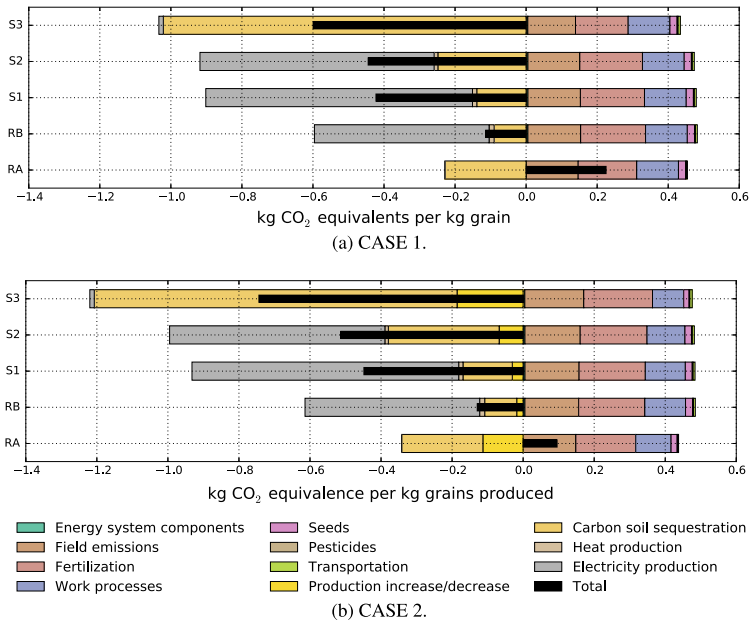

(a) CASE 1.

(b) CASE 2.

Fig. 6. LCIA result for both cases with functional unit kg grains produced.

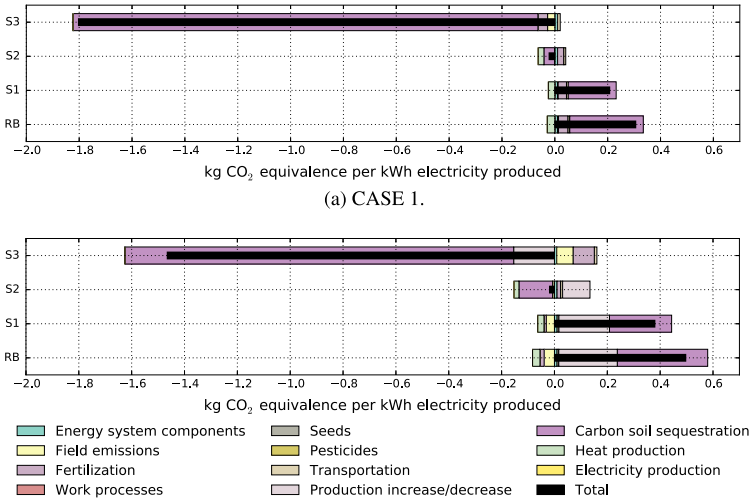

(a) CASE 1.

(b) CASE 2.

Fig. 7. LCIA result for both cases with functional unit kW h electricity produced.

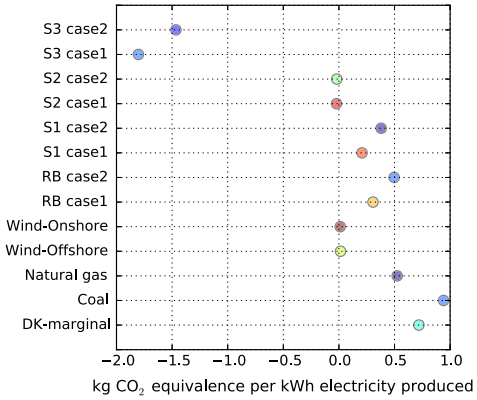

Fig. 8. Result of the straw utilization in reference to alternative resource utilization.

in the agricultural system analyzed in this research are CO_2 and N_2O, both of which have increasing contribution over time but stabilize in around 20 years when looking at the 100 year time horizon [24]. This can mean that because no significant short-lived gases are emitted to the atmosphere, the 100 year time horizons analysis is appropriate.

When observing the results of the two cases it is obvious that the carbon soil sequestration effect and substituted electricity production are dominant. However, what is striking is that increasing the carbon in the GBC at the cost of the energy efficiency of the gasifier has positive effect on decrease of the global warming potential. This is the case both when looking at it from the agricultural system (per kg grain) perspective and from the energy system perspective (per kW h electricity). For Case 2, this is even more evident than in Case 1 as the yield increase by added nitrogen fertilization with lowered nitrate leaching is better than decreasing nitrogen fertilization for constant yield.

In the sensitivity analysis the GBC stability was varied to show how an increase in decay with CC decrease would affect the total results. Despite including that in the analysis it is not expected to change by changing the carbon conversion to 80–86% for a climate neutral resource as long as the pyrolysis phase of the gasifier is fully completed and is independent of the CC change in the gasification phase, which could be the case for the Pyroneer gasifier. However, although the Low CC scenario assumes CC of 20% the gasifier must be analyzed for the Lowest CC an yet a full pyrolyses

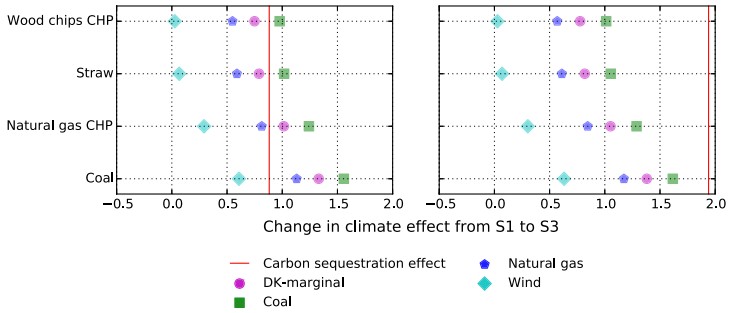

Fig. 9. Sensitivity analysis for Cases 1 and 2, low CC scenario.

operation, to ensure maximum stability in the soil. Moreover, in the sensitivity analysis of the substituted products it was demonstrated that great care must be taken when deciding on the best CC which strongly depends on what is substituted in the consequential LCA analysis.

What was not included in the modeling is the change in the soil's water retention for the different scenarios. This is expected to occur, and it would lower necessary nitrogen supply to the field in Case 1 and increase the yield in Case 2 as even less nitrogen would be leached from the soil. Both of these would contribute in favor of returning more GBC to the field and decreasing the CC.

It would be interesting to expand the analysis to include more environmental impacts and economic impact of decreased CC. To further establish the system as an environmental impact mitigating technology other impact factors should be analyzed, e.g. eutrophication, ecotoxicity and non-renewable resource demand. For this recycling of nutrients, heavy metal accumulation and the possible decrease in nitrate leaching would be of special notice.

It could be that lowering the CC would increase the value of the fertile GBC and thus mitigate the revenue losses from decreased efficiency. Additionally, a gasifer with a low CC could be smaller and it is expected that for the same input the investment cost would be less. However, the revenues from electricity and district heat sales would be less also, but the GBC could be worth more with increased biochar content. It would be interesting to do an economics analysis to fully judge the economics of these systems.

5. Conclusion

The article has presented a study of the decrease in global warming potential of wheat production and combined heat and power production based on a integrated solution. The wheat straw is used in thermal gasification to produce fuel for the CHP plant, while the GBC contains carbon and nutrients which is recycled to the next year's wheat production. Based on the results of the study, the main conclusions are that:

1. Utilization of straw from wheat fields for heat and power production has a positive impact on the GWP of the total system, mainly due to the substituted electricity production.
2. Decreasing the carbon conversion of the gasifier, and thus allowing more carbon in the GBC, at the expense of the gasifier efficiency, further improved the GWP of the system. This result will hold despite 18% and 19% decrease in the carbon soil sequestration effect for Cases 1 and 2, respectively.
3. At a carbon conversion of 80% and 86%, the system was climate change mitigating in terms of kW h produced for Cases 1 and 2, respectively. However, before deciding on the appropriate CC in a specific area, the products substituted must be analyzed with great care.

These conclusion underline the importance of considering the GBC from the LT-CFB gasifier as an important fertilizer and soil amendment product. However, taking into account the possible changes in the soil's water retention, the positive effect on the environmental impact can be demonstrated as even greater.

Acknowledgement

This study was financially supported by the Villum Foundation.

References

[1] IPCC. Fourth assessment report: climate change 2007: the AR4 synthesis report, Geneva: IPCC; 2007.
[2] IPCC. Fourth assessment report: climate change 2007: working group iii report: mitigation of climate change, Geneva: IPCC; 2007.
[3] Ahrenfeldt J, Thomsen TP, Henriksen U, Clausen LR. Biomass gasification cogeneration – a review of state of the art technology and near future perspectives. Appl Therm Eng 2013;50(2):1407–17. http://dx.doi.org/10.1016/j.applthermaleng.2011.12.040. Combined Special Issues: {ECP} 2011 and {IMPRES} 2010.
[4] Djomo SN, Witters N, Dael MV, Gabrielle B, Ceulemans R. Impact of feedstock, land use change, and soil organic carbon on energy and greenhouse gas performance of biomass cogeneration technologies. Appl Energy 2015;154:122–30. http://dx.doi.org/10.1016/j.apenergy.2015.04.097. <http://www.sciencedirect.com/science/article/pii/S0306261915005607>.
[5] Sastre C, González-Arechavala Y, Santos A. Global warming and energy yield evaluation of spanish wheat straw electricity generation – a {LCA} that takes into account parameter uncertainty and variability. Appl Energy 2015;154:900–11. http://dx.doi.org/10.1016/j.apenergy.2015.05.108. <http://www.sciencedirect.com/science/article/pii/S0306261915007412>.
[6] Yang J, Chen B. Global warming impact assessment of a crop residue gasification project – a dynamic {LCA} perspective. Appl Energy 2014;122:269–79. http://dx.doi.org/10.1016/j.apenergy.2014.02.034. <http://www.sciencedirect.com/science/article/pii/S0306261914001706>.
[7] Parajuli R, Løkke S, østergaard PA, Knudsen MT, Schmidt J, Dalgaard T. Life cycle assessment of district heat production in a straw fired {CHP} plant. Biomass Bioenergy 2014;68:115–34. http://dx.doi.org/10.1016/j.biombioe.2014.06.005. <http://www.sciencedirect.com/science/article/pii/S0961953414003079>.
[8] Petersen BM, Knudsen MT, Hermansen JE, Halberg N. An approach to include soil carbon changes in life cycle assessments. J Cleaner Prod 2013;52:217–24. http://dx.doi.org/10.1016/j.jclepro.2013.03.007.
[9] Guest G, Cherubini F, StrÃm¸man AH. The role of forest residues in the accounting for the global warming potential of bioenergy. GCB Bioenergy 2013;5(4):459–66. http://dx.doi.org/10.1111/gcbb.12014.
[10] Cherubini F, Stromman AH, Hertwich E. Effects of boreal forest management practices on the climate impact of CO_2 emissions from bioenergy. Ecol Model 2011;223(1):59–66. http://dx.doi.org/10.1016/j.ecolmodel.2011.06.021.
[11] Kuligowski K, Poulsen TG, Rubak GH, Sorensen P. Plant-availability to barley of phosphorus in ash from thermally treated animal manure in comparison to other manure based materials and commercial fertilizer. Eur J Agron 2010;33(4):293–303. http://dx.doi.org/10.1016/j.eja.2010.08.003.
[12] Muller-Stover D, Ahrenfeldt J, Holm J, Shalatet S, Henriksen U, Hauggaard-Nielsen H. Soil application of ash produced by low-temperature fluidized bed gasification: effects on soil nutrient dynamics and crop response. Nutr Cycl Agroecosyst 2012;94(2–3):193–207. http://dx.doi.org/10.1007/s10705-012-9533-x.
[13] Brandao M, Levasseur A, Kirschbaum M, Weidema B, Cowie A, et al. Key issues and options in accounting for carbon sequestration and temporary storage in life cycle assessment and carbon footprinting. Int J Life Cycle Assess 2013;18(1):230–40. http://dx.doi.org/10.1007/s11367-012-0451-6.
[14] Hansen V, Müller-Stöver D, Ahrenfeldt J, Holm JK, Henriksen UB, Hauggaard-Nielsen H. Gasification biochar as a valuable by-product for carbon sequestration and soil amendment. Biomass Bioenergy 2015;72:300–8. http://dx.doi.org/10.1016/j.biombioe.2014.10.013. <http://www.sciencedirect.com/science/article/pii/S0961953414004693>.
[15] Nguyen TLT, Hermansen JE, Mogensen L. Environmental performance of crop residues as an energy source for electricity production: the case of wheat straw in denmark. Appl Energy 2013;104(0):633–41. http://dx.doi.org/10.1016/j.apenergy.2012.11.057.
[16] Nguyen TLT, Hermansen JE, Nielsen RG. Environmental assessment of gasification technology for biomass conversion to energy in comparison with other alternatives: the case of wheat straw. J Cleaner Prod 2013;53:138–48. http://dx.doi.org/10.1016/j.jclepro.2013.04.004.
[17] Petersen BM, Olesen JE, Heidmann T. A flexible tool for simulation of soil carbon turnover. Ecol Model 2002;151(1):1–14. http://dx.doi.org/10.1016/S0304-3800(02)00034-0.
[18] Petersen BM, Berntsen J, Hansen S, Jensen LS. Cn-sim - a model for the turnover of soil organic matter. I. Long-term carbon and radiocarbon development. Soil Biol Biochem 2005;37(2):359–74. http://dx.doi.org/10.1016/j.soilbio.2004.08.006.
[19] Elmegaard B, Houbak N, et al., Dna – a general energy system simulation tool. In: Proceedings of SIMS, Citeseer; 2005. p. 1–10.
[20] Mutel C, Brightway2, a framework for advanced life cycle assessment calculations; 2014. <http://brightwaylca.org/>.
[21] Vassilev SV, Baxter D, Andersen LK, Vassileva CG. An overview of the chemical composition of biomass. Fuel 2010;89:913–33.
[22] ecoinvent Centre 2013, ecoinvent centre (2013). ecoinvent data v3.1., swiss Centre for Life Cycle Inventories, Dübendorf; 2013, retrieved from: <www.ecoinvent.org>.
[23] NaturErhvervstyrelsen, Vejledning om gØdsknings- og harmoniregler, Tech. rep., Ministeriet for Fødevarer, Landbrug og Fiskeri; 2013.
[24] Myhre G, Shindell D, Bréon FM, Collins W, Fuglestvedt J, Huang J, et al. Anthropogenic and natural radiative forcing. In: Stocker TF, Qin D, Plattner G-K, Tignor M, Allen SK, Boschung J, et al., editors. Climate change 2013: The physical science basis. Contribution of working group I to the fifth assessment report of the intergovernmental panel on climate change. Cambridge, United Kingdom and New York, NY, USA: Cambridge University Press; 2013. p. 659–740. http://dx.doi.org/10.1017/CBO9781107415324.018.

[25] DMI, Danmarks climate 2014. Danmarks Meteorologiske Institut; 2014. <http://www.dmi.dk/en/vejr/arkiver/decadal-mean-weather/>.
[26] Nemecek T, Schnetzer J. Methods of assessment of direct field emissions for lcis of agricultural production systems. Agroscope Reckenholz-TlniNRn Research Station ART.
[27] E. Research Centre of the Netherlands. Phyllis2, database for biomass and waste. <https://www.ecn.nl/phyllis2>.
[28] Hauschild M, Potting J. Spatial differentiation in life cycle impact assessment – the edip2003 methodology, Tech. rep., Institute for Product Development - Technical University of Denmark; 2005.
[29] Roy R, Misra R, Lesschen J, Smaling E. Assessment of soil nutrient balance: approaches and methodologies, Tech. rep., Food and Agriculture Organization of the United Nations; 2003. <ftp://ftp.fao.org/docrep/fao/006/y5066e/y5066e00.pdf>.
[30] Willigen P de. An analysis of the calculation of leaching and denitrification losses as practised in the NUTMON approach. Rapport-Plant Res Int 2000;18.
[31] Nielsen P, Nielsen A, Weidema B, Dalgaard R, Halberg N. Lca food data base; 2003. <www.lcafood.dk>.
[32] Eggleston S, Buendia L, Miwa K. 2006 IPCC guidelines for national greenhouse gas inventories [recurso electrónico]: industrial processes and product use. Kanagawa, JP: Institute for Global Environmental Strategies; 2006.
[33] Asman WA. Ammonia emission in Europe: updated emission and emission variations. the Netherlands: National Institute of Public Health and Environmental Protection Bilthoven; 1992.
[34] Faist Emmenegger M, Reinhard J, Zah R., SQCB – Sustainability Quick Check for Biofuels, Empa, 2009, intermediate Background Report.
[35] Cherubini F, Guest G, StrÃm¸man AH. Application of probability distributions to the modeling of biogenic CO_2 fluxes in life cycle assessment. GCB Bioenergy 2012;4(6):784–98. http://dx.doi.org/10.1111/j.1757-1707.2011.01156.x.
[36] Joos F, Bruno M, Fink R, Siegenthaler U, Stocker TF, Le Quere C, et al. An efficient and accurate representation of complex oceanic and biospheric models of anthropogenic carbon uptake. Tellus B 1996;48(3):397–417. http://dx.doi.org/10.1034/j.1600-0889.1996.t01-2-00006.x.
[37] Joos F, Prentice IC, Sitch S, Meyer R, Hooss G, Plattner G-K, et al. Global warming feedbacks on terrestrial carbon uptake under the intergovernmental panel on climate change (IPCC) emission scenarios. Global Biogeochem Cycles 2001;15(4):891–907. http://dx.doi.org/10.1029/2000GB001375.
[38] Nemecek T, Kagi T. Life cycle inventories of agricultural production systems, Tech. rep., Reckenholz-Tanikon Research Station ART, ecoinvent report No. 15; 2007.
[39] Green M et al. Energy in pesticide manufacture, distribution and use. Energy World Agric 1987(2):166–77.
[40] Bhat MG, English BC, Turhollow AF, Nyangito HO. Energy in synthetic fertilizers and pesticides: revisited, ORNL/Sub/90-99732/2. Oak Ridge National Laboratory, Oak Ridge, TN, US Dept. Energy.
[41] Hartley D, Kidd H, et al. The agrochemicals handbook. 2nd ed. The Royal Society of Chemistry; 1987.
[42] Tomlin C, editor. British Crop Protection Council. British Crop Protection Council; 1997.
[43] Petersen BM, Berntsen J. Ther turnover of soil organic matter on different farm types, DARCOFenews, <http://orgprints.org/4665/1/4665.PDF> (September 2003).

PROCEEDINGS OF ECOS 2015 - THE 28TH INTERNATIONAL CONFERENCE ON
EFFICIENCY, COST, OPTIMIZATION, SIMULATION AND ENVIRONMENTAL IMPACT OF ENERGY SYSTEMS
JUNE 30-JULY 3, 2015, PAU, FRANCE

CLIMATE EFFECT OF BIOENERGY AND AGRICULTURE INTEGRATION BASED ON LOWTAR GASIFICATION OF WOOD CHIPS

Hafthor Ægir Sigurjonsson[a+], Brian Elmegaard[a] and Lasse Røngaard Clausen[a]

[a] *Technical University of Denmark, Kongens Lyngby, Denmark, +hafsig@mek.dtu.dk*

Abstract:
To mitigate the increasing pressure on Earth´s biosphere through increased concentration of carbon dioxide in the atmosphere, processes in the anthroposphere must change from being fossil- to renewable resource driven. Bioenergy utilization of forest residues can be a step towards achieving that goal. The climate change mitigating effect of different bioenergy scenarios is however not obvious. In recent years, finding the right way to quantify the effect of biogenic carbon emissions associated with bioenergy has gathered attention. This paper analyses the global warming potential of an integrated bioenergy and agricultural system through a polygenerating energy system, producing electricity, district heat and fertile biochar for agricultural soil application. The case analysis is based on utilization of forest residues from a sustainably harvested forest. Quantification of the biogenic global warming potential is included in the analysis, by accounting for both the atmospheric load of biogenic carbon emissions and the carbon captured by forest re-growth. The energy conversion is based on thermal gasification. The gasifier allows changing the carbon conversion fraction, from the conventional maximum energy generation to maximum biochar production. For a 100 year time horizon the biogenic global warming potential varies from 0.65 for maximum energy generation to 0.30 for maximum biochar production. The total carbon footprint per kWh electricity produced decreases towards maximum biochar production, such that in this analysis it outperforms an alternative offshore wind power generation. However, the maximum energy generation scenario just about outperforms an alternative natural gas fuelled power generation. Concluding that for this type of a system, producing more biochar at the expense of energy generation improves its carbon footprint.

Keywords:
Bioenergy, forest residues, gasification, biochar, system integration, biogenic GWP.

1. Introduction

Renewable biomass feedstock for transportation fuels, heat and power generation is generally perceived as a relevant resource to mitigate climate change caused by fossil fuel utilization. However, the effectiveness of bioenergy systems to combat climate change can vary greatly. Depending on, e.g. what type of biomass it is, how it is harvested or collected, distance to end use, and what its utilization will ultimately substitute. Recently, focus on analysing carbon balance within the biomass life cycle has increased.

Soil carbon is estimated to amount to 2157-2293 Pg in the world, of which 684-724 Pg are estimated to be soil organic carbon in the upper 30 cm of soils [1]. However, since the industrial revolution depletion of soil organic carbon has contributed 66-90 Pg to carbon in the atmosphere, this can be compared to the 240-300 Pg contributed by fossil fuel combustion [2]. Additionally, some cultivated soils have lost up to two thirds of their organic carbon, indicating a lot of potential in using the soil carbon pools as carbon sink.

This article presents a consequential Life Cycle Assessment (LCA) of heat, power and fertilizer (gasification ash and biochar) production , utilizing forestry residue (FR) in the TwoStage down draft gasifier [3]. The fertilizer is termed GBC throughout the article. Where the objective is to

determine the value of the integration and compare climate effect and energy efficiency when varying operation in the energy system from maximum energy generation to maximum biochar production.

For the analysis, the total system is modelled by combining the use of energy system software and carbon soil simulation software for both agricultural soils and forestry soils, interconnected with Python. The software used are Dynamic Network Analysis (DNA) [4], C-Tool [5] and Yasso2007 [6] for the energy system, agricultural and forestry soils, respectively.

The novelty of this article is the holistic integrated model of bioenergy and agriculture and the use of a detailed biogenic carbon balance in a case analysis, using the approach of [7-8]. Additionally, the approach of [9] is used for accounting the biochar carbon emission from agricultural soil. Moreover, the energy system is modelled with a comprehensive energy system modelling tool and the carbon conversion in the gasifier is varied, allowing maximum energy efficiency or maximum biochar production in this polygeneration energy system to be simulated.

2. Methods

2.1. Analytical Approach

The analysis is made in a life cycle perspective, based on the Life Cycle Assessment (LCA) methodology over a 100 year time horizon, using the consequential approach [10] and IPCC's global warming potential 100a Life Cycle Impact Assessment (LCIA) method. The system operates to produce electricity and GBC, and the functional unit is 1 kWh electricity produced. This enables comparison with a provision of the service by other feedstock, where the output is 1 kWh electricity produced [11]. The analysis accounts for the upstream impact of removing the residues from the forest and downstream impact of applying GBC to an agricultural field to increase its soil carbon content. The carbon conversion factor (CC) in the gasifier governs the amount emitted from the power plant and the agricultural field, i.e. whether operation is aimed at maximum energy generation or maximum biochar production. The two scenarios are termed High gasifier CC and Low gasifier CC, respectively.

The developed program integrates LCA, energy system, and carbon balance models. The LCA part of the calculation script is done by connecting to the Brightway2 open source LCA program [12] which enables communication with the ecoinvent database for Life Cycle Inventory analysis (LCI) and Life Cycle Impact Assessment [13]. The energy system modelling is done with the Dynamic Network Analysis software developed in the Thermal Energy Section at the Technical University of Denmark. Carbon balance modelling includes a time integrated calculation of the impulse response function and carbon captured by forest re-growth. Along with carbon decay on forest floor and agricultural soil where Yasso07 [6] and C-tool [5] software are used, respectively.

2.2. System Description

The system analysed is an integrated bioenergy and agricultural system, where the waste from the bioenergy system is a resource for the agricultural system. FR is the feedstock for the bioenergy system which generates heat, power and fertilizer. Available FR are divided into above ground FR and below ground FR, the total extraction efficiency is 46%, where 75% of the above ground FR are removed and 0% of the below ground FR. The extracted FR enter the energy system as wood chips which are gasified in the TwoStage gasifier [3] producing product gas and GBC. The GBC is applied to an agricultural field as fertilizer, but the product gas is combusted in a gas engine for heat and power. A simple schematic of the integrated system can be seen in Figure 1.

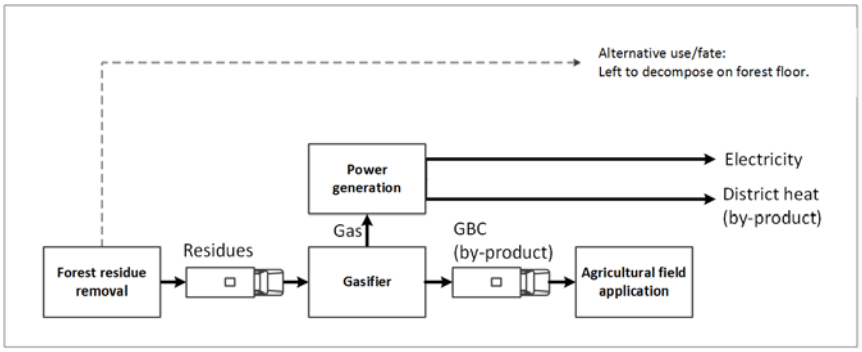

Fig. 1. Schematic of the overall system.

It can be seen in the figure that the total system can be aggregated into four subsystems: forest residue removal, gasifier, power generation and agricultural field application. The forest residue removal LCI is modelled using the strong sustainability concept with the recycled content or cut-off allocation approach [14]. FR are considered as a secondary product of a sustainable harvested forest (logs or stems being the primary product) and using the cut-off allocation approach only the impact associated with the forest residues are accounted for. Other by-products of the system, i.e. district heat in the power generation subsystem and GBC in the gasifier subsystem, are allocated using the system expansion approach.

2.3. Carbon Balance

Carbon balance is made and a biogenic global warming potential GWP_{bio} is calculated for the FR originating CO_2 emissions. This includes carbon emission from product gas combustion in the gas engine, carbon emission from FR on the forest floor, carbon emitted from biochar in the agricultural soil and carbon captured during re-growth. The GWP_{bio} impact factor is based on the integrated radiative forcing difference between biogenic emission and an equivalent fossil carbon pulse emission [7-8]. Carbon will be oxidise to carbon dioxide (CO_2) when entering the atmosphere and all global warming potential (GWP) values are generally benchmarked to CO_2. Thus knowing the resulting carbon concentration change in the atmosphere over a specific time horizon as a consequence of the production of the functional unit, the GWP_{bio} can be found.

The principles of the method from [8] was used in calculating the GWP_{bio}, but adapted in only account for FR and including the biochar carbon decay.

$$GWP_{bio} = \frac{AGWP_{CO_2,bio}}{AGWP_{CO_2}} = \frac{C_0 \cdot \left(w \cdot CC \cdot A_T + w \cdot (1-CC) B_T + (1-w) \cdot F_T - G_T\right)}{C_0 \cdot w \cdot A_t} \quad (1)$$

Where $AGWP$ represents the absolute global warming potential or cumulative radiative forcing (CFR), C_0 is the carbon content of the wood chips, w is the FR extraction efficiency (FR carbon extracted / FR carbon available). A_T, B_T and F_T are the time integrated atmospheric CO_2 load of a pulse emission, biochar decay emission and FR decay emission, respectively. G_T is then the time integrated captured load of CO_2 by forest regrowth.

The Bern carbon cycle model [12-13] is used to describe the impulse response function for CO_2 decay in the atmosphere over a specific time horizon, as it is absorbed by the many sinks in Earth's system, e.g. oceans, forests, etc... Modelling the decay of carbon in the FR on the forest floor is done with Yasso07, a dynamic carbon soil model for forest applications [6]. From the result of that

model F_T can be calculated by multiplying the FR decomposition rate with the impulse response function. The decay modelling of GBC was done in a similar way but utilizing the C-tool dynamic carbon soil model for agricultural applications [5]. Like for the FR, the C-tool model calculates the annual decomposition rate which enables B_T calculation. To represent the rate of carbon captured by the re-growth of FR over the time horizon, Schnute model is used [17]. The Schnute model is a versatile growth model based on statistically stable parameters. G_T could then be calculated by multiplying the rate of carbon captured with the impulse response function.

2.4. Energy System Modelling

The energy system is combined with the gasifier and power generation subsystems. It is analysed by modelling its thermodynamic process using the energy system simulation tool Dynamic Network Analysis (DNA) [4]. Figure 2 gives the process flow diagram of the energy system.

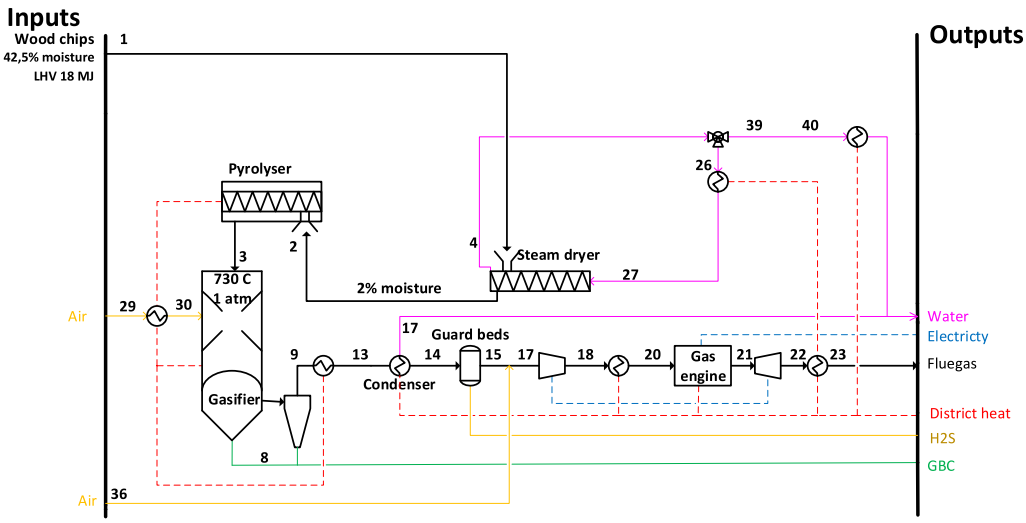

Fig. 2. Process Flow Diagram of the energy system.

Its main components are: The TwoStage gasifier [18], a steam dryer and a gas engine. The FR enters the energy system as wood chips with 42.5% moisture content. They are dried in a steam dryer which operates at 200°C before they enter the two stage pyrolysis and gasification thermochemical converter, i.e. the TwoStage gasifier. The evaporated moisture from the steam dryer is used to generate heat for district heating. After the gasification the hot producer gas is used to fuel the pyrolysis process and to preheat the gasification agent (air), the producer gas is then cooled down to condense out its water content and then cleaned to get rid of H_2S. The gas is then combusted in a turbocharged gas engine to produce electricity for the national grid and district heating for the local community.

The TwoStage gasifier has a separate pyrolysis and gasification unit and a high temperature tar cracking zone in-between. This allows the gasification producer gas to have very low tar content, which enables it to be utilized in a gas engine [3]. The gasifier component model in DNA was developed for [19]. As mentioned in Section 2.1, one of the main parts of the analysis is to show the difference in the results when the gasifier is operated with different levels of carbon conversion. This is included in the energy system model and the system is simulated with a large range of CC values. Key parameters of the energy system, for the two scenarios are given in Table 1.

Table 1. Key inputs to the energy system model.

Key value	*Unit*	*High gasifier CC*	*Low gasifier CC*
Gasifier carbon conversion	-	0.99	0.60
Gasification temperature	°C	730	730
Moisture content after dryer	%	2.0	2.0
Component pressure drops	bar	0.0	0.0
Temperature inside dryer	°C	200	200
Gas engine power efficiency	%	38	38
Air–fuel equivalence ratio	-	2	2

The performance of the energy system is measured by the electrical efficiency, fuel utilization and exergetic efficiency of the whole unit. Electrical efficiency is based on the first law of thermodynamics and is calculated by dividing the net electricity generated with the energy content of the input. Similarly, the fuel utilization is also based on the first law of thermodynamics and is calculated by dividing the net energy generated (heat and power) with the energy content of the wood chips. However, the exergetic efficiency is a concept of the second law of thermodynamics and is calculated by dividing the systems product exergy value with the exergy value of its fuel [20]. In this system the fuel is defined as the wood chips input and the product is defined as the net electricity and heat generated, along with the GBC produced. But, exergetic efficiency of an energy system most often discounts the ash and char by-products as loss or destroyed exergy. For reference the exergetic efficiency of the energy system discounting the GBC is included. It should be mentioned that only the chemical exergy of GBC is included in the efficiency calcuation and the physical exergy is assumed to be dissipated to the environment.

2.5. Life Cycle Assessment

The carbon balance calculation and the energy system modelling are tied together in LCA. They are joined by other elements of the life cycle inventory (LCI), e.g. extraction and transport of the FR, and the transport and application of the GBC to the agricultural field. Along with the assumed change in fertilization requirements of the agricultural field by the potassium (K) and phosphorus (P) input from GBC. The mineral fertilizer value of these elements in GBC are assumed to be 100% as done in [15-16] for GBC from a low temperature gasification. Along with the input of phosphorus and potassium in the ash, the nitrogen input is expected to be affected as well. However, not enough data could be collected to include that in the analysis.

As the assessment is consequential, the substituted marginal needs to be found for K and P fertilizers, and the district heating. For the P and K fertilizers the marginal substituted products are diammonium phosphate and potassium chloride fertilizers as done in [23] which is based on [18-19], respectively. The heat producing technology substituted is assumed to be the heat generated part of a decentralised natural gas fired combined heat and power plant.

3. Results

3.1. Carbon Balance

The cumulated decomposition curves of the FR and GBC is given in Figure 3, along with the growth rate and cumulated growth of FR. The FR decomposition curve is split into above ground and below ground FR curves.

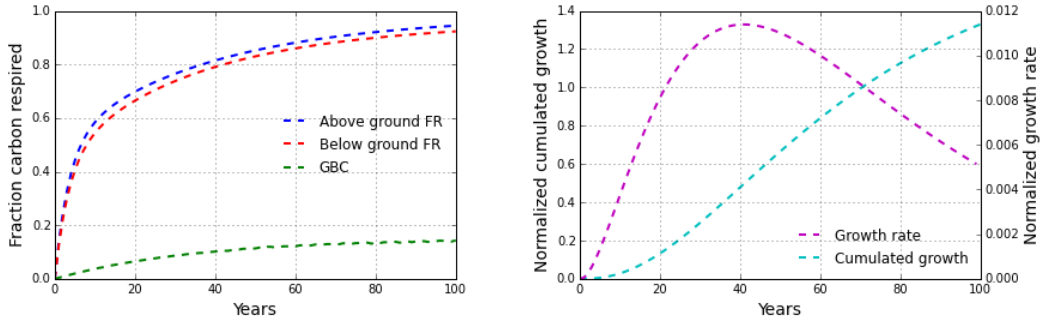

a) b)

Fig. 3. Rate of carbon emission and capture: a) Simulated carbon respiration, b) simulated growth rate and cumulated growth.

It can be seen in Figure 3 a) that GBC carbon respires very slowly compared to FR. This should benefit the Low gasification CC scenario as most of the carbon applied to the agricultural field can be considered to be sequestered in the soil in a 100 year timeframe. Figure 3 b) provides an insight into how rapidly after emitting biogenic carbon it is captured again with the 100 year rotating sustainable forestry.

The atmospheric CO_2 loads over the time horizon for each part of the GWP_{bio} formula is given in Figure 4, along with the $AGWP_{bio,CO_2}$ or CRF at each stage of the time horizon for the two scenarios and the $AGWP_{CO_2}$ reference, which its integration represent the numerator and denominator in (1), respectively.

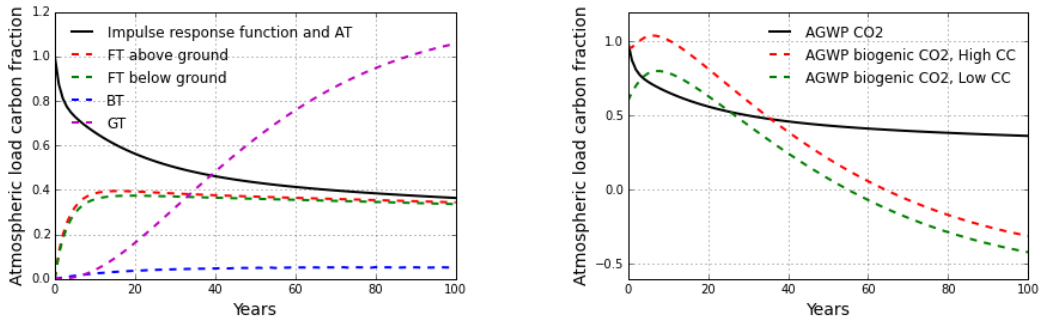

a) b)

Fig. 4. Atmospheric CO_2 loads: a) Individual parts of (1), b) Total loads of the two scenarios and fossil CO_2 as a reference.

Figure 4 a) give an insight into the relative importance of each part of the carbon balance. The difference between the two scenarios is the distribution between A_T and B_T. The High gasification CC scenario has high A_T and low B_T, but the Low gasification CC scenario maximizes the potential of the B_T part of the equation (lowering A_T as a consequence) which decreases its $AGWP_{bio,CO_2}$. This effect can be observed in Figure 4 b). The resulting GWP_{bio} for the High and Low gasification CC scenarios are 0.65 and 0.30, respectively.

3.2. Energy System Modelling

The values presented here are given in rates, i.e. mass flow, power, etc… The modelling assumed that 9000 tonnes of wet wood chips would enter the system and be used over the whole year with the capacity factor of 0.9. Table 2 displays the main outputs of the energy system simulation, other properties of the energy system can be found in Tables A1 and A2 in Appendix for the two scenarios. Figure 5 displays these resulting efficiencies for a range of CC values, i.e. from 0.60 to 0.99.

Table 2. Main outputs of the energy system simulation.

Key values	*Unit*	*High gasifier CC*	*Low gasifier CC*
Gasifier cold gas efficiency	%	93.4	60.6
Net power production	kW	1055	628
Net district heat production	kW	1576	978
GBC output flow	kg/s	0.0025	0.0373

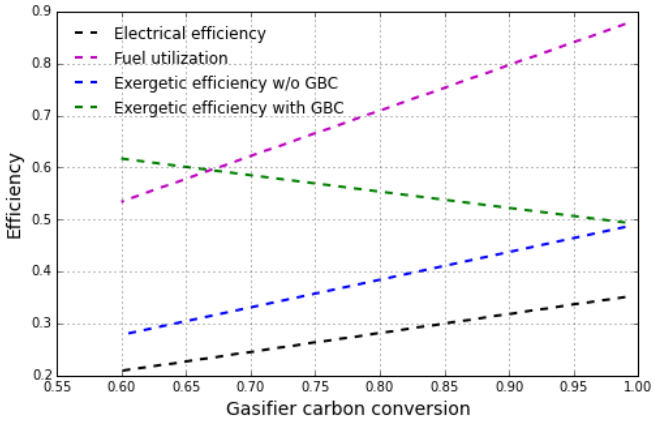

Fig. 5. Efficiencies of the energy system of a range of CC values.

It can be seen in the figure that the electrical efficiency, fuel utilization and exgetic efficiency where GBC is a loss of the system, declines as the CC is decrease from maximum energy generation to maximum GBC production. However, if the energy system approached as a polygeneration system, producing electricity, heat for district heating and GBC as a high carbon fertilizer for agricultural soils the exergetic efficiency increases with decreased CC.

3.3. Life Cycle Assessment

The LCI results includes the main parts of the system, i.e. residue recovery and chipping, transportation to and from the energy system, P and K value of the GBC, and carbon balance disaggregated to show what is allocated to power plant emissions, carbon from forest floor removal and carbon in agricultural soil sequestration. Since the functional unit is kWh electricity produced the LCI data is given in per kWh also. LCI results are presented in Table 3.

It can be seen in Table 3 that the LCI for the two scenarios changes with CC. The Low gasification CC scenario requires more input to produce the same amount of electricity as the High gasification CC scenario, which subsequently affects other parts of the system. Figure 6. displays the LCIA results for the overall system.

Table 3. Life Cycle Inventory per kWh electricity produced.

Key values	*Unit*	*High gasifier CC*	*Low gasifier CC*
Mass input	kg	1.06	1.65
Misc. energy system electricity use	kWh	0.13	0.22
Residue recovery	MJ	0.12	0.18
Chipping	MJ	0.05	0.07
Transport	tonne × km	0.054	0.092
District heat produced	MJ	4.75	4.59
GBC output flow	kg	0.0085	0.1943

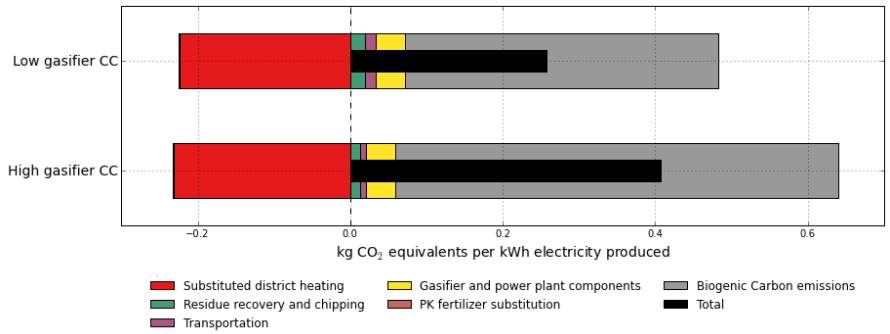

Fig. 6. IPCC GWP 100a total Life Cycle Impact Assessment results.

It can be seen in the figure that the main contributions to the results are from the energy technology substitution and biogenic carbon emissions. Also, it shows that lowering the carbon conversion in the gasifier decreases the carbon footprint of the FR fuelled power generation.

To put the results of Figure 6 into context, a comparison is made with LCA results from alternative power generation from the ecoinvent database [13]. These alternatives are fuelled with coal, natural gas and wind. The coal and natural gas fuelled production co-generate heat for district heating. To justify the comparison, this heat substitutes the same district heating as the two scenarios did. Additionally, forest floor emissions are included in the LCA of the alternatives, as it is assumed that the FR used in the two scenarios are now allowed to decompose on the forest floor. Figure 7 displays the IPCC GWP 100a LCIA for producing 1 kWh of electricity from the two scenarios and the alternatives.

It can be observed in Figure 7 a) and b) that the two scenarios perform better than the fossil fuelled alternatives. However, the High gasifier CC scenario just marginally outperforms natural gas fuelled production. Conversely, the Low gasifier CC scenario marginally outperforms offshore wind power generation.

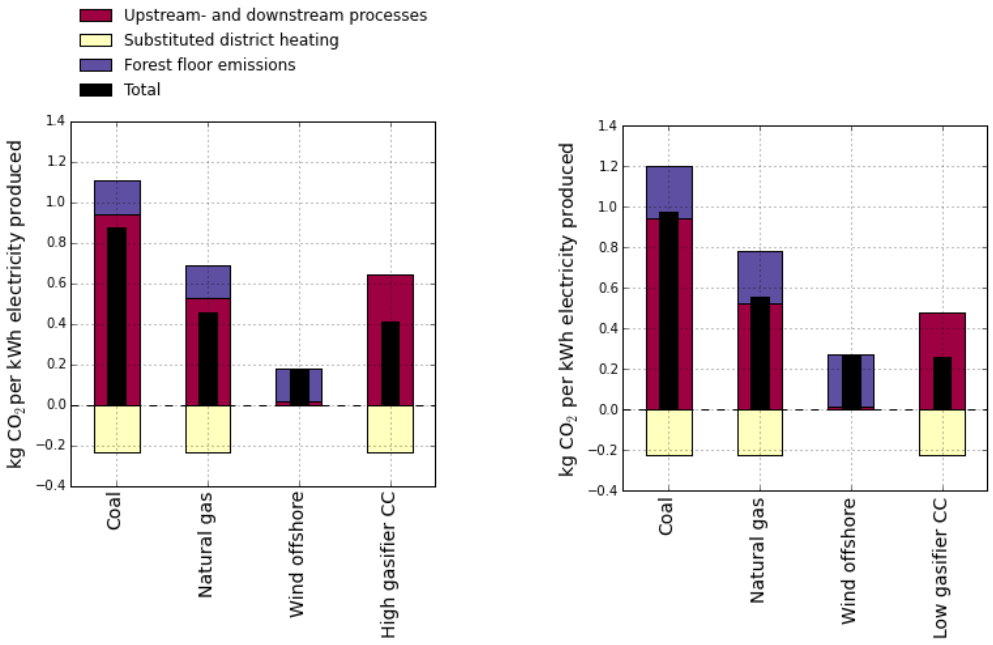

a) b)

Fig. 7 Comparison of LCIA per kWh for scenarios and from other resources: a) High gasification CC scenario, b) Low gasification CC scenario.

4. Discussion

When observing the results of the two scenarios it is clear that the effect of the GWP_{bio} is important. However, what is striking is that increasing the carbon in the GBC at the cost of the energy efficiency of the gasifier has positive effect the carbon footprint of the system. Also, from the results of the energy system simulation, the exergetic efficiency when including the GBC as a product showed an increase with decreased energy efficiency. This is important as there is increasing focus on treating "waste" as a product of a system. These results indicate that designing processes in that way could result in a better performing systems both in terms of environmental and exergetic performance.

The change in GWP_{bio} with CC is noteworthy. The cause is the change in the first year pulse emitted CO_2 per mass input to the energy system when CC is lowered. Almost all of the carbon input to the energy system is pulse emitted at the beginning of the timeframe in the high gasifier CC scenario, but a large part of it is slowly decomposed in the agricultural system for the low gasifier CC scenario. Based on these results it looks like pyrolysis could be an interesting thermochemical conversion process for biomass in terms of carbon footprint when accounting for the positive effects of the biochar.

As indicated in Section 2.5 the effect on the nitrogen balance of the agricultural soil by the input of GBC is not included. However, it has been observed that there are positive effects on the agricultural soil's water retention with increased biochar input [26]. It is also expected that nitrogen will build up as carbon is built up in the soil [27]. Both of these effects would contribute in favour of returning the GBC to an agricultural field and decrease the CC.

In Figure 7 a notable comparison was made between the scenarios and alternative energy systems. In that comparative analysis the alternatives were credited the FR forest floor emissions as they are left unutilized. The scenarios are modelled by taking into account all above- and below ground FR, but with FR extraction efficiency of 46%. It is expected that the performance of the scenarios will be better with increased FR extraction efficiency and worse with decreased efficiency. It would be interesting to expand the analysis to include the primary production of the sustainably harvested forest in a dedicated forestry bioenergy system.

In this analysis only LCIA associated with climate change was observed. However, a lot of different environmental impacts could (and should) be analysed to further assess the value of a decreased CC in a gasifier. It would also be interesting to do an economic analysis of such system integration, as it could be that lowering the CC would increase the value of the fertile GBC and thus mitigate the revenue losses from decreased efficiency. Additionally, a gasifier with a low CC could be smaller and is therefore expected to be cheaper than a gasifier with a high CC.

5. Conclusion

The article has presented a carbon footprint LCA study of an integrated bioenergy and agriculture system using wood chips from forest residues. The wood chips are used in thermal gasification to produce fuel for the CHP plant, while the GBC is applied to an agricultural soil containing biochar and nutrients.

Based on the results of the study, the main conclusions are that:

1. Utilization of forest residues, by removing them from the forest floor and presenting them as wood chips to an energy efficient energy system barely hold the comparison with fossil fuel energy systems. It does perform better then a coal based energy system, but is only marginally superior to a natural gas energy system.

2. Decreasing the carbon conversion of the gasifier, and thus allowing more carbon in the GBC, at the expense of the gasifier efficiency, improves the GWP_{bio} of the system. Such a system can even outperform offshore wind energy system in a carbon based LCA. However, those results depend on the FR extraction efficiency and the allocation between the primary and secondary production of the sustainably harvested forest.

These conclusions underline the importance of considering the GBC from a gasification system as an important fertilizer and soil amendment product. However, taking into account the possible changes in the soil's water retention, the positive effect on the environmental impact can possibly be demonstrated as even greater.

Acknowledgments

This study was funded by the Villum foundation.

References

[1] N. H. Batjes, "Total carbon and nitrogen in the soils of the world," *Eur. J. Soil Sci.*, vol. 65, no. 1, pp. 10–21, Jan. 2014.

[2] R. Lal, "Soil carbon sequestration to mitigate climate change," *Geoderma*, vol. 123, no. 1–2, pp. 1–22, Nov. 2004.

[3] J. Ahrenfeldt, T. P. Thomsen, U. Henriksen, and L. R. Clausen, "Biomass gasification cogeneration – A review of state of the art technology and near future perspectives," *Appl. Therm. Eng.*, vol. 50, no. 2, pp. 1407–1417, Feb. 2013.

[4] B. Elmegaard and N. Houbak, "DNA – A General Energy System Simulation Tool," *Proc. SIMS 2005*, pp. 43–52, 2005.

[5] B. M. Petersen, J. E. Olesen, and T. Heidmann, "A flexible tool for simulation of soil carbon turnover," *Ecol. Modell.*, vol. 151, no. 1, pp. 1–14, May 2002.

[6] J. Liski, T. Palosuo, M. Peltoniemi, and R. Sievänen, "Carbon and decomposition model Yasso for forest soils," *Ecol. Modell.*, vol. 189, no. 1–2, pp. 168–182, Nov. 2005.

[7] F. Cherubini, A. H. Strømman, and E. Hertwich, "Effects of boreal forest management practices on the climate impact of CO2 emissions from bioenergy," *Ecol. Modell.*, vol. 223, no. 1, pp. 59–66, Dec. 2011.

[8] G. Guest, F. Cherubini, and A. H. Strømman, "The role of forest residues in the accounting for the global warming potential of bioenergy," *GCB Bioenergy*, vol. 5, no. 4, pp. 459–466, Jul. 2013.

[9] B. M. Petersen, M. T. Knudsen, J. E. Hermansen, and N. Halberg, "An approach to include soil carbon changes in life cycle assessments," *J. Clean. Prod.*, vol. 52, pp. 217–224, Aug. 2013.

[10] M. Brander, R. Tipper, C. Hutchison, and G. Davis, "Consequential and attributional approaches to LCA: a Guide to policy makers with specific reference to greenhouse gas LCA of biofuels," *Econom. Press*, no. April, pp. 1–14, 2008.

[11] F. Cherubini and A. H. Strømman, "Life cycle assessment of bioenergy systems: state of the art and future challenges.," *Bioresour. Technol.*, vol. 102, no. 2, pp. 437–51, Jan. 2011.

[12] C. Mutel, "Brightway2." 2015.

[13] B. P. Weidema, C. Bauer, R. Hischier, C. Mutel, T. Nemecek, J. Reinhard, C. O. Vadenbo, and G. Wernet, "The ecoinvent database: Overview and methodology, Data quality guideline for the database version 3." 2013.

[14] R. Frischknecht, "LCI modelling approaches applied on recycling of materials in view of environmental sustainability, risk perception and eco-efficiency," *Int. J. Life Cycle Assess.*, vol. 15, no. 7, pp. 666–671, Jun. 2010.

[15] F. JOOS, M. BRUNO, R. FINK, U. SIEGENTHALER, T. F. STOCKER, C. LE QUERE, and J. L. SARMIENTO, "An efficient and accurate representation of complex oceanic and

biospheric models of anthropogenic carbon uptake," *Tellus B*, vol. 48, no. 3, pp. 397–417, Jul. 1996.

[16] F. Joos, I. C. Prentice, S. Sitch, R. Meyer, G. Hooss, G.-K. Plattner, S. Gerber, and K. Hasselmann, "Global warming feedbacks on terrestrial carbon uptake under the Intergovernmental Panel on Climate Change (IPCC) Emission Scenarios," *Global Biogeochem. Cycles*, vol. 15, no. 4, pp. 891–907, Dec. 2001.

[17] J. Schnute, "A Versatile Growth Model with Statistically Stable Parameters," *Can. J. Fish. Aquat. Sci.*, vol. 38, no. 9, pp. 1128–1140, Sep. 1981.

[18] B. Gøbel, C. Hindsgaul, U. B. Henriksen, J. Ahrenfeldt, F. Fock, N. Houbak, and E. B. Qvale, "High Performance Gasification with the Two-Stage Gasifier," in *Proceedings of the 12. European Biomass Conference. ETA-Florence & WIP-Munich*, 2002, pp. 389–395.

[19] L. R. Clausen, B. Elmegaard, J. Ahrenfeldt, and U. Henriksen, "Thermodynamic analysis of small-scale dimethyl ether (DME) and methanol plants based on the efficient two-stage gasifier," *Energy*, vol. 36, no. 10, pp. 5805–5814, Oct. 2011.

[20] A. Bejan, G. Tsatsaronis, and M. J. Moran, *Thermal Design and Optimization*. John Wiley & Sons, 1996.

[21] T. L. T. Nguyen, J. E. Hermansen, and R. G. Nielsen, "Environmental assessment of gasification technology for biomass conversion to energy in comparison with other alternatives: the case of wheat straw," *J. Clean. Prod.*, vol. 53, pp. 138–148, Aug. 2013.

[22] T. L. T. Nguyen, J. E. Hermansen, and L. Mogensen, "Environmental performance of crop residues as an energy source for electricity production: The case of wheat straw in Denmark," *Appl. Energy*, vol. 104, pp. 633–641, Apr. 2013.

[23] L. Hamelin, M. Wesnæs, H. Wenzel, and B. M. Petersen, "Environmental consequences of future biogas technologies based on separated slurry.," *Environ. Sci. Technol.*, vol. 45, no. 13, pp. 5869–77, Jul. 2011.

[24] F. Tenkorang and J. Lowenberg-DeBoer, "Forecasting long-term global fertilizer demand," *Nutr. Cycl. Agroecosystems*, vol. 83, no. 3, pp. 233–247, Oct. 2008.

[25] FOOD & AGRICULTURE ORGANIZATION OF THE UNITED NATIONS, "Current world fertilizer trends and outlook to 2013," 2009.

[26] V. Hansen, D. Müller-Stöver, J. Ahrenfeldt, J. K. Holm, U. B. Henriksen, and H. Hauggaard-Nielsen, "Gasification biochar as a valuable by-product for carbon sequestration and soil amendment," *Biomass and Bioenergy*, vol. 72, pp. 300–308, Jan. 2015.

[27] B. M. Petersen, L. S. Jensen, S. Hansen, A. Pedersen, T. M. Henriksen, P. Sørensen, I. Trinsoutrot-Gattin, and J. Berntsen, "CN-SIM: a model for the turnover of soil organic matter. II. Short-term carbon and nitrogen development," *Soil Biol. Biochem.*, vol. 37, no. 2, pp. 375–393, Feb. 2005.

Appendix A

Table A1. Flow properties at each stage of the energy system. High gasification CC scenario.

State	*Mass flow rate (kg/s)*	*Temperature (°C)*	*Pressure (bar)*	Enthalpy (kJ/kg)
1	0.32	15	-	-9793.3
2	0.19	115	-	-5345.7
3	0.18	115	-	-5138.7
4	2.33	115	1.013	-13264.7
8	0.00	730	-	-5268.5
9	0.40	730	1.013	-1871.2
13	0.40	150	1.013	-2732.9
14	0.40	50	1.013	-2872.7
15	0.40	50	1.013	-2872.9
17	2.07	24	1.013	-638.6
18	2.07	108	2.000	-547.3
20	2.07	25	2.000	-637.1
21	2.07	658	2.000	-1435.4
22	2.07	577	1.216	-1532.5
23	2.07	125	1.216	-2039.4
26	2.20	115	1.013	-13264.7
27	2.20	200	1.013	-13095.7
29	0.22	15	1.013	-98.8
30	0.22	700	1.013	632.6
36	1.66	15	1.013	-98.8
37	0.00	50	1.013	-15761.7
39	0.13	115	1.013	-13264.7
40	0.13	50	1.013	-15761.7

Table A2. Flow properties at each stage of the energy system. Low gasification CC scenario.

State	*Mass flow rate (kg/s)*	*Temperature (°C)*	*Pressure (bar)*	Enthalpy (kJ/kg)
1	0.32	15	-	-9793.3
2	0.19	115	-	-5345.7
3	0.18	115	-	-5138.7
4	2.33	115	1.013	-13264.7
8	0.04	730	-	153.6
9	0.26	730	1.013	-3247.9
13	0.26	112	1.013	-4276.0
14	0.26	50	1.013	-4371.4
15	0.26	50	1.013	-4372.0
17	1.36	24	1.013	-917.1
18	1.36	108	2.000	-824.0
20	1.36	25	2.000	-916.3
21	1.36	558	2.000	-1800.3
22	1.36	475	1.139	-1899.4
23	1.36	125	1.139	-2295.9
26	2.20	115	1.013	-13264.7
27	2.20	200	1.013	-13095.7
29	0.11	15	1.013	-98.8
30	0.11	700	1.013	632.6
36	1.10	15	1.013	-98.8
37	0.00	50	1.013	-15761.7
39	0.13	115	1.013	-13264.7
40	0.13	50	1.013	-15761.7

Integrated model of bioenergy and agriculture system

Hafthor Ægir Sigurjonsson[1] Brian Elmegaard[1] Lasse Røngaard Clausen[1]

[1]DTU Mechanical Engineering, Technical University of Denmark (DTU), Denmark,
{hafsig,be,lrc}@mek.dtu.k

Abstract

Due to increased burden on the environment caused by human activities, focus on industrial ecology designs are gaining more attention. In that perspective an environmentally effective integration of bionergy and agriculture systems has significant potential. This work introduces a modeling approach that builds on Life Cycle Inventory and carries out Life Cycle Impact Assessment for a consequential Life Cycle Assessment on integrated bioenergy and agriculture systems. The model framework is built in Python which connects various freely available software that handle different aspects of the overall model. C-TOOL and Yasso07 are used in the carbon balance of agriculture, Dynamic Network Analysis is used for the energy simulation and Brightway2 is used to build a Life Cycle Inventory compatible database and processes it for various impacts assessment methods. The model is successfully demonstrated using a manure utilization case study where the manure is used to produce biogas and then heat and power, whereas its digestate is used as an organic fertilizer to a wheat field. The case study is compared with direct manure to wheat field application.
Keywords: Life cycle assessment, energy efficiency, sustainability

1 Introduction

Environmental conscious design of industrial systems has gained more interest in recent years and the development of industrial ecosystems and eco-industrial parks are now relevant topics for policy-makers. This is in large part due to increasing public awareness of the environmental burden from human activity on the environment. Denmark's future energy plan for 2050 is to be completely independent of fossil fuels for all energy consumption in the country (Danish Ministry of Climate. Energy and Buildings). This includes all electricity and heat consumption, along with transportation fuels. For this to be possible and make sense, the utilization of energy resources needs to be environmentally effective and the available options going forward need to be thoroughly investigated. Along with this focus on more environmentally friendly energy system in Denmark, the environmental burden of its agricultural industry also needs to addressed, which today releases about 15% of the total national greenhouse gas emissions (Government (2013a)). A climate change mitigation potentials inter-ministerial working group report identified a few connection with the energy industry to mitigate those emissions (Government (2013b)).

Finding the best possible integration between these two industries in terms of net environmental impact is the motivation of this work. Systems are analyzed using the Life Cycle Assessment framework (LCA) (Rebitzer et al. (2004)) using the Brightway2 software (Mutel (2015)). Building the Life Cycle Inventory (LCI) (Suh and Huppes (2005)) requires detailed models of the inputs and outputs of the agricultural and energy systems, along with possible interactions between them. Integration between bioenergy and agriculture can be done in various ways. In this work the focus has been on producing electricity and district heat by using residual resources in the agricultural system and thus not affect its capacity to produce food and related products. Additionally, the organic residues from the biomass conversion in the energy system are returned back to the agricultural system to ensure that most of the essential elements, e.g. macro-nutrient, for agricultural activities are recycled. The agricultural system base model is a field which mainly produces wheat grain, located in Zealand Denmark. In its reference state, it is fertilized with mineral fertilizers and has expected yield according to the national agricultural guidelines (NaturErhvervstyrelsen (2013)). The LCI model is built on top of an extensive model gathered from the Ecoinvent3 database (Weidema et al. (2013)) and follows their basic modeling principles, in addition to a comprehensive atmospheric carbon balance modeling procedure adopted from (Cherubini et al. (2011) and Petersen et al. (2013)) and using results generated by the soil carbon balance simulation software C-TOOL (Petersen et al. (2002) and Petersen et al. (2005)). The energy system utilizes biomass resources and can be either based on biochemical or thermochemical conversion (or both) before heat and power generation in a gas engine or a steam cycle and will always deliver its residues to the agricultural system as organic fertilizer. Modeling of the energy system is done in the Dynamic Network Analysis (DNA) (Elmegaard and Houbak (2005)). Like the agricultural system the energy

system LCI model is built on top of a model gathered from Ecoinvent3 but using results from DNA. The Life Cycle Impact Assessment (Pennington et al. (2004)) results are given in four levels, from a normalized and weighted endpoint result combining seventeen different environmental indicators into one numerical result to disaggregating the most important indicators to specific inputs and outputs of the system analyzed using midpoint level LCIA. This is to allow for evaluation of the total environmental impact and what inputs and outputs are mostly effecting that outcome.

This articles describes the methodology of the integrated agriculture and bioenergy environmental impact assessment model. How the LCIs are built from mass, energy and substance balances of the sub-systems, and how the four levels LCIA analysis gives overall environmental impact and the major contributors to that impact as a result. The model is demonstrated by analyzing manure based biogas production and utilization. Additionally, a direct manure to field application is analyzed as a reference case.

2 Method

2.1 Case description

The modeling and analysis methods introduced in this paper are demonstrated by a case study on biogas production and utilization from pig manure, and a reference case with direct pig manure to field application. The objective of the analysis is to report the environmental impact change to one hectare agricultural field and to identify the main impacts and contributors to the final result. A simple flow chart of the system can be seen in Figure 1.

The system for each case is divided into three subsystems, i.e. agricultural, storage and transportation, and energy. The energy sub-system consist of the biochemical conversion of biomass to biogas, and heat and power generation. Before the pig manure is converted to biogas and digestate, it is stored and then de-watered in a decanter. The liquid manure is stored in an outdoor storage before it is applied to the agricultural sub-system. However, the solid manure is converted in an anaerobic digester to biogas and digestate. The digestate follows the same process as the liquid manure, but the biogas is combusted in a gas engine producing electricity and district heat.

The agricultural sub-system is a cereal grain production using conventional practices. For the analysis the manure is modeled as a recycled content (Frischknecht (2010)), i.e. only the impacts it induces follow the flow and other parts of the pork production are excluded. Moreover, as raw manure, liquid manure or digestate are applied to the field its effective macro-nutrient content replaces mineral fertilizer and modifies the field emissions.

2.2 Model formulation

2.2.1 Agricultural sub-system model

The objective of this model is to produce a Life Cycle Inventory (LCI) of the system described by the user. A database is used to form the base of a LCI, which is then manipulated and modified based on the actual condition and substance balances of the system. To describe that process the agricultural sub-system model is divided into three modeling sections representing, nutrients-, carbon- and heavy metals balance which will deliver new unit processes and elementary flows for the LCI.

The nutrient balance model is based on the macronutrients required to grow crops, i.e. nitrogen (N), phosphorus (P) and potassium (K). The flow of these nutrients through the system are governed by conservation of mass and each substance is modeled individually. Only N is modeled to change in the control volume by immobilization and mineralization in the agricultural soil, for both P and K the outputs are equal to the inputs.

The reference mineral fertilization is based on national guidelines for fertilization (NaturErhvervstyrelsen (2013)) and the change in nutrient balance is regulated by the mineral fertilizer input. Uptake by harvest, grain and straw (if harvested), are a part of the nutrient output of a field. The uptake by grain is based on the yield and its chemical composition. Yields are assumed based on the soil type using national guidelines (NaturErhvervstyrelsen (2013)) and chemical composition is extracted from a biomass database adopted from (Vassilev et al. (2010)). Same principles apply to straw, along with extraction efficiency, i.e. how much of the total straw are harvested. For P model, leaching, surface run-off and erosion are included and estimated based on (Nemecek and Schnetzer (2012)). Figures 2 and 3 display the phosphorus inputs and output of the agricultural sub-system.

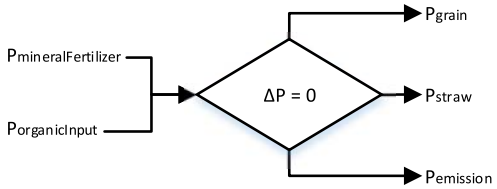

Figure 2. Phosphorus balance in the agricultural sub-system.

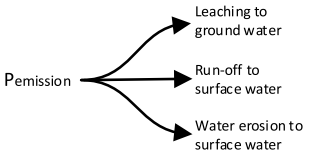

Figure 3. Phosphorus emissions in the agricultural sub-system.

DOI
10.3384/ecp15119211

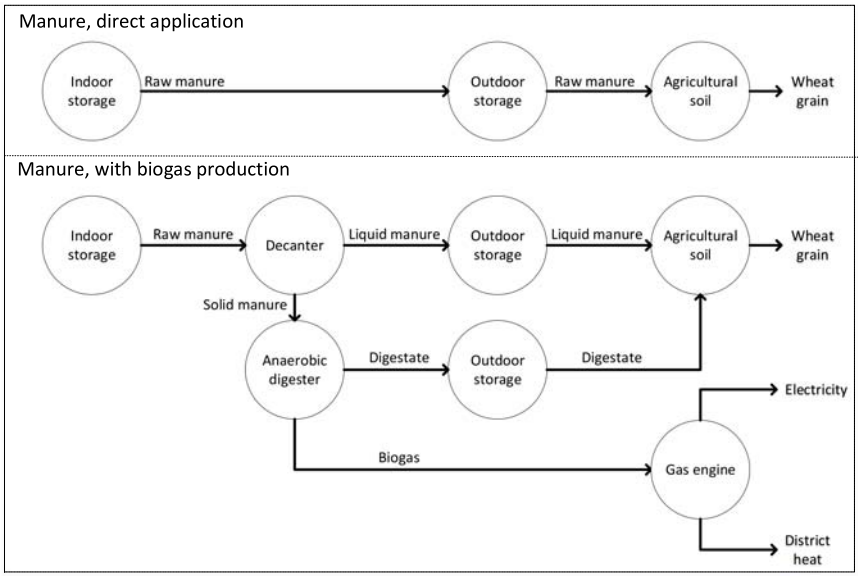

Figure 1. Flow diagram for the case study and the reference.

K model also includes leaching as an emission, but the calculations are based on a method adopted from (de Willigen (2000)) recommended by Food and Agriculture Organization (FAO) in Assessment of nutrient balances: Approaches and methodologies (Roy et al. (2003)). Figures 4 and 5 display the potassium inputs and output of the agricultural sub-system.

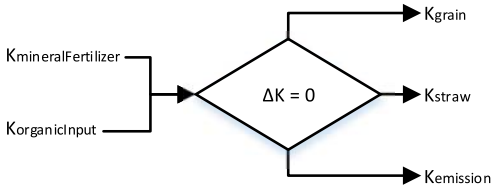

Figure 4. Potassium balance in the agricultural sub-system.

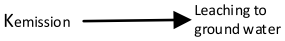

Figure 5. Potassium emissions in the agricultural sub-system.

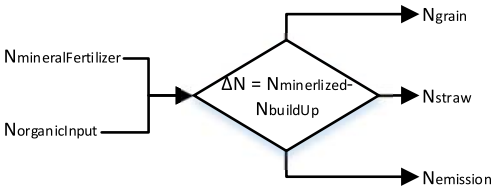

Figure 6. Nitrogen balance in the agricultural sub-system.

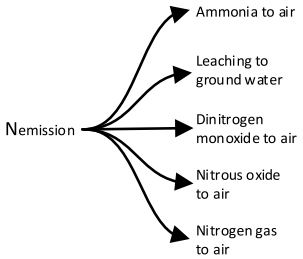

Figure 7. Nitrogen emissions in the agricultural sub-system.

Nitrogen outputs include leaching (NO_3^-), along with nitrous oxide (N_2O), nitrogen gas (N_2) and ammonia (NH_3) emissions. These nitrogen outputs are calculated in different ways depending on the input resource. Figures 6 and 7 display the nitrogen inputs and output of the agricultural sub-system.

For pig manure sourced inputs (raw slurry, liquid fraction, solid fraction, digestate, liquid digestate and solid digestate) the nitrogen outputs were calculated using the same methods as in (Hamelin et al. (2011)). The methods of assessing direct field emissions for LCIs of agricultural production sub-system (Nemecek and Schnetzer (2012)) are used for mineral and cereal straw sourced inputs.

The carbon (C) balance model is based on the flow through the whole system and follows the law of mass conservation. Similarly to the nutrient balance model the C output of the agricultural sub-system is based on the uptake (photosynthesis) by harvest and associated emis-

sion. However, the input is equal to the total carbon captured by photosynthesis of the whole growth on the field (harvest and residues) in addition to any organic or inorganic C input through fertilization. The uptake is based on the chemical composition, yield and extraction efficiency in the same manner as described above. Figures 8 and 9 display the carbon inputs and output of the agricultural sub-system. Additionally, to describe the photosynthesis the growth period displayed in Figure 10 is simulated based on the Schnute model (Schnute (1981)), a versatile growth model based on statistically stable parameters. C emissions from the agricultural sub-system is based on the respiration of decaying residues and organic fertilizer. The magnitude of these residues is based on the straw extraction efficiency and any other organic input to the soil. C decay from the residues and other organic carbon inputs are simulated by C-TOOL (Petersen et al. (2002, 2005)), a software for whole-profile carbon storage simulation in temperate agricultural soils. This also needs to be considered for other biomass potentially utilized in the overall system. C balance for a wood chips feedstock is thus modeled in a forest sub-system. That model follows the same principles as the agricultural sub-system but uses data extracted from Yasso07 (Liski et al. (2005)), a carbon and decomposition software for forest soils, to simulate the decay of forest residues. It can be seen in Figure 11, that the carbon emission from decaying biomass is gradual over time. The impact factor related to greenhouse gas emissions is in reference of pulse emission of carbon dioxide, i.e. all carbon is emitted in the first year, but the influence on climate change is then based on the integrated radiative forcing of carbon dioxide in the atmosphere. Thus the load of carbon dioxide in the atmosphere needs to adequately accounted for in the case of biomass decay carbon dioxide emissions. When emitted it starts to be absorbed by earth's many sink, e.g. ocean and terrestrial forests, this is simulated by the impulse response function (Joos et al. (1996, 2001)) which needs to be combined with the biomass decay emissions to get their atmospheric load over a time horizon. Figure 12, displays the atmospheric load of carbon emission from different sources in reference to pulse emitted CO_2. The global warming potential

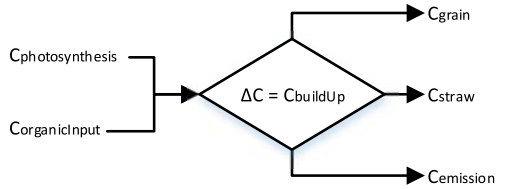

Figure 8. Carbon balance in the agricultural sub-system.

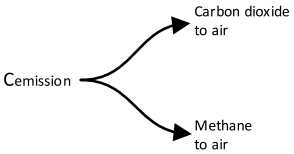

Figure 9. Carbon emissions in the agricultural sub-system.

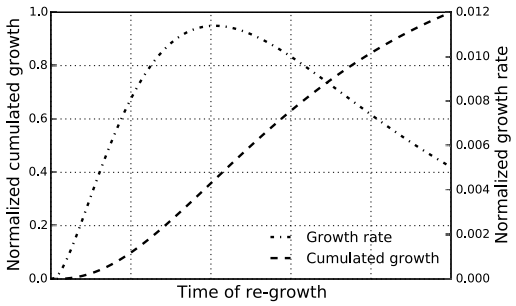

Figure 10. Carbon captured by photosynthesis in the agricultural and forestry sub-system.

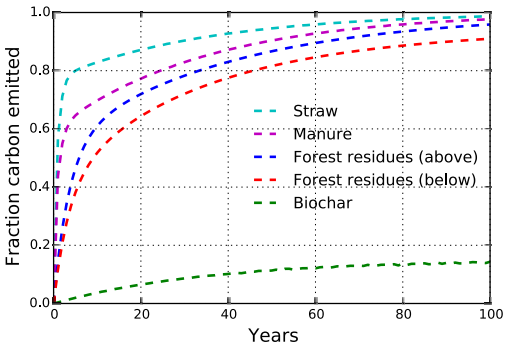

Figure 11. Carbon emissions from decomposition in the agricultural and forestry sub-system.

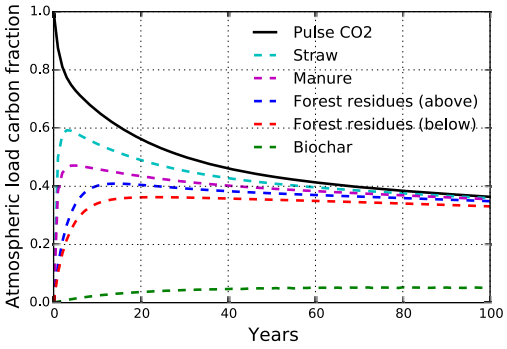

Figure 12. Atmospheric load due to carbon dioxide emissions.

DOI
10.3384/ecp15119211

for the biomass decay carbon dioxide emission can then be calculated by referencing their atmospheric load to that of the pulse carbon dioxide. The global warming potential of the different biomass decay emissions is displayed graphically overt time in Figure 13.

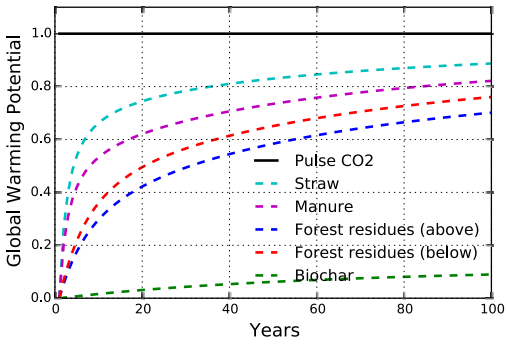

Figure 13. Evolution of the global warming potential over time.

It can be seen in Figure 13 the curve representing manure ends at a value about 0.81. This indicates that the global warming potential of 1 kg manure carbon dioxide decay is about 0.81 kg carbon dioxide equivalent. However, there are two elements to the total global warming potential of a biomass and the other is the sub-sequent regrowth of carbon in the biomass type. This is described in Figure 10 above, and for carbon in manure which mainly comes from annual rotation agricultural crops the value is -1 as its carbon is captured within a year.

The Heavy metals balance model is like the other balance models based on the flow through the whole system and follows the law of mass conservation. The heavy metals modeled are: Cadmium (Cd), copper (Cu), zinc (Zn), lead (Pb), nickel (Ni), chromium (Cr) and mercury (Hg). Inputs to the agricultural field are based on the heavy metals content of fertilizers, pesticides, seeds and disposition. The heavy metals can either accumulate or diminish from the soil based on the balance and are accounted for as emission to the soil (can be positive or negative). For the reference system the emissions are modeled according to ecoinvent modules which use SALCA-heavy metal (Nemecek and Schnetzer (2012)) as its reference. The emission is divided between soil emissions, leaching to ground water and erosion to surface water. Figures 14 and 15 display the heavy metals inputs and output of the agricultural sub-system. The leaching and erosion are modeled in SALCA-heavy metal based on constants, so when inputs change in the reference system the accumulation or demission in soil is only affected, thus causing increase or decrease in soil emissions.

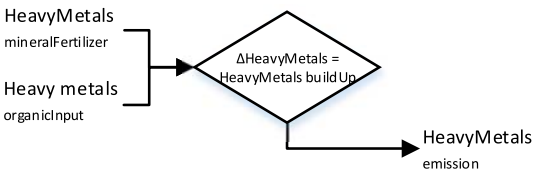

Figure 14. Heavy metals balance in the agricultural sub-system.

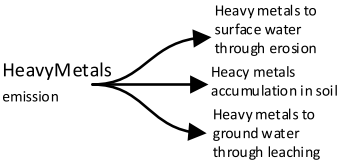

Figure 15. Heavy metals emissions in the agricultural sub-system.

2.2.2 Energy sub-system model

The energy sub-system is modeled with the Dynamic Network Analysis (DNA) energy system simulation tool (Elmegaard and Houbak (2005)). By using DNA it is possible to use the library of energy components already modeled there. Specific models of the energy sub-system for use in this project are modeled in DNA. In all of those pre-made models, the inputs requirements are the ultimate chemical composition, energy content and specific heat of the resource utilized. Optionally, the operation parameters which are to be varied can be defined. The ultimate chemical composition of the resource used is found in the same way as in Section 2.2.1. Additionally, the Higher Heating Value (HHV) and specific heat (cp) are estimated on a dry basis with the following equations from (Friedl et al. (2005)) and (Dupont et al. (2014)) for each resource, respectively.

$$HHV_{dry} = 341.7 \cdot C + 1322.1 \cdot H + 119.8 \cdot (O+N) - 123.2 \cdot S/10000 - 15.3 \cdot A \quad (1)$$

Where C, H, O, N, S, A are the carbon, hydrogen, oxygen, nitrogen, sulfur and ash content of the resource given by its ultimate chemical composition.

$$CP = (5.340 \cdot T(K) - 299)/1000 \quad (2)$$

DNA already handles all mass and energy balances over the whole energy sub-system it simulates and delivers the properties of each state of the energy sub-system and all necessary information about its products, e.g. electricity, district heat, digestate, biochar and ash, and fuel.

DNA provides information about the emissions from the power plant. For a thermochemical conversion system the power plant consists of a gasifier and either a steam cycle or a gas engine, and for a biochemical conversion system the power plant consist of an anaerobic digester

and either a steam cycle or a gas engine. By doing all this, DNA handles the nutrient and carbon balance through the power plants. It is worth noting that the nutrient balance differs in one significant way for power plants using biochemical- or thermochemical conversions. This can be observed in Figures 16a and 16b. It can be seen the figures that the nitrogen input is lost as emissions when the resource is thermochemically converted, whereas it is retained in the digestate, making it available to the agricultural sub-system again, when biochemically converted.

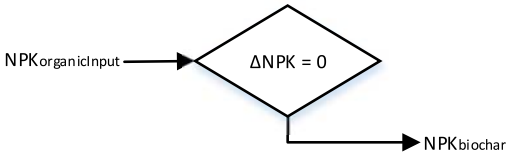

(a) Biochemical conversion.

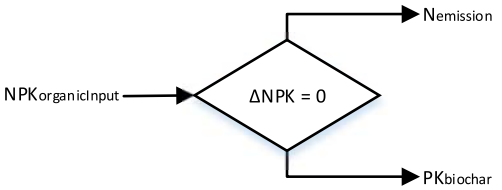

(b) Thermochemical conversion.

Figure 16. Nutrient balance for inputs to the power plants.

As mentioned in above the carbon balance for the power plants is performed in DNA. The inputs and outputs from DNA are the carbon input of the organic material to be converted and then either digestate or biochar for biochemical or thermochemical conversion respectively, and emissions which can be both carbon dioxide and methane or just carbon dioxide corresponding to Figure 9 in Section 2.2.1.

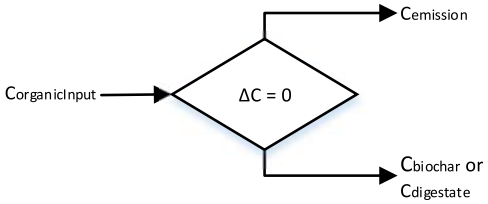

Figure 17. Carbon balance for inputs to the power plants.

2.2.3 Storage and transportation sub-system model

The P and K nutrient balance of the storage and transportation sub-system are modeled with an organic input and an organic output, which are equal for both P and K. However for the decanter the distribution between liquid and solid fraction differs according to (Hamelin et al. (2011)), which also gives the distribution for N. Most often the balance for N is equivalent to P and K, but special attention is drawn to storage of manure type resources. In those cases N emissions need to be accounted for, which are the same as introduced in Sections 2.2.1 and 2.2.2 except nitrate leaching is added. Figures 18 and 19 display the nitrogen inputs and output of the storage and transportation sub-system. It can be seen in the figures that there are a-lot of similarities to Figures 6 and 7 and the amounts are calculated according to (Hamelin et al. (2011)) like for pig manure sourced emissions from agricultural field, but these emission are specific to indoor and outdoor storage.

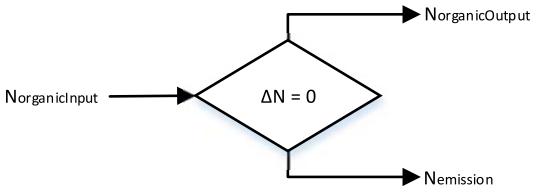

Figure 18. Nitrogen balance in the storage sub-system.

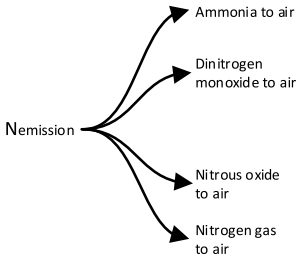

Figure 19. Nitrogen emissions in the storage sub-system.

The carbon balance is equivalent to the nitrogen balance, but with emissions corresponding to Figure 9 and the magnitude of the emissions are calculated according to (Hamelin et al. (2011)).

2.3 Performance analysis model

LCIA results are given in four levels, where the total endpoint results are disaggregated to each impact category and sub-system. Before the results are disaggregated to the main impact categories for each input and output of the LCI at midpoint level. Figure 20 displays the elements of the four level LCIA method.

First the total endpoint results are given. Those results give the total environmental impact asserted by the system analysed. These endpoint results are given in relation to its subcategories, i.e. ecosystem quality, human health and resources, which are then given for each sub-system. Those results are then further disaggregated into their impact subcategories; for ecosystem quality, i.e. agricul-

DOI
10.3384/ecp15119211

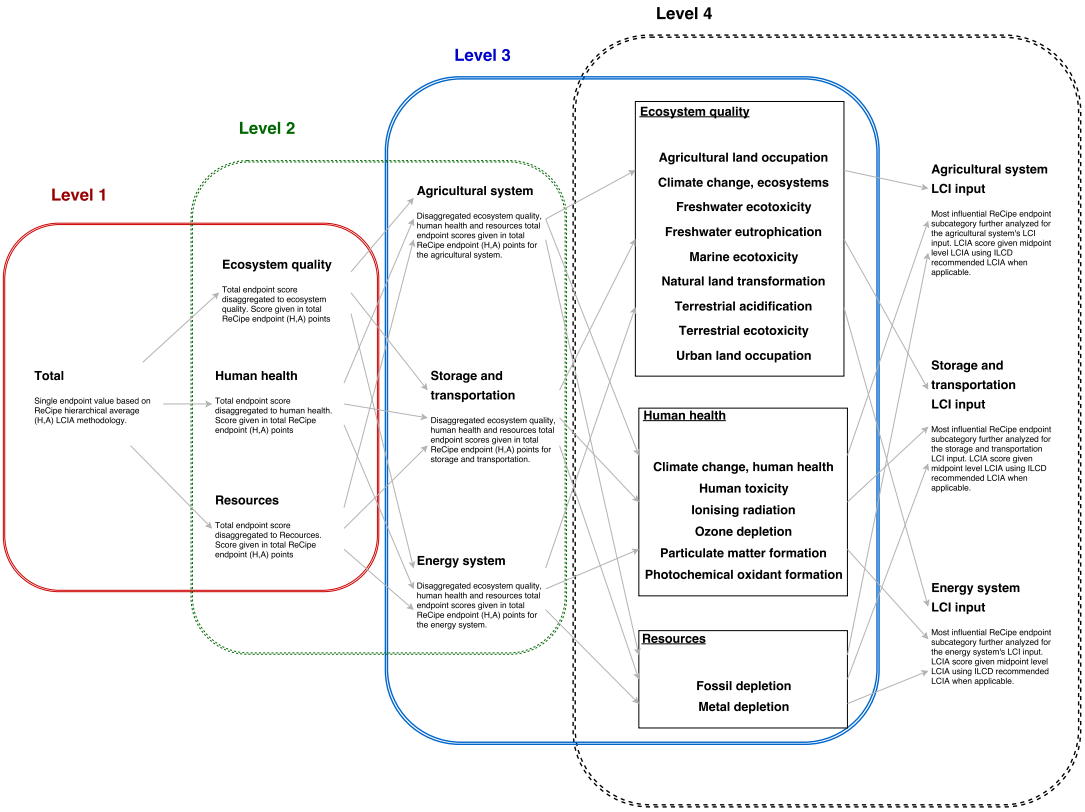

Figure 20. Elements of the four level LCIA method.

tural land occupation, climate change, freshwater ecotoxicity, freshwater eutrophication, marine ecotoxicity, natural land transformation, terrestrial acidification, terrestrial ecotoxicity and urban land occupation; for human health, i.e. climate change, human toxicity, ionizing radiation, ozone depletion, particulate matter formation and photochemical oxidant formation; and for resources, i.e. fossil depletion and metal depletion. Level four then takes the most important impact categories and gives midpoint results for each input and output of the LCI. By doing this the elements of greatest influences to the environmental impact can be identified. For endpoint results the ReCipe method Goedkoop et al. (6 January 2009) is used and the International Reference Life Cycle Data System (ILCD) recommended methods (Hauschild et al. (2010)) are used for the midpoint results.

3 Model implementation

Python 2.7 was used to design of the integrated agricultural and bioenergy model. The open source advanced life cycle assessment software Brightway2 Mutel (2015) is imported as a module, which enables easy communication with the Ecoinvent3 database Weidema et al. (2013) once uploaded. Communication to other software within the model script is done by interacting with the operating system and with file manipulation using the os and shutil python modules, respectively. Pandas is used for data structures and as a data analysis tool to import and manipulate data within the python script, and the numpy module is used for all numerical calculation. A basic flowchart of the main processes it goes through when used is displayed in Figure 21. Figure 21 uses five different objects to describe various functions in the model. Those functions are; internal process, external process, decision, input/output and local database. The meaning behind internal processes is that these objects are created in and operate fully in the python script the model is written in by the author. However, external processes operate outside the model script and an object has been made for communication within the model script. Local databases are also outside of the script model but no processes are operating within them as they simply pass on data to either internal or external processes that operate on them. The decision function basically contains information on what

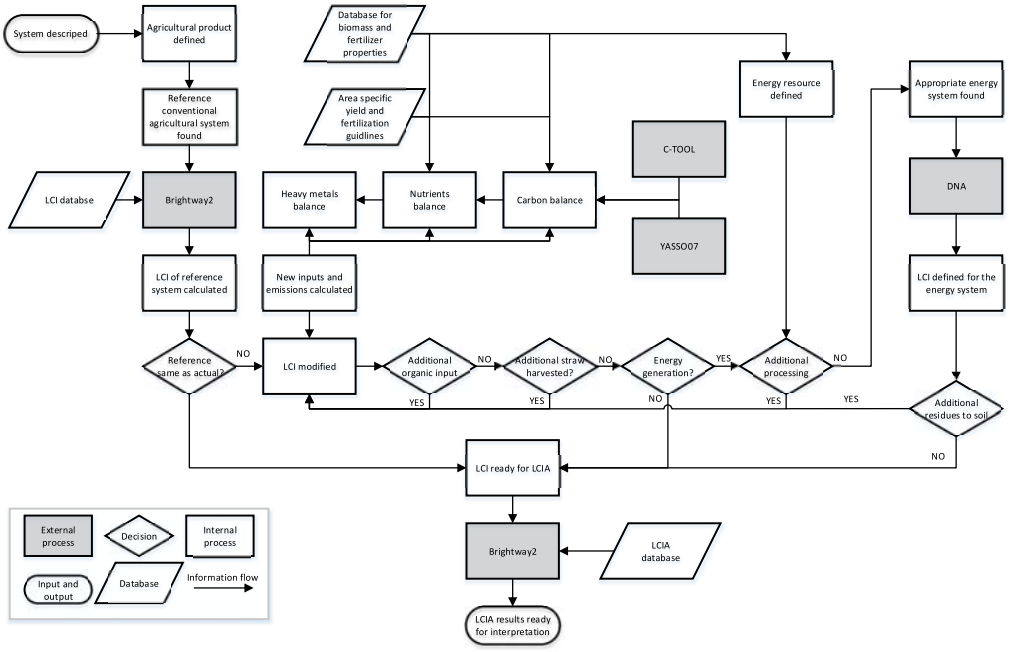

Figure 21. Basic flowchart of the integrated system model.

to do when different cases and/or situations are modeled. Input/output functions communicate information with the user of the model, i.e the input information required to use the model and the output it gives based on those information. The arrows describe the main information flow in the model. It is beneficial to use the case study and its reference to further explain the procedures of the model. Starting with the reference case, the system analyzed is defined, i.e. direct manure application on a field whose main product is wheat grain. The agricultural product of wheat grain is identified and a reference case with a complete LCI is found from the ecoinvent database using Brightway2.

For a wheat grain product the model automatically finds a predefined reference which has similar properties as such a system in Denmark where the case study is located. At this point, a full LCI is ready for LCIA. However, this system is not fully descriptive to the system being analyzed. Therefore, a modification of the LCI generated is required for new unit processes and emissions of the system. This is done by first gathering information about the fertilization requirements and expected yield, then the nutrient-, heavy metal- and carbon balances are made for the new properties of the system. At this point, the agricultural product is produced as the reference but representing specific conditions in Denmark.

Next the model reacts to an additional organic input, e.g. manure, if there are no further organic inputs the LCI is ready for LCIA. If there is an additional organic input the LCI is modified similarly as before, but now balances are made including the organic input with its properties. Likewise, if the straws are removed their properties are removed as-well which affects the balances and the LCI is modified. If the straws are not removed the LCI is ready for LCIA (as the straws are not removed in the reference). The calculation of the LCI is finished here for the reference case.

For the case study the process is the same until the model reacts to additional organic input as there is a liquid manure and an input from the energy sub-system, i.e. digestate. Then the LCI needs to be modified again taking those inputs to consideration. The energy sub-system can be connected to the agricultural sub-system by utilizing its straws but it can also use an external source as done in the case study with the raw pig manure. Either way there is a need to check if additional processes, e.g. storage and/or separation, are required. If the sub-system requires additional processes before resources can be utilized in a power plant the inputs and emissions need to be calculated and LCI is modified.

At this point the appropriate energy sub-system needs to be found which is available and built in DNA prior to running the model. From DNA, all balances are calculated and its data can directly be post-processed into a LCI. Now the LCI in the agricultural sub-system is modified if the residues from the energy sub-system are sent to it and a combined LCI ready for LCIA is fully defined. As described in Section 2.3, there are a few steps the model

DOI
10.3384/ecp15119211

makes when compiling the LCIA results before they are displayed to the user.

4 Case study results

LCI tables are given in Appendix A.1 for both the case study and the reference case. Those tables display the inputs and outputs for each sub-system, where the values are given as a changes from conventional wheat production in Denmark. The LCIA results are given in reference to the LCIA levels described in Section 2.3 and in Figure 20. Figure 22 gives the Level 1 endpoint results of the direct field application reference and the biogas production and utilization case.

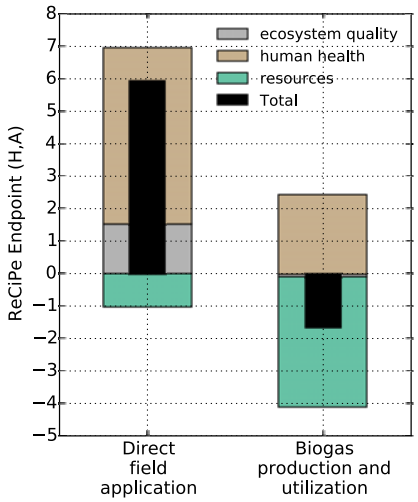

Figure 22. Life Cycle Assessment endpoint results (Level 1).

It can be seen in Figure 22 that the total score of the case study has a lower overall environmental impact then its reference and has a net mitigating environmental effect, whereas the reference has an intensifying effect.

Figure 23 gives the results of the Level 2 analysis, by disaggregating the results from Figure 22 into the main sections of the overall system, i.e. agricultural sub-system, storage and transportation, and energy system, for the three aggregated endpoint categories.

It can be seen in the 23 that the case study outperforms its reference in all three aggregated endpoint LCIA categories. Further, the distribution between the sections indicates large changes in the agricultural sub-system for the ecosystem quality and human health categories, but the largest changes are in the energy sub-system for the resources category. This can be further investigated in a Level 3 analysis. Figures 24 - 26 disaggregate the results from Figure 23 in to subcategories of ecosystem quality, human health and resources, respectively. In Figure 24 it can see that the greatest contributor to the ecosystem quality impact is climate change and there is very little impact in the other subcategories. In the agricultural subsystem both the case study and its reference show a mitigating effect on climate change, but the case study offers considerably greater mitigation. However, in storage and transportation the impact is intensified. There the case study is less intensive than its reference, but for the energy sub-system the case study also has an intensifying effect whereas the reference does not have an impact as it has no processes in the energy sub-system. To further investigate those results it is relevant to take a closer look at the climate change impact in a Level 4 analysis.

Figure 27 in the Appendix, displays the results using the midpoint category IPCC's global warming potential over a 100 time horizon. for each section. But disaggregated to the inputs and outputs of the system in relation to the LCI. In Figure 27a the difference in the impact of the agricultural sub-system can be found to be due to the carbon dioxide emission and the mineral nitrogen fertilizer input. The amount of carbon dioxide emitted from the agricultural sub-system can be found in tables 3 and 4, but the reason can be found in Section 2.2.1. There it is stated that the carbon dioxide emission from the agricultural subsystem is carbon respiration from decaying organic matter in the soil. Digested manure has less carbon then raw manure because a large portion of it is transformed into biogas in the anaerobic digester. The amount of substituted mineral nitrogen fertilization is given in tables 1 and 2. The reason for greater substitution in the case study can be found in the nitrogen balance of the agricultural subsystem described in Section 2.2.1, there it is stated that less nitrogen in the digested manure is immobilized in the soil compared to nitrogen in raw manure and thus more nitrogen available to the growing plants. It can be observed in Figure 27b that the difference in impact is due to the difference in methane emission. In Section 2.2.3 it is stated that the carbon balance of the storage units is based on Hamelin et al. (2011), where the digested manure has mostly slowly degradable volatile solids and the emissions are based on the amount of volatile solids stored.

The greatest impact factors in the energy sub-system found by observing Figure 27c are the carbon dioxide emission and the substitution of natural gas fueled heat and power generation. The carbon emission is from the carbon that was taken from the manure in the anaerobic digester is the reason for the decrease in carbon emission between the case study and the reference in the agricultural sub-system. What is interesting is that although the net carbon emission from the agricultural and energy subsystems is greater in the case study the substitution of fossil fueled heat and power generation counterweights that and contributes in making the biogas production and utilization case superior to its reference in terms of climate change impact.

Figure 25 displays the human health environmental im-

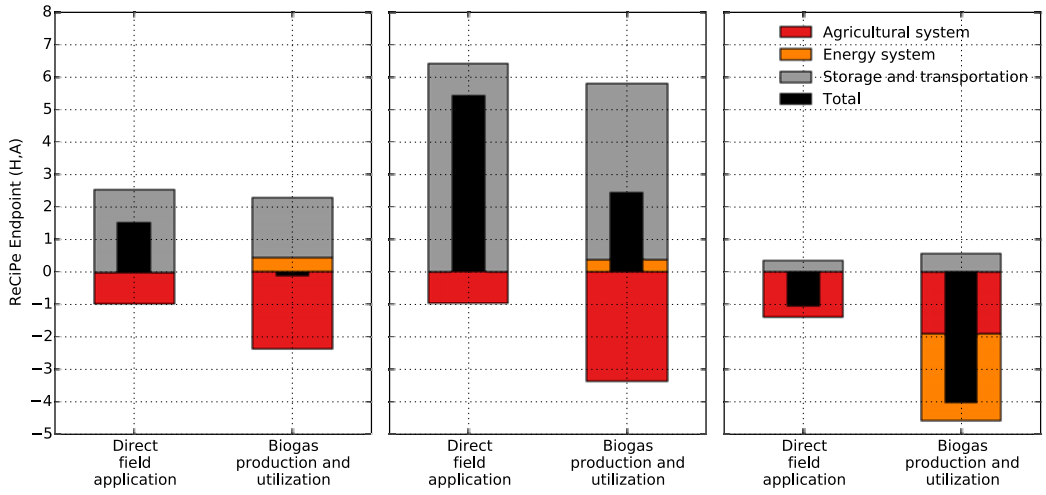

(a) Ecosystem quality. **(b)** Human health. **(c)** Resources.

Figure 23. Disaggregated Life Cycle Assessment ecosystem quality endpoint results (Level 2).

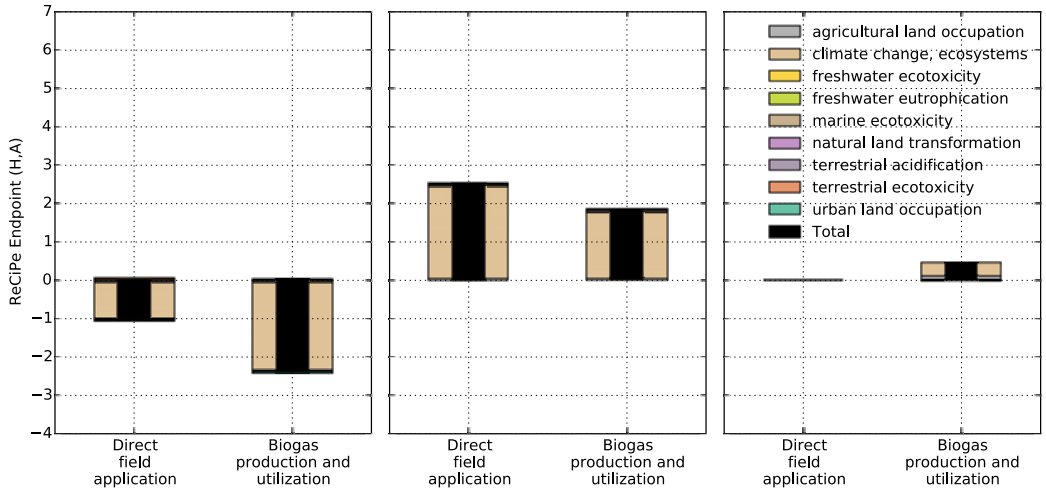

(a) Agricultural sub-system. **(b)** Storage and transportation. **(c)** Energy sub-system.

Figure 24. Disaggregated Life Cycle Assessment human health endpoint results.

pact and it can be seen that particulate matter formation and climate change are the largest contributors. Having discussed the climate change impact in depth above, the Level 4 analysis is on the particulate matter formation part of the total environmental impact. From the Figures in 28 it can be seen the main contributor to particulate matter formation is ammonia emission in the agricultural sub-system, and storage and transportation sub-system. The emission of ammonia is calculated in the nitrogen balance in described in Section 2.2.1 and 2.2.3 both are based on Hamelin et al. (2011) which refers to national guidelines of nitrogen accounting.

In Figure 26, which displays the environmental impact on resources, it can be observed that the greatest category of the two available is fossil depletion. Furthermore, that category is also where the greatest difference is observed between the case study and the reference. From the Figures in 29 the decrease in nitrogen mineral fertilization and the substitution of fossil resources for heat and power generation are most influential.

DOI
10.3384/ecp15119211

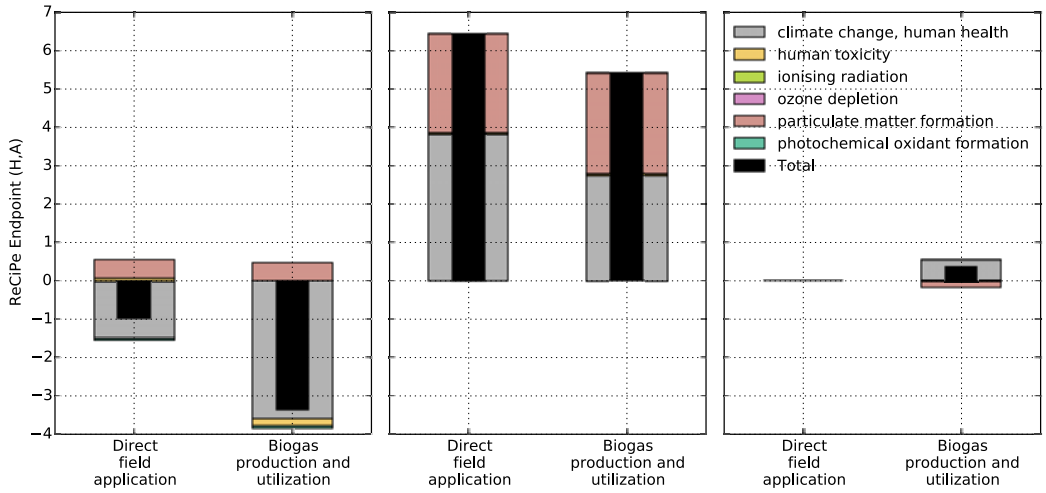

(a) Agricultural sub-system. **(b)** Storage and transportation. **(c)** Energy sub-system.

Figure 25. Disaggregated Life Cycle Assessment resources endpoint results.

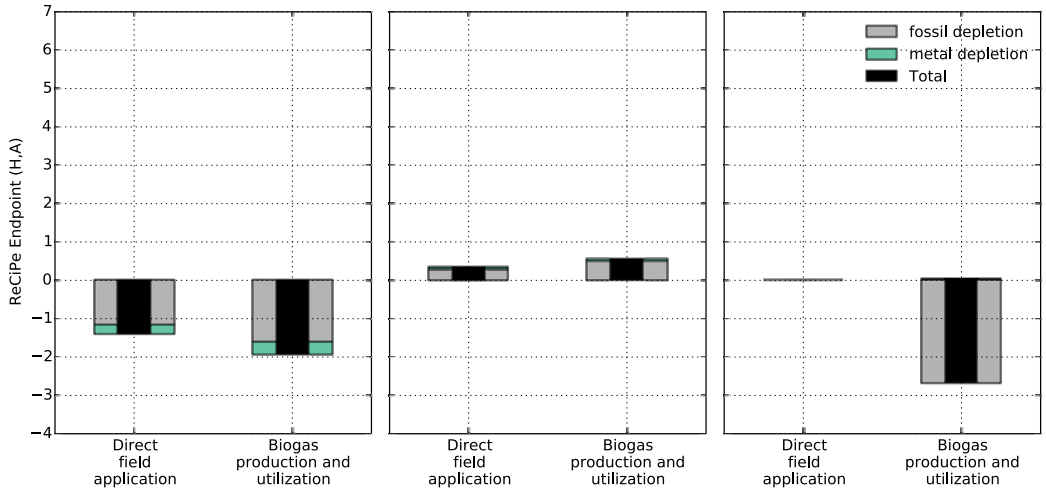

(a) Agricultural sub-system. **(b)** Storage and transportation. **(c)** Energy sub-system.

Figure 26. Disaggregated Life Cycle Assessment endpoint results.

5 Discussion

When observing the results of the case study, it seems that for a system like these, analyzing the environmental impact categories climate change and fossil depletion, as particulate matter formation was basically the same for the case study and its reference, might by sufficient to reach an informed decisions. There is a general acceptance of the climate change impact method from IPCC and every impact assessment method in general use, uses that approach. However, this is not the case for resource depletion environmental impact. For that impact category it is generally recognized that improvements are needed (Hauschild et al. (2010)). Although generally not recognized to reflect resource scarcity, which is a requirement by the ILCD for an impact method, exergy and cumulative exergy could be used to reflect the efficiency of resource utilization in a life cycle sense and thus aid in the decision making. It could be added to the overall analysis but outside of the LCA results where an impact method reflecting scarcity would

be used.

Displaying the results using four levels as introduced in Section 2.3 gives a great deal of insight into the system analyzed. It can also help in finding weaknesses in the modeling, e.g. if one of the greatest contributors is based on uncertain data or the greatest impact is calculated with LCIA method which will need further development. It is also worth noting that the level of detail could be decrease by jumping from level one to level 4 result and showing only the top contributers for main impacts for simplicity.

As mentioned in the introduction, all parts of the processes in the model are freely available. This includes all the external software used. However, the LCI database used in this case study was Ecoinvent3. To be able to use Ecoinvent3 a user will need a license, which is not free of charge. To get around this there are new and constantly expanding freely available LCI databases, e.g. ELCD, USDA, Agribalyse and bioenergiedat.

6 Conclusion

The article introduces a model that successfully uses only freely available software to model Life Cycle Assessment of an integrated bioenergy and agriculture sub-system. This was demonstrated with a case study of biogas production from manure and field application of the residual digestate, in reference to direct manure to field application.

The case study unveiled the studied case to be better in terms of overall environmental impact than its reference, where the greatest difference from the reference were observed in the climate change and fossil depletion impact categories.

The model still uses ecoinvent, a commercial LCI database. But with new freely available LCI database, the possibility for a completely free software based on the model introduced is getting greater.

References

Francesco Cherubini, Anders H. Stromman, and Edgar Hertwich. Effects of boreal forest management practices on the climate impact of CO2 emissions from bioenergy. *Ecological Modelling*, 223(1):59–66, December 2011. ISSN 03043800. doi:10.1016/j.ecolmodel.2011.06.021.

Danish Ministry of Climate. Energy and Buildings. OUR FUTURE ENERGY. Technical report, Danish Ministry of Climate. Energy and Buildings, Copenhagen.

P. de Willigen. An analysis of the calculation of leaching and denitrification losses as practised in the NUTMON approach. *Rapport-Plant Research International*, (18), 2000.

Capucine Dupont, Rodica Chiriac, Guillaume Gauthier, and François Toche. Heat capacity measurements of various biomass types and pyrolysis residues. *Fuel*, 115:644–651, January 2014. ISSN 00162361. doi:10.1016/j.fuel.2013.07.086.

Brian Elmegaard and Niels Houbak. Dna: A general energy system simulation tool. *Proceedings of SIMS 2005*, pages 43–52, 2005.

A. Friedl, E. Padouvas, H. Rotter, and K. Varmuza. Prediction of heating values of biomass fuel from elemental composition. *Analytica Chimica Acta*, 544(1-2):191–198, July 2005. ISSN 00032670. doi:10.1016/j.aca.2005.01.041.

Rolf Frischknecht. LCI modelling approaches applied on recycling of materials in view of environmental sustainability, risk perception and eco-efficiency. *The International Journal of Life Cycle Assessment*, 15(7):666–671, June 2010. ISSN 0948-3349. doi:10.1007/s11367-010-0201-6.

M. J. Goedkoop, R Heijungs, M. Huijbregts, A. De Schryver, J. Struijs, and R. Van Zelm. Recipe 2008, a life cycle impact assessment method which comprises harmonised category indicators at the midpoint and the endpoint level; first edition report i: Characterisation. Technical report, 6 January 2009. Homepage: http://www.lcia-recipe.net/.

The Danish Government. The Danish Climate Policy Plan Towards a low carbon society. Technical report, Danish Government, Copenhagen, 2013a. Retrieved from: http://www.ens.dk/sites/ens.dk/files/policy/danish-climate-energy-policy/danishclimatepolicyplan_uk.pdf.

The Danish Government. Catalogue of Danish Climate Change Mitigation Measures. Technical report, Danish Government, Copenhagen, 2013b. Retrienved from: http://www.ens.dk/sites/ens.dk/files/policy/danish-climate-energy-policy/dk_climate_change_mitigation_uk.pdf.

Lorie Hamelin, Marianne Waesnes, Henrik Wenzel, and Bjorn M Petersen. Environmental consequences of future biogas technologies based on separated slurry. *Environmental science & technology*, 45(13):5869–77, July 2011. ISSN 1520-5851. doi:10.1021/es200273j.

Michael Hauschild, GOEDKOOP Mark, GUINEE Jerome, HEIJUNGS Reinout, HUIJBREGTS Mark, JOLLIET Olivier, MARGNI Manuele, and DE SCHRYVER An. Recommendations for Life Cycle Impact Assessment in the European context - based on existing environmental impact assessment models and factors (International Reference Life Cycle Data System - ILCD handbook), October 2010. ISSN 1018-5593.

Fortunat Joos, Michele Bruno, Roger Fink, Ulrich Siegenthaler, Thomas F. Stocker, Corinne Le Quere, and Jorge L. Sarmiento. An efficient and accurate representation of complex oceanic and biospheric models of anthropogenic carbon uptake. *Tellus B*, 48(3):397–417, July 1996. ISSN 0280-6509. doi:10.1034/j.1600-0889.1996.t01-2-00006.x.

Fortunat Joos, I. Colin Prentice, Stephen Sitch, Robert Meyer, Georg Hooss, Gian-Kasper Plattner, Stefan Gerber, and Klaus Hasselmann. Global warming feedbacks on terrestrial carbon uptake under the Intergovernmental Panel on Climate Change (IPCC) Emission Scenarios. *Global Biogeochemical Cycles*, 15(4):891–907, December 2001. ISSN 08866236. doi:10.1029/2000GB001375.

Jari Liski, Taru Palosuo, Mikko Peltoniemi, and Risto Sievänen. Carbon and decomposition model Yasso for forest soils. *Ecological Modelling*, 189(1-2):168–182, November 2005. ISSN 03043800. doi:10.1016/j.ecolmodel.2005.03.005.

Chris Mutel. Brightway2, 2015. Homepage: www.brightwaylca.org.

NaturErhvervstyrelsen. Vejledning om gØdsknings- og harmoniregler. Technical report, Ministeriet for Fødevarer, Landbrug og Fiskeri, 2013.

Thomas Nemecek and Julian Schnetzer. Methods of assessment of direct field emissions for LCIs of agricultural production systems. *Data v3. 0*, 2012.

D.W. Pennington, J. Potting, G. Finnveden, E. Lindeijer, O. Jolliet, T. Rydberg, and G. Rebitzer. Life cycle assessment part 2: Current impact assessment practice. *Environment International*, 30(5):721 – 739, 2004. ISSN 0160-4120. doi:http://dx.doi.org/10.1016/j.envint.2003.12.009.

Bjorn M. Petersen, Jorgen E. Olesen, and Tove Heidmann. A flexible tool for simulation of soil carbon turnover. *Ecological Modelling*, 151(1):1–14, May 2002. ISSN 03043800. doi:10.1016/S0304-3800(02)00034-0.

Bjorn M. Petersen, Lars S. Jensen, Sø ren Hansen, Anders Pedersen, Trond M. Henriksen, Peter Sø rensen, Isabelle Trinsoutrot-Gattin, and Jø rgen Berntsen. CN-SIM: a model for the turnover of soil organic matter. II. Short-term carbon and nitrogen development. *Soil Biology and Biochemistry*, 37(2):375–393, February 2005. ISSN 00380717. doi:10.1016/j.soilbio.2004.08.007.

Bjorn Molt Petersen, Marie Trydeman Knudsen, John Erik Hermansen, and Niels Halberg. An approach to include soil carbon changes in life cycle assessments. *Journal of Cleaner Production*, 52:217–224, August 2013. ISSN 09596526. doi:10.1016/j.jclepro.2013.03.007.

G. Rebitzer, T. Ekvall, R. Frischknecht, D. Hunkeler, G. Norris, T. Rydberg, W.-P. Schmidt, S. Suh, B.P. Weidema, and D.W. Pennington. Life cycle assessment: Part 1: Framework, goal and scope definition, inventory analysis, and applications. *Environment International*, 30(5):701 – 720, 2004. ISSN 0160-4120. doi:http://dx.doi.org/10.1016/j.envint.2003.11.005.

R. N. Roy, R.V. Misra, J.P. Lesschen, and E.M. Smaling. Assessment of soil nutrient balance: Approaches and methodologies. Technical report, Food and Agriculture Organization of the United Nations, 2003. Retrieved from: ftp://ftp.fao.org/docrep/fao/006/y5066e/y5066e00.pdf.

Jon Schnute. A Versatile Growth Model with Statistically Stable Parameters. *Canadian Journal of Fisheries and Aquatic Sciences*, 38(9):1128–1140, September 1981. ISSN 0706-652X. doi:10.1139/f81-153.

Sangwon Suh and Gjalt Huppes. Methods for life cycle inventory of a product. *Journal of Cleaner Production*, 13(7):687 – 697, 2005. ISSN 0959-6526. doi:http://dx.doi.org/10.1016/j.jclepro.2003.04.001.

Stanislav V. Vassilev, David Baxter, Lars K. Andersen, and Christina G. Vassileva. An overview of the chemical composition of biomass. *Fuel*, 89(5):913–933, May 2010. ISSN 00162361. doi:10.1016/j.fuel.2009.10.022.

B.P. Weidema, Ch. Bauer, R. Hischier, Ch. Mutel, T. Nemecek, J. Reinhard, C.O. Vadenbo, and G. Wernet. The ecoinvent database: Overview and methodology, Data quality guideline for the database version 3, 2013. Homepage: www.ecoinvent.org.

A Appendix

A.1 LCI data

Table 1. Life Cycle Inventory for processes, direct field application.

	Unit	Agricultural	Storage and trans.
market for potassium chloride, as K2O	kilogram	-75.735	0.000
liquid manure spreading, by vacuum tanker	cubic meter	21.283	0.000
market for phosphate fertiliser, as P2O5	kilogram	-43.510	0.000
market for nitrogen fertiliser, as N	kilogram	-116.115	0.000
market for fertilising, by broadcaster	hectare	-3.263	0.000
transport, tractor and trailer, agricultural	ton kilometer	0.000	445.265
market for electricity, low voltage	kilowatt hour	0.000	15.916
market for liquid manure storage and processing...	cubic meter	0.000	0.001

Table 2. Life Cycle Inventory for emissions, direct field application.

	Unit	Agricultural	Storage and trans.
Phosphate	kilogram	0.134	0.000
Carbon dioxide, fossil	kilogram	-3151.968	0.000
Zinc	kilogram	1.216	0.000
Copper	kilogram	0.183	0.000
Ammonia	kilogram	12.568	0.000
Dinitrogen monoxide	kilogram	0.322	0.000
Mercury	kilogram	0.001	0.000
Nitrogen oxides	kilogram	-0.274	0.000
Nitrate	kilogram	-1.264	0.000
Chromium	kilogram	-0.007	0.000
Carbon dioxide, from soil or biomass stock	kilogram	2376.740	0.000
Lead	kilogram	0.001	0.000
Cadmium	kilogram	-0.001	0.000
Nickel	kilogram	0.010	0.000
Methane, from soil or biomass stock	kilogram	0.000	69.100
Ammonia	kilogram	0.000	31.519
Dinitrogen monoxide	kilogram	0.000	3.676
Nitrogen oxides	kilogram	0.000	1.932
Nitrogen	kilogram	0.000	5.410
Carbon dioxide, from soil or biomass stock	kilogram	0.000	57.454

DOI
10.3384/ecp15119211

Table 3. Life Cycle Inventory for processes, biogas production and utilization.

	Unit	Agricultural	Storage and trans.	Energy
market for fertilising, by broadcaster	hectare	-3.475	0.000	0.000
liquid manure spreading, by vacuum tanker	cubic meter	21.685	0.000	0.000
market for potassium chloride, as K2O	kilogram	-75.735	0.000	0.000
market for phosphate fertiliser, as P2O5	kilogram	-43.510	0.000	0.000
market for nitrogen fertiliser, as N	kilogram	-129.017	0.000	0.000
market for polyacrylamide	kilogram	0.000	0.000	20.002
transport, tractor and trailer, agricultural	ton kilometer	0.000	0.000	427.653
market for electricity, low voltage	kilowatt hour	0.000	0.000	64.168
market for liquid manure storage and processing...	cubic meter	0.000	0.000	0.001
anaerobic digestion plant construction, agricul...	unit	0.000	0.000	0.000
heat and power co-generation, natural gas, 1MW ...	megajoule	0.000	-7548.223	0.000
heat and power co-generation, natural gas, 1MW ...	kilowatt hour	0.000	-1822.929	0.000
heat and power co-generation unit construction,...	unit	0.000	0.000	0.000
heat and power co-generation unit construction,...	unit	0.000	0.000	0.000
heat and power co-generation unit construction,...	unit	0.000	0.000	0.000
market for lubricating oil	kilogram	0.000	0.533	0.000
market for waste mineral oil	kilogram	0.000	-0.533	0.000

Table 4. Life Cycle Inventory for emissions, dbiogas production and utilization.

	Unit	Agricultural	Storage and trans.	Energy
Lead	kilogram	-0.000	0.000	0.000
Cadmium	kilogram	-0.001	0.000	0.000
Chromium	kilogram	-0.011	0.000	0.000
Carbon dioxide, fossil	kilogram	-3151.968	0.000	0.000
Phosphate	kilogram	0.134	0.000	0.000
Nickel	kilogram	0.004	0.000	0.000
Carbon dioxide, from soil or biomass stock	kilogram	1533.367	0.000	0.000
Nitrogen oxides	kilogram	-0.281	0.000	0.000
Ammonia	kilogram	10.933	0.000	0.000
Copper	kilogram	0.106	0.000	0.000
Nitrate	kilogram	19.052	0.000	0.000
Dinitrogen monoxide	kilogram	0.730	0.000	0.000
Zinc	kilogram	0.703	0.000	0.000
Mercury	kilogram	0.001	0.000	0.000
Methane, from soil or biomass stock	kilogram	0.000	0.000	36.086
Carbon dioxide, from soil or biomass stock	kilogram	0.000	0.000	34.204
Nitrogen oxides	kilogram	0.000	0.000	1.706
Nitrogen	kilogram	0.000	0.000	4.778
Ammonia	kilogram	0.000	0.000	32.096
Dinitrogen monoxide	kilogram	0.000	0.000	3.357
Methane, from soil or biomass stock	kilogram	0.000	5.719	0.000
NMVOC, non-methane volatile organic compounds, ...	kilogram	0.000	0.036	0.000
Platinum	kilogram	0.000	0.000	0.000
Sulfur dioxide	kilogram	0.000	1.067	0.000
Carbon monoxide, from soil or biomass stock	kilogram	0.000	0.854	0.000
Dinitrogen monoxide	kilogram	0.000	0.044	0.000
Nitrogen oxides	kilogram	0.000	0.267	0.000
Carbon dioxide, from soil or biomass stock	kilogram	0.000	1492.460	0.000

A.2 LCIA level 4 results

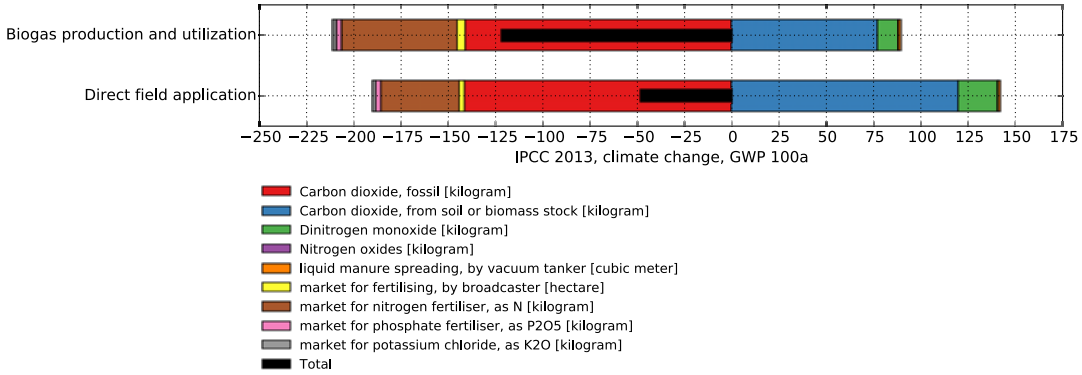

(a) Agricultural system.

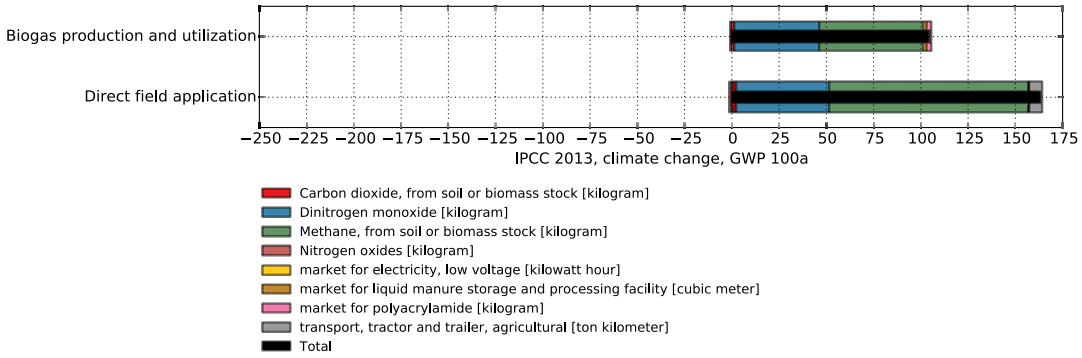

(b) Storage and transportation.

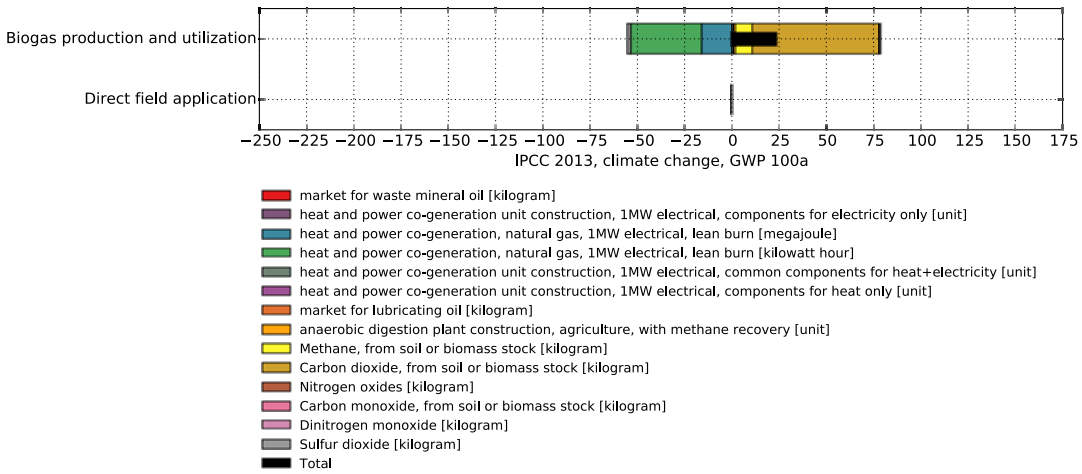

(c) Energy system.

Figure 27. Level 4 climate change, disaggregated LCIA midpoint results in kg Carbon dioxide-equivalence per hectare.

DOI
10.3384/ecp15119211

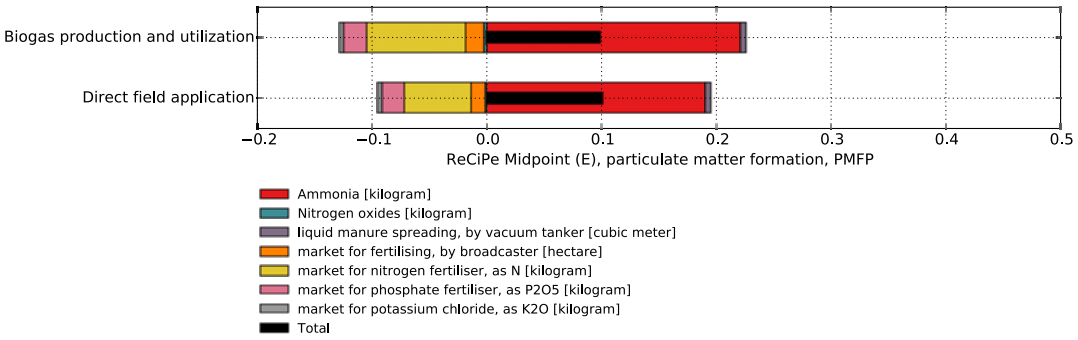

(a) Agricultural system.

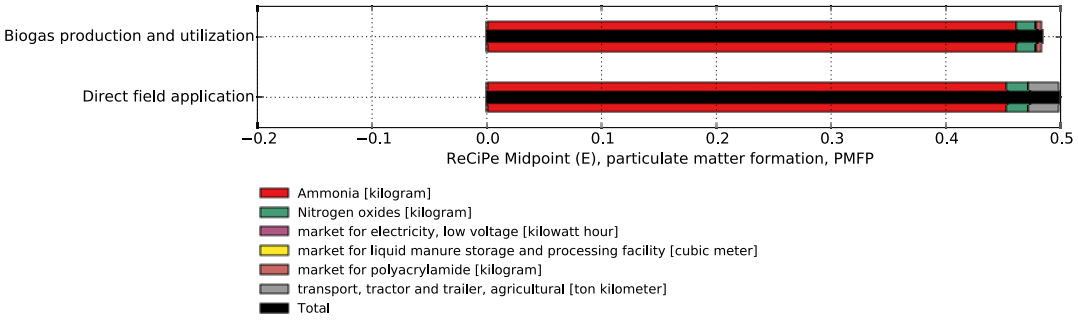

(b) Storage and transportation.

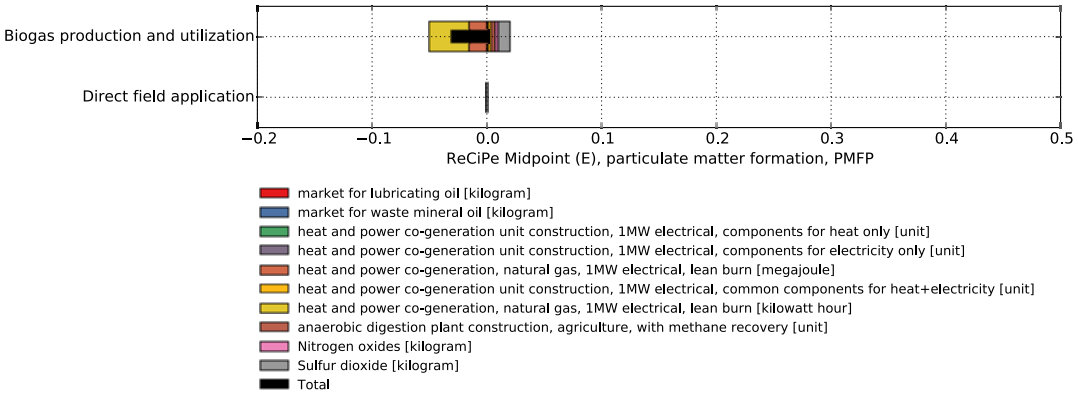

(c) Energy system.

Figure 28. Level 4 particulate matter formation, disaggregated LCIA midpoint results in kg PM10-equivalence per hectare.

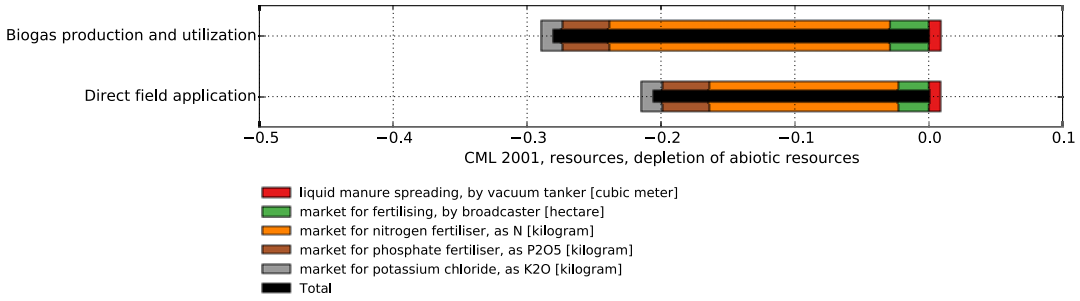

(a) Agricultural system.

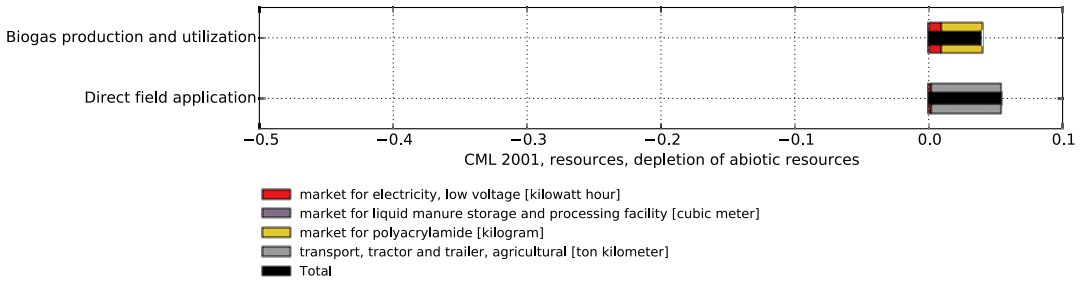

(b) Storage and transportation.

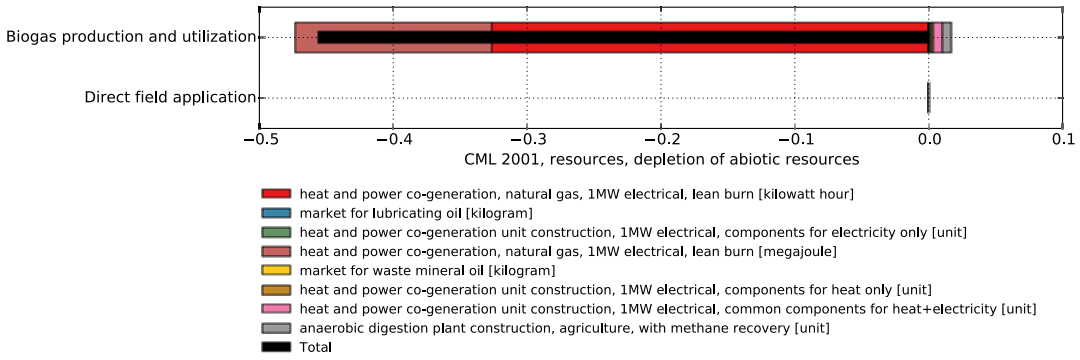

(c) Energy system.

Figure 29. Level 4 depletion of abiotic resources, disaggregated LCIA midpoint results in kg Antimony-equivalence per hectare.

DOI
10.3384/ecp15119211

Multi-Criteria Analysis of an Integrated Polygeneration Energy System and Agriculture Utilizing Cereal Straw

Hafthor Ægir Sigurjonsson,[a,1], Brian Elmegaard[a], Lasse Røngaard Clausen[a]

[a] *Technical University of Denmark, Department of Mechanical Engineering, Building 403, DK-2800 Kgs. Lyngby, Denmark*

Abstract

In order to contribute to climate change mitigation, Denmark aims to be completely independent from fossil fuels for all its energy by 2050. Biomass is commonly seen as a good alternative fuel option to fossil fuels, but intensified use of land, mineral resource depletion and soil degradation put increased pressure on effective biomass utilization by energy systems. From that perspective, an energy system utilizing cereal straw in a polygeneration power plant producing heat, power and biochar is modelled and evaluated. The energy system is based on a Low Temperature Circulating Fluidized Bed gasifier and a steam boiler power plant. The overall system is evaluated using multi-criteria analysis, based on environmental impact, renewable energy indicators and profitability of the required investment. The main results of the article are that the LT-CFB gasifier polygeneration power plant is economically feasible. Additionally, the maximum bioenergy production operation scenario of the polygeneration power plant is more environmentally friendly then the maximum energy generation operation scenario, although decreased biochar production by increasing energy generation is the more profitable and efficient renewable energy generation operation. Nevertheless, when energy generation is maximized, carbon build-up in soil will be decreased, so that carbon conversion would need to be decreased to 91% to have an equivalent carbon build-up over a 100-year time horizon to leaving straw on the field.

Keywords: Bioenergy, Polygeneration, Gasification, Biochar, Multi-criteria
2010 MSC: 00-01, 99-00

1. Introduction

It is commonly believed that increased use of biomass feedstock for energy generation can mitigate climate change, increase security of energy supply and minimize the issues of fossil fuel depletion. However, other concerns associated with agriculture which directly and indirectly affect the food supply, such as land use, mineral depletion and soil degradation, have increased the awareness of effective biomass utilization for both energy generation and food production. Denmark is planning to be completely independent of fossil fuels for all of its energy consumption by 2050 [1]. In addition, the climate targets set by the government are set to decrease greenhouse gas emissions by 40% compared with 1990 emission levels [2].

According to the annual energy statistics which were last published by the Danish Energy Agency in 2013, electricity production in Denmark is mainly made up of wind turbines and combined heat and power (CHP) plants [3]. About 50% of all energy generated by CHP plants is fuelled with fossil fuels and only 23% with biomass [3]. Cherubini et al. [4] divides biomass for bioenergy into residues and dedicated energy crops, where residues are defined as biomass obtained as a result of economic activity, not specifically produced to be used in the energy system. Agricultural land covered about 61.5% of the total area of Denmark in 2013, according to the World Bank. About 60% of this land is used for production of cereal crops [5] from which

[1] Corresponding author.

2464.78 million kg straw can be harvested for alternative purpose based on 80% feasible extraction limit [6]. This amounts to about 35.6 PJ, of which an average of 21.30 PJ has been harvested and used in the energy system over the last 5 years and 14.28 PJ is left on the field.

The incorporation of crop residues such as cereal straw can be essential for retaining soil quality as it can increase soil organic carbon [7]. Additionally, crops require nutrients and the demand for organic or mineral fertilizers can be decreased by leaving straw on fields, as nutrients in crop residues can be utilized by the following crop. Harvesting straw can thus have an adverse effect on soil quality and increase dependency on mineral fertilizers. However, as shown by Nguyen et al. [8] and Sigurjonsson et al. [9] an energy system based on low-temperature gasification that can collect and return the ash and char has the potential to mitigate those effects.

This paper builds on the analysis made by Sigurjonsson et al. [9] but expands the analysis to include a renewable energy generation indicator and an economic analysis in a multi-criteria analysis. It also refines the environmental impact analysis by including uncertainty and a broader range of alternatives for avoided energy generation. Furthermore, this paper includes a more detailed mathematical model of the energy system and an analysis of the projected development of soil carbon for straw utilization compared with the increasingly more common practice of leaving straw on the field.

2. Methods

2.1. System Description

An alternative system was modelled for comparison in which the harvested straw is utilized in a direct combustion CHP plant. The reference system when evaluating the environmental impact is when cereal straw is not harvested and the corresponding energy is generated in a CHP plant fuelled by natural gas.

In the analysed system, the straw is harvested and utilized in an energy system. This system is a thermal power plant which consists of a Low Temperature Circulating Fluidized Bed (LT-CFB) gasifier and a conventional steam boiler power plant (the quantity of tar in the syngas is too high for gas engines and gas turbines [10]). This power plant produces heat and power, along with ash and char (referred to collectively as biochar). The LT-CFB gasifier was developed by Peder Christian Stoholm and the Technical University of Denmark (DTU) [11, 12].

This gasifier was designed to be able to utilize biomass resources with a relatively high quantity of low-melting ash compounds compared with woody biomass [10], by keeping the process temperature below the melting point of these ash compounds [11]. This will allow the ash to be extracted in solid form, enabling it to be applied to an agricultural field as a source of fertilizer [13, 14]. Additionally, unconverted carbon or char is captured with the ash, which can then be used for soil amendment and long-term carbon sequestration if applied on an agricultural field [15]. Figure 1 displays a simple schematic of the overall concept.

The amount of unconverted carbon or biochar produced can be controlled by changing the operation of the gasifier. This is described by the carbon conversion factor, which gives the ratio of carbon in the biomass input to the carbon in the syngas leaving the gasifier. For the LT-CFB gasifier and straw resource the practical carbon conversion ranges from 0.98 to 0.70, where the lower estimate is found by the ratio of fixed carbon to total carbon in the cereal straw input and the energy required to sustain the pyrolysis process, which is fuelled with char combustion. The 0.98 carbon conversion operation is referred to as the maximum energy generation scenario while the 0.70 carbon conversion operation is referred to as the maximum biochar production scenario.

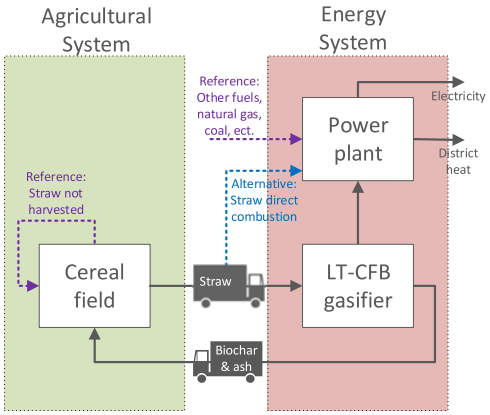

Figure 1: A simple schematic of the overall system.

2.2. Analytical Framework

The evaluation is done by multi-criteria analysis, comprising environmental impact, a renewable energy indicator and a profitability analysis. Environmental impact is calculated by using the LCI data and the IPCC 2013 Life Cycle Impact Assessment (LCIA) method [16], representing only climate change. The renewable energy indicator combines exergy analysis and Life Cycle Assessment (LCI) by using the LCI data and Cumulative Exergy Demand [17] CExD) LCIA method, along with the exergy output of the system. For the technoeconomic analysis, the methods described by Bejan et al. [18] are used to find the real payback period of the required investment and the levelized annual revenues required for electricity generation. The Technique for Order Preference by Similarity (TOPSIS) method was used to find the best alternative, based on the weighting of each criteria to another [19], and in which only a judgement of the weighting is required [20]. TOPSIS can identify the alternative that is closest to the ideal solution, based on the specified multi-criteria [21], which in this analysis are environmental impact, renewable energy generation and profitability. A ternary graph is used to show the best solution for all weights between each criteria. This is described in Figure 2.

The system is modelled and simulated by combining energy system simulation and Life Cycle Inventory (LCI) analysis. For the energy simulation part, the DNA [22] (Dynamic Network Analysis) tool developed at DTU was used. The results of the simulation represent the foreground LCI data for the energy system in the overall analysis. All background data used in the LCI was collected using the ecoinvent 3.1 database [23]. Communication with the database was done using Brightway2, an advanced open-source life cycle assessment framework [24]. The foreground LCI data for the agricultural system was divided into macro-nutrients and carbon substance flow analysis. In the macro-nutrients analysis, the methods used by Nguyen et al. [25, 8] were applied, whereas for the carbon analysis the methods of Cherubini et al. [26, 27, 28] and Petersen et al. [29] were used and the calculation was supported by simulating soil carbon using C-TOOL [30, 31].

Both the environmental impact and the renewable energy indicator are found by applying the principles of LCI (The environmental impact analysis is consequential and the renewable energy indicator is attributional), using the ecoinvent database for all background data. The ecoinvent database has a specific way of reporting uncertainty [32], which was originally described by Weidema and Wesnæs [33, 34]. Two types of uncertainty are defined: basic uncertainty and additional uncertainty. Basic uncertainty includes variation and stochastic error of the values that describe the exchanges; for this type of uncertainty, ecoinvent has

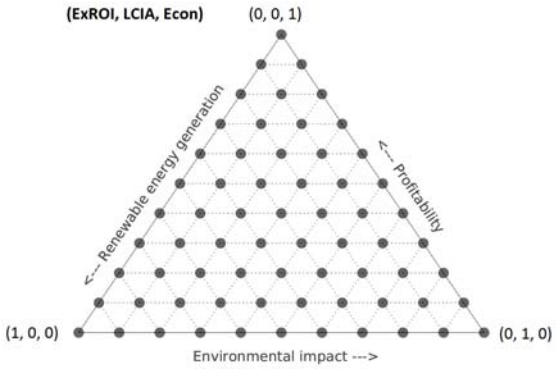

Figure 2: Descriptive ternary graph.

defined the default variance that is applied to specific type LCA data [32]. The additional uncertainty covers the use of estimates, incompleteness of samples, and extrapolation from temporally and spatially different conditions. Additional variance on LCI data is defined based on the description of the collected data. The confidence interval (5% lower bound and 95% upper bound) is then found using the default and additional variance, along with a Monte Carlo simulation using 1000 trials of random samples. For the profitability analysis, the main parameters are varied in a sensitivity analysis using multiplication factors from 0.1 to 1.9.

2.3. Modelling and Simulation

The overall system is modelled as a system integration between agricultural and bioenergy systems, connected by the transportation of resources between these two systems. A steam-drying process, which is operated at 200°C and in which the moisture content is decreased from 10.1% to 2.0%, precedes the gasifier. The extracted water vapour is used to generate district heating and the heat required by the drying process is supplied by the flue gas from the steam boiler. The gasifier is operated at atmospheric pressure and the temperatures inside the pyrolysis chamber and the char gasification chamber are assumed to be 630°C and 700°C respectively. A gasifier component has been developed in DNA, using Gibbs minimization to calculate the outlet gas composition at chemical equilibrium for the defined operation [35]. Clausen used the same component in DNA to simulate the operation of a two-stage gasifier fuelled with wood chips, but for more realistic simulation the equilibrium temperature was assumed to be slightly above the outlet temperature and the methane content of the syngas was adjusted to measured data from experiments [35]. In the steam boiler power plant, the live steam temperature and pressure are 650°C and 80 bar respectively. Table 1 gives the main parameters used in the simulation of the energy system.

Table 1: Main parameters defining the energy system.

Feedstock	1 kg/s cereal straw, where the dry and ash free composition (daf) is assumed to be (wt %): 46.1% C, 5.7% H, 40.7% O, 0.7% N, 0.16% S, 6.63% ASH, LHV = 18.23 MJ/kg daf. cp = 1.35 kJ/ (kg dry· K). The biomass input is 5 MW to the gasifier (LHV dry), moisture content at steam dryer input = 45.0%.
Gasifier air blown	P = 1.0 bar. Carbon conversion = 98% - 70%. Heat loss = 3% of the cereal straw thermal input (LHV dry). Texit = 730C. The gas (excl. CH4) is assumed to be in chemical equilibrium at 750C. Pyrolysis is modelled by assuming a cp = 1.85 kJ/ (kg*K) for completely dry and ash free biomass. cp of ash = 1 kJ/(kg*K). Steam to straw (dry) input mass flow ratio is 0.82 at 630C and air to straw (dry) ratio is 1.13 at 700C.

... continued

Power plant	Live steam temperature is set to 650C and live steam pressure is set to 80 bar. $\eta_{isentropic}$ = 90%, $\eta_{mechanical}$ = 98%.
Heat production	All surplus heat in both modes of operation will used to produce district heat where forward temperature is 80C and return temperature is 40C.

LCI data for the energy system infrastructure was estimated by using the ecoinvent 3.1 database [23] and includes the gasification unit and the steam boiler power plant. The resource inputs are accounted for by excluding the electricity and heating required to operate the system, which are supplied by the system itself. Estimations of the emission profile of the bioenergy system were based on data from Nguyen et al. [8] and included only emissions affecting climate change, i.e. SO_2 , NO_x , N_2O, CH_4 and CO_2. For the CO_2 emissions a resource-unique biogenic impact factor was calculated which represents the climate effect due to changes in the radiative forcing by the carbon cycle in the overall system. This is described further in the description of the agricultural system model below.

LCI background data were found by using ecoinvent 3.1 for the field work processes and production of the mineral fertilizers used. The changes in field work processes include baling straw and loading the bales, along with the avoided process of drilling down the straw. The field emissions and changes in the fertilization requirements are modelled by macro-nutrients and carbon balances, based on the inputs and outputs to and from the soil as done by Sigurjonsson et al. [9]. When straw is harvested, the nutrients and carbon within it cannot be utilized by the following crop, which results in increased fertilizer requirements and changes in field emissions, along with changes in the development of soil carbon as less carbon can be sequestered in soil.

2.4. Climate Change Impact

The climate change impact is calculated by the LCIA method developed for the Intergovernmental Panel of Climate Change (IPCC) 2013 assessment report which builds on previous methods developed for preceding reports [16], using the LCI data gathered from modelling and simulating the system. The radiative forcing caused by the time lag between the combustion of syngas from straw gasification and the regrowth of straw is taken into account in the LCI carbon-balance calculation by using the methods developed by Cherubini et al. [26, 27, 36] and Petersen et al. [29] cf. Sigurjonsson et al. [9] as noted above. Climate change impact results are given by including the estimated displaced energy generation using a few alternatives, i.e. CHP fuelled with biomass, natural gas and coal, where the displaced electricity generation represents either the marginal grid or the actual electricity generated in the alternative CHP plant. Marginal electricity generation in Denmark is defined as a mix of wind power, natural gas CHP and coal power plants [37]. The results are presented independently from the displaced energy generation and are disaggregated to the main parts of the model to highlight the difference between the operation scenarios.

2.5. Renewable Energy Indicator

Exergy Return on Investment (ExROI) was used as the renewable energy indicator. ExROI is an extension of the Energy Return on Investment (EROI) developed by Cleveland et al. [38]. The ExROI concept utilizes the second law of thermodynamics to find the ratio of exergy required to obtain and process a given resource to the exergy acquired by its utilization [39]. The exergy required to supply and process the straw is found by using the LCI data from modelling and simulation of the overall system and by the Cumulative Exergy Demanded (CExD) LCIA method, which is equivalent to the Cumulative Exergy Consumed (CExC) method defined by Szargut and Morris [40] as the cumulative sum of exergy over all resources required by a product. The CExD has been fully coupled with the ecoinvent LCI database by Bösch et al. [17].

The net electricity produced is assumed to be equivalent to exergy, while the exergy of the district heating produced is based on the heat transfer occurring at the thermodynamic average temperature and constant

pressure between the upper and lower temperature levels of the district heating system, as defined by Bejan et al. [18].

$$\dot{E}_q = 1 - \frac{T_0}{T_a} \cdot \dot{Q} \tag{1}$$

Here, $\dot{E}_q$, T_0, T_a and $\dot{Q}$ represent the exergy rate transferred to district heating, the temperature of the exergy reference environment (15°C), the thermodynamic average temperature and the heat rate transferred to the district heating system. The thermodynamic average temperature is calculated by the specific enthalpy (h) and specific entropy (s) of water at the upper (e) and lower (i) temperature levels of the district heating system.

$$T_a = \frac{h_e - h_i}{s_e - s_i} \tag{2}$$

Both the specific enthalpies and entropies are found from the Coolprop C++ library, which can apply pure and pseudo-pure fluid equations of state and transportation properties [41]. The renewable energy indicator is thus found by the sum of the exergy of the electricity and district heating products (biochar is utilized within the system boundaries) and then dividing by the CExD of the non-renewable material and energy resources needed.

$$ExROI = \frac{E_p}{nCExD_p} \tag{3}$$

Here, E_p and $nCExD_p$ are the product exergy and cumulative sum of all non-renewable resources required to obtain and process the products. Mora et al. [42] noted that if ExROI is above 1, then the exergy required from non-renewable resources is less then the products' exergy content, thus making the energy generation renewable. An ExROI beyond 1 indicates that the system is even more effective from a renewable energy point of view.

2.6. Technoeconomic Analysis

The levelized annual average revenues required for electricity generation were found by using the methods described by Bejan et al. [18], where the sum of the present values of the total revenues required (TRR) for each year are subsequently converted to an equivalent annuity using the uniform series present worth factor (U_f).

$$U_f = \frac{(1+i)^T - 1}{i \cdot (1+i)^T} \tag{4}$$

Here, T is the lifetime of the unit and i is the discount rate. The real payback period (τ_{pb}) is then found by assuming that the price received is equivalent to the premium feed-in tariff subsidy scheme defined by the Danish Promotion of Renewable Energy Act §44 par. 2 VE-Lov as 0.793 DKK.

TRR is found by calculating the total capital recovery (TCR), the minimum return on investment (ROI) for common equity and debt, and the variable cost and benefits over the assumed 25-year economic lifetime of the investment. The TCR was based on the investment cost of the gasification unit and the power generating unit, which are given in the report on technology data for energy plants issued by the Danish Energy Agency [43] for the LT-CFB gasifier and a straw-fired combustion power plant. To account for the avoided components when sending product gas to the power plant instead of straw, the investment cost of the straw fired combustion power plant was multiplied by a factor of 0.8.

The same report from the Danish Energy Agency [43] was used to account for the operation and maintained cost of the LT-CFB gasifier and the power plant, applying the same reduction factor to the power plant data as that used for the investment cost. A report by EA (Energy Analysis) for the Danish Energy Agency was used to estimate the current and projected straw prices during the lifetime of the investment [44]. The benefits of the co-products are also included because these affect the levelized cost of electricity generation, as the energy system is a combined heat and power plant which also generates biochar with a fertilization value

and carbon sequestration potential. District heat is accounted for by charges derived from the production cost, which is a thermodynamic allocation method based on energy. The biochar is assumed to be sold for the equivalent price of the fertilizers it replaces, using the Import/Export data from the United Nations Statistics Database which is reported in the ecoinvent database [23]. The benefits of carbon sequestration by producing biochar are accounted for by using the current and projected carbon quota prices over the lifetime of the investment, as reported in a report by the Danish Energy Agency [45].

3. Results and discussion

The results are given for the maximum energy generation, the maximum biochar production operation scenarios and the direct combustion alternative for each single criteria. However, in the multi-criteria analysis the whole range between the 0.98 maximum and 0.70 minimum carbon conversion in the gasifier is covered. The simulation results of the energy system are also given.

3.1. System Simulation

The modelled energy system was simulated in DNA and the results of that simulation are given in Table 2, where the mass flow, temperature and exergy flow are given in relation to each state defined in the process flow diagram given in Figure 3.

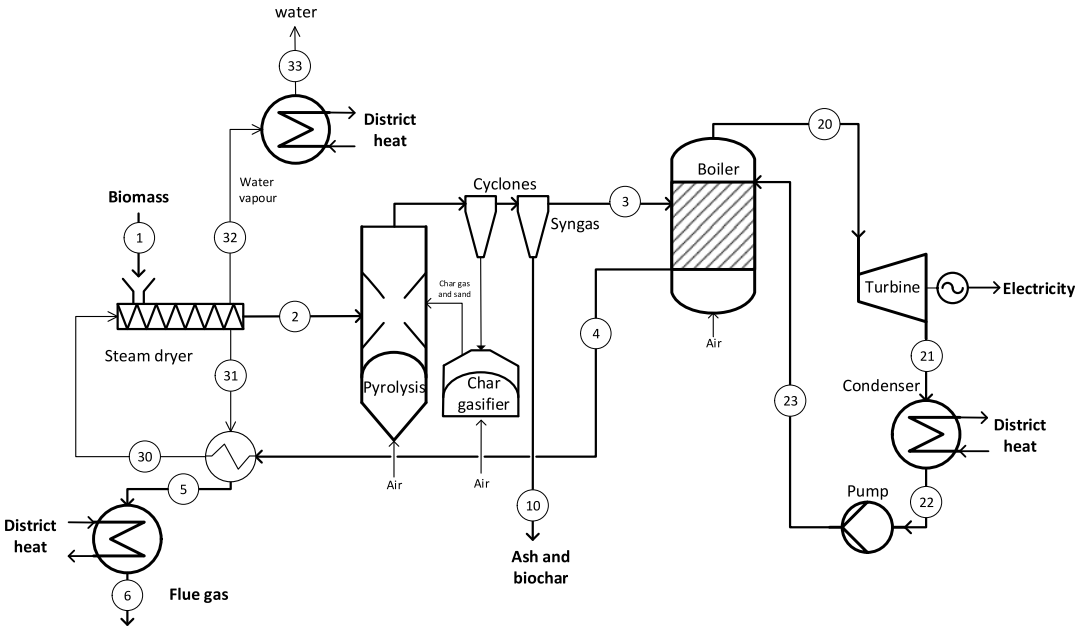

Figure 3: Process flow diagram of the LT-CFB gasifier and the steam boiler power plant.

Table 2: Resulting mass, temperature and exergy at each state of the energy system from simulation.

STATE	kg/s (max energy)	kg/s (max biochar)	$Celsius$ (max energy)	$Celsius$ (max biochar)	kJ/s (max energy)	kJ/s (max biochar)
1	1.00	1.00	15.00	15.00	16385.17	16385.17
2	0.99	0.99	115.00	115.00	16242.43	16242.43
3	2.36	1.83	630.00	630.00	13223.03	9657.02
4	9.31	6.67	205.00	205.00	1004.49	770.71
5	9.31	6.67	186.39	179.49	932.00	699.09
6	9.31	6.67	120.00	120.00	717.60	561.26
10	0.07	0.18	630.00	630.00	290.97	4126.11
20	3.74	2.74	650.00	650.00	6365.12	4658.21
21	3.74	2.74	94.85	94.79	1958.97	1432.73
22	3.74	2.74	94.85	94.79	146.72	107.23
23	3.74	2.74	95.58	95.52	178.29	130.34
30	1.11	1.11	200.00	200.00	690.89	690.89
31	1.11	1.11	115.00	115.00	629.12	629.12
32	0.01	0.01	115.00	115.00	1398.29	1024.53
33	0.01	0.01	50.00	50.00	327.73	240.13

As noted in Section 2.3, the gasifier is operated at atmospheric pressure and the live steam pressure is 80 bar. It can be seen in Figure 3 that the water evaporated from the straw in the steam dryer is condensed and cooled to provide heat for the district heating grid, along with the condensation component in the steam boiler plant, while in Table 2 the simulation results are normalized to 1 kg/s mass flow as input to the energy system. Table 3 gives the resulting energy and exergy efficiency for both maximum energy generation and maximum biochar production operation scenarios of the three products produced in this polygeneration system.

Table 3: Straw utilization system integration energy and exergy efficiencies (energy/exergy).

Scenarios	Biochar	Electricity	District heat
Max energy generation	1.86% / 1.78%	26.98% / 26.78%	50.18% / 7.97%
Max biochar production	26.65% / 25.18%	19.61% / 19.91%	36.93% / 5.76%

As seen in Table 3, there is a shift of energy and exergy towards the biochar from electricity and district heat when moving from a maximum energy generation operation to maximum biochar production. The removal of straw and the difference in biochar production affects the carbon build-up in soil: by not harvesting the straw, the soil carbon build-up has the potential to be about 7.8 kg per kg carbon in straw incorporated in soil continuously over a 100-year period based on C-TOOL simulations. However, this carbon build-up will be changed by removing the straw and only returning a specific factor (proportion) of the carbon originally in straw back to the agricultural system. This specific factor is 1 - carbon conversion in the gasifier and is 0.02 for maximum energy generation and 0.30 for the maximum biohcar production scenario. Figure 4 displays the change in carbon sequestration over a 100-year time-frame when harvesting straw and utilizing it in the LT-CFB gasifier with biochar production for a few carbon conversion factors. As shown in Figure 4, there is a net loss of carbon if the energy system is operated for maximum energy generation. However, if the carbon conversion in the gasifier is decreased to 0.91 the carbon content will potentially be the same in 100 years compared with not harvesting the straw, while the maximum biochar production scenario could increase the carbon content in soil beyond the potential of straw incorporation. This analysis could be used to define an upper limit on the carbon conversion from this type of a system to protect soil quality.

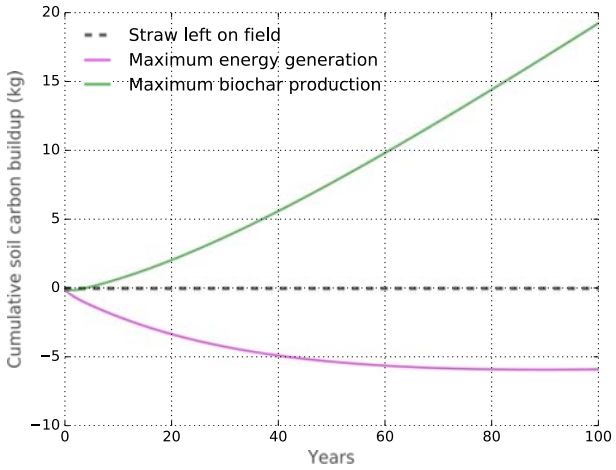

Figure 4: Development of soil carbon for straw utilization in reference to the reference scenario.

3.2. Climate Change Impact

The results of the climate change impact, including displaced energy generation for both operation scenarios and the combustion alternative, are given in Figure 5. The results include confidence intervals found by Monte Carlo simulation.

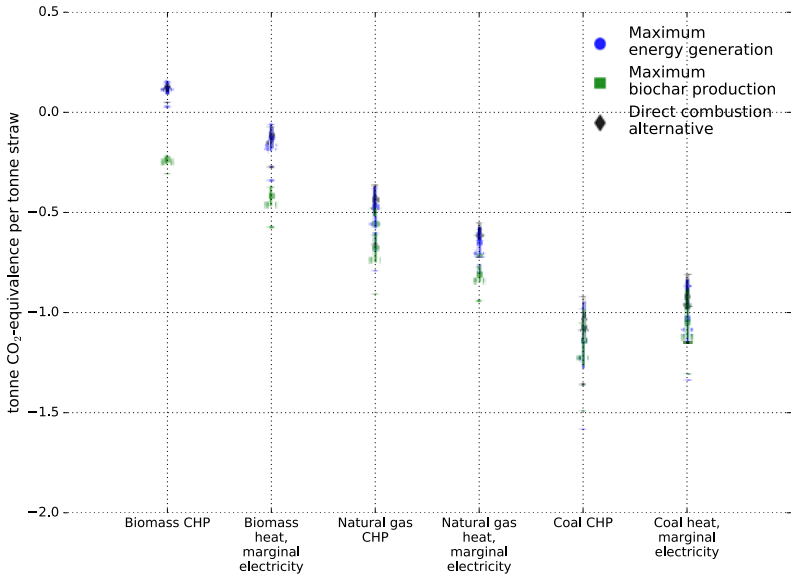

Figure 5: LCIA results for climate change impact in system integration by straw utilization including confidence intervals.

It can be seen in Figure 5 that the gasification system outperforms the combustion alternative. This is true for all displaced energy alternatives, except for biomass where the combustion alternative slightly outperforms the maximum energy generation scenario. In addition, the maximum biochar production scenario outperforms the maximum energy generation scenario for all displaced energy generation alternatives, except for coal-fuelled CHP where the results are equal. The figure also shows that there is an overlap in the confidence intervals in some cases, although this should not affect the conclusion drawn from these between the scenarios and the combustion alternative, as the uncertainty is mainly in the displaced energy generation and any change in value there will be experienced almost equally for all scenarios as the electricity to district heat ratio is almost the same.

The effect of decreased energy generation can be seen when comparing the results from displaying climate-friendly production (biomass fuelled) and coal-fuelled production, because the difference in climate change impact decreases as production using dirtier fuel is avoided. The reason for the difference in climate change impact for the two scenarios can be analysed by disaggregating the impacts to specific processes within the system. These results are displayed in Figure 6 for the two scenarios and the direct combustion alternative, excluding the avoided energy generation, as Figure 6 shows the biochar incorporation process. The reason

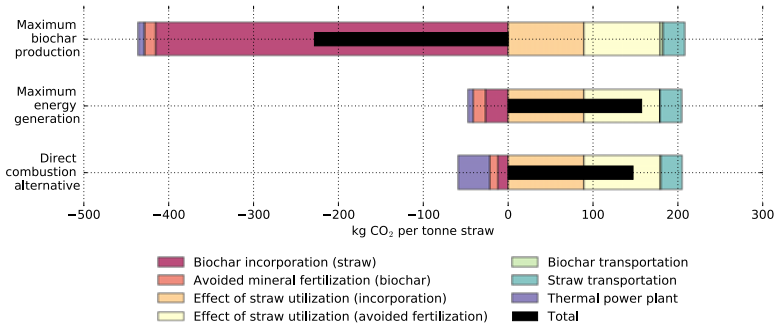

Figure 6: LCIA results for climate change impact in system integration by straw utilization, disaggregated to components.

for the large mitigating effect of biochar incorporation is that the resource (straw) is from an annual crop rotation, i.e. the carbon within that resource is captured by photosynthesis every year. Nevertheless, the carbon that is left in the biochar is very stable and will not dissipate to the atmosphere after the thermal treatment during pyrolysis in the LT-CFB gasifier. It can also be seen that the impacts as a result of emissions from the thermal plant are different for the gasification system and the direct combustion alternative. This is because the NO_x and SO_2 emissions, which mitigate greenhouse gas effects but are otherwise undesired because of other environmental and human health impacts, are greater in the direct combustion system. It should be noted here that as found in an article by Sigurjonsson et al. [9] al climate change impacts are mitigated at carbon conversion factors below 0.88.

3.3. Renewable Energy Indicator

The ExROI final scores for the maximum energy generation scenario and maximum biochar production scenario are 10.05 and 6.22 respectively, while the final score of the direct combustion alternative is 8.08. These results, along with their confidence intervals from Monte Carlo simulation, are displayed in Figure 7. It can be seen in the figure that the ExROI scores of the scenarios and the alternative are not found within the confidence intervals of each other and no result is below 1.0, indicating that both scenarios and the alternative are renewable energy generators. The CExD results used to find the ExROI score are then disaggregated into specific processes for both systems as well as for the combustion alternative. Those results

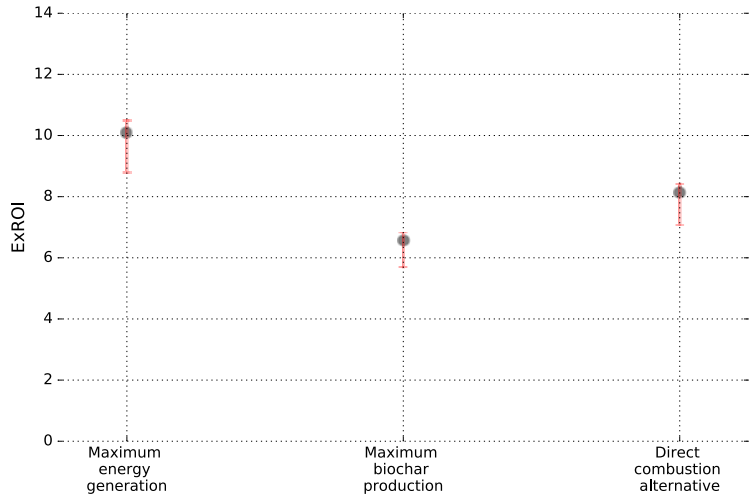

Figure 7: Exergy Return on Investment results for system integration by straw utilization, including confidence intervals from a Monte Carlo simulation.

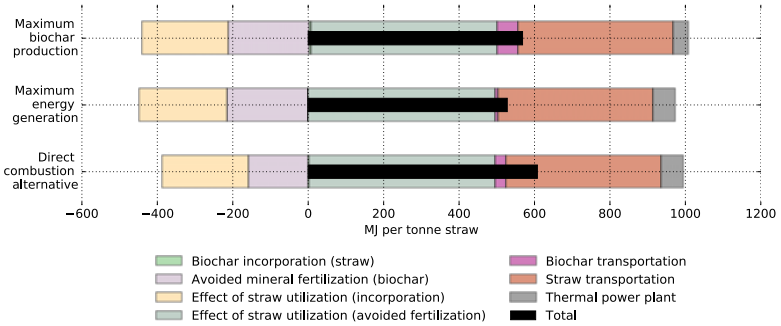

Figure 8: Cumulative Exergy Demand results of the system integration by straw utilization disaggregated to components.

are displayed in Figure 8. It can be seen when viewing these results that the difference is relatively small between the scenarios and the combustion alternative. This indicates that the ExROI results are governed by the exergetic efficiency of the energy systems. The exergetic efficiency of the energy system can be seen in Table 4, which shows the efficiency of electricity, district heat and biochar production. As the biochar is processed within the system and affects the CExD without much impact, the efficiency of electricity and district heat are the most important indicators for ExROI.

3.4. Technoeconomic Analysis

The levelized cost of electricity production and the investment payback period, assuming sales at the fixed premium tariff price along with the share of carrying charges, expenses and benefits of biochar production, are given in Table 4 for both scenarios as well as for the combustion alternative.

Table 4: Results of the economic analysis in the straw utilization case study.

	Maximum energy generation	Maximum biochar production	Combustion alternative
Levelized cost euro/MWh	70.4	83.0	68.7
Payback period years	9.5	12.4	8.3
Carrying charges %	54.2	49.8	49.4
Expenses %	48.0	55.9	52.5
Benefits %	-2.2	-5.6	-1.9

As shown in the figure, both of the scenarios and the combustion alternative have a payback period shorter than the economic lifetime of the investment, making them economically feasible. It can also be seen that the combustion alternative outperforms both gasification scenarios, with a lower levelized cost and investment payback period. Furthermore, the distribution between carrying charges, expenses and benefits changes for the two systems and the two gasification scenarios.

A sensitivity analysis was done by varying the main parameters used to calculate the investment payback period. The results of this analysis are given in Figures 9a and 9b for the two gasification scenarios respectively. The results of the sensitivity analysis show that the investment payback period is most sensitive

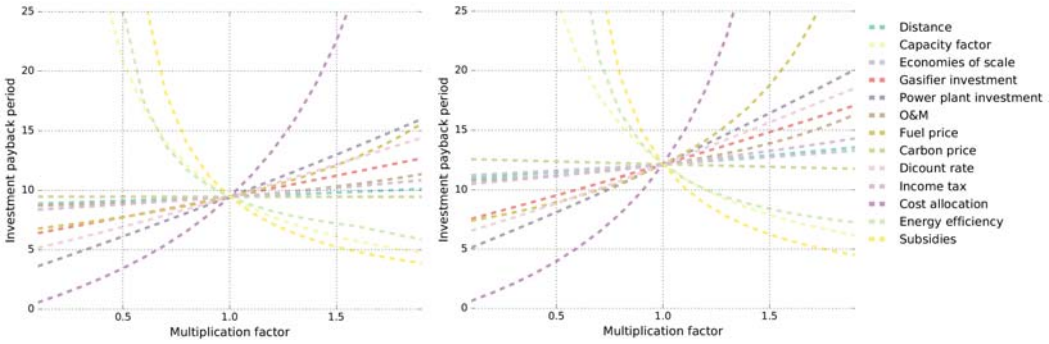

(a) Maximum energy generation.

(b) Maximum biochar production.

Figure 9: Sensitivity analysis of the economic parameters for the gasification case in the straw utilization case study.

to changes in the capacity factor, power plant investment cost, discount rate, fuel prices and the gasifier investment cost parameters.

The main difference between the direct combustion and the gasification systems lies in the carrying charges, as shown in Table 4. The carrying charges are governed by the investment cost. The data used for the investment cost of both systems is the same, except that the burner and boiler unit of the straw-fired combustion power plant – which is the reference – is replaced by the LT-CFB gasifier, resulting in the assumed reduction in the total power plant investment of 20%. However, the cost of installing the LT-CFB gasifier and a boiler is more than this reduction, which would need to be about 37% for the investment payback period to be equal to the direct combustion alternative and the maximum energy generation scenario of the LT-CFB gasification system.

These results are based on a 70% capacity factor, which is assumed to be the upper limit, while the lower limit is assumed to be 30%. If the lower limit is used as a capacity factor, the gasification case still has a

payback period below 25 years. The capacity factor cannot be lower than 30% if the payback period is to be before the technical lifetime of the investment.

3.5. Multi-Criteria Analysis

The results given above for the LT-CFB gasifier energy system include only the maximum energy generation and maximum biochar production operation scenarios. However, the multi-criteria analysis combines the results of the climate change impact, renewable energy indicator and profitability for the whole carbon conversion range between maximum energy generation (0.98) to maximum biochar production (0.70). Figure 10 displays the results of the three criteria.

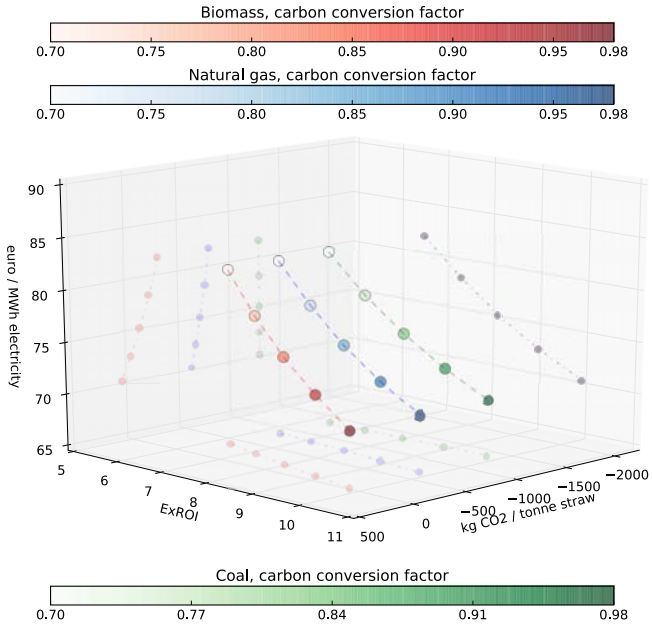

Figure 10: 3d graph with climate change impact, Exergy Return on Investment and levelized cost of electricity generation for the straw utilization case study.

It can be seen in the figure that the profitability represented by a levelized cost of electricity and the renewable energy indicator found with ExROI are optimized at maximum carbon conversion but the environmental impact based on climate change is optimized at minimum carbon conversion. Figure 11 shows the results of the TOPSIS MCDA analysis when the avoided energy generation is a CHP plant fuelled by natural gas. The arrows point to criteria of interest, e.g. because profitability points to the top of the triangle, the optimum carbon conversion factor is purely based on profitability.

As shown in Figure 11 , the decision on optimum carbon conversion if based purely on profitability and environmental impact can be the whole range between the maximum and minimum values, depending on the importance of each criteria. However, if a renewable energy generation indicator is also included in the calculations, the optimum carbon conversion is more likely to be at maximum carbon conversion, i.e. maximum energy generation. To get an indication of the importance of each of these, the Delphi technique [46] could be used for each of them, together with all stakeholders, which can then ultimately be used to identify the optimum operation of the LT-CFB gasifier.

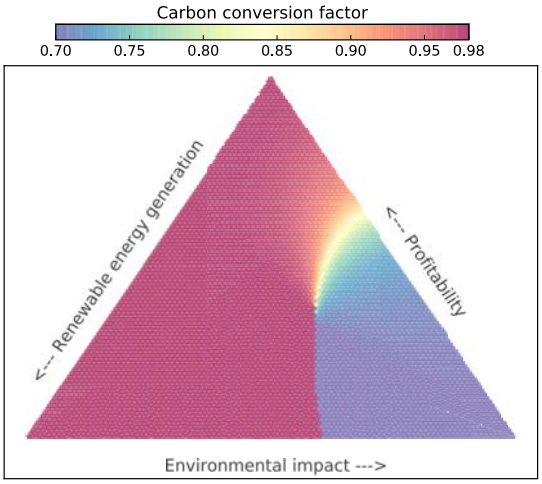

Figure 11: Ternary graphs of the multi-criteria decision analysis for the straw utilization integrated system.

4. Conclusion

The article presents a study on the multi-criteria analysis of cereal straw utilization in a LT-CFB heat, power and biochar polygeneration plant using renewable energy generation, environmental impact and profitability criteria. The system is compared with a direct combustion CHP plant fuelled by cereal straw and analysed over a range of operation scenarios.

1. Based on the results of the study, the main conclusions are that the polygeneration power plant is economically feasible given the current rate of the premium feed-in tariff. Additionally, it has a lower environmental impact based on climate change and higher renewable energy generation based on ExROI than the direct combustion alternative. However, the alternative was found to have a lower levelized cost and a lower investment payback period than the polygeneration plant.

2. For the polygeneration plant, the maximum biochar production operation at the expense of energy generation was found to have a lower environmental impact. However, the maximum energy generation is the optimum operation based on profitability and renewable energy generation, and therefore when all three criteria are included it is most likely that maximum energy generation would be the optimal operation.

3. If using cereal straw in the energy system instead of leaving it on the field, the system would need to be operated at maximum biochar production (70% carbon conversion) for the carbon build-up to be increased within a few years if the biochar is returned to the same field. At maximum energy generation operation, the carbon build-up in soil would decrease. However, 91% carbon conversion suffices for an equivalent carbon build-up over a 100-year time horizon.

Acknowledgements

This research was funded by the Villum foundation.

References

[1] Danish Ministry of Climate. Energy and Buildings, Our Future Energy, Tech. rep., Danish Ministry of Climate. Energy and Buildings, Copenhagen.
URL http://www.ens.dk/sites/ens.dk/files/policy/danish-climate-energy-policy/our_future_energy.pdf

[2] G. Working, The Danish Climate Policy Plan Towards a low carbon society, Tech. rep., Inter-ministerial, Copenhagen (2013).
URL http://www.ens.dk/sites/ens.dk/files/policy/danish-climate-energy-policy/danishclimatepolicyplan_uk.pdf

[3] Energy Statistics 2013: Data, tables, staristics and maps, Tech. rep., Danish Energy Agency, Copenhagen (2015).

[4] Energy- and greenhouse gas-based LCA of biofuel and bioenergy systems: Key issues, ranges and recommendations, Resources, Conservation and Recycling 53 (8) (2009) 434–447. doi:10.1016/j.resconrec.2009.03.013.
URL http://www.sciencedirect.com/science/article/pii/S0921344909000500

[5] Statistics Denmark, https://www.dst.dk/en, accessed: 2016-01-31.
URL https://www.dst.dk/en

[6] L. Elsgaard, U. Jørgensen, M. Gylling, T. Holst, H. Andersen, L. Nikolaisen, Anvendelsesmuligheder for halm til energiformål, 2011.

[7] D. S. Powlson, M. J. Glendining, K. Coleman, A. P. Whitmore, Implications for Soil Properties of Removing Cereal Straw: Results from Long-Term Studies, Agronomy Journal 103 (1) (2011) 279. doi:10.2134/agronj2010.0146s.
URL https://dl.sciencesocieties.org/publications/aj/abstracts/103/1/279

[8] T. L. T. Nguyen, J. E. Hermansen, R. G. Nielsen, Environmental assessment of gasification technology for biomass conversion to energy in comparison with other alternatives: the case of wheat straw, Journal of Cleaner Production 53 (0) (2013) 138 – 148. doi:http://dx.doi.org/10.1016/j.jclepro.2013.04.004.

[9] H. Æ. Sigurjonsson, B. Elmegaard, L. R. Clausen, J. Ahrenfeldt, Climate effect of an integrated wheat production and bioenergy system with low temperature circulating fluidized bed gasifier, Applied Energy 160 (2015) 511–520.

[10] J. Ahrenfeldt, T. P. Thomsen, U. Henriksen, L. R. Clausen, Biomass gasification cogeneration – a review of state of the art technology and near future perspectives, Applied Thermal Engineering 50 (2) (2013) 1407 – 1417. doi:http://dx.doi.org/10.1016/j.applthermaleng.2011.12.040.

[11] R. Nielsen, E. Qvale, U. Henriksen, P. Stoholm, Optimering af lav temperatur cirkulerende fluid bed forgasningsprocessen til biomasse med højt askeindhold, Ph.D. thesis (2007).

[12] P. Stoholm, R. Nielsen, L. Sarbæk, L. Tobiasen, U. Henriksen, M. Fock, K. Richardt, B. Sander, L. Wolff, The Low Temperature CFB Gasifier - Further Test Results and Possible Applications, ETA-Florence & WIP-Munich, 2002, pp. 706–709.

[13] K. Kuligowski, T. G. Poulsen, G. H. Rubak, P. Sorensen, Plant-availability to barley of phosphorus in ash from thermally treated animal manure in comparison to other manure based materials and commercial fertilizer, European Journal of Agronomy 33 (4) (2010) 293 – 303. doi:http://dx.doi.org/10.1016/j.eja.2010.08.003.

[14] D. Muller-Stover, J. Ahrenfeldt, J. Holm, S. Shalatet, U. Henriksen, H. Hauggaard-Nielsen, Soil application of ash produced by low-temperature fluidized bed gasification: effects on soil nutrient dynamics and crop response, Nutrient Cycling in Agroecosystems 94 (2-3) (2012) 193–207. doi:10.1007/s10705-012-9533-x.

[15] V. Hansen, D. Müller-Stöver, J. Ahrenfeldt, J. K. Holm, U. B. Henriksen, H. Hauggaard-Nielsen, Gasification biochar as a valuable by-product for carbon sequestration and soil amendment, Biomass and Bioenergy 72 (2015) 300 – 308. doi:http://dx.doi.org/10.1016/j.biombioe.2014.10.013.
URL http://www.sciencedirect.com/science/article/pii/S0961953414004693

[16] G. Myhre, D. Shindell, F. Bréon, W. Collins, J. Fuglestvedt, J. Huang, D. Koch, J. Lamarque, D. Lee, B. Mendoza, et al., Anthropogenic and Natural Radiative Forcing. In: Climate Change 2013: The Physical Science Basis. Contribution of Working Group 1 to the Fifth Assessment Report of the Intergovernmental Panel on Climate Change, Table 8 (2013) 714.

[17] M. E. Bosch, M. E., S. Hellweg, M. Huijbregts, R. Frischknecht, Applying cumulative exergy demand (cexd) indicators to the database, The International Journal of Life Cycle Assessment 12 (3) (2007) 181–190. doi:10.1065/lca2006.11.282.

[18] Thermal Design and Optimization, John Wiley & Sons, 1996.
URL https://books.google.com/books?hl=en&lr=&id=sTi2crXeZYgC&pgis=1

[19] C.-L. Hwang, K. Yoon, Multiple attribute decision making: methods and applications a state-of-the-art survey, Vol. 186, Springer Science & Business Media, 2012.

[20] I. B. Huang, J. Keisler, I. Linkov, Multi-criteria decision analysis in environmental sciences: ten years of applications and trends, Science of the total environment 409 (19) (2011) 3578–3594.

[21] M. Behzadian, S. Khanmohammadi Otaghsara, M. Yazdani, J. Ignatius, A state-of the-art survey of TOPSIS applications, Expert Systems with Applications 39 (17) (2012) 13051–13069. doi:10.1016/j.eswa.2012.05.056.
URL http://www.sciencedirect.com/science/article/pii/S0957417412007725

[22] B. Elmegaard, N. Houbak, et al., DNA – a general energy system simulation tool, in: Proceedings of SIMS, Citeseer, 2005, pp. 1–10.

[23] E. C. 2013, Ecoinvent centre (2013), ecoinvent data v3.1., swiss Centre for Life Cycle Inventories, Dübendorf, 2013, retrieved from: www.ecoinvent.org.

[24] C. Mutel, Brightway2, http://brightwaylca.org/., accessed: 2015-11-31, a framework for advanced life cycle assessment calculations (2014).
URL http://brightwaylca.org/.

[25] T. L. T. Nguyen, J. E. Hermansen, L. Mogensen, Environmental performance of crop residues as an energy source for

electricity production: The case of wheat straw in denmark, Applied Energy 104 (0) (2013) 633 – 641. doi:http://dx.doi.org/10.1016/j.apenergy.2012.11.057.

[26] F. Cherubini, G. P. Peters, T. Berntsen, A. H. Stromman, E. Hertwich, CO2 emissions from biomass combustion for bioenergy: atmospheric decay and contribution to global warming, GCB Bioenergy 3 (5) (2011) 413–426. doi:10.1111/j.1757-1707.2011.01102.x.
URL http://doi.wiley.com/10.1111/j.1757-1707.2011.01102.x

[27] F. Cherubini, A. H. Stromman, E. Hertwich, Effects of boreal forest management practices on the climate impact of CO2 emissions from bioenergy, Ecological Modelling 223 (1) (2011) 59–66. doi:10.1016/j.ecolmodel.2011.06.021.

[28] G. Guest, F. Cherubini, A. H. StrÃ¸mman, The role of forest residues in the accounting for the global warming potential of bioenergy, GCB Bioenergy 5 (4) (2013) 459–466. doi:10.1111/gcbb.12014.
URL http://dx.doi.org/10.1111/gcbb.12014

[29] B. M. Petersen, M. T. Knudsen, J. E. Hermansen, N. Halberg, An approach to include soil carbon changes in life cycle assessments, Journal of Cleaner Production 52 (0) (2013) 217 – 224. doi:http://dx.doi.org/10.1016/j.jclepro.2013.03.007.

[30] B. M. Petersen, J. E. Olesen, T. Heidmann, A flexible tool for simulation of soil carbon turnover, Ecological Modelling 151 (1) (2002) 1 – 14. doi:http://dx.doi.org/10.1016/S0304-3800(02)00034-0.

[31] B. M. Petersen, C-TOOL version 1.1 a Tool for Simulation of Soil Carbon Turnover : Description and users guide, Tech. rep., Danish Institute of Agricultural Sciences: Department of Agroecology (2003).

[32] B. Weidema, C. Bauer, R. Hischier, C. Mutel, T. Nemecek, J. Reinhard, C. Vadenbo, G. Wernet, The ecoinvent database: Overview and methodology, Data quality guideline for the database version 3. Ecoinvent Report 1 (v3), Tech. rep. (2013).
URL www.ecoinvent.org

[33] B. P. Weidema, M. S. Wesnæ s, Data quality management for life cycle inventories—an example of using data quality indicators, Journal of Cleaner Production 4 (3-4) (1996) 167–174. doi:10.1016/S0959-6526(96)00043-1.
URL http://www.sciencedirect.com/science/article/pii/S0959652696000431

[34] B. P. Weidema, Multi-user test of the data quality matrix for product life cycle inventory data, The International Journal of Life Cycle Assessment 3 (5) (1998) 259–265. doi:10.1007/BF02979832.
URL http://link.springer.com/10.1007/BF02979832

[35] L. R. Clausen, Design of novel dme/methanol synthesis plants based on gasification of biomass, Ph.D. thesis, PhD Thesis, DTU Mechanical Engineering, Technical University of Denmark, Denmark (2011).

[36] G. Guest, F. Cherubini, A. H. Stromman, The role of forest residues in the accounting for the global warming potential of bioenergy, GCB Bioenergy 5 (4) (2013) 459–466. doi:10.1111/gcbb.12014.

[37] H. Lund, B. V. Mathiesen, P. Christensen, J. H. Schmidt, Energy system analysis of marginal electricity supply in consequential LCA, The International Journal of Life Cycle Assessment 15 (3) (2010) 260–271. doi:10.1007/s11367-010-0164-7.
URL http://link.springer.com/10.1007/s11367-010-0164-7

[38] C. J. Cleveland, R. Costanza, C. A. Hall, R. Kaufmann, Energy and the u.s. Economy: a biophysical perspective., Science (New York, N.Y.) 225 (4665) (1984) 890–7. doi:10.1126/science.225.4665.890.
URL http://science.sciencemag.org/content/225/4665/890.abstract

[39] E. Font de Mora, C. Torres, A. Valero, Assessment of biodiesel energy sustainability using the exergy return on investment concept, Energy 45 (1) (2012) 474–480. doi:10.1016/j.energy.2012.02.072.
URL http://www.sciencedirect.com/science/article/pii/S0360544212001867

[40] J. Szargut, D. Morris, F. Steward, Exergy analysis of thermal, chemical, and metallurgical processes.
URL http://www.osti.gov/scitech/biblio/6157620

[41] I. H. Bell, J. Wronski, S. Quoilin, V. Lemort, Pure and pseudo-pure fluid thermophysical property evaluation and the open-source thermophysical property library coolprop, Industrial & Engineering Chemistry Research 53 (6) (2014) 2498–2508. arXiv:http://pubs.acs.org/doi/pdf/10.1021/ie4033999, doi:10.1021/ie4033999.
URL http://pubs.acs.org/doi/abs/10.1021/ie4033999

[42] E. F. de Mora, C. Torres, A. Valero, Thermoeconomic analysis of biodiesel production from used cooking oils, Sustainability 7 (5) (2015) 6321–6335.

[43] Technology data for energy plants - Generation of Electricity and District Heating, Energy Storage and Energy Carrier Generation and Conversion, Tech. rep., The Danish Energy Agency and Energinet.dk.
URL http://www.energinet.dk/SiteCollectionDocuments/Danskedokumenter/Forskning/Technology_data_for_energy_plants.pdf

[44] C. Bang, A. Vitina, J. S. Gregg, H. H. Lindboe, Analysis of biomass prices - Future Danish prices for straw, wood chips and wood pellets, Tech. rep., Ea Energy Analyses (2013).
URL http://www.ens.dk/sites/ens.dk/files/undergrund-forsyning/vedvarende-energi/bioenergi/analyse-bioenergi-danmark/analysis_of_biomass_prices_2013.06.18_-_final_report.pdf

[45] Energistyrelsen, Forudsætning for samfunsøkonomiske analyser på energiområdet, Tech. rep., Energistyrelsen, (2014).

[46] F. Hasson, S. Keeney, H. McKenna, Research guidelines for the delphi survey technique, Journal of advanced nursing 32 (4) (2000) 1008–1015.

B. DNA Code

The Dynamic Network Analysis (DNA) software was used to model and simulate the thermal power plant and biogas engine in this thesis. There were two DNA models of the thermal power plant made, one for resources under 20% moisture content and another for inputs above 20%. Only one biogas engine model was made.

```
c ########################################
c ############## Inputs ##################
c ########################################
c ########################################

solid sol C 0.4751 O 0.3902 H 0.0595
+ N 0.0075 S 0.0012 ASH 0.0665
 + HHV 19236.0 CP 1.24

addco ZA Dryer 2 0.02
addco m MIX 99 0.5 m MIX 98 0.5
addco ZA Gasifier 11 1.0
addco ZA Gasifier 19 0.101
addco za burner 1 1.7
addco t superheater 61 520
addco p 58 120
addco p 62 12

c #### Media ####
media 98 sol 99 STEAM-HF 1 resource 2 Dry
media 30 STANDARD_AIR 9 SynGas 8 Ash
media 11 FlueGas 40 STANDARD_AIR
media 60 STEAM-HF

c ########################################
c ----------- Steam Dryer ---------------
c ########################################
struc MIX sllqmx_1 98 99 1 0
addco t MIX 99 15

struc Dryer DRYER_04 1 27 2 4 301
addco t Dryer 1 15 p 1 1.013
addco t Dryer 2 115 t Dryer 4 115 t Dryer 27 200 c Temperature of the steam loop
addco q Dryer 301 0
addco p 27 1.013 p 2 1.013

struc splitter splitter2 3 4 26 5
addco p 5 1.013

struc DH heatsnk0 5 85 322 0
addco t DH 5 80
addco t DH 85 45

struc HEX heatsrc0 26 27 302 0

c ########################################
c ------------- Gasifier ----------------
c ########################################
struc Gasifier GASIFI_3_VENZIN 8 2 7 30 9 8 304 303 901 1 3 4 6 7 9 11 36
addco M Gasifier 7 0 T Gasifier 7 150
addco P 8 1.013 p 9 1.013
addco T Gasifier 9 630 T Gasifier 8 630 c Temperature of the syngas and biochar
addco ZA Gasifier 17 0.015 c Ratio of heat lost.
addco ZA Gasifier 18 0
addco ZA Gasifier 21 630 c Equilibrium temperature
addco ZA Gasifier 22 0.005
addco ZA Gasifier 28 1

struc air_preheater heatsrc0 29 30 395 0
addco t air_preheater 29 15

struc syngas_cooling heatsnk0 9 10 395 0
addco t syngas_cooling 10 630

struc biochar_cooling heatsnk0_1 8 69 399 0
addco t biochar_cooling 69 20

struc air_heater heatsrc0 40 41 399 0
addco t air_heater 40 15

c ########################################
c ----------- Steam Cycle ---------------
c ########################################
struc burner gasbur_3 41 10 11 305 1
addco q burner 305 0

struc turbine turbin_1 61 62 101 0.95

struc splitter2 splitter 62 63 64

struc dummy valve_01 64 65
addco p 65 12

struc heat1 heatsnk0 65 66 302 0
addco t heat1 66 120 c Outlet temperature

struc heat3 heatsrc0 63 90 390 0
```

```
struc condenser heatex_2 71 72 80 5 346 5 0 0
addco t condenser 80 40
addco x condenser 72 0
addco q condenser 346 0

struc watmix watmix_2 72 67 74

struc pump liqpum_1 74 58 201 0.9

struc superheater heatex_1 11 42 60 61 341 0 0
addco q superheater 341 0
addco x superheater 60 1 c Steam quality at superheater inlet

struc heat4 heatsnk0 42 91 390 0

c #### HRSG ####
struc evaporator heatex_1 91 43 59 60 342 0 0
addco q evaporator 342 0
addco x evaporator 59 0

struc economizer heatex_1 43 44 58 59 343 0 0
addco q economizer 343 0
addco t economizer 44 205

struc dryer_heat heatsnk0 44 45 302 0
addco t dryer_heat 45 120

c #### For drying and district heat ####
struc dh1 heatex_1 45 46 82 5 323 0 0
addco t dh1 82 40
addco t dh1 46 120
addco q dh1 323 0
addco t dh1 5 115

struc dh2 heatex_1 66 67 83 5 324 0 0
addco t dh2 83 40
addco t dh2 67 45
addco q dh2 324 0
addco t dh2 5 115

c Reference conditions for exergy
xergy p 1.013 t 15

C ~~~~~~~~~~~~~~~~~~~~~~~~~~~~~~~~~~~~~~~~~~~~~~~~~~~~~~~~~~~~~~~~~~~~~~~~~~~~~~~~
C ~~ Start of list of generated initial guesses.
C ~~ The values are the results of the latest simulation.
C ~~~~~~~~~~~~~~~~~~~~~~~~~~~~~~~~~~~~~~~~~~~~~~~~~~~~~~~~~~~~~~~~~~~~~~~~~~~~~~~~
START M     MIX                        98  0.4000000000000000E+00 {~~}
START P                           98  0.1013000000000000E+01 {~~}
START H     MIX                        98 -0.5802671882868591E+04 {~~}
START M     MIX                        99  0.6000000000000001E+00 {~~}
START P                           99  0.1013000000000000E+01 {~~}
START H     MIX                        99 -0.1590799997036134E+05 {~~}
START M     MIX                         1 -0.1000000000000000E+01 {~~}
START P                            1  0.1013000000000000E+01 {~~}
START H     MIX                         1 -0.1186586873536424E+05 {~~}
START X_J   resource                   H2          0.2280000000000000E-01 {~~}
START X_J   resource                   O2          0.1628800000000000E+00 {~~}
START X_J   resource                   N2          0.2600000000000000E-02 {~~}
START X_J   resource                   CO          0.0000000000000000E+00 {~~}
START X_J   resource                   NO          0.0000000000000000E+00 {~~}
START X_J   resource                   CO2         0.0000000000000000E+00 {~~}
START X_J   resource                   H2O-L       0.6000000000000000E+00 {~~}
START X_J   resource                   NH3         0.0000000000000000E+00 {~~}
START X_J   resource                   H2S         0.0000000000000000E+00 {~~}
START X_J   resource                   SO2         0.0000000000000000E+00 {~~}
START X_J   resource                   CH4         0.0000000000000000E+00 {~~}
START X_J   resource                   C2H6        0.0000000000000000E+00 {~~}
START X_J   resource                   C3H8        0.0000000000000000E+00 {~~}
START X_J   resource                   C4H10-N     0.0000000000000000E+00 {~~}
START X_J   resource                   C4H10-I     0.0000000000000000E+00 {~~}
START X_J   resource                   C5H12       0.0000000000000000E+00 {~~}
START X_J   resource                   C6H14       0.0000000000000000E+00 {~~}
START X_J   resource                   C7H16       0.0000000000000000E+00 {~~}
START X_J   resource                   C8H18       0.0000000000000000E+00 {~~}
START X_J   resource                   C2H4        0.0000000000000000E+00 {~~}
START X_J   resource                   C3H6        0.0000000000000000E+00 {~~}
START X_J   resource                   C5H10       0.0000000000000000E+00 {~~}
START X_J   resource                   C6H12-1     0.0000000000000000E+00 {~~}
START X_J   resource                   C7H14       0.0000000000000000E+00 {~~}
START X_J   resource                   C2H2        0.0000000000000000E+00 {~~}
START X_J   resource                   C6H6        0.0000000000000000E+00 {~~}
START X_J   resource                   C6H12-C     0.0000000000000000E+00 {~~}
START X_J   resource                   C           0.1845600000000000E+00 {~~}
START X_J   resource                   S           0.6400000000000003E-03 {~~}
START X_J   resource                   NO2         0.0000000000000000E+00 {~~}
START X_J   resource                   HCN         0.0000000000000000E+00 {~~}
```

```
START X_J   resource                NO3          0.0000000000000000E+00 {~~}
START X_J   resource                SO3          0.0000000000000000E+00 {~~}
START X_J   resource                AR           0.0000000000000000E+00 {~~}
START X_J   resource                ASH          0.2652000000000000E-01 {~~}
START X_J   resource                TAR          0.0000000000000000E+00 {~~}
START M     Dryer                     1  0.1000000000000000E+01 {~~}
START H     Dryer                     1 -0.1186586873536424E+05 {~~}
START M     Dryer                    27  0.9566790205763516E+01 {~~}
START P                           27  0.1013000000000000E+01 {~~}
START H     Dryer                    27 -0.1309566421515521E+05 {~~}
START M     Dryer                     2 -0.4081632653061225E+00 {~~}
START P                            2  0.1013000000000000E+01 {~~}
START H     Dryer                     2 -0.5874810951642397E+04 {~~}
START M     Dryer                     4 -0.1015862694045740E+02 {~~}
START P                            4  0.1013000000000000E+01 {~~}
START H     Dryer                     4 -0.1326473150905305E+05 {~~}
START Q     Dryer                   301  0.0000000000000000E+00 {~~}
START ZA    Dryer                     1  0.1617431331376768E+04 {~~}
START ZA    Dryer                     2  0.2000000000000000E-01 {~~}
START ZA    Dryer                     3  0.0000000000000000E+00 {~~}
START X_J   Dry                       H2           0.5586000000000000E-01 {~~}
START X_J   Dry                       O2           0.3990560000000000E+00 {~~}
START X_J   Dry                       N2           0.6370000000000002E-02 {~~}
START X_J   Dry                       CO           0.0000000000000000E+00 {~~}
START X_J   Dry                       NO           0.0000000000000000E+00 {~~}
START X_J   Dry                       CO2          0.0000000000000000E+00 {~~}
START X_J   Dry                       H2O-L        0.2000000000000000E-01 {~~}
START X_J   Dry                       NH3          0.0000000000000000E+00 {~~}
START X_J   Dry                       H2S          0.0000000000000000E+00 {~~}
START X_J   Dry                       SO2          0.0000000000000000E+00 {~~}
START X_J   Dry                       CH4          0.0000000000000000E+00 {~~}
START X_J   Dry                       C2H6         0.0000000000000000E+00 {~~}
START X_J   Dry                       C3H8         0.0000000000000000E+00 {~~}
START X_J   Dry                       C4H10-N      0.0000000000000000E+00 {~~}
START X_J   Dry                       C4H10-I      0.0000000000000000E+00 {~~}
START X_J   Dry                       C5H12        0.0000000000000000E+00 {~~}
START X_J   Dry                       C6H14        0.0000000000000000E+00 {~~}
START X_J   Dry                       C7H16        0.0000000000000000E+00 {~~}
START X_J   Dry                       C8H18        0.0000000000000000E+00 {~~}
START X_J   Dry                       C2H4         0.0000000000000000E+00 {~~}
START X_J   Dry                       C3H6         0.0000000000000000E+00 {~~}
START X_J   Dry                       C5H10        0.0000000000000000E+00 {~~}
START X_J   Dry                       C6H12-1      0.0000000000000000E+00 {~~}
START X_J   Dry                       C7H14        0.0000000000000000E+00 {~~}
START X_J   Dry                       C2H2         0.0000000000000000E+00 {~~}
START X_J   Dry                       C6H6         0.0000000000000000E+00 {~~}
START X_J   Dry                       C6H12-C      0.0000000000000000E+00 {~~}
START X_J   Dry                       C            0.4521720000000001E+00 {~~}
START X_J   Dry                       S            0.1568000000000000E-02 {~~}
START X_J   Dry                       NO2          0.0000000000000000E+00 {~~}
START X_J   Dry                       HCN          0.0000000000000000E+00 {~~}
START X_J   Dry                       COS          0.0000000000000000E+00 {~~}
START X_J   Dry                       N2O          0.0000000000000000E+00 {~~}
START X_J   Dry                       NO3          0.0000000000000000E+00 {~~}
START X_J   Dry                       SO3          0.0000000000000000E+00 {~~}
START X_J   Dry                       AR           0.0000000000000000E+00 {~~}
START X_J   Dry                       ASH          0.6497400000000000E-01 {~~}
START X_J   Dry                       TAR          0.0000000000000000E+00 {~~}
START M     splitter                  4  0.1015862694045740E+02 {~~}
START H     splitter                  4 -0.1326473150905305E+05 {~~}
START M     splitter                 26 -0.9566790205763516E+01 {~~}
START P                           26  0.1013000000000000E+01 {~~}
START H     splitter                 26 -0.1326473150905305E+05 {~~}
START M     splitter                  5 -0.5918367346938780E+00 {~~}
START P                            5  0.1013000000000000E+01 {~~}
START H     splitter                  5 -0.1326473150905306E+05 {~~}
START M     DH                        5  0.2514318555011430E+02 {~~}
START H     DH                        5 -0.1563608739894910E+05 {~~}
START M     DH                       85 -0.2514318555011430E+02 {~~}
START P                           85  0.1013000000000000E+01 {~~}
START H     DH                       85 -0.1578256163014351E+05 {~~}
START Q     DH                      322 -0.3682828773231356E+04 {~~}
START M     HEX                      26  0.9566790205763516E+01 {~~}
START H     HEX                      26 -0.1326473150905305E+05 {~~}
START M     HEX                      27 -0.9566790205763516E+01 {~~}
START H     HEX                      27 -0.1309566421515521E+05 {~~}
START Q     HEX                     302  0.1617431331376763E+04 {~~}
START M     Gasifier                  2  0.4081632653061225E+00 {~~}
START H     Gasifier                  2 -0.5874810951642397E+04 {~~}
START M     Gasifier                  7  0.0000000000000000E+00 {~~}
START P                            7  0.1018000000000000E+01 {~~}
START H     Gasifier                  7 -0.1319461892147020E+05 {~~}
START M     Gasifier                 30  0.3191422503280371E+00 {~~}
START P                           30  0.1018000000000000E+01 {~~}
START H     Gasifier                 30  0.5073026313769964E+03 {~~}
START M     Gasifier                  9 -0.6970943156341596E+00 {~~}
START P                            9  0.1013000000000000E+01 {~~}
START H     Gasifier                  9 -0.3055442950116309E+04 {~~}
```

```
START H     Gasifier                    8 -0.1026264441489806E+05 {~~}
START Q     Gasifier                  304 -0.2039983975143750E+03 {~~}
START Q     Gasifier                  303  0.0000000000000000E+00 {~~}
START ZC                          901  0.6799946583812501E+04 {~~}
START ZA    Gasifier                    1  0.6742249677413554E+05 {~~}
START ZA    Gasifier                    2 -0.8980798449980357E+04 {~~}
START ZA    Gasifier                    3  0.8968858913821123E+05 {~~}
START ZA    Gasifier                    4  0.3053220296332986E+06 {~~}
START ZA    Gasifier                    5  0.1218135433410215E+06 {~~}
START ZA    Gasifier                    6  0.1766240805386200E+06 {~~}
START ZA    Gasifier                    7 -0.7720690210601007E+04 {~~}
START ZA    Gasifier                    8  0.8938421640752452E+00 {~~}
START ZA    Gasifier                    9  0.9012651094667627E+00 {~~}
START ZA    Gasifier                   10  0.9116270844776427E+00 {~~}
START ZA    Gasifier                   11  0.9800000000000000E+00 {~~}
START ZA    Gasifier                   12  0.7401744000000003E-01 {~~}
START ZA    Gasifier                   13  0.3318208904045270E-05 {~~}
START ZA    Gasifier                   14  0.3807106499720268E-02 {~~}
START ZA    Gasifier                   15  0.6780007726669643E+04 {~~}
START ZA    Gasifier                   16  0.7297599999999999E+04 {~~}
START ZA    Gasifier                   17  0.3000000000000000E-01 {~~}
START ZA    Gasifier                   18  0.0000000000000000E+00 {~~}
START ZA    Gasifier                   19  0.2000000000000000E-01 {~~}
START ZA    Gasifier                   20  0.1013000000000000E+01 {~~}
START ZA    Gasifier                   21  0.5700000000000000E+03 {~~}
START ZA    Gasifier                   22  0.5000000000000000E-02 {~~}
START ZA    Gasifier                   23 -0.6948897677711638E-01 {~~}
START ZA    Gasifier                   24  0.3577842159742293E-03 {~~}
START ZA    Gasifier                   25  0.1440690488632838E+00 {~~}
START ZA    Gasifier                   26  0.0000000000000000E+00 {~~}
START ZA    Gasifier                   27  0.0000000000000000E+00 {~~}
START ZA    Gasifier                   28  0.1000000000000000E+01 {~~}
START ZA    Gasifier                   29  0.1847970786707476E+05 {~~}
START ZA    Gasifier                   30  0.2687929349843844E-02 {~~}
START ZA    Gasifier                   31  0.1221798538290437E+00 {~~}
START ZA    Gasifier                   32  0.3197211711010624E+00 {~~}
START ZA    Gasifier                   33  0.1185177008041819E+00 {~~}
START ZA    Gasifier                   34  0.2662159125706949E+00 {~~}
START ZA    Gasifier                   35  0.1408545697750505E+00 {~~}
START ZA    Gasifier                   36  0.1501872372447156E+00 {~~}
START ZA    Gasifier                   37  0.1931413418922040E-01 {~~}
START ZA    Gasifier                   38  0.2724598761375971E-01 {~~}
START ZA    Gasifier                   39  0.2695112727286954E+00 {~~}
START ZA    Gasifier                   40  0.8938421640752452E+00 {~~}
START ZA    Gasifier                   41  0.0000000000000000E+00 {~~}
START ZA    Gasifier                   42  0.1529250793954289E-05 {~~}
START ZA    Gasifier                   43  0.3917125872334746E-05 {~~}
START Y_J   SynGas                     H2          0.1162286340270520E+00 {~~}
START Y_J   SynGas                     O2          0.0000000000000000E+00 {~~}
START Y_J   SynGas                     N2          0.3135460334992817E+00 {~~}
START Y_J   SynGas                     CO          0.2610741827119988E+00 {~~}
START Y_J   SynGas                     NO          0.0000000000000000E+00 {~~}
START Y_J   SynGas                     CO2         0.1381340857132503E+00 {~~}
START Y_J   SynGas                     H2O-G       0.1931413418922040E-01 {~~}
START Y_J   SynGas                     NH3         0.0000000000000000E+00 {~~}
START Y_J   SynGas                     H2S         0.7243063414772655E-03 {~~}
START Y_J   SynGas                     SO2         0.0000000000000000E+00 {~~}
START Y_J   SynGas                     CH4         0.1472865007910629E+00 {~~}
START Y_J   SynGas                     NO2         0.0000000000000000E+00 {~~}
START Y_J   SynGas                     HCN         0.0000000000000000E+00 {~~}
START Y_J   SynGas                     COS         0.0000000000000000E+00 {~~}
START Y_J   SynGas                     AR          0.3692122726656691E-02 {~~}
START X_J   Ash                        C           0.1221798538290437E+00 {~~}
START X_J   Ash                        ASH         0.8778201461709563E+00 {~~}
START M     air_preheater               29  0.3191422503280371E+00 {~~}
START P                           29  0.1018000000000000E+01 {~~}
START H     air_preheater               29 -0.9883452766878590E+02 {~~}
START M     air_preheater               30 -0.3191422503280371E+00 {~~}
START H     air_preheater               30  0.5073026313769964E+03 {~~}
START Q     air_preheater             395  0.1934439769453143E+03 {~~}
START M     syngas_cooling              9  0.6970943156341596E+00 {~~}
START H     syngas_cooling              9 -0.3055442950116309E+04 {~~}
START M     syngas_cooling             10 -0.6970943156341596E+00 {~~}
START P                           10  0.1013000000000000E+01 {~~}
START H     syngas_cooling             10 -0.3332943386724136E+04 {~~}
START Q     syngas_cooling             395 -0.1934439769453143E+03 {~~}
START M     biochar_cooling             8  0.3021120000000001E-01 {~~}
START H     biochar_cooling             8 -0.1026264441489806E+05 {~~}
START M     biochar_cooling            69 -0.3021120000000001E-01 {~~}
START P                           69  0.1013000000000000E+01 {~~}
START H     biochar_cooling            69 -0.1087264441489806E+05 {~~}
START Q     biochar_cooling            399 -0.1842883200000000E+02 {~~}
START M     air_heater                 40  0.3155375420457260E+01 {~~}
START P                           40  0.1013000000000000E+01 {~~}
START H     air_heater                 40 -0.9883452766878590E+02 {~~}
START M     air_heater                 41 -0.3155375420457260E+01 {~~}
START P                           41  0.1013000000000000E+01 {~~}
START H     air_heater                 41 -0.9299407144905359E+02 {~~}
```

```
START H     burner                    41 -0.9299407144905359E+02 {~~}
START M     burner                    10  0.6970943156341596E+00 {~~}
START H     burner                    10 -0.3332943386724136E+04 {~~}
START M     burner                    11 -0.3852469736091420E+01 {~~}
START P                          11  0.1013000000000000E+01 {~~}
START H     burner                    11 -0.6792544200929583E+03 {~~}
START Q     burner                   305  0.0000000000000000E+00 {~~}
START ZA    burner                     1  0.1700000000000000E+01 {~~}
START Y_J   FlueGas                  O2          0.7094148307630707E-01 {~~}
START Y_J   FlueGas                  N2          0.7073473253664888E+00 {~~}
START Y_J   FlueGas                  NO          0.0000000000000000E+00 {~~}
START Y_J   FlueGas                  CO2         0.1146064214411883E+00 {~~}
START Y_J   FlueGas                  H2O-G       0.9854188072308205E-01 {~~}
START Y_J   FlueGas                  SO2         0.1515654784847850E-03 {~~}
START Y_J   FlueGas                  NO2         0.0000000000000000E+00 {~~}
START Y_J   FlueGas                  AR          0.8411323914448954E-02 {~~}
START M     turbine                   61  0.1788651390200589E+01 {~~}
START P                          61  0.1000000000000000E+03 {~~}
START H     turbine                   61 -0.1249421060208165E+05 {~~}
START M     turbine                   62 -0.1788651390200589E+01 {~~}
START P                          62  0.8500000000000000E+01 {~~}
START H     turbine                   62 -0.1312754540714483E+05 {~~}
START W     turbine                  101 -0.1132815179538679E+04 {~~}
START M     splitter2                 62  0.1788651390200589E+01 {~~}
START H     splitter2                 62 -0.1312754540714483E+05 {~~}
START M     splitter2                 63 -0.1247439359153316E+01 {~~}
START P                          63  0.8500000000000000E+01 {~~}
START H     splitter2                 63 -0.1312754540714483E+05 {~~}
START M     splitter2                 64 -0.5412120310472732E+00 {~~}
START P                          64  0.8500000000000000E+01 {~~}
START H     splitter2                 64 -0.1312754540714483E+05 {~~}
START M     dummy                     64  0.5412120310472732E+00 {~~}
START H     dummy                     64 -0.1312754540714483E+05 {~~}
START M     dummy                     65 -0.5412120310472732E+00 {~~}
START P                          65  0.8500000000000000E+01 {~~}
START H     dummy                     65 -0.1312754540714483E+05 {~~}
START M     heat1                     65  0.5412120310472732E+00 {~~}
START H     heat1                     65 -0.1312754540714483E+05 {~~}
START M     heat1                     66 -0.5412120310472732E+00 {~~}
START P                          66  0.8500000000000000E+01 {~~}
START H     heat1                     66 -0.1546683660761298E+05 {~~}
START Q     heat1                    302 -0.1266052541816380E+04 {~~}
START M     turbin2                   90  0.1247439359153316E+01 {~~}
START H     turbin2                   90 -0.1312754540714483E+05 {~~}
START M     turbin2                   71 -0.1247439359153316E+01 {~~}
START P                          71  0.3089018451772466E+00 {~~}
START H     turbin2                   71 -0.1364677209482745E+05 {~~}
START W     turbin2                  102 -0.6477038065381097E+03 {~~}
START M     condenser                 71  0.1247439359153316E+01 {~~}
START H     condenser                 71 -0.1364677209482745E+05 {~~}
START M     condenser                 72 -0.1247439359153316E+01 {~~}
START P                          72  0.3089018451772466E+00 {~~}
START H     condenser                 72 -0.1567902891242899E+05 {~~}
START M     condenser                 80  0.2448418119350408E+02 {~~}
START P                          80  0.1013000000000000E+01 {~~}
START H     condenser                 80 -0.1580345468692628E+05 {~~}
START M     condenser                  5 -0.2448418119350408E+02 {~~}
START H     condenser                  5 -0.1569991366498447E+05 {~~}
START Q     condenser                346  0.0000000000000000E+00 {~~}
START ZA    condenser                  1  0.2535117142183827E+04 {~~}
START M     watmix                    72  0.1247439359153316E+01 {~~}
START H     watmix                    72 -0.1567902891242899E+05 {~~}
START M     watmix                    67  0.5412120310472732E+00 {~~}
START P                          67  0.8500000000000000E+01 {~~}
START H     watmix                    67 -0.1578190720615766E+05 {~~}
START M     watmix                    74 -0.1788651390200589E+01 {~~}
START P                          74  0.2220213082662809E+00 {~~}
START H     watmix                    74 -0.1571015793544858E+05 {~~}
START M     pump                      74  0.1788651390200589E+01 {~~}
START H     pump                      74 -0.1571015793544858E+05 {~~}
START M     pump                      58 -0.1788651390200589E+01 {~~}
START P                          58  0.1000000000000000E+03 {~~}
START H     pump                      58 -0.1569886781340417E+05 {~~}
START E     pump                     201  0.2019409249026819E+02 {~~}
START M     superheater               11  0.3852469736091420E+01 {~~}
START H     superheater               11 -0.6792544200929583E+03 {~~}
START M     superheater               42 -0.3852469736091420E+01 {~~}
START P                          42  0.1013000000000000E+01 {~~}
START H     superheater               42 -0.1028117733841838E+04 {~~}
START M     superheater               60  0.1788651390200589E+01 {~~}
START P                          60  0.1000000000000000E+03 {~~}
START H     superheater               60 -0.1324560652283701E+05 {~~}
START M     superheater               61 -0.1788651390200589E+01 {~~}
START H     superheater               61 -0.1249421060208165E+05 {~~}
START Q     superheater              341  0.0000000000000000E+00 {~~}
START ZA    superheater                1  0.1343985358250124E+04 {~~}
START M     evaporator                91  0.3852469736091420E+01 {~~}
START H     evaporator                91 -0.1028117733841838E+04 {~~}
```

```
START H     evaporator                43 -0.1639864508045476E+04 {~~}
START M     evaporator                59  0.1788651390200589E+01 {~~}
START P                            59  0.1000000000000000E+03 {~~}
START H     evaporator                59 -0.1456321147743175E+05 {~~}
START M     evaporator                60 -0.1788651390200589E+01 {~~}
START H     evaporator                60 -0.1324560652283701E+05 {~~}
START Q     evaporator               342  0.0000000000000000E+00 {~~}
START ZA    evaporator                 1  0.2356735933771066E+04 {~~}
START M     economizer                43  0.3852469736091420E+01 {~~}
START H     economizer                43 -0.1639864508045476E+04 {~~}
START M     economizer                44 -0.3852469736091420E+01 {~~}
START P                            44  0.1013000000000000E+01 {~~}
START H     economizer                44 -0.2167134914636148E+04 {~~}
START M     economizer                58  0.1788651390200589E+01 {~~}
START H     economizer                58 -0.1569886781340417E+05 {~~}
START M     economizer                59 -0.1788651390200589E+01 {~~}
START H     economizer                59 -0.1456321147743175E+05 {~~}
START Q     economizer               343  0.0000000000000000E+00 {~~}
START ZA    economizer                 1  0.2031293284127184E+04 {~~}
START M     dryer_heat                44  0.3852469736091420E+01 {~~}
START H     dryer_heat                44 -0.2167134914636148E+04 {~~}
START M     dryer_heat                45 -0.3852469736091420E+01 {~~}
START P                            45  0.1013000000000000E+01 {~~}
START H     dryer_heat                45 -0.2258343623238978E+04 {~~}
START Q     dryer_heat               302 -0.3513787895603837E+03 {~~}
START M     dh1                       45  0.3852469736091420E+01 {~~}
START H     dh1                       45 -0.2258343623238978E+04 {~~}
START M     dh1                       46 -0.3852469736091420E+01 {~~}
START P                            46  0.1013000000000000E+01 {~~}
START H     dh1                       46 -0.2258343623238978E+04 {~~}
START M     dh1                       82  0.0000000000000000E+00 {~~}
START P                            82  0.1013000000000000E+01 {~~}
START H     dh1                       82 -0.1580345468692628E+05 {~~}
START M     dh1                        5  0.0000000000000000E+00 {~~}
START H     dh1                        5 -0.1326473150905305E+05 {~~}
START Q     dh1                      323  0.0000000000000000E+00 {~~}
START ZA    dh1                        1  0.0000000000000000E+00 {~~}
START M     dh2                       66  0.5412120310472732E+00 {~~}
START H     dh2                       66 -0.1546683660761298E+05 {~~}
START M     dh2                       67 -0.5412120310472732E+00 {~~}
START H     dh2                       67 -0.1578190720615766E+05 {~~}
START M     dh2                       83  0.6716762191634354E-01 {~~}
START P                            83  0.1013000000000000E+01 {~~}
START H     dh2                       83 -0.1580345468692628E+05 {~~}
START M     dh2                        5 -0.6716762191634354E-01 {~~}
START H     dh2                        5 -0.1326473150905305E+05 {~~}
START Q     dh2                      324  0.0000000000000000E+00 {~~}
START ZA    dh2                        1  0.1705199985616474E+03 {~~}
C ~~~~~~~~~~~~~~~~~~~~~~~~~~~~~~~~~~~~~~~~~~~~~~~~~~~~~~~~~~~~~~~~~~~~~~~~~~~~~~~~
C ~~ End of generated initial guesses.
C ~~~~~~~~~~~~~~~~~~~~~~~~~~~~~~~~~~~~~~~~~~~~~~~~~~~~~~~~~~~~~~~~~~~~~~~~~~~~~~~~
```

```
c ########################################
c ############## Inputs ##################
c ########################################
c ########################################

solid sol C 0.4614 O 0.4072 H 0.057
+ N 0.0065 S 0.0016 ASH 0.0663
 + HHV 18244.0 CP 1.24
 addco ZA Dryer 2 0.02
addco m MIX 99 0.15 m MIX 98 0.85
addco ZA Gasifier 11 1.0
addco ZA Gasifier 19 0.101
addco za burner 1 1.7
addco t superheater 61 520
addco p 58 120
addco p 62 12

c #### Media ####
media 98 sol 99 STEAM-HF 1 resource 2 Dry
media 30 STANDARD_AIR 9 SynGas 8 Ash
media 11 FlueGas 40 STANDARD_AIR
media 60 STEAM-HF

c ########################################
c ---------- Steam Dryer ---------------
c ########################################
struc MIX sllqmx_1 98 99 1 0
addco t MIX 99 15

struc Dryer DRYER_04 1 27 2 4 301
addco t Dryer 1 15 p 1 1.013
addco t Dryer 2 115 t Dryer 4 115 t Dryer 27 200
addco q Dryer 301 0
addco p 27 1.013 p 2 1.013

struc splitter splitter2 3 4 26 5
addco p 5 1.013

struc DH heatsnk0 5 85 322 0
addco t DH 5 80
addco t DH 85 40

struc HEX heatsrc0 26 27 302 0

c ########################################
c ------------ Gasifier ----------------
c ########################################
struc Gasifier GASIFI_3_VENZIN 8 2 7 30 9 8 304 303 901 1 3 4 6 7 9 11 36
addco M Gasifier 7 0 T Gasifier 7 150
addco P 8 1.013 p 9 1.013
addco T Gasifier 9 630 T Gasifier 8 630 c Temperature of the syngas and biochar
addco ZA Gasifier 17 0.015 c Ratio of heat lost.
addco ZA Gasifier 18 0
addco ZA Gasifier 21 630 c Equilibrium temperature
addco ZA Gasifier 22 0.005
addco ZA Gasifier 28 1

struc air_preheater heatsrc0 29 30 395 0
addco t air_preheater 29 15

struc syngas_cooling heatsnk0 9 10 395 0
addco t syngas_cooling 10 630

struc biochar_cooling heatsnk0_1 8 69 399 0
addco t biochar_cooling 69 20

struc air_heater heatsrc0 40 41 399 0
addco t air_heater 40 15

c ########################################
c ---------- Steam Cycle ---------------
c ########################################
struc burner gasbur_3 41 10 11 305 1
addco q burner 305 0

struc turbine turbin_1 61 62 101 0.95

struc splitter2 splitter 62 63 64
addco m splitter2 64 -0.000001

struc dummy valve_01 64 65
addco p 65 12

struc heat1 heatsnk0 65 66 302 0
addco t heat1 66 120 c Outlet temperature

struc heat3 heatsrc0 63 90 390 0
```

```
struc condenser heatex_2 71 72 80 5 346 5 0 0
addco t condenser 80 40
addco x condenser 72 0
addco q condenser 346 0

struc watmix watmix_2 72 67 74

struc pump liqpum_1 74 58 201 0.9

c #### HRSG ####
struc superheater heatex_1 11 42 60 61 341 0 0
addco q superheater 341 0
addco x superheater 60 1 c Steam quality at superheater inlet

struc heat4 heatsnk0 42 91 390 0

struc evaporator heatex_1 91 43 59 60 342 0 0
addco q evaporator 342 0
addco x evaporator 59 0

struc economizer heatex_1 43 44 58 59 343 0 0
addco q economizer 343 0
addco t economizer 44 205

c #### For drying and district heat ####
struc dryer_heat heatsnk0 44 45 302 0

struc dh1 heatex_1 45 46 82 5 323 0 0
addco t dh1 82 40
addco t dh1 46 120
addco q dh1 323 0
addco t dh1 5 115

c media 83 STEAM-HF
struc dh2 heatex_1 66 67 83 5 324 0 0
addco t dh2 83 40
addco t dh2 67 45
addco q dh2 324 0
addco t dh2 5 115

c Reference conditions for exergy
xergy p 1.013 t 15


C ~~~~~~~~~~~~~~~~~~~~~~~~~~~~~~~~~~~~~~~~~~~~~~~~~~~~~~~~~~~~~~~~~~~~~~~~~~~~~~~~~~~~~~~~~~~~
C ~~ Start of list of generated initial guesses.
C ~~ The values are the results of the latest simulation.
C ~~~~~~~~~~~~~~~~~~~~~~~~~~~~~~~~~~~~~~~~~~~~~~~~~~~~~~~~~~~~~~~~~~~~~~~~~~~~~~~~~~~~~~~~~~~~
START M     MIX                        98  0.8500000000000000E+00 {~~}
START P                              98  0.1013000000000000E+01 {~~}
START H     MIX                        98 -0.5802601696582135E+04 {~~}
START M     MIX                        99  0.1500000000000000E+00 {~~}
START P                              99  0.1013000000000000E+01 {~~}
START H     MIX                        99 -0.1590799997036134E+05 {~~}
START M     MIX                         1 -0.1000000000000000E+01 {~~}
START P                               1  0.1013000000000000E+01 {~~}
START H     MIX                         1 -0.7318411437649015E+04 {~~}
START X_J   resource                   H2          0.4845000000000000E-01 {~~}
START X_J   resource                   O2          0.3461200000000000E+00 {~~}
START X_J   resource                   N2          0.5525000000000000E-02 {~~}
START X_J   resource                   CO          0.0000000000000000E+00 {~~}
START X_J   resource                   NO          0.0000000000000000E+00 {~~}
START X_J   resource                   CO2         0.0000000000000000E+00 {~~}
START X_J   resource                   H2O-L       0.1499999999999999E+00 {~~}
START X_J   resource                   NH3         0.0000000000000000E+00 {~~}
START X_J   resource                   H2S         0.0000000000000000E+00 {~~}
START X_J   resource                   SO2         0.0000000000000000E+00 {~~}
START X_J   resource                   CH4         0.0000000000000000E+00 {~~}
START X_J   resource                   C2H6        0.0000000000000000E+00 {~~}
START X_J   resource                   C3H8        0.0000000000000000E+00 {~~}
START X_J   resource                   C4H10-N     0.0000000000000000E+00 {~~}
START X_J   resource                   C4H10-I     0.0000000000000000E+00 {~~}
START X_J   resource                   C5H12       0.0000000000000000E+00 {~~}
START X_J   resource                   C6H14       0.0000000000000000E+00 {~~}
START X_J   resource                   C7H16       0.0000000000000000E+00 {~~}
START X_J   resource                   C8H18       0.0000000000000000E+00 {~~}
START X_J   resource                   C2H4        0.0000000000000000E+00 {~~}
START X_J   resource                   C3H6        0.0000000000000000E+00 {~~}
START X_J   resource                   C5H10       0.0000000000000000E+00 {~~}
START X_J   resource                   C6H12-1     0.0000000000000000E+00 {~~}
START X_J   resource                   C7H14       0.0000000000000000E+00 {~~}
START X_J   resource                   C2H2        0.0000000000000000E+00 {~~}
START X_J   resource                   C6H6        0.0000000000000000E+00 {~~}
START X_J   resource                   C6H12-C     0.0000000000000000E+00 {~~}
START X_J   resource                   C           0.3921900000000000E+00 {~~}
START X_J   resource                   S           0.1360000000000000E-02 {~~}
START X_J   resource                   NO2         0.0000000000000000E+00 {~~}
```

```
START X_J   resource                N2O          0.0000000000000000E+00 {~~}
START X_J   resource                NO3          0.0000000000000000E+00 {~~}
START X_J   resource                SO3          0.0000000000000000E+00 {~~}
START X_J   resource                AR           0.0000000000000000E+00 {~~}
START X_J   resource                ASH          0.5635500000000000E-01 {~~}
START X_J   resource                TAR          0.0000000000000000E+00 {~~}
START M     Dryer                     1  0.1000000000000000E+01 {~~}
START H     Dryer                     1 -0.7318411437649015E+04 {~~}
START M     Dryer                    27  0.2740357943744428E+01 {~~}
START P                           27  0.1013000000000000E+01 {~~}
START H     Dryer                    27 -0.1309566421515521E+05 {~~}
START M     Dryer                     2 -0.8673469387755103E+00 {~~}
START P                            2  0.1013000000000000E+01 {~~}
START H     Dryer                     2 -0.5874810951642395E+04 {~~}
START M     Dryer                     4 -0.2873011004968918E+01 {~~}
START P                            4  0.1013000000000000E+01 {~~}
START H     Dryer                     4 -0.1326473150905305E+05 {~~}
START Q     Dryer                   301  0.0000000000000000E+00 {~~}
START ZA    Dryer                     1  0.4633049018603111E+03 {~~}
START ZA    Dryer                     2  0.2000000000000000E-01 {~~}
START ZA    Dryer                     3  0.0000000000000000E+00 {~~}
START X_J   Dry                     H2           0.5585999999999999E-01 {~~}
START X_J   Dry                     O2           0.3990560000000000E+00 {~~}
START X_J   Dry                     N2           0.6370000000000000E-02 {~~}
START X_J   Dry                     CO           0.0000000000000000E+00 {~~}
START X_J   Dry                     NO           0.0000000000000000E+00 {~~}
START X_J   Dry                     CO2          0.0000000000000000E+00 {~~}
START X_J   Dry                     H2O-L        0.2000000000000000E-01 {~~}
START X_J   Dry                     NH3          0.0000000000000000E+00 {~~}
START X_J   Dry                     H2S          0.0000000000000000E+00 {~~}
START X_J   Dry                     SO2          0.0000000000000000E+00 {~~}
START X_J   Dry                     CH4          0.0000000000000000E+00 {~~}
START X_J   Dry                     C2H6         0.0000000000000000E+00 {~~}
START X_J   Dry                     C3H8         0.0000000000000000E+00 {~~}
START X_J   Dry                     C4H10-N      0.0000000000000000E+00 {~~}
START X_J   Dry                     C4H10-I      0.0000000000000000E+00 {~~}
START X_J   Dry                     C5H12        0.0000000000000000E+00 {~~}
START X_J   Dry                     C6H14        0.0000000000000000E+00 {~~}
START X_J   Dry                     C7H16        0.0000000000000000E+00 {~~}
START X_J   Dry                     C8H18        0.0000000000000000E+00 {~~}
START X_J   Dry                     C2H4         0.0000000000000000E+00 {~~}
START X_J   Dry                     C3H6         0.0000000000000000E+00 {~~}
START X_J   Dry                     C5H10        0.0000000000000000E+00 {~~}
START X_J   Dry                     C6H12-1      0.0000000000000000E+00 {~~}
START X_J   Dry                     C7H14        0.0000000000000000E+00 {~~}
START X_J   Dry                     C2H2         0.0000000000000000E+00 {~~}
START X_J   Dry                     C6H6         0.0000000000000000E+00 {~~}
START X_J   Dry                     C6H12-C      0.0000000000000000E+00 {~~}
START X_J   Dry                     C            0.4521720000000000E+00 {~~}
START X_J   Dry                     S            0.1568000000000000E-02 {~~}
START X_J   Dry                     NO2          0.0000000000000000E+00 {~~}
START X_J   Dry                     HCN          0.0000000000000000E+00 {~~}
START X_J   Dry                     COS          0.0000000000000000E+00 {~~}
START X_J   Dry                     N2O          0.0000000000000000E+00 {~~}
START X_J   Dry                     NO3          0.0000000000000000E+00 {~~}
START X_J   Dry                     SO3          0.0000000000000000E+00 {~~}
START X_J   Dry                     AR           0.0000000000000000E+00 {~~}
START X_J   Dry                     ASH          0.6497399999999999E-01 {~~}
START X_J   Dry                     TAR          0.0000000000000000E+00 {~~}
START M     splitter                  4  0.2873011004968918E+01 {~~}
START H     splitter                  4 -0.1326473150905305E+05 {~~}
START M     splitter                 26 -0.2740357943744428E+01 {~~}
START P                           26  0.1013000000000000E+01 {~~}
START H     splitter                 26 -0.1326473150905305E+05 {~~}
START M     splitter                  5 -0.1326530612244898E+00 {~~}
START P                            5  0.1013000000000000E+01 {~~}
START H     splitter                  5 -0.1326473150905304E+05 {~~}
START M     DH                        5  0.5244684761014108E+02 {~~}
START H     DH                        5 -0.1563608739894910E+05 {~~}
START M     DH                       85 -0.5244684761014108E+02 {~~}
START P                           85  0.1013000000000000E+01 {~~}
START H     DH                       85 -0.1580345468692628E+05 {~~}
START Q     DH                      322 -0.8777886647461781E+04 {~~}
START M     HEX                      26  0.2740357943744428E+01 {~~}
START H     HEX                      26 -0.1326473150905305E+05 {~~}
START M     HEX                      27 -0.2740357943744428E+01 {~~}
START H     HEX                      27 -0.1309566421515521E+05 {~~}
START Q     HEX                     302  0.4633049018603124E+03 {~~}
START M     Gasifier                  2  0.8673469387755103E+00 {~~}
START H     Gasifier                  2 -0.5874810951642395E+04 {~~}
START M     Gasifier                  7  0.0000000000000000E+00 {~~}
START P                            7  0.1018000000000000E+01 {~~}
START H     Gasifier                  7 -0.1319461892147020E+05 {~~}
START M     Gasifier                 30  0.6984645375474748E+00 {~~}
START P                           30  0.1018000000000000E+01 {~~}
START H     Gasifier                 30  0.4977350706477748E+03 {~~}
START M     Gasifier                  9 -0.1509456476322985E+01 {~~}
START P                            9  0.1013000000000000E+01 {~~}
```

```
START P                              8  0.10130000000000000E+01 {~~}
START H     Gasifier                 8 -0.11775263157894740E+05 {~~}
START Q     Gasifier               304 -0.43349659471804690E+03 {~~}
START Q     Gasifier               303  0.00000000000000000E+00 {~~}
START ZC                           901  0.14449886490601560E+05 {~~}
START ZA    Gasifier                 1  0.67568546996349210E+05 {~~}
START ZA    Gasifier                 2 -0.95620209323654530E+04 {~~}
START ZA    Gasifier                 3  0.89642170264382410E+05 {~~}
START ZA    Gasifier                 4  0.30572454401193130E+06 {~~}
START ZA    Gasifier                 5  0.12163304098257930E+06 {~~}
START ZA    Gasifier                 6  0.17652905563477160E+06 {~~}
START ZA    Gasifier                 7 -0.16591414995523690E+05 {~~}
START ZA    Gasifier                 8  0.91111509996330590E+00 {~~}
START ZA    Gasifier                 9  0.91763638796934180E+00 {~~}
START ZA    Gasifier                10  0.91111509996330590E+00 {~~}
START ZA    Gasifier                11  0.10000000000000000E+01 {~~}
START ZA    Gasifier                12  0.64973999999999990E-01 {~~}
START ZA    Gasifier                13  0.72621260433792340E-05 {~~}
START ZA    Gasifier                14  0.79616340658619620E-02 {~~}
START ZA    Gasifier                15  0.14407516419172990E+05 {~~}
START ZA    Gasifier                16  0.15507400000000000E+05 {~~}
START ZA    Gasifier                17  0.30000000000000000E-01 {~~}
START ZA    Gasifier                18  0.00000000000000000E+00 {~~}
START ZA    Gasifier                19  0.20000000000000000E-01 {~~}
START ZA    Gasifier                20  0.10130000000000000E+01 {~~}
START ZA    Gasifier                21  0.57000000000000000E+03 {~~}
START ZA    Gasifier                22  0.50000000000000000E-02 {~~}
START ZA    Gasifier                23 -0.69488976777116350E-01 {~~}
START ZA    Gasifier                24  0.36848711038322070E-03 {~~}
START ZA    Gasifier                25  0.14837878570672990E+00 {~~}
START ZA    Gasifier                26  0.00000000000000000E+00 {~~}
START ZA    Gasifier                27  0.00000000000000000E+00 {~~}
START ZA    Gasifier                28  0.10000000000000000E+01 {~~}
START ZA    Gasifier                29  0.18479707867074750E+05 {~~}
START ZA    Gasifier                30  0.23595185347771270E-02 {~~}
START ZA    Gasifier                31  0.00000000000000000E+00 {~~}
START ZA    Gasifier                32  0.32338279880961970E+00 {~~}
START ZA    Gasifier                33  0.11346979544869210E+00 {~~}
START ZA    Gasifier                34  0.27258348812352070E+00 {~~}
START ZA    Gasifier                35  0.13617553607470840E+00 {~~}
START ZA    Gasifier                36  0.14985368067431770E+00 {~~}
START ZA    Gasifier                37  0.17492064413027600E-01 {~~}
START ZA    Gasifier                38  0.27407186811784020E-01 {~~}
START ZA    Gasifier                39  0.26826042330796680E+00 {~~}
START ZA    Gasifier                40  0.91111509996330590E+00 {~~}
START ZA    Gasifier                41  0.00000000000000000E+00 {~~}
START ZA    Gasifier                42  0.15620176400457400E-05 {~~}
START ZA    Gasifier                43  0.39873211160130010E-05 {~~}
START Y_J   SynGas                  H2          0.11148497447777050E+00 {~~}
START Y_J   SynGas                  O2          0.00000000000000000E+00 {~~}
START Y_J   SynGas                  N2          0.31772616606277670E+00 {~~}
START Y_J   SynGas                  CO          0.26781544019133630E+00 {~~}
START Y_J   SynGas                  NO          0.00000000000000000E+00 {~~}
START Y_J   SynGas                  CO2         0.13379354482621100E+00 {~~}
START Y_J   SynGas                  H2O-G       0.17492064413027600E-01 {~~}
START Y_J   SynGas                  NH3         0.00000000000000000E+00 {~~}
START Y_J   SynGas                  H2S         0.71286671659166950E-03 {~~}
START Y_J   SynGas                  SO2         0.00000000000000000E+00 {~~}
START Y_J   SynGas                  CH4         0.14723243043943330E+00 {~~}
START Y_J   SynGas                  NO2         0.00000000000000000E+00 {~~}
START Y_J   SynGas                  HCN         0.00000000000000000E+00 {~~}
START Y_J   SynGas                  COS         0.00000000000000000E+00 {~~}
START Y_J   SynGas                  AR          0.37425128728529150E-02 {~~}
START X_J   Ash                     C           0.00000000000000000E+00 {~~}
START X_J   Ash                     ASH         0.10000000000000000E+01 {~~}
START M     air_preheater            29  0.69846453754747480E+00 {~~}
START P                             29  0.10180000000000000E+01 {~~}
START H     air_preheater           29 -0.98834527668785900E+02 {~~}
START M     air_preheater           30 -0.69846453754747480E+00 {~~}
START H     air_preheater           30  0.49773507064777480E+03 {~~}
START Q     air_preheater          395  0.41668270860305940E+03 {~~}
START M     syngas_cooling           9  0.15094564763229850E+01 {~~}
START H     syngas_cooling           9 -0.29929651561141940E+04 {~~}
START M     syngas_cooling          10 -0.15094564763229850E+01 {~~}
START P                             10  0.10130000000000000E+01 {~~}
START H     syngas_cooling          10 -0.32690133331494760E+04 {~~}
START Q     syngas_cooling         395 -0.41668270860305940E+03 {~~}
START M     biochar_cooling          8  0.56355000000000000E-01 {~~}
START H     biochar_cooling          8 -0.11775263157894740E+05 {~~}
START M     biochar_cooling         69 -0.56355000000000000E-01 {~~}
START P                             69  0.10130000000000000E+01 {~~}
START H     biochar_cooling         69 -0.12385263157894740E+05 {~~}
START Q     biochar_cooling        399 -0.34376549999999950E+02 {~~}
START M     air_heater              40  0.68250605101753990E+01 {~~}
START P                             40  0.10130000000000000E+01 {~~}
START H     air_heater              40 -0.98834527668785900E+02 {~~}
START M     air_heater              41 -0.68250605101753990E+01 {~~}
START P                             41  0.10130000000000000E+01 {~~}
```

```
START M     burner                    41  0.6825060510175399E+01 {~~}
START H     burner                    41 -0.9379771518210562E+02 {~~}
START M     burner                    10  0.1509456476322985E+01 {~~}
START H     burner                    10 -0.3269013333149476E+04 {~~}
START M     burner                    11 -0.8334516986498384E+01 {~~}
START P                            11  0.1013000000000000E+01 {~~}
START H     burner                    11 -0.6688580079413597E+03 {~~}
START Q     burner                   305  0.0000000000000000E+00 {~~}
START ZA    burner                     1  0.1700000000000000E+01 {~~}
START Y_J   FlueGas                   O2          0.7097789182107306E-01 {~~}
START Y_J   FlueGas                   N2          0.7084657593190736E+00 {~~}
START Y_J   FlueGas                   NO          0.0000000000000000E+00 {~~}
START Y_J   FlueGas                   CO2         0.1149496691977463E+00 {~~}
START Y_J   FlueGas                   H2O-G       0.9703292013857254E-01 {~~}
START Y_J   FlueGas                   SO2         0.1489795279019163E-03 {~~}
START Y_J   FlueGas                   NO2         0.0000000000000000E+00 {~~}
START Y_J   FlueGas                   AR          0.8424779995632582E-02 {~~}
START M     turbine                   61  0.3976160519166992E+01 {~~}
START P                            61  0.1000000000000000E+03 {~~}
START H     turbine                   61 -0.1249421060208165E+05 {~~}
START M     turbine                   62 -0.3976160519166992E+01 {~~}
START P                            62  0.8500000000000000E+01 {~~}
START H     turbine                   62 -0.1312754540714483E+05 {~~}
START W     turbine                  101 -0.2518240847306546E+04 {~~}
START M     splitter2                 62  0.3976160519166992E+01 {~~}
START H     splitter2                 62 -0.1312754540714483E+05 {~~}
START M     splitter2                 63 -0.3976159519166992E+01 {~~}
START P                            63  0.8500000000000000E+01 {~~}
START H     splitter2                 63 -0.1312754540714483E+05 {~~}
START M     splitter2                 64 -0.1000000000000000E-05 {~~}
START P                            64  0.8500000000000000E+01 {~~}
START H     splitter2                 64 -0.1312754540714483E+05 {~~}
START M     dummy                     64  0.1000000000000000E-05 {~~}
START H     dummy                     64 -0.1312754540714483E+05 {~~}
START M     dummy                     65 -0.1000000000000000E-05 {~~}
START P                            65  0.8500000000000000E+01 {~~}
START H     dummy                     65 -0.1312754540714483E+05 {~~}
START M     heat1                     65  0.1000000000000000E-05 {~~}
START H     heat1                     65 -0.1312754540714483E+05 {~~}
START M     heat1                     66 -0.1000000000000000E-05 {~~}
START P                            66  0.8500000000000000E+01 {~~}
START H     heat1                     66 -0.1546683660761298E+05 {~~}
START Q     heat1                    302 -0.2339291200468147E-02 {~~}
START M     turbin2                   90  0.3976159519166992E+01 {~~}
START H     turbin2                   90 -0.1312754540714483E+05 {~~}
START M     turbin2                   71 -0.3976159519166992E+01 {~~}
START P                            71  0.5200355717155932E+00 {~~}
START H     turbin2                   71 -0.1357805599950551E+05 {~~}
START W     turbin2                  102 -0.1791301980300490E+04 {~~}
START M     condenser                 71  0.3976159519166992E+01 {~~}
START H     condenser                 71 -0.1357805599950551E+05 {~~}
START M     condenser                 72 -0.3976159519166992E+01 {~~}
START P                            72  0.5200355717155932E+00 {~~}
START H     condenser                 72 -0.1562648089111446E+05 {~~}
START M     condenser                 80  0.5219750080427055E+02 {~~}
START P                            80  0.1013000000000000E+01 {~~}
START H     condenser                 80 -0.1580345468692628E+05 {~~}
START M     condenser                  5 -0.5219750080427055E+02 {~~}
START H     condenser                  5 -0.1564741533625677E+05 {~~}
START Q     condenser                346  0.0000000000000000E+00 {~~}
START ZA    condenser                  1  0.8144864132069551E+04 {~~}
START M     watmix                    72  0.3976159519166992E+01 {~~}
START H     watmix                    72 -0.1562648089111446E+05 {~~}
START M     watmix                    67  0.1000000000000000E-05 {~~}
START P                            67  0.8500000000000000E+01 {~~}
START H     watmix                    67 -0.1578190720615766E+05 {~~}
START M     watmix                    74 -0.3976160519166992E+01 {~~}
START P                            74  0.5200353785959876E+00 {~~}
START H     watmix                    74 -0.1562648093020401E+05 {~~}
START M     pump                      74  0.3976160519166992E+01 {~~}
START H     pump                      74 -0.1562648093020401E+05 {~~}
START M     pump                      58 -0.3976160519166992E+01 {~~}
START P                            58  0.1000000000000000E+03 {~~}
START H     pump                      58 -0.1561508966980987E+05 {~~}
START E     pump                     201  0.4529347984271815E+02 {~~}
START M     superheater               11  0.8334516986498384E+01 {~~}
START H     superheater               11 -0.6688580079413597E+03 {~~}
START M     superheater               42 -0.8334516986498384E+01 {~~}
START P                            42  0.1013000000000000E+01 {~~}
START H     superheater               42 -0.1027327586827635E+04 {~~}
START M     superheater               60  0.3976160519166992E+01 {~~}
START P                            60  0.1000000000000000E+03 {~~}
START H     superheater               60 -0.1324560652283701E+05 {~~}
START M     superheater               61 -0.3976160519166992E+01 {~~}
START H     superheater               61 -0.1249421060208165E+05 {~~}
START Q     superheater              341  0.0000000000000000E+00 {~~}
START ZA    superheater                1  0.2987607794370586E+04 {~~}
START M     evaporator                91  0.8334516986498384E+01 {~~}
```

```
START P                          43  0.10130000000000000E+01 {~~}
START H     evaporator            43 -0.16559193587090090E+04 {~~}
START M     evaporator            59  0.39761605191669920E+01 {~~}
START P                          59  0.10000000000000000E+03 {~~}
START H     evaporator            59 -0.14563211477431750E+05 {~~}
START M     evaporator            60 -0.39761605191669920E+01 {~~}
START H     evaporator            60 -0.13245606522837010E+05 {~~}
START Q     evaporator           342  0.00000000000000000E+00 {~~}
START ZA    evaporator             1  0.52390088003184260E+04 {~~}
START M     economizer            43  0.83345169864983840E+01 {~~}
START H     economizer            43 -0.16559193587090090E+04 {~~}
START M     economizer            44 -0.83345169864983840E+01 {~~}
START P                          44  0.10130000000000000E+01 {~~}
START H     economizer            44 -0.21577404655928330E+04 {~~}
START M     economizer            58  0.39761605191669920E+01 {~~}
START H     economizer            58 -0.15615089669809870E+05 {~~}
START M     economizer            59 -0.39761605191669920E+01 {~~}
START H     economizer            59 -0.14563211477431750E+05 {~~}
START Q     economizer           343  0.00000000000000000E+00 {~~}
START ZA    economizer             1  0.41824365395066490E+04 {~~}
START M     dryer_heat            44  0.83345169864983840E+01 {~~}
START H     dryer_heat            44 -0.21577404655928330E+04 {~~}
START M     dryer_heat            45 -0.83345169864983840E+01 {~~}
START P                          45  0.10130000000000000E+01 {~~}
START H     dryer_heat            45 -0.22133288774131750E+04 {~~}
START Q     dryer_heat           302 -0.46330256256911190E+03 {~~}
START M     dh1                   45  0.83345169864983840E+01 {~~}
START H     dh1                   45 -0.22133288774131750E+04 {~~}
START M     dh1                   46 -0.83345169864983840E+01 {~~}
START P                          46  0.10130000000000000E+01 {~~}
START H     dh1                   46 -0.22488741645192010E+04 {~~}
START M     dh1                   82  0.11669362054011500E+00 {~~}
START P                          82  0.10130000000000000E+01 {~~}
START H     dh1                   82 -0.15803454686926280E+05 {~~}
START M     dh1                    5 -0.11669362054011500E+00 {~~}
START H     dh1                    5 -0.13264731509053050E+05 {~~}
START Q     dh1                  323  0.00000000000000000E+00 {~~}
START ZA    dh1                    1  0.29625279917513600E+03 {~~}
START M     dh2                   66  0.10000000000000000E-05 {~~}
START H     dh2                   66 -0.15466836607612980E+05 {~~}
START M     dh2                   67 -0.10000000000000000E-05 {~~}
START H     dh2                   67 -0.15781907206157660E+05 {~~}
START M     dh2                   83  0.12410592903186330E-06 {~~}
START P                          83  0.10130000000000000E+01 {~~}
START H     dh2                   83 -0.15803454686926280E+05 {~~}
START M     dh2                    5 -0.12410592903186330E-06 {~~}
START H     dh2                    5 -0.13264731509053050E+05 {~~}
START Q     dh2                  324  0.00000000000000000E+00 {~~}
START ZA    dh2                    1  0.31507059854468210E-03 {~~}
C ~~~~~~~~~~~~~~~~~~~~~~~~~~~~~~~~~~~~~~~~~~~~~~~~~~~~~~~~~~~~~~~~~~~~~~~~~~~~~~~~
C ~~ End of generated initial guesses.
C ~~~~~~~~~~~~~~~~~~~~~~~~~~~~~~~~~~~~~~~~~~~~~~~~~~~~~~~~~~~~~~~~~~~~~~~~~~~~~~~~
```

```
c ########################################
c ############### Inputs #################
c ########################################
c ########################################

fluid biogas co2 0.38 ch4 0.62
addco m air_mix 5 1.0

c #### Media ####
media 5 biogas
media 16 STANDARD_AIR 17 EngineFuel 21 FlueGas 99 STEAM-HF

struc air_mix mixer_01 5 16 17
addco p 5 1.013
addco t air_mix 5 15
addco t air_mix 16 15

c ########################################
c ----------- Biogas engine -------------
c ########################################
struc GasEngine engine_1_za 17 21 511 311 312
addco za GasEngine 3 0.40
addco za GasEngine 5 0.05
addco za GasEngine 1 1
addco za GasEngine 2 2
c addco za GasEngine 4 0.52
addco t GasEngine 21 120

c #### district heat ####
struc dh heatsrc0 99 98 312 0
addco p 99 2.013
start m dh 99 1
addco t dh 99 40
addco t dh 98 80

c Reference conditions for exergy
xergy t 15 p 1.013

C ~~~~~~~~~~~~~~~~~~~~~~~~~~~~~~~~~~~~~~~~~~~~~~~~~~~~~~~~~~~~~~~~~~~~~~~~~~~~~~~~~~~~~~~~~~~~~~~~~~
C ~~ Start of list of generated initial guesses.
C ~~ The values are the results of the latest simulation.
C ~~~~~~~~~~~~~~~~~~~~~~~~~~~~~~~~~~~~~~~~~~~~~~~~~~~~~~~~~~~~~~~~~~~~~~~~~~~~~~~~~~~~~~~~~~~~~~~~~~
START M     air_mix                 5  0.1000000000000000E+01 {~~}
START P                          5  0.1013000000000000E+01 {~~}
START H     air_mix                 5 -0.7360960946381470E+04 {~~}
START M     air_mix                16  0.1293019000842311E+02 {~~}
START P                         16  0.1013000000000000E+01 {~~}
START H     air_mix                16 -0.9883452766878590E+02 {~~}
START M     air_mix                17 -0.1393019000842311E+02 {~~}
START P                         17  0.1013000000000000E+01 {~~}
START H     air_mix                17 -0.6201573821540101E+03 {~~}
START Y_J   EngineFuel             H2          0.0000000000000000E+00 {~~}
START Y_J   EngineFuel             O2          0.1914790697674419E+00 {~~}
START Y_J   EngineFuel             N2          0.7132249302325582E+00 {~~}
START Y_J   EngineFuel             CO          0.0000000000000000E+00 {~~}
START Y_J   EngineFuel             NO          0.0000000000000000E+00 {~~}
START Y_J   EngineFuel             CO2         0.2961637209302325E-01 {~~}
START Y_J   EngineFuel             H2O-G       0.9320186046511629E-02 {~~}
START Y_J   EngineFuel             NH3         0.0000000000000000E+00 {~~}
START Y_J   EngineFuel             H2S         0.0000000000000000E+00 {~~}
START Y_J   EngineFuel             SO2         0.0000000000000000E+00 {~~}
START Y_J   EngineFuel             CH4         0.4786976744186047E-01 {~~}
START Y_J   EngineFuel             C2H6        0.0000000000000000E+00 {~~}
START Y_J   EngineFuel             C3H8        0.0000000000000000E+00 {~~}
START Y_J   EngineFuel             C4H10-N     0.0000000000000000E+00 {~~}
START Y_J   EngineFuel             C4H10-I     0.0000000000000000E+00 {~~}
START Y_J   EngineFuel             C5H12       0.0000000000000000E+00 {~~}
START Y_J   EngineFuel             C6H14       0.0000000000000000E+00 {~~}
START Y_J   EngineFuel             C7H16       0.0000000000000000E+00 {~~}
START Y_J   EngineFuel             C8H18       0.0000000000000000E+00 {~~}
START Y_J   EngineFuel             C2H4        0.0000000000000000E+00 {~~}
START Y_J   EngineFuel             C3H6        0.0000000000000000E+00 {~~}
START Y_J   EngineFuel             C5H10       0.0000000000000000E+00 {~~}
START Y_J   EngineFuel             C6H12-1     0.0000000000000000E+00 {~~}
START Y_J   EngineFuel             C7H14       0.0000000000000000E+00 {~~}
START Y_J   EngineFuel             C2H2        0.0000000000000000E+00 {~~}
START Y_J   EngineFuel             C6H6        0.0000000000000000E+00 {~~}
START Y_J   EngineFuel             C6H12-C     0.0000000000000000E+00 {~~}
START Y_J   EngineFuel             C           0.0000000000000000E+00 {~~}
START Y_J   EngineFuel             S           0.0000000000000000E+00 {~~}
START Y_J   EngineFuel             NO2         0.0000000000000000E+00 {~~}
START Y_J   EngineFuel             HCN         0.0000000000000000E+00 {~~}
START Y_J   EngineFuel             COS         0.0000000000000000E+00 {~~}
START Y_J   EngineFuel             N2O         0.0000000000000000E+00 {~~}
START Y_J   EngineFuel             NO3         0.0000000000000000E+00 {~~}
START Y_J   EngineFuel             SO3         0.0000000000000000E+00 {~~}
START Y_J   EngineFuel             AR          0.8489674418604650E-02 {~~}
START Y_J   EngineFuel             ASH         0.0000000000000000E+00 {~~}
```

```
START Y_J   EngineFuel              C2H5OH      0.0000000000000000E+00 {~~}
START Y_J   EngineFuel              C2H5OH-L    0.0000000000000000E+00 {~~}
START Y_J   EngineFuel              CH3OCH3     0.0000000000000000E+00 {~~}
START Y_J   EngineFuel              CH3OCH3-L   0.0000000000000000E+00 {~~}
START M     GasEngine                17  0.1393019000842311E+02 {~~}
START H     GasEngine                17 -0.6201573821540101E+03 {~~}
START M     GasEngine                21 -0.1393019000842311E+02 {~~}
START P                          21  0.1013000000000000E+01 {~~}
START H     GasEngine                21 -0.1538565816083909E+04 {~~}
START E     GasEngine               511 -0.7087312329821085E+04 {~~}
START Q     GasEngine               311 -0.9325410960290901E+03 {~~}
START Q     GasEngine               312 -0.4773750564131617E+04 {~~}
START ZA    GasEngine                 1  0.1000000000000000E+01 {~~}
START ZA    GasEngine                 2  0.2000000000000000E+01 {~~}
START ZA    GasEngine                 3  0.3800000000000000E+00 {~~}
START ZA    GasEngine                 4  0.2559538976061760E+00 {~~}
START ZA    GasEngine                 5  0.5000000000000000E-01 {~~}
START Y_J   FlueGas                 O2          0.9573953488372094E-01 {~~}
START Y_J   FlueGas                 N2          0.7132249302325582E+00 {~~}
START Y_J   FlueGas                 NO          0.0000000000000000E+00 {~~}
START Y_J   FlueGas                 CO2         0.7748613953488373E-01 {~~}
START Y_J   FlueGas                 H2O-G       0.1050597209302326E+00 {~~}
START Y_J   FlueGas                 SO2         0.0000000000000000E+00 {~~}
START Y_J   FlueGas                 NO2         0.0000000000000000E+00 {~~}
START Y_J   FlueGas                 AR          0.8489674418604650E-02 {~~}

C ~~~~~~~~~~~~~~~~~~~~~~~~~~~~~~~~~~~~~~~~~~~~~~~~~~~~~~~~~~~~~~~~~~~~~~~~~~~~~~~~~~~~~~~~~~~~~~~~
C ~~ End of generated initial guesses.
C ~~~~~~~~~~~~~~~~~~~~~~~~~~~~~~~~~~~~~~~~~~~~~~~~~~~~~~~~~~~~~~~~~~~~~~~~~~~~~~~~~~~~~~~~~~~~~~~~
```

C. Python Code

Python programming language was used to model the integrated bioenergy and agricultural system concepts and to evaluate them based on climate change impact, non-renewable resource utilization and economic feasibility.

Here it is spit into four parts, first the code for the bioenergy system models, where the calculation of all components are given in relation to the bioenergy system are given. Then the agricultural system models are presented showing the computational code for the agricultural system part. After that the code to bridge from Python to DNA and C-TOOL is presented and finally the utility functions are give that facilitate the other models.

I. Bioenergy System Models

The bioenergy system models is split into four classes: thermal power plant, anaerobic digestion, biogas engine, storage units and separation processes.

```
from DatabaseSearch import *
from DNA import *
from copy import deepcopy
from utilities import lci_write, lci_write_uncert, eng_str, calcLCA_tot, calcLCA_uniProc

class ThermalPowerPlant:
    """

    A class that builds thermal power plant LCI dataset based on DNA simulation.
        0) Function that returns the energy generation and biochar production
        1) To establish the unit process of this component,
        2) To establish the chemical composition at the outlet,
        3) Extract the LCI data to use in LCIA.
        4) Update LCI data and assign uncertainties.
        5) Write LCI data to LaTex.
        6) Returns economics of the thermal plant

    """
    def __init__(self, input1, input2, input3, input4, input5, input6, input7, input8, input9):
        self.input1 = input1 #String statement, resource type (e.g. 'rawManure').
        self.input2 = deepcopy(input2) #Pandas dataframe, mass, DM, C, N, K, P info.
        self.input3 = input3 #Carbon conversion factor
        self.input4 = input4 #Steam input factor
        self.input5 = input5 #combustion temp
        self.input6 = input6 #life steam temp
        self.input7 = input7 #life steam pressure
        self.input8 = input8 #life steam pressure
        self.input9 = input9 #life steam pressure

    def energy_generation(self):
        """

        A function that feeds inputs to and runs a thermal power plant DNA model and
        returns the results of the simulation.

        ** This function returns the energy generation and biochar production, along with emissions
            based on simulation of the DNA model

        """
        mass = deepcopy(self.input2[0])
        ult_inp = deepcopy(self.input2[1][0])
        maj_inp = deepcopy(self.input2[1][1])
        hm_inp = deepcopy(self.input2[1][2])

        ###################################################
        ################## Write to DNA ###################
        ###################################################

        dna_input = self.input2

        sec_year = 365 * 24 * 3600
        hour_year = 365 * 24

        DNA_script = DNA_input_thermo(dna_input, self.input4)

        feedstock = DNA_script

        parameter1 = ''
        addco = '\naddco ZA Gasifier 11 '
        b = addco + str(self.input3)
        parameter1 += b

        parameter2 = ''
        addco = '\naddco ZA Gasifier 19 '
        b = addco + str(self.input9)
        parameter2 += b

        parameter3 = ''
        addco = '\naddco za burner 1 '
        b = addco + str(self.input5)
        parameter3 += b

        parameter4 = ''
        addco = '\naddco t superheater 61 '
        b = addco + str(self.input6)
        parameter4 += b

        parameter5 = ''
        addco = '\naddco p 58 '
        b = addco + str(self.input7)
        parameter5 += b

        parameter6 = ''
        addco = '\naddco p 62 '
        b = addco + str(self.input8)
        parameter5 += b
```

```
##################################################
################### Run DNA ######################
##################################################

MOI = ult_inp.M / mass
if MOI <= 0.189 and self.input3 > 0.69:
    'first'
    dna = pyroneer_dryer_str(feedstock, parameter1, parameter2, parameter3, parameter4, parameter5, parameter6)
elif MOI <= 0.20 and self.input3 > 0.79:
    'first'
    dna = pyroneer_dryer_str(feedstock, parameter1, parameter2, parameter3, parameter4, parameter5, parameter6)
elif MOI <= 0.211 and self.input3 > 0.89:
    'first'
    dna = pyroneer_dryer_str(feedstock, parameter1, parameter2, parameter3, parameter4, parameter5, parameter6)
elif MOI <= 0.23 and self.input3 > 0.98:
    'first'
    dna = pyroneer_dryer_str(feedstock, parameter1, parameter2, parameter3, parameter4, parameter5, parameter6)
else:
    dna = pyroneer_dryer_man(feedstock, parameter1, parameter2, parameter3, parameter4, parameter5, parameter6)

##################################################
################### PostProcessing ###############
##################################################

el_rec = 83 *(mass-ult_inp.M) * 1e-3

Q_rh = abs(float(dna['Q heat3 390'][0]))
Q_hr = abs(float(dna['M superheater 11'][0]))*\
        abs(float(dna['H superheater 11'][0])-float(dna['H economizer 44'][0]))
Q = abs(float(dna['Q DH 322'][0]))*(hour_year/float(sec_year))*mass * 3.6 # MJ
Q_hrsg = (Q_rh+Q_hr)*(hour_year/float(sec_year))*mass * 3.6

EL = (abs(float(dna['W turbin2 102']))+abs(float(dna['W turbine 101']))  - abs(float(dna['E pump 201'])))*\
     hour_year/float(sec_year)*mass - el_rec
EL_mj = EL * 3.6
Q_mj = Q
m3_syngas = abs(float(dna['M Gasifier 9'][0])*mass)
MOLMA = (abs(float(dna['MOLMA FlueGas '])))

mass_to_steam = abs(float(dna['M dummy 64'][0]))*mass

Nitrogen = abs(float(dna['Y_J FlueGas N2'])) * (14/MOLMA)*abs(float(dna['M Gasifier 9'][0]))*mass
CarbonDioxide = abs(float(dna['Y_J FlueGas CO2'])) * (44/MOLMA)*abs(float(dna['M Gasifier 9'][0]))*mass
SulfurDioxide = abs(float(dna['Y_J FlueGas SO2'])) * (64/MOLMA)*abs(float(dna['M Gasifier 9'][0]))*mass

lhv_syngas = (abs(float(dna['LHV SynGas ']))) * abs(float(dna['M Gasifier 9']))
lhv_resource = (abs(float(dna['FUEL_CONSU MPTION_HHV ']))) * abs(float(dna['M Dryer 1']))
lhv_ash = (float(dna['LHV Ash '])* abs(float(dna['M Gasifier 8'])))

mj_fuel = lhv_resource* (hour_year/float(sec_year))*mass * 3.6
mj_syngas = lhv_syngas* (hour_year/float(sec_year))*mass * 3.6
mj_ash = lhv_ash* (hour_year/float(sec_year))*mass * 3.6

el_eff = EL_mj / mj_fuel
q_eff = Q_mj / mj_fuel

outData = pd.DataFrame([EL, Q, mj_syngas, mj_fuel, mj_ash, Q_hrsg, el_eff, q_eff, m3_syngas,
                        Nitrogen, CarbonDioxide,
                        SulfurDioxide],
                       index = ['EL', 'Q', 'mj_syngas', 'mj_fuel', 'mj_ash', 'mj_hrsg', 'el_eff',
                                'q_eff', 'm3', 'N2', 'CO2', 'SO2'],
                       columns = [self.input1]).T

syngas_flow = abs(float(dna['M Gasifier 9'][0]))
ash_flow = abs(float(dna['M Gasifier 8'][0]))
air_flow = abs(float(dna['M Gasifier 30'][0]))
bio_flow = abs(float(dna['M Gasifier 2'][0]))

mass_bal = pd.DataFrame([bio_flow, air_flow, syngas_flow, ash_flow],
                        ['Biomass input', 'Air input', 'Syngas output', 'Biochar output'])
eff = 0.95

inp_ult = ult_inp
inp_ult.C = (1-self.input3)*ult_inp.C
inp_ult.O = 0
inp_ult.H = 0
inp_ult.N = 0
inp_ult.S = 0
inp_ult.A = inp_ult.A*eff

inp_ult.M = (inp_ult.C+inp_ult.A*eff)*1.3
mass_biochar = inp_ult.C+inp_ult.A*eff+inp_ult.M
out_ult = inp_ult
out_biochar = mass_biochar, [out_ult, maj_inp*eff, hm_inp]

return outData, out_biochar, mass_bal, mass_to_steam
```

```
def unit_process(self):
    """

    A function that make the LCI unit process for the thermal power plant class.

    """
    data_pp = self.energy_generation()[0]
    EL = data_pp.EL[0]

    unit1 = 1.1529E-11
    unit1_new = unit1*((np.divide(500, 100))**(1-0.7))
    unit2 = 5.8988E-13
    unit2_new = unit2*((np.divide(500, 100))**(1-0.7))

    dry_ratio = (self.input2[1][0].M / EL) * 0.7
    gasifi_ratio = (self.input2[0]/ 1.1122) / EL
    pp1_ratio = EL / EL
    pp2_ratio = data_pp.Q[0] / EL

    steam_dryer = ['drying of feed grain',
                   'litre', 'CH']
    activity_dryer = technosphereData(steam_dryer)
    lci_dryer = {}
    for exc in activity_dryer.technosphere():
        lci_dryer.update({exc.input:exc.amount * dry_ratio})

    LCI_dryer = pd.Series(lci_dryer)

    rem_values = []
    rem_keys = []
    for i in np.arange(len(lci_dryer)):
        if 'heat' in LCI_dryer.index[i]['name']:
            rem_values.append(LCI_dryer.values[i])
            rem_keys.append((LCI_dryer.index[i]['database'], LCI_dryer.index[i]['code']))
        elif 'electricity' in LCI_dryer.index[i]['name']:
            rem_values.append(LCI_dryer.values[i])
            rem_keys.append((LCI_dryer.index[i]['database'], LCI_dryer.index[i]['code']))
        elif 'building' in LCI_dryer.index[i]['name']:
            rem_values.append(LCI_dryer.values[i])
            rem_keys.append((LCI_dryer.index[i]['database'], LCI_dryer.index[i]['code']))
    for i in np.arange(len(rem_keys)):
        lci_dryer.pop(rem_keys[i])

    LCIdryer = pd.Series(lci_dryer)

    gasifier = ['synthetic gas production, from wood, at fluidized bed gasifier',
                'cubic meter', 'CH']
    activity = technosphereData(gasifier)

    lci1 = {}
    for exc in activity.technosphere():
        lci1.update({exc.input:exc.amount*gasifi_ratio})

    LCI_1 = pd.Series(lci1)

    rem_values = []
    rem_keys = []
    for i in np.arange(len(lci1)):
        if 'wood' in LCI_1.index[i]['name']:
            rem_values.append(LCI_1.values[i])
            rem_keys.append((LCI_1.index[i]['database'], LCI_1.index[i]['code']))
        elif 'zeolite' in LCI_1.index[i]['name']:
            rem_values.append(LCI_1.values[i])
            rem_keys.append((LCI_1.index[i]['database'], LCI_1.index[i]['code']))
        elif 'dolomite' in LCI_1.index[i]['name']:
            rem_values.append(LCI_1.values[i])
            rem_keys.append((LCI_1.index[i]['database'], LCI_1.index[i]['code'])) #check if runs
        elif 'sodium hydroxide' in LCI_1.index[i]['name']:
            rem_values.append(LCI_1.values[i])
            rem_keys.append((LCI_1.index[i]['database'], LCI_1.index[i]['code'])) #check if runs
        elif 'sulfuric acid' in LCI_1.index[i]['name']:
            rem_values.append(LCI_1.values[i])
            rem_keys.append((LCI_1.index[i]['database'], LCI_1.index[i]['code'])) #check if runs
        elif 'electricity' in LCI_1.index[i]['name']:
            rem_values.append(LCI_1.values[i])
            rem_keys.append((LCI_1.index[i]['database'], LCI_1.index[i]['code'])) #check if runs
    for i in np.arange(len(rem_keys)):
        lci1.pop(rem_keys[i], None)

    powerplant = ['hard coal power plant construction, 100MW','unit','GLO']
    activity = technosphereData(powerplant)
    LCIplant = pd.Series({activity: unit1_new*pp1_ratio+unit2_new*pp2_ratio})
    LCIgasifi = pd.Series(lci1)
    LCI_1 = pd.concat([LCIgasifi, LCIplant, LCIdryer])
    LCI_1.columns = ['Power plant']

    lci_write([LCI_1], "Power plant", u'kilowatt hour', 'EL+Q', self.input1)
```

```
    db = Database('Power plant')
    IP0 = db.query(NF('Power plant'))
    activity = db.get(next(iter(IP0.keys()))[1])
    dict = {activity: 1}
    unitProcess = pd.DataFrame(dict, index = ['Engine components']).T

    return unitProcess


def elementary_flow(self):
    """

    A function that make the LCI elementary flows for the thermal power plant class.

    """
    data_PP = deepcopy(self.energy_generation()[0])
    EL = data_PP.EL[0]
    C_inp = deepcopy(self.input2[1][0].C)
    mj_syngas = data_PP.mj_syngas[0]
    rts = pd.read_csv('climate_indicators.csv', index_col=0).sum()
    C_CH4 = 12.0107/float(12.0107+(4*1.00794))
    C_CO = 12.0107/float(15.9994+12.0107)
    C_CO2 = 12.0107/float(2*15.9994+12.0107)

    CH4 = 0.000505263*1e-3 * mj_syngas / EL
    CO = 0.021122807*1e-3  * mj_syngas / EL
    CO2 = ((C_inp * self.input3 - CH4 * C_CH4 - CO * C_CO) / C_CO2) / EL
    tot_C = CH4*C_CH4 + CO*C_CO + CO2*C_CO2


    N2O = 0.001403509*1e-3 *mj_syngas / EL
    NOx = 0.08*1e-3 *mj_syngas / EL
    SO2 = 0.019087719*1e-3 *mj_syngas / EL
    PM25 = 4.91228E-05*1e-3 *mj_syngas / EL
    PM10 = 7.01754E-05*1e-3 *mj_syngas / EL

    CO2_emi = ['Carbon dioxide, from soil or biomass stock', 'air',
               'low population density, long-term']
    N2O_nam = ['Dinitrogen monoxide', 'air', 'non-urban air or from high stacks']
    NOx_nam = ['Nitrogen oxides', 'air', 'non-urban air or from high stacks']
    CH4_nam = ['Methane, from soil or biomass stock', 'air', 'low population density, long-term']
    SO2_nam = ['Sulfur dioxide', 'air', 'non-urban air or from high stacks']
    PM10_nam = ['Particulates, > 2.5 um, and < 10um', 'air', 'non-urban air or from high stacks']
    PM25_nam = ['Particulates, < 2.5 um', 'air', 'non-urban air or from high stacks']
    CO_nam = ['Carbon monoxide, from soil or biomass stock', 'air', 'low population density, long-term']

    emissions = [CO2_emi, N2O_nam, NOx_nam, CH4_nam, SO2_nam, PM25_nam, PM10_nam, CO_nam]

    exchanges = []
    for i in np.arange(len(emissions)):
        exchanges.append(biosphereData_exact(emissions[i]))

    dictStruc2 = {exchanges[0]: CO2-(tot_C*rts['1 year']*(1.0/C_CO2)),
                  exchanges[1]: N2O, exchanges[2]: NOx, exchanges[3]: CH4,
                  exchanges[4]: SO2, exchanges[5]: PM10, exchanges[6]: PM25,
                  exchanges[7]: CO}

    elementaryFlow = pd.DataFrame(dictStruc2, index = ['Plant emission']).T

    return elementaryFlow


def get_lci(self):
    """

    A function that returns the LCI dataset of the transportation class.

    """
    data_PP = deepcopy(self.energy_generation()[0]) #/ self.input2[0]
    EL = data_PP.EL[0]

    db = Database("Thermal plant")
    if db.load() == {}:
        LCI_1 = self.unit_process(); LCI_1.columns = ["Thermal plant"]
        LCI_2 = self.elementary_flow(); LCI_2.columns = ["Thermal plant"]
        lci_write([LCI_1, LCI_2], "Thermal plant", u'kilowatt hour', 'EL+Q', self.input1)
        db = Database("Thermal plant")
        IP0 = db.query(NF("Thermal plant"))
        activity = db.get(next(iter(IP0.keys()))[1])
    else:
        IP0 = db.query(NF("Thermal plant"))
        activity = db.get(next(iter(IP0.keys()))[1])
    unitProcess = pd.Series({activity:EL})

    return unitProcess
```

```
def update_database(self):
    """

    A function that updates the database built by the thermal power plant class and
    assigns uncertainty factors.

    """
    uncert_int = pd.read_excel('uncertainty_energy.xlsx')
    uncert_fact_uni = [uncert_int['sd']['Infrastructure']]
    uncert_fact_ele = [uncert_int['sd']['CO2'], uncert_int['sd']['N2O'],
                       uncert_int['sd']['NOX'], uncert_int['sd']['CH4'],
                       uncert_int['sd']['SO2'],
                       uncert_int['sd']['PM25'], uncert_int['sd']['PM10'],
                       uncert_int['sd']['CO']]
    uncert_fact = [uncert_fact_uni, uncert_fact_ele]
    LCI_1 = self.unit_process(); LCI_1.columns = ["Thermal plant"]
    LCI_2 = self.elementary_flow(); LCI_2.columns = ["Thermal plant"]
    lci_write_uncert([LCI_1, LCI_2], "Thermal plant", u'kilowatt hour', 'EL+Q', self.input1, uncert_fact)
    print('New databse written')


def get_lcia(self, input1, input2):
    """

    A function that returns the LCIA results of all associated with all unit processes and
    elementary flows.

    """
    data_PP = deepcopy(self.energy_generation()[0])
    EL = data_PP.EL[0]
    method = input1
    if input2 == 'simple':
        lci = self.get_lci()
        return calcLCA_uniProc(method, lci)

    elif input2 =='full':
        LCI_1 = self.unit_process()
        LCI_2 = self.elementary_flow()*EL
        lci1 = {}
        for exc in LCI_1.index[0].technosphere():
            lci1.update({exc.input:exc.amount*EL})
        LCI_1 = pd.Series(lci1)
        return calcLCA_tot(method, LCI_1, LCI_2.T.sum())


def lci_to_latex(self, filename1, filename2, yes_no):
    """

    A function that returns the LCI data in a LaTex table.

    """
    activity5 = self.get_lci()
    unip_n, unip_u, unip_v, unip_sd = [], [], [], []
    for activity in activity5.index[0].technosphere():
        for exc in activity.input.technosphere():
            unip_n.append(exc.input['name'])
            unip_u.append(exc.input['unit'])
            unip_v.append(eng_str(exc.amount*self.input2[0], 3))
            unip_sd.append(eng_str(pd.read_excel('uncertainty_energy.xlsx')['sd']['Infrastructure']
                                   *exc.amount*self.input2[0], 3))
    unip_table = pd.DataFrame([unip_u, unip_v, unip_sd], ['Unit', 'Amount', 'Standard deviation'], unip_n).T
    if yes_no == 'yes':
        unip_table.to_latex(filename1)
    else:
        pass

    elem_n, elem_u, elem_v, elem_sd = [], [], [], []
    for exc in activity5.index[0].biosphere():
        elem_n.append(exc.input['name']+' to '+exc.input['categories'][0])
        elem_u.append(exc.input['unit'])
        elem_v.append(eng_str(exc.amount*self.input2[0], 3))
        elem_sd.append(eng_str(exc.uncertainty['scale']*self.input2[0], 3))
    elem_table = pd.DataFrame([elem_u, elem_v, elem_sd], ['Unit', 'Amount', 'Standard deviation'], elem_n).T
    if yes_no == 'yes':
        elem_table.to_latex(filename2)
    else:
        pass

    return unip_table, elem_table
```

```
from DatabaseSearch import *
from DNA import *
from copy import deepcopy
from utilities import round_sig, lci_write, lci_write_uncert, eng_str, calcLCA_tot, calcLCA_uniProc

class AnaerobicDigester:
    """

    A class that builds Anaerobic digester LCI dataset predefined assumptions.
        1) To establish the unit process of this component,
        2) To establish the chemical composition at the outlet,
        3) Extract the LCI data to use in LCIA.
        4) Update LCI data and assign uncertainties.
        5) Write LCI data to LaTex.
    """

    def __init__(self, input1, input2):
        self.input1 = input1 #String statement, resource type (e.g. 'rawManure').
        self.input2 = deepcopy(input2) #Pandas dataframe, mass, DM, C, N, K, P info.

    def unit_process(self):
        """

        A function that make the LCI unit process for the anaerobic digester class.

        """
        Bioreactor = ['anaerobic digestion plant construction, agriculture, with methane recovery', 'unit', 'RoW']
        activity = technosphereData(Bioreactor)
        dictStruc = {activity: 1.6295E-07/1.128}
        unitProcess = pd.DataFrame(dictStruc, index = ['Digester']).T

        return unitProcess

    def elementary_flow(self):
        """

        A function that make the LCI elementary flows for the anaerobic digester class.
        ** This function also returns the value of the digestate and biogas at outlet.

        """

        mass_inp = deepcopy(self.input2[0])
        input_ult = deepcopy(self.input2[1][0])

        C_CH4 = 12.0107/float(12.0107+(4*1.00794))
        H_CH4 = 1-C_CH4
        C_CO2 = 12.0107/float(2*15.9994+12.0107)
        O_CO2 = 1-C_CO2

        ch4_ratio = 0.62

        DM_inp = mass_inp-input_ult.M
        totC = input_ult.C
        totN = input_ult.N
        totA = input_ult.A
        totFC = float(deepcopy(self.input2[-1]))

        CN_ratio = totC/totN

        totVS = DM_inp-totA-totFC

        if CN_ratio < 23.5:
            ch4_vol = np.divide(-0.8475*CN_ratio**2 + 45.36*CN_ratio - 345.3, 1000)
        else:
            ch4_vol = np.divide(-1.16*CN_ratio**2 + 71.16*CN_ratio - 781.4, 1000)

        ch4_vol = ch4_vol * totVS

        bio_vol = ch4_vol/ch4_ratio
        mass_bio = bio_vol*1.158

        CH4_bio = mass_bio*float(ch4_ratio)
        CO2_bio = mass_bio*float(1.0-ch4_ratio)
        CO2C_bio = CO2_bio*C_CO2
        CH4C_bio = CH4_bio*C_CH4
        C_bio = CO2C_bio+CH4C_bio
        H_bio = CH4_bio*H_CH4
        O_bio = CO2_bio*O_CO2

        rts = pd.read_csv('climate_indicators.csv', index_col=0).sum()


        CH4 = CH4_bio*0.01
        CO2 = CH4*1.42
        tot_C = CH4*C_CH4 + CO2*C_CO2

        CH4_nam = ['Methane, from soil or biomass stock', 'air', 'low population density, long-term']
        CO2_emi = ['Carbon dioxide, from soil or biomass stock', 'air', 'low population density, long-term']
```

```
    CO2_reg = ['Carbon dioxide, fossil', 'air', 'low population density, long-term']
    emissions = [CH4_nam, CO2_emi, CO2_reg]

    exchanges = []
    for i in np.arange(len(emissions)):
        exchanges.append(biosphereData(emissions[i]))

    dictStruc2 = {exchanges[0]: CH4, exchanges[1]: CO2, exchanges[2]:(-tot_C/C_CO2)*rts['1 year']}
    elementaryFlow = pd.DataFrame(dictStruc2, index = ['Digester emission']).T



    mass_out = mass_inp-mass_bio
    DM_out = DM_inp-mass_bio

    if DM_out/mass_out > 0.3:
        mass_out = mass_out * ((DM_out/mass_out)/0.3)
    else:
        mass_out = mass_out

    mass_in = mass_out+mass_bio

    C_out =  totC-C_bio-(CH4*C_CH4)-(CO2*C_CO2)

    if CN_ratio < 23.5:
        heat_rec1 = DM_inp*CP((10.0+32.0)/2)*(32-10)
        heat_rec2 = (mass_in-DM_inp)*4.179*(32-10)
        heat_rec = (heat_rec1+heat_rec2)*1e-3
    else:
        heat_rec1 = DM_inp*CP((10.0+52.0)/2)*(52-10)
        heat_rec2 = (DM_inp)*4.179*(52-10)
        heat_rec = (heat_rec1+heat_rec2)*1e-3

    el_rec = 0.033464 * mass_in #kWh per input from ecoinvent
    data_biogas = pd.DataFrame([mass_bio, CH4_bio, CO2_bio, el_rec, heat_rec],
                               ['mass', 'CH4', 'CO2', 'EL', 'Q'], ['biogas']).T
    inp_total = input_ult

    inp_total.C = C_out
    inp_total.M = mass_out-DM_out-H_bio-O_bio
    out_total = inp_total
    out_data = mass_out, [out_total, deepcopy(self.input2[1][1]), deepcopy(self.input2[1][2])], C_out

    return elementaryFlow / data_biogas.mass[0], data_biogas, out_data


def get_lci(self):
    """

    A function that returns the LCI dataset of the storage tank class.

    """
    db = Database(self.input1+' Digestion')
    if db.load() == {}:
        LCI_1 = self.unit_process(); LCI_1.columns = [self.input1+' Digestion']
        LCI_2 = self.elementary_flow()[0]; LCI_2.columns = [self.input1+' Digestion']
        lci_write([LCI_1, LCI_2], self.input1+' Digestion', u'mass', u'kilogram*km', self.input1)
        db = Database(self.input1+' Digestion')
        IP0 = db.query(NF(self.input1+' Digestion'))
        activity = db.get(next(iter(IP0.keys()))[1])
    else:
        IP0 = db.query(NF(self.input1+' Digestion'))
        activity = db.get(next(iter(IP0.keys()))[1])

    data_biogas, dataDigestate = self.elementary_flow()[1:]
    mass_bio = data_biogas.mass[0]
    unitProcess = pd.Series({activity:mass_bio})

    return unitProcess, data_biogas, dataDigestate


def update_database(self):
    """

    A function that updates the database built by the anaerobic digester class and
    assigns uncertainty factors.

    """
    uncert_int = pd.read_excel('uncertainty_energy.xlsx')
    uncert_fact_uni = [uncert_int['sd']['Infrastructure']]
    uncert_fact_ele = [uncert_int['sd']['CH4'], uncert_int['sd']['CO2'], uncert_int['sd']['CO2']]
    uncert_fact = [uncert_fact_uni, uncert_fact_ele]

    LCI_1 = self.unit_process(); LCI_1.columns = [self.input1+' Digestion']
    LCI_2 = self.elementary_flow()[0]; LCI_2.columns = [self.input1+' Digestion']
    lci_write_uncert([LCI_1, LCI_2], self.input1+' Digestion', u'mass', u'kilogram*km', self.input1,
                     uncert_fact)
```

```
        print('New databse written')


    def get_lcia(self, input1, input2):
        """

        A function that returns the LCIA results of all associated with all unit processes and
        elementary flows.

        """
        mass = deepcopy(self.get_output()[0].mass)

        method = input1
        if input2 == 'simple':
            lci = self.get_lci()[0]

            return calcLCA_uniProc(method, lci)

        elif input2 =='full':
            LCI_1 = self.unit_process()*float(mass)
            LCI_2 = self.elementary_flow()[0]*float(mass)

            return calcLCA_tot(method, LCI_1.T.sum(), LCI_2.T.sum())


class BiogasEngine:
    """

    A class that builds biogas engine LCI dataset based on DNA simulation.
        0) Function that returns the energy generation of the biogas plant
        1) To establish the unit process of this component,
        2) To establish the chemical composition at the outlet,
        3) Extract the LCI data to use in LCIA.
        4) Update LCI data and assign uncertainties.
        5) Write LCI data to LaTex.
        6) Returns economics of the biogas plant

    """
    def __init__(self, input1, input2, input3):
        self.input1 = input1 #String statement, resource type (e.g. 'rawManure').
        self.input2 = (input2.T/input2.mass[0]).T #Pandas dataframe, mass, DM, C, N, K, P info.
        self.input3 = input3


    def energy_generation(self):
        """

        A function that feeds inputs to and runs a biogas engine DNA model and
        returns the results of the simulation.

        ** This function returns the energy generation, along with emissions
            based on simulation of the DNA model

        """
        sec_year = 365 * 24 * 3600
        hour_year = 365 * 24
        dataCO2 = self.input2.CO2[0]

        ##################################################
        ################## Write to DNA ##################
        ##################################################

        DNA_script = 'fluid '+'biogas'+' co2 '+str(dataCO2)+' ch4 '+str(1-dataCO2)
        feedstock = DNA_script
        num = 1

        parameter = ''
        addco = '\naddco m air_mix 5 '
        b = addco + str(self.input2.mass[0])
        parameter += b

        ##################################################
        ################### Run DNA ######################
        ##################################################

        dna = biogas_engine(feedstock, parameter, num)

        ##################################################
        ################## PostProcessing ################
        ##################################################

        Q = abs(float(dna['Q GasEngine 312'][0]))*\
             (hour_year/float(sec_year)) * 3.6 - self.input2.Q[0]*1e-3
        EL = abs(float(dna['E GasEngine 511']))*(hour_year/float(sec_year))
        EL -= 0.05 * (EL + Q / 3.6)
        dna.T.to_excel('dna_bio.xlsx')
        LHV_bio = float(dna['FUEL_CONSU MPTION_LHV '])
```

```
    el_eff = abs(float(dna['E GasEngine 511'])) / LHV_bio

    outData = pd.DataFrame([EL*self.input3, Q*self.input3, LHV_bio, el_eff],
                           index = ['EL', 'Q', 'LHV_bio', 'el_eff'],
                           columns = [self.input1]).T

    return outData


def unit_process(self):
    """

    A function that make the LCI unit process for the biogas engine class.

    """
    engine = ['heat and power co-generation, biogas, gas engine', 'kilowatt hour', 'DK']
    activity = technosphereData(engine)

    lci1a = {}
    for exc in activity.technosphere():
         lci1a.update({exc.input:exc.amount})

    LCI_1a = pd.Series(lci1a)
    rem_values = []
    rem_keys = []
    for i in np.arange(len(lci1a)):
        if 'biogas' in LCI_1a.index[i]['name']:
            rem_values.append(LCI_1a.values[i])
            rem_keys.append((LCI_1a.index[i]['database'], LCI_1a.index[i]['code']))

    for i in np.arange(len(rem_keys)):
        lci1a.pop(rem_keys[i], None)

    LCIbiogas = pd.Series(lci1a)
    LCIbiogas.columns = ['Biogas engine uni']
    lci_write([LCIbiogas], "Biogas engine uni", 'electricity+heat', u'kilowatt hour', self.input1)

    db = Database('Biogas engine uni')
    IP0 = db.query(NF('Biogas engine uni'))
    activity = db.get(next(iter(IP0.keys()))[1])
    dict = {activity: 1}
    unitProcess = pd.DataFrame(dict, index = ['Engine components']).T

    return unitProcess


def elementary_flow(self):
    """

    A function that make the LCI elementary flows for the biogas engine class.

    """
    rts = pd.read_csv('climate_indicators.csv', index_col=0).sum()
    C_CH4 = 12.0107/float(12.0107+(4*1.00794))
    C_CO2 = 12.0107/float(2*15.9994+12.0107)

    CH4 = 0.00052037 #434.0*1e-3 * LHV_bio
    CO2 = (self.input2.CO2[0] * C_CO2 + self.input2.CH4[0] * C_CH4 - CH4 * C_CH4) / C_CO2
    tot_C = CH4*C_CH4 + CO2*C_CO2

    N2O = 3.2523E-05
    NOx = 0.00045532
    SO2 = 3.5775E-06
    PM25 =  9.7569E-07

    CO2_emi = ['Carbon dioxide, from soil or biomass stock', 'air', 'low population density, long-term']
    N2O_nam = ['Dinitrogen monoxide', 'air', 'non-urban air or from high stacks']
    NOx_nam = ['Nitrogen oxides', 'air', 'non-urban air or from high stacks']
    CH4_nam = ['Methane, from soil or biomass stock', 'air', 'low population density, long-term']
    SO2_nam = ['Sulfur dioxide', 'air', 'non-urban air or from high stacks']
    PM25_nam = ['Particulates, > 2.5 um, and < 10um', 'air', 'non-urban air or from high stacks']
    emissions = [CO2_emi, N2O_nam, NOx_nam, CH4_nam, SO2_nam, PM25_nam]

    exchanges = []
    for i in np.arange(len(emissions)):
        exchanges.append(biosphereData_exact(emissions[i]))

    dictStruc2 = {exchanges[0]: CO2-tot_C*rts['1 year']*(1/C_CO2),
                  exchanges[1]: N2O, exchanges[2]: NOx, exchanges[3]: CH4,
                  exchanges[4]: SO2, exchanges[5]: PM25}
    elementaryFlow = pd.DataFrame(dictStruc2, index = ['Engine emission']).T

    return elementaryFlow


def get_lci(self):
    """
```

```
    A function that returns the LCI dataset of the transportation class.

    """
    data_pp = self.energy_generation()[0]
    EL = data_pp.EL[0]

    db = Database("Biogas engine")
    if db.load() == {}:
        LCI_1 = self.unit_process(); LCI_1.columns = ["Biogas engine"]
        LCI_2 = self.elementary_flow(); LCI_2.columns = ["Biogas engine"]
        lci_write([LCI_1, LCI_2], "Biogas engine", u'electricity+heat', u'kilowatt hour', self.input1)
        db = Database("Biogas engine")
        IP0 = db.query(NF("Biogas engine"))
        activity = db.get(next(iter(IP0.keys()))[1])
    else:
        IP0 = db.query(NF("Biogas engine"))
        activity = db.get(next(iter(IP0.keys()))[1])
    unitProcess = pd.Series({activity:EL})

    return unitProcess, data_pp


def update_database(self):
    """

    A function that updates the database built by the biogas engine class and
    assigns uncertainty factors.

    """
    uncert_int = pd.read_excel('uncertainty_energy.xlsx')
    uncert_fact_uni = [uncert_int['sd']['Infrastructure']]
    uncert_fact_ele = [uncert_int['sd']['CO2'], uncert_int['sd']['N2O'],
                       uncert_int['sd']['NOX'], uncert_int['sd']['CH4'],
                       uncert_int['sd']['SO2'],
                       uncert_int['sd']['PM25']]
    uncert_fact = [uncert_fact_uni, uncert_fact_ele]

    LCI_1 = self.unit_process(); LCI_1.columns = ["Biogas engine"]
    LCI_2 = self.elementary_flow(); LCI_2.columns = ["Biogas engine"]
    lci_write_uncert([LCI_1, LCI_2], "Biogas engine", u'electricity+heat', u'kilowatt hour', self.input1, uncert_fact)
    print('New databse written')


def get_lcia(self, input1, input2):
    """

    A function that returns the LCIA results of all associated with all unit processes and
    elementary flows.

    """
    data_pp = self.energy_generation()[0]
    EL = data_pp.EL[0]

    method = input1
    if input2 == 'simple':
        lci = self.get_lci()[0]
        return calcLCA_uniProc(method, lci)

    elif input2 =='full':
        LCI_1 = self.unit_process()*EL
        LCI_2 = self.elementary_flow()*EL
        return calcLCA_tot(method, LCI_1.T.sum(), LCI_2.T.sum())
```

```
import sys
from DatabaseSearch import *
from utilities import eng_str, lci_write, lci_write_uncert, calcLCA_tot, calcLCA_uniProc
from DNA import *

class StorageTank:
    """

    A class that builds storage tanks (indoor and outdoor)  process model

    ** Functions within this class can be used:
        1) Establish a mass and substance balance.
        2) Extract the LCI data to use in LCIA.
        3) Update LCI data and assign uncertainties.
        4) Write LCI data to LaTex.
        5) Get the investment and O&M costs

    """

    def __init__(self, input1, input2, input3):
        biomass = deepcopy(input2)
        self.input1 = input1    # String statement, resource type (e.g. 'rawManure').
        self.input2 = biomass   # Pandas dataframe, DM, C, N, K, P info.
        self.input3 = input3    # String statement, indoor(In) or outdoor(Out) storage.

    def unit_process(self):
        """

        A function that make the LCI unit process for the storage tank class.

        """
        DM_inp = (self.input2[0]-float(self.input2[1][0].M)) / self.input2[0] # Dry matter at inlet
        density = 1000 - 11.2*DM_inp + 1.19*DM_inp**2 - 0.0235*DM_inp**2 # Density of input
        tank = ['liquid manure storage and processing facility construction',
                'cubic meter', 'RoW']
        electricity = ['market for electricity, medium voltage',
                       'kilowatt hour', 'DK']
        processes = [tank, electricity]
        activities = []
        for i in np.arange(len(processes)):
            activities.append(technosphereData_exact(processes[i]))
        unitProcess = pd.DataFrame([(1.0/density)*3.47e-5, (1.0/density)*0.375],
                                   index = [activities] ,
                                   columns = [self.input3+'door storage facility,'])

        return unitProcess


    def elementary_flow(self):
        """

        A function that make the LCI elementary flows for the storage tank class.
        ** This function also returns the value of the biomass at outlet.

        """
        rts = pd.read_csv('climate_indicators.csv', index_col=0).sum()
        C_CH4 = (12.0107/float(12.0107+(4*1.00794)))
        C_CO2 = float(12.0107)/float(2*15.9994+12.0107)

        N2O = ['Dinitrogen monoxide', 'air', 'low population density, long-term']
        NH3 = ['Ammonia', 'air', 'low population density, long-term']
        NOx = ['Nitrogen oxides', 'air', 'low population density, long-term']
        N2 = ['Nitrogen', 'air']
        emissions1 = [N2O, NH3, NOx, N2]

        input_ult = deepcopy(self.input2[1][0])

        mass_inp = deepcopy(self.input2[0])
        DM_inp = deepcopy(self.input2[0]-float(self.input2[1][0].M)) / mass_inp
        N_inp = deepcopy(self.input2[1][0].N) / mass_inp
        C_inp = deepcopy(self.input2[1][0].C) / mass_inp

        exchanges1 = []
        for i in np.arange(len(emissions1)):
            exchanges1.append(biosphereData_exact(emissions1[i]))

            CH4 = ['Methane, from soil or biomass stock', 'air',
                   'low population density, long-term']
            CO2_emi = ['Carbon dioxide, fossil', 'air', 'low population density, long-term']
            CO2_reg = ['Carbon dioxide, from soil or biomass stock', 'air',
                       'low population density, long-term']
            emissions2 = [CH4, CO2_emi, CO2_reg]

            exchanges2 = []
            for i in np.arange(len(emissions2)):
                exchanges2.append(biosphereData(emissions2[i]))

        if self.input1 == 'rawManure' and self.input3 == 'In':
```

```
        # NITROGEN EMISSIONS
        NH3N = N_inp*0.16
        NH3 = NH3N *(17.03052/14.0067)
        dirN2ON = N_inp*0.002
        NOxN = dirN2ON
        NOx = NOxN *(30.00610/14.0067)
        indN2ON = (NH3N+NOxN)*0.01
        N2O = (indN2ON+dirN2ON) *(44.01280/14.0067)
        N2 = dirN2ON*3.0 *((2*14.0067)/14.0067)

        totN = indN2ON+dirN2ON+NH3N+NOxN+N2 * 0.5

        nitrogenEmission = pd.DataFrame([N2O, NH3, NOx, N2],
                                        index = [exchanges1] ,
                                        columns = [self.input3+'door storage emission, '
                                                    ''+self.input1])
        # CARBON EMISSIONS
        CH4 = DM_inp*0.8*0.45*0.66*0.03
        CO2 = C_inp*0.1 - CH4*C_CH4
        totC = CH4*C_CH4+CO2*C_CO2
        C_seq = totC*rts['1 year']
        CO2_seq = np.divide(C_seq, C_CO2)

        totC = CH4*C_CH4+CO2*C_CO2

        carbonEmission = pd.DataFrame([CH4, CO2, -CO2_seq], index = [exchanges2] ,
                            columns = [self.input3+'door storage emission, '+self.input1])

    elif self.input1 == 'rawManure2' and self.input3 == 'In':
        # NITROGEN EMISSIONS
        NH3N = N_inp*0.16
        NH3 = NH3N *(17.03052/14.0067)
        dirN2ON = N_inp*0.002
        NOxN = dirN2ON
        NOx = NOxN *(30.00610/14.0067)
        indN2ON = (NH3N+NOxN)*0.01
        N2O = (indN2ON+dirN2ON) *(44.01280/14.0067)
        N2 = dirN2ON*3.0 *((2*14.0067)/14.0067)
        totN = indN2ON+dirN2ON+NH3N+NOxN+N2 * 0.5
        nitrogenEmission = pd.DataFrame([N2O, NH3, NOx, N2],
                                        index = [exchanges1] ,
                                        columns = [self.input3+'door storage emission, '
                                                    ''+self.input1])
        # CARBON EMISSIONS
        CH4 = DM_inp*0.8*0.45*0.66*0.03
        CO2 = C_inp*0.1 - CH4*C_CH4
        totC = CH4*C_CH4+CO2*C_CO2
        C_seq = totC*rts['1 year']
        CO2_seq = np.divide(C_seq, C_CO2)
        totC = CH4*C_CH4+CO2*C_CO2
        carbonEmission = pd.DataFrame([CH4, CO2, -CO2_seq], index = [exchanges2] ,
                            columns = [self.input3+'door storage emission, '+self.input1])

    elif self.input1 == 'rawManure' and self.input3 == 'Out':
        # NITROGEN EMISSIONS
        NH3N = N_inp*0.02
        NH3 = NH3N *(17.03052/14.0067)
        dirN2ON = N_inp*0.005
        NOxN = dirN2ON
        NOx = NOxN *(30.00610/14.0067)
        indN2ON = (NH3N+NOxN)*0.01
        N2O = (indN2ON+dirN2ON) *(44.01280/14.0067)
        N2 = dirN2ON*3.0 *((2*14.0067)/14.0067)
        totN = indN2ON+dirN2ON+NH3N+NOxN+N2 * 0.5
        nitrogenEmission = pd.DataFrame([N2O, NH3, NOx, N2], index = [exchanges1] ,
                            columns = [self.input3+'door storage emission, '+self.input1])
        # CARBON EMISSIONS
        CH4 = DM_inp*0.8*0.45*0.66*0.10
        CO2 = C_inp*0.05 - CH4*C_CH4
        totC = CH4*C_CH4+CO2*C_CO2
        C_seq = totC*rts['1 year']
        CO2_seq = np.divide(C_seq, C_CO2)
        totC = CH4*C_CH4+CO2*C_CO2
        carbonEmission = pd.DataFrame([CH4, CO2, -CO2_seq], index = [exchanges2] ,
                            columns = [self.input3+'door storage emission, '+self.input1])

    elif self.input1 == 'lmManure' and self.input3 == 'Out':
        # NITROGEN EMISSIONS
        NH3N = N_inp*0.02
        NH3 = NH3N *(17.03052/14.0067)
        dirN2ON = N_inp*0.005
        NOxN = dirN2ON
        NOx = NOxN *(30.00610/14.0067)
        indN2ON = (NH3N+NOxN)*0.01
        N2O = (indN2ON+dirN2ON) *(44.01280/14.0067)
        N2 = dirN2ON*3.0 *((2*14.0067)/14.0067)
        totN = indN2ON+dirN2ON+NH3N+NOxN+N2 * 0.5
        nitrogenEmission = pd.DataFrame([N2O, NH3, NOx, N2], index = [exchanges1] ,
```

```
                        columns = [self.input3+'door storage emission, '+self.input1])
    # CARBON EMISSIONS
    CH4 = DM_inp*0.8*0.45*0.66*0.10
    CO2 = CH4 * 1.67
    totC = CH4*C_CH4+CO2*C_CO2
    C_seq = totC*rts['1 year']
    CO2_seq = np.divide(C_seq, C_CO2)
    totC = CH4*C_CH4+CO2*C_CO2
    carbonEmission = pd.DataFrame([CH4, CO2, -CO2_seq], index = [exchanges2] ,
                        columns = [self.input3+'door storage emission, '+self.input1])

elif self.input1 == 'smManure' and self.input3 == 'Out':
    # NITROGEN EMISSIONS
    NH3N = N_inp*0.02 * (1-0.12)
    NH3 = NH3N *(17.03052/14.0067)
    dirN2ON = N_inp*0.005 * (1-0.99)
    NOxN = dirN2ON
    NOx = NOxN *(30.00610/14.0067)
    indN2ON = (NH3N+NOxN)*0.01
    N2O = (indN2ON+dirN2ON) *(44.01280/14.0067)
    N2 = dirN2ON*3.0 *((2*14.0067)/14.0067)
    totN = indN2ON+dirN2ON+NH3N+NOxN+N2 * 0.5
    nitrogenEmission = pd.DataFrame([N2O, NH3, NOx, N2], index = [exchanges1] ,
                        columns = [self.input3+'door storage emission, '+self.input1])
    # CARBON EMISSIONS
    CH4 = DM_inp*0.8*0.45*0.66*0.10 * (1.0-0.88)
    CO2 = CH4 * 1.67
    totC = CH4*C_CH4+CO2*C_CO2
    C_seq = totC*rts['1 year']
    CO2_seq = np.divide(C_seq, C_CO2)
    totC = CH4*C_CH4+CO2*C_CO2
    carbonEmission = pd.DataFrame([CH4, CO2, -CO2_seq], index = [exchanges2] ,
                        columns = [self.input3+'door storage emission, '+self.input1])

elif self.input1 == 'dManure' and self.input3 == 'Out':
    # NITROGEN EMISSIONS
    NH3N = N_inp*0.02
    NH3 = NH3N *(17.03052/14.0067)
    dirN2ON = N_inp*0.005*0.4
    NOxN = dirN2ON
    NOx = NOxN *(30.00610/14.0067)
    indN2ON = (NH3N+NOxN)*0.01
    N2O = (indN2ON+dirN2ON) *(44.01280/14.0067)
    N2 = dirN2ON*3.0 *((2*14.0067)/14.0067)
    totN = indN2ON+dirN2ON+NH3N+NOxN+N2 * 0.5
    nitrogenEmission = pd.DataFrame([N2O, NH3, NOx, N2], index = [exchanges1] ,
                        columns = [self.input3+'door storage emission, '+self.input1])
    # CARBON EMISSIONS
    CH4 = DM_inp*0.8*0.45*0.66*0.10*0.5
    CO2 = CH4*1.67
    totC = CH4*C_CH4+CO2*C_CO2
    C_seq = totC*rts['1 year']
    CO2_seq = np.divide(C_seq, C_CO2)
    totC = CH4*C_CH4+CO2*C_CO2
    carbonEmission = pd.DataFrame([CH4, CO2, -CO2_seq], index = [exchanges2] ,
                        columns = [self.input3+'door storage emission, '+self.input1])

elif self.input1 == 'ldManure' and self.input3 == 'Out':
    # NITROGEN EMISSIONS
    NH3N = N_inp*0.02
    NH3 = NH3N *(17.03052/14.0067)
    dirN2ON = N_inp*0.005*0.4
    NOxN = dirN2ON
    NOx = NOxN *(30.00610/14.0067)
    indN2ON = (NH3N+NOxN)*0.01
    N2O = (indN2ON+dirN2ON) *(44.01280/14.0067)
    N2 = dirN2ON*3.0 *((2*14.0067)/14.0067)
    totN = indN2ON+dirN2ON+NH3N+NOxN+N2 * 0.5
    nitrogenEmission = pd.DataFrame([N2O, NH3, NOx, N2], index = [exchanges1] ,
                        columns = [self.input3+'door storage emission, '+self.input1])
    # CARBON EMISSIONS
    CH4 = DM_inp*0.8*0.45*0.66*0.10*0.5
    CO2 = CH4*1.67
    totC = CH4*C_CH4+CO2*C_CO2
    C_seq = totC*rts['1 year']
    CO2_seq = np.divide(C_seq, C_CO2)
    totC = CH4*C_CH4+CO2*C_CO2
    carbonEmission = pd.DataFrame([CH4, CO2, -CO2_seq], index = [exchanges2] ,
                        columns = [self.input3+'door storage emission, '+self.input1])

elif self.input1 == 'sdManure' and self.input3 == 'Out':
    # NITROGEN EMISSIONS
    NH3N = N_inp*0.13
    NH3 = NH3N *(17.03052/14.0067)
    dirN2ON = N_inp*0.0004
    NOxN = dirN2ON
    NOx = NOxN *(30.00610/14.0067)
    indN2ON = (NH3N+NOxN)*0.01
```

```
            N2O = (indN2ON+dirN2ON) *(44.01280/14.0067)
            N2 = dirN2ON*3.0 *((2*14.0067)/14.0067)
            totN = indN2ON+dirN2ON+NH3N+NOxN+N2 * 0.5
            nitrogenEmission = pd.DataFrame([N2O, NH3, NOx, N2], index = [exchanges1] ,
                               columns = [self.input3+'door storage emission, '+self.input1])
            # CARBON EMISSIONS
            CH4 = C_inp*0.0017
            CO2 = C_inp*0.019
            totC = CH4*C_CH4+CO2*C_CO2
            C_seq = totC*rts['1 year']
            CO2_seq = np.divide(C_seq, C_CO2)
            totC = CH4*C_CH4+CO2*C_CO2
            carbonEmission = pd.DataFrame([CH4, CO2, -CO2_seq], index = [exchanges2] ,
                               columns = [self.input3+'door storage emission, '+self.input1])

        else:
            print('ERROR IN INPUT TO STORAGETANK !!!')
            sys.exit()

        elementaryFlow = pd.concat([nitrogenEmission, carbonEmission])
        out_total = input_ult
        out_total.C = input_ult.C-(totC*mass_inp)
        out_total.N = input_ult.N-(totN*mass_inp)
        FC_out = self.input2[-1]
        out_data = self.input2[0]-(totN*mass_inp)-(totC*mass_inp), \
                   [out_total, self.input2[1][1], self.input2[1][2]], FC_out

        return elementaryFlow, out_data


    def get_lci(self):
        """

        A function that returns the LCI dataset of the storage tank class.

        """
        db = Database(self.input3+'door storage, '+self.input1)
        if db.load() == {}:
            LCI_1 = self.unit_process(); LCI_1.columns = [self.input3+'door storage, '+self.input1]
            LCI_2 = self.elementary_flow()[0]; LCI_2.columns = [self.input3+'door storage, '+self.input1]
            lci_write([LCI_1, LCI_2], self.input3+'door storage, '+self.input1,
                      u'volume', u'kilogram', self.input3+'door storage, '+self.input1)
            db = Database(self.input3+'door storage, '+self.input1)
            IP0 = db.query(NF(self.input3+'door storage, '+self.input1))
            activity = db.get(next(iter(IP0.keys()))[1])
            uniProc = pd.Series({activity:self.input2[0]})
        else:
            IP0 = db.query(NF(self.input3+'door storage, '+self.input1))
            activity = db.get(next(iter(IP0.keys()))[1])
            uniProc = pd.Series({activity:self.input2[0]})

        return uniProc


    def update_database(self):
        """

        A function that updates the database built by the storage class.

        """
        uncert_int = pd.read_excel('uncertainty_intermittent_new.xlsx')
        uncert_fact_uni = [uncert_int['sd']['Infrastructure'], uncert_int['sd']['Energy']]
        uncert_fact_ele = [uncert_int['sd']['N2O'], uncert_int['sd']['NH3'],
                           uncert_int['sd']['NOX'], uncert_int['sd']['N2'],
                           uncert_int['sd']['CH4'], uncert_int['sd']['CO2'], uncert_int['sd']['CO2']]
        uncert_fact = [uncert_fact_uni, uncert_fact_ele]

        LCI_1 = self.unit_process(); LCI_1.columns = [self.input3+'door storage, '+self.input1]
        LCI_2 = self.elementary_flow()[0]; LCI_2.columns = [self.input3+'door storage, '+self.input1]
        lci_write_uncert([LCI_1, LCI_2], self.input3+'door storage, '+self.input1,
                  u'volume', u'kilogram', self.input3+'door storage, '+self.input1, uncert_fact)


    def get_lcia(self, input1, input2):
        """

        A function that returns the LCIA results of all associated with all unit processes and
        elementary flows.

        """
        method = input1
        if input2 == 'simple':
            lci = self.get_lci()
            return calcLCA_uniProc(method, lci)

        elif input2 =='full':
            LCI_1 = self.unit_process()*self.input2[0]
            LCI_2 = self.elementary_flow()[0]*self.input2[0]
```

```
        return calcLCA_tot(method, LCI_1.T.sum(), LCI_2.T.sum())


def lci_to_latex(self, filename1, filename2, yes_no):
    """

    A function that returns the LCI data in a LaTex table.

    """
    activity5 = self.get_lci()
    unip_n, unip_u, unip_v, unip_sd = [], [], [], []
    for exc in activity5.index[0].technosphere():
        unip_n.append(exc.input['name'])
        unip_u.append(exc.input['unit'])
        unip_v.append(eng_str(exc.amount, 3))
        unip_sd.append(eng_str(exc.uncertainty['scale'], 3))
    unip_table = pd.DataFrame([unip_u, unip_v, unip_sd], ['Unit', 'Amount', 'Standard deviation'], unip_n).T

    if yes_no == 'yes':
        unip_table.to_latex(filename1)
    else:
        pass

    elem_n, elem_u, elem_v, elem_sd = [], [], [], []
    for exc in activity5.index[0].biosphere():
        elem_n.append(exc.input['name']+' to '+exc.input['categories'][0])
        elem_u.append(exc.input['unit'])
        elem_v.append(eng_str(exc.amount, 3))
        elem_sd.append(eng_str(exc.uncertainty['scale'], 3))
    elem_table = pd.DataFrame([elem_u, elem_v, elem_sd], ['Unit', 'Amount', 'Standard deviation'], elem_n).T

    if yes_no == 'yes':
        elem_table.to_latex(filename2)
    else:
        pass

    return unip_table, elem_table
```

```
import sys
from DatabaseSearch import *
from utilities import eng_str, lci_write, lci_write_uncert, calcLCA_tot, calcLCA_uniProc
from DNA import *

class Separation:
    """

    A class that builds separators LCI dataset based on type and resource input.
        1) To establish the unit process of this component,
        2) To establish the chemical composition at the outlet,
        3) Extract the LCI data to use in LCIA.
        4) Update LCI data and assign uncertainties.
        5) Write LCI data to LaTex.

    """

    def __init__(self, input1, input2, input3):
        self.input1 = input1    # String statement, resource type (e.g. 'rawManure').
        self.input2 = input2    # String statement,sSeparator type (e.g., 'decanter or screw-press).
        self.input3 = deepcopy(input3)    # Pandas dataframe, mass, DM, C, N, K, P info


    def unit_process(self):
        """

        A function that make the LCI unit process for the separation class.
        ** This function also returs the composition of the liquid and solid
            states at the outlet.

        """
        if self.input2 == 'decanterPAM':
            el_comp = 2.18/1000
        elif self.input2 == 'decanter1':
            el_comp = 2.18/1000
        elif self.input2 == 'decanter2':
            el_comp = 2.18/1000
        elif self.input2 == 'screw_press1':
            el_comp = 0.95/1000
        elif self.input2 == 'screw_press2':
            el_comp = 0.95/1000
        else:
            print('ERROR IN INPUT TO SEPARATOR TYPE INPUT !!!')
            sys.exit()

        if self.input2 == 'decanterPAM':
            electricity = ['market for electricity, low voltage', 'kilowatt hour', 'DK']
            polyacrylamide = ['market for polyacrylamide', 'kilogram', 'GLO']
            steel_a = ['market for steel, low-alloyed', 'kilogram', 'GLO']
            steel_b = ['market for steel, chromium steel 18/8, hot rolled', 'kilogram', 'GLO']
            copper = ['market for copper', 'kilogram', 'GLO']
            electronics = ['computer production, laptop', 'unit', 'GLO']
            processes = [electricity, polyacrylamide, steel_a, steel_b, copper, electronics]

            activities = []
            for i in np.arange(len(processes)):
                activities.append(technosphereData_exact(processes[i]))
            unitProcess = pd.DataFrame([el_comp, 0.9*1e-3, 5.86*1e-6, 9.3*1e-6,
                                        0.023*1e-3, 6.7*1e-10], index = [activities] ,
                                        columns = [self.input2+' separator, '+self.input1])
        elif self.input2 == 'decanter1' or self.input2 == 'decanter2' \
                or self.input2 == 'screw_press1'or self.input2 == 'screw_press2':
            electricity = ['market for electricity, low voltage', 'kilowatt hour', 'DK']
            steel_a = ['market for steel, low-alloyed', 'kilogram', 'GLO']
            steel_b = ['market for steel, chromium steel 18/8, hot rolled', 'kilogram', 'GLO']
            copper = ['market for copper', 'kilogram', 'GLO']
            electronics = ['computer production, laptop', 'unit', 'GLO']
            processes = [electricity, steel_a, steel_b, copper, electronics]

            activities = []
            for i in np.arange(len(processes)):
                activities.append(technosphereData_exact(processes[i]))
            unitProcess = pd.DataFrame([el_comp, 5.86*1e-6, 9.3*1e-6, 0.023*1e-3, 6.7*1e-10],
                                       index = [activities] ,
                                       columns = [self.input2+' separator, '+self.input1])
        else:
            print('ERROR IN INPUT TO SEPARATOR (unit process) !!!')
            sys.exit()
        return unitProcess


    def get_lci(self):
        """

        A function that returns the LCI dataset of the separator class.

        """
        db = Database(self.input2+' separator')
```

```
    if db.load() == {}:
        LCI_1 = self.unit_process(); LCI_1.columns = [self.input2+' separator']
        lci_write([LCI_1], self.input2+' separator',
                  u'volume', u'kilogram', self.input2+' separator')
        db = Database(self.input2+' separator')
        IP0 = db.query(NF(self.input2+' separator'))
        activity = db.get(next(iter(IP0.keys()))[1])
        uniProc = pd.Series({activity})
    else:
        IP0 = db.query(NF(self.input2+' separator'))
        activity = db.get(next(iter(IP0.keys()))[1])
        print(activity, 'activity')
        uniProc = pd.Series({activity:self.input3[0]})

    return uniProc


def update_database(self):
    """

    A function that updates the database built by the separator class.

    """
    uncert_int = pd.read_excel('uncertainty_intermittent_new.xlsx')
    uncert_fact_uni = [uncert_int['sd']['Energy'], uncert_int['sd']['Working material'],
                       uncert_int['sd']['Working material'], uncert_int['sd']['Working material'],
                       uncert_int['sd']['Working material']]
    uncert_fact_ele = 0
    uncert_fact = [uncert_fact_uni, uncert_fact_ele]
    LCI_1 = self.unit_process(); LCI_1.columns = [self.input2+' separator']
    lci_write_uncert([LCI_1], self.input2+' separator',
              u'volume', u'kilogram', self.input2+' separator', uncert_fact)


def get_output(self):
    """

    A function that returns the chemical composition at the output of the separator.

    """
    elem = deepcopy(self.input3)

    if self.input2 == 'decanterPAM':
        eff_mass = 0.229
        eff_DM = 0.872
        eff_N = 0.419
        eff_P = 0.90
        eff_K = 0.14
        eff_A = (eff_P*(elem[1][1].P2O5/2.29)+eff_K*(elem[1][1].K2O/1.20)) /\
                (elem[1][1].P2O5/2.29+elem[1][1].K2O/1.20)
        eff_Cu = 1.0
        eff_Zn =0.992
        eff_HM = (eff_Cu*elem[1][2].Cu+eff_Zn*elem[1][2].Zn) /\
                 (elem[1][2].Cu+elem[1][2].Zn)
    elif self.input2 == 'decanter1':
        eff_mass = 0.242
        eff_DM = 0.609
        eff_N = 0.212
        eff_P = 0.662
        eff_K = 0.097
        eff_A = (eff_P*(elem[1][1].P2O5/2.29)+eff_K*(elem[1][1].K2O/1.20)) /\
                (elem[1][1].P2O5/2.29+elem[1][1].K2O/1.20)
        eff_Cu = 0.362
        eff_Zn =0.422
        eff_HM = (eff_Cu*elem[1][2].Cu+eff_Zn*elem[1][2].Zn) /\
                 (elem[1][2].Cu+elem[1][2].Zn)
    elif self.input2 == 'screw_press1':
        eff_mass = 0.052
        eff_DM = 0.296
        eff_N = 0.068
        eff_P = 0.091
        eff_K = 0.029
        eff_A = (eff_P*(elem[1][1].P2O5/2.29)+eff_K*(elem[1][1].K2O/1.20)) /\
                (elem[1][1].P2O5/2.29+elem[1][1].K2O/1.20)
        eff_Cu = 0.064
        eff_Zn =0.063
        eff_HM = (eff_Cu*elem[1][2].Cu+eff_Zn*elem[1][2].Zn) /\
                 (elem[1][2].Cu+elem[1][2].Zn)
    elif self.input2 == 'decanter2':
        eff_mass = 0.16
        eff_DM = 0.595
        eff_N = 0.21
        eff_A = 0.432
        eff_P = 0.736
        eff_K = 0.141
        eff_Cu = 0.199
        eff_Zn =0.273
        eff_HM = (eff_Cu*elem[1][2].Cu+eff_Zn*elem[1][2].Zn) /\
```

```
            (elem[1][2].Cu+elem[1][2].Zn)
elif self.input2 == 'screw_press2':
    eff_mass = 0.11335
    eff_DM = 0.344
    eff_N = 0.112
    eff_A = 0.137
    eff_P = 0.133
    eff_K = 0.105
    eff_Cu = 0.102
    eff_Zn =0.099
    eff_HM = (eff_Cu*elem[1][2].Cu+eff_Zn*elem[1][2].Zn) /\
            (elem[1][2].Cu+elem[1][2].Zn)
else:
    print('ERROR IN INPUT TO SEPARATOR TYPE INPUT (elementary flow)!!!')
    sys.exit()

dm_out = (elem[0]-elem[1][0].M)*eff_DM
N_out = elem[1][0].N*eff_N
A_out = elem[1][0].A*eff_A

sum_ult = elem[1][0].C+elem[1][0].O+elem[1][0].H+elem[1][0].S
diff_C = elem[1][0].C/sum_ult
diff_O = elem[1][0].O/sum_ult
diff_H = elem[1][0].H/sum_ult
diff_S = elem[1][0].S/sum_ult

diff_ult = elem[1][0].C+elem[1][0].O+elem[1][0].H+elem[1][0].S+N_out+A_out-dm_out

C_out = elem[1][0].C - diff_ult*diff_C
O_out = elem[1][0].O - diff_ult*diff_O
H_out = elem[1][0].H - diff_ult*diff_H
S_out = elem[1][0].S - diff_ult*diff_S
mass_out = elem[0]* eff_mass
M_out = mass_out - dm_out

ULT_elem = pd.Series([C_out, O_out, H_out, N_out, S_out, A_out, M_out],
                     ['C', 'O', 'H', 'N', 'S', 'A', 'M'])

K2O_out = elem[1][1].K2O*eff_K
P2O5_out = elem[1][1].P2O5*eff_P

sum_maj = elem[1][1].SiO2+elem[1][1].CaO+elem[1][1].Al2O3+elem[1][1].MgO+elem[1][1].Fe2O3+\
          elem[1][1].SO3+elem[1][1].Na2O+elem[1][1].TiO2
diff_SiO2 = elem[1][1].SiO2/sum_maj
diff_CaO = elem[1][1].CaO/sum_maj
diff_Al2O3 = elem[1][1].Al2O3/sum_maj
diff_MgO = elem[1][1].MgO/sum_maj
diff_Fe2O3 = elem[1][1].Fe2O3/sum_maj
diff_SO3 = elem[1][1].SO3/sum_maj
diff_Na2O = elem[1][1].Na2O/sum_maj
diff_TiO2 = elem[1][1].TiO2/sum_maj

diff_maj = elem[1][1].SiO2+elem[1][1].CaO+elem[1][1].Al2O3+elem[1][1].MgO+elem[1][1].Fe2O3+\
          elem[1][1].SO3+elem[1][1].Na2O+elem[1][1].TiO2+K2O_out+P2O5_out - A_out

SiO2_out = elem[1][1].SiO2 - diff_maj*diff_SiO2
CaO_out = elem[1][1].CaO - diff_maj*diff_CaO
Al2O3_out = elem[1][1].Al2O3 - diff_maj*diff_Al2O3
MgO_out = elem[1][1].MgO - diff_maj*diff_MgO
Fe2O3_out = elem[1][1].Fe2O3 - diff_maj*diff_Fe2O3
SO3_out = elem[1][1].SO3 - diff_maj*diff_SO3
Na2O_out = elem[1][1].Na2O - diff_maj*diff_Na2O
TiO2_out = elem[1][1].TiO2 - diff_maj*diff_TiO2

MAJ_elem = pd.Series([SiO2_out, CaO_out, K2O_out, P2O5_out, Al2O3_out,
                      MgO_out, Fe2O3_out, SO3_out, Na2O_out, TiO2_out],
                     ['SiO2', 'CaO', 'K2O', 'P2O5', 'Al2O3', 'MgO', 'Fe2O3', 'SO3', 'Na2O', 'TiO2'])

HM_elem = elem[1][2]*eff_HM
HM_elem.Cu = eff_Cu*elem[1][2].Cu
HM_elem.Zn = eff_Zn*elem[1][2].Zn

eff_C = C_out / elem[1][0].C
FC_out = elem[-1]*eff_C

outSolid = mass_out, [ULT_elem, MAJ_elem, HM_elem], FC_out

ult_liquid = elem[1][0][:-1]-ULT_elem[:-1].T
mass_liquid = elem[0]-mass_out

moi_liquid = pd.Series([mass_liquid-ult_liquid.sum()], ['M'])
ult_liquid_new = pd.concat([ult_liquid, moi_liquid], axis=1).T.sum()
ult_liquid_index = ['C', 'O', 'H', 'N', 'S', 'A', 'M']
ult_liquid_new = ult_liquid_new[ult_liquid_index].T


outLiquid = mass_liquid, [ult_liquid_new, elem[1][1]-MAJ_elem.T, elem[1][2]-HM_elem.T], elem[-1]-FC_out
```

```
    outLiquid[1][0] = outLiquid[1][0].T
    outLiquid[1][1] = outLiquid[1][1].T
    outLiquid[1][2] = outLiquid[1][2].T

    return outSolid, outLiquid


def get_lcia(self, input1, input2):
    """

    A function that returns the LCIA results of all associated with all unit processes and
    elementary flows.

    """
    method = input1
    if input2 == 'simple':
        lci = self.get_lci()

        return calcLCA_uniProc(method, lci)

    elif input2 =='full':
        LCI_1 = self.get_lci()
        lci1 = {}
        for exc in LCI_1.index[0].technosphere():
             print(exc.amount)
             lci1.update({exc.input:exc.amount*self.input3[0]})

        LCI_1 = pd.Series(lci1)

        return calcLCA_uniProc(method, LCI_1)


def lci_to_latex(self, filename1, yes_no):
    """

    A function that returns the LCI data in a LaTex table.

    """
    activity5 = self.get_lci()
    unip_n, unip_u, unip_v, unip_sd = [], [], [], []
    for exc in activity5.index[0].technosphere():
        unip_n.append(exc.input['name'])
        unip_u.append(exc.input['unit'])
        unip_v.append(eng_str(exc.amount*self.input3[0], 3))
        unip_sd.append(eng_str(exc.uncertainty['scale']*self.input3[0], 3))
    unip_table = pd.DataFrame([unip_u, unip_v, unip_sd], ['Unit', 'Amount', 'Standard deviation'], unip_n).T

    if yes_no == 'yes':
        unip_table.to_latex(filename1)
    else:
        pass
    return unip_table


def get_econ(self, input1, input2):
    """

    A function that returns the cost of separator in euro/kg input.

    """
    if input1 == 'decanter 1' or input1 == 'decanter 2':
        inv_cost = 0.148e6 * input2
        # fx_cost = 0.018 * input2 * 24*365
        op_cost = inv_cost*0.03
    elif input1 == 'screw press 1' or input1 == 'screw press 2':
        inv_cost = 0.071e6 * input2
        # fx_cost = 0.018 * input2 * 24*365
        op_cost = inv_cost*0.03
    else:
        print('ERROR IN INPUT TO SEPARATOR TYPE INPUT (elementary flow)!!!!')
        sys.exit()

    return inv_cost, op_cost
```

II. Agricultural System Models

The bioenergy system models is split into three classes: organic fertilizers, biochar and mineral fertilizers.

```
import pandas as pd
import numpy as np
import sys

from DatabaseSearch import *
from utilities import lci_write, lci_write_uncert, calcLCA_tot, calcLCA_uniProc, eng_str
from resources import hm_nitrogen, hm_phosphorus, hm_potassium
from copy import deepcopy

class OrganicFertilizer:
    """

    A class that builds organic fertilizer LCI dataset based biomass composition.
    ** This includes all manure sourced inputs, straw and biochar.
        1) To establish the unit process of this component,
        2) To establish the chemical composition at the outlet,
        3) Extract the LCI data to use in LCIA.
        4) Update LCI data and assign uncertainties.
        5) Write LCI data to LaTex.

    """

    def __init__(self, input1, input2, input3, input4):
        self.input1 = input1 #String statement, resource type (e.g. 'rawManure').
        self.input2 = input2 #String statement, separator type (e.g. 'decanter').
        self.input3 = deepcopy(input3) #Pandas dataframe, DM, C, N, K, P info.
        self.input5 = input4 #String statement, are solids combusted.


    def unit_process(self):
        """

        A function that make the LCI unit process for the organic fertilizer class.

        """

        if self.input1 == 'rawManure' or self.input1 == 'lmManure' or \
                        self.input1 == 'ldManure' or self.input1 == 'dManure':
            DM = (self.input3[0]-self.input3[1][0].M)/self.input3[0]
            density = 100 / ((DM*100) / 2500  + (100 - (DM*100)) / 1000)
            application = ['market for liquid manure spreading, by vacuum tanker',
                    'cubic meter', 'GLO']
            activity = technosphereData(application)
            dictStruc = {activity: 1.0/float(density)}
            unitProcess = pd.DataFrame(dictStruc,
                                       index = [self.input1+' application']).T
            return unitProcess

        elif self.input1 == 'straw':
            application = ['tillage, harrowing, by rotary harrow',
                           'hectare', 'GLO']
            activity = technosphereData(application)
            dictStruc = {activity: 0.00039101*0.55}
            unitProcess = pd.DataFrame(dictStruc,
                                       index = [self.input1+' drill-down']).T

            return unitProcess

        else:
            application = ['market for solid manure loading and spreading, by hydraulic loader and spreader',
                    'kilogram', 'GLO']
            activity = technosphereData(application)
            dictStruc = {activity: 1.0}
            unitProcess = pd.DataFrame(dictStruc,
                                       index = [self.input1+' application']).T


            return unitProcess


    def elementary_flow(self):
        """

        A function that make the LCI elementary flows for the storage tank class.

        """
        rts = pd.read_csv('climate_indicators.csv', index_col=0).sum()
        C_CO2 = float(12.0107)/float(2*15.9994+12.0107)

        N2O = ['Dinitrogen monoxide', 'air', 'non-urban air or from high stacks']
        NH3 = ['Ammonia', 'air', 'non-urban air or from high stacks']
        NOx = ['Nitrogen oxides', 'air', 'non-urban air or from high stacks']
        NO3 = ['Nitrate', 'water', 'ground-']
        N2 = ['Nitrogen', 'air']
        emissions1 = [N2O, NH3, NOx, NO3, N2]

        mass_inp = deepcopy(self.input3[0])
        C_inp = deepcopy(self.input3[1][0].C)/mass_inp
```

```
N_inp = deepcopy(self.input3[1][0].N)/mass_inp
P_inp = (deepcopy(self.input3[1][1].P2O5) / 2.29)/mass_inp

n_index = []
for i in np.arange(len(emissions1)):
    n_index.append(biosphereData_exact(emissions1[i]))

if self.input5 == 'Biochar':
    CO2 = C_inp*rts['Biochar']*(1.0/C_CO2)
    CO2_seq = C_inp*rts['1 year']*(1.0/C_CO2)

elif self.input5 == 'Biochar [combustion]':
    CO2 = C_inp*rts['Biochar']*(1.0/C_CO2)
    CO2_seq = C_inp*rts['1 year']*(1.0/C_CO2)

elif self.input5 == 'Straw':
    CO2 = C_inp*rts['Plant residue']*(1.0/C_CO2)
    CO2_seq = C_inp*rts['1 year']*(1.0/C_CO2)

    default_CN = 6.8651669019
    CN_to_default = (C_inp/N_inp) / default_CN

else:
    CO2 = C_inp*rts['Manure']*(1.0/C_CO2)
    CO2_seq = C_inp*rts['1 year']*(1.0/C_CO2)

    default_CN = 6.8651669019
    CN_to_default = (C_inp/N_inp) / default_CN

CO2_emi = ['Carbon dioxide, from soil or biomass stock', 'air',
           'low population density, long-term']
c_index = biosphereData(CO2_emi)

Cd = ['Cadmium', 'soil', 'agricultural']
Cu = ['Copper', 'soil', 'agricultural']
Zn = ['Zinc', 'soil', 'agricultural']
Pb = ['Lead', 'soil', 'agricultural']
Ni = ['Nickel', 'soil', 'agricultural']
Cr = ['Chromium', 'soil', 'agricultural']
Hg = ['Mercury', 'soil', 'agricultural']
hm_emissions1 = [Cd, Cu, Zn, Pb, Ni, Cr, Hg]

hm_index = []
for i in np.arange(len(hm_emissions1)):
    hm_index.append(biosphereData(hm_emissions1[i]))

if 'Biochar' == self.input5:
    NO3N =  -0.1*C_inp*0.25*0.5
    N2ON_ind = 0.0075*NO3N
    N2ON = N2ON_ind
    N2O = N2ON*(44.01280/14.0067)
    NO3 = NO3N*(62.0049/14.0067)
    NH3 = 0.0
    NOx = 0.0
    N2 = 0.0

elif self.input1 == 'rawManure':
    default_N = 156 #Nitrogen fertilizer per hectare
    NH4N = N_inp*0.79
    N2ON_dir = N_inp*0.01
    NH3N= NH4N*0.138 #For whole crop rotation.
    NOxN = 0.1*N2ON_dir
    N2N = 4.5*N2ON_dir
    NO3N =  21.37*(N_inp/default_N)+(0.0037*(765.0/(12.0*1.7))*
              (N_inp-N_inp*0.392*0.75))+ \
              (N_inp - NOxN - NH3N - N2ON_dir - N2N -
               N_inp*0.392*0.75-0.1*C_inp*0.25)*0.5
    N2ON_ind = 0.01*(NH3N+NOxN)+0.0075*NO3N
    N2ON = N2ON_dir + N2ON_ind
    N2O = N2ON*(44.01280/14.0067)
    NO3 = NO3N*(62.0049/14.0067)
    NH3 = NH3N*(17.03052/14.0067)
    NOx = NOxN*(30.00610/14.0067)
    N2 = N2N

elif CN_to_default <= 1.0:
    default_N = 156 #Nitrogen fertilizer per hectare
    NH4N_1 = N_inp*0.79
    N2ON_dir = N_inp*0.01
    NH3N_1 = NH4N_1*0.138*0.5
    NH3N_2 = N_inp*0.02
    NH3N = NH3N_1*(1-CN_to_default)+NH3N_2*CN_to_default
    NOxN = 0.1*N2ON_dir
    N2N = 4.5*N2ON_dir
    NO3N_1 = 21.37*(N_inp/default_N)+(0.0037*(765.0/(12.0*1.7))*
                                                (N_inp-N_inp*0.392*0.75))+ \
              (N_inp - NOxN - NH3N - N2ON_dir - N2N -
               N_inp*0.392*0.75-0.1*C_inp*0.25)*0.5
```

```
        NO3N_2 = 21.37*(N_inp/default_N)+(0.0037*(765.0/(12.0*1.7))*
                                                (N_inp-N_inp*0.392))+ \
                 (N_inp - NOxN - NH3N - N2ON_dir - N2N -
                  N_inp*0.392)*0.5
        NO3N = (NO3N_1*(1-CN_to_default)+NO3N_2*CN_to_default)
        N2ON_ind = 0.01*(NH3N+NOxN)+0.0075*NO3N
        N2ON = N2ON_dir + N2ON_ind
        N2O = N2ON*(44.01280/14.0067)
        NO3 = NO3N*(62.0049/14.0067)
        NH3 = NH3N*(17.03052/14.0067)
        NOx = NOxN*(30.00610/14.0067)
        N2 = N2N

    elif CN_to_default > 1.0:
        if self.input1 == 'straw':
            Nmineral = (1-0.7)*N_inp
            default_N = 156 #Nitrogen fertilizer per hectare
            NH4N = Nmineral*0.79
            N2ON_dir = Nmineral*0.01
            NH3N= NH4N*0.138 #For whole crop rotation.
            NOxN = 0.1*N2ON_dir
            N2N = 4.5*N2ON_dir
            NO3N =  21.37*(Nmineral/default_N)+(0.0037*(765.0/(12.0*1.7))*
                     (Nmineral-Nmineral*0.69))+ \
                     (Nmineral - NOxN - NH3N - N2ON_dir - N2N -
                      Nmineral*0.392)*0.5
            N2ON_ind = 0.01*(NH3N+NOxN)+0.0075*NO3N
            N2ON = N2ON_dir + N2ON_ind
            N2O = N2ON*(44.01280/14.0067)
            NO3 = NO3N*(62.0049/14.0067)
            NH3 = NH3N*(17.03052/14.0067)
            NOx = NOxN*(30.00610/14.0067)
            N2 = N2N

        else:
            default_N = 156 #Nitrogen fertilizer per hectare
            NH4N = N_inp*0.25
            N2ON_dir = N_inp*0.01
            NH3N= NH4N*0.40 #For whole crop rotation.
            NOxN = 0.1*N2ON_dir
            N2N = 4.5*N2ON_dir
            NO3N =  21.37*(N_inp/default_N)+(0.0037*(765.0/(12.0*1.7))*
                     (N_inp-N_inp*0.392*0.75))+ \
                     (N_inp - NOxN - NH3N - N2ON_dir - N2N -
                      N_inp*0.392*0.75-0.1*C_inp*0.25)*0.5
            if NO3N < 0:
                NO3N = 0
            N2ON_ind = 0.01*(NH3N+NOxN)+0.0075*NO3N
            N2ON = N2ON_dir + N2ON_ind
            N2O = N2ON*(44.01280/14.0067)
            NO3 = NO3N*(62.0049/14.0067)
            NH3 = NH3N*(17.03052/14.0067)
            NOx = NOxN*(30.00610/14.0067)
            N2 = N2N

    else:
        print('ERROR IN INPUT TO ORGANIC FERTILIZER INPUT 1 !!!')
        sys.exit()

    nitrogenEmission = pd.DataFrame([N2O, NH3, NOx, NO3, N2],
                                    index = [n_index] ,
                                    columns = [self.input1+' field emissions'])

    p_nam = 'Phosphorus', 'water', 'surface water'
    p_index = biosphereData_exact(p_nam)
    p_dict = {p_index: P_inp * 0.03}
    phosphorusEmission = pd.DataFrame(pd.Series(p_dict))
    phosphorusEmission.columns = [self.input1+' field emissions']

    heavyM = deepcopy(self.input3[1][2]) / mass_inp

    heavymetalsEmission = pd.DataFrame([heavyM.Cd, heavyM.Cu, heavyM.Zn,
                                        heavyM.Pb, heavyM.Ni, heavyM.Cr,
                                        heavyM.Hg], index=[hm_index],
                                        columns = [self.input1+' field emissions'])


    carbonEmission = pd.DataFrame({c_index: CO2-CO2_seq}, [self.input1+' field emissions'])

    elementaryFlow = pd.concat([nitrogenEmission, carbonEmission.T,
                                phosphorusEmission, heavymetalsEmission], axis=0)

    return elementaryFlow


def get_lci(self):
    """
```

```
    A function that returns the LCI dataset of the organic fertilizer class.

    """
    db = Database(self.input1+' ['+self.input2+"] fertilizer")

    if db.load() == {}:
        LCI_1 = self.unit_process(); LCI_1.columns = [self.input1+' ['+self.input2+"] fertilizer"]
        LCI_2 = self.elementary_flow(); LCI_2.columns = [self.input1+' ['+self.input2+"] fertilizer"]
        lci_write([LCI_1, LCI_2], self.input1+' ['+self.input2+"] fertilizer",
                  u'volume', u'kilogram', self.input1+' ['+self.input2+"] fertilizer")
        db = Database(self.input1+' ['+self.input2+"] fertilizer")
        IP0 = db.query(NF(self.input1+' ['+self.input2+"] fertilizer"))
        activity = db.get(next(iter(IP0.keys()))[1])
        uniProc = pd.Series({activity:self.input3[0]})
    else:
        IP0 = db.query(NF(self.input1+' ['+self.input2+"] fertilizer"))
        activity = db.get(next(iter(IP0.keys()))[1])
        uniProc = pd.Series({activity:self.input3[0]})

    return uniProc


def update_database(self):
    """

    A function that updates the database built by the organic fertilizer class and
    assigns uncertainty factors.

    """

    uncert_int = pd.read_excel('uncertainty_agriculture_new.xlsx')
    uncert_fact_uni = [uncert_int['sd']['Working material']]
    uncert_fact_ele = [uncert_int['sd']['N2O'], uncert_int['sd']['NH3'],
                       uncert_int['sd']['NOX'], uncert_int['sd']['NO3'],
                       uncert_int['sd']['N2'], uncert_int['sd']['CO2'],
                       uncert_int['sd']['P'], uncert_int['sd']['Cd'],
                       uncert_int['sd']['Cu'], uncert_int['sd']['Zn'],
                       uncert_int['sd']['Pd'], uncert_int['sd']['Ni'],
                       uncert_int['sd']['Cr'], uncert_int['sd']['Hg']]
    uncert_fact = [uncert_fact_uni, uncert_fact_ele]

    LCI_1 = self.unit_process(); LCI_1.columns = [self.input1+' ['+self.input2+"] fertilizer"]
    LCI_2 = self.elementary_flow(); LCI_2.columns = [self.input1+' ['+self.input2+"] fertilizer"]
    lci_write_uncert([LCI_1, LCI_2], self.input1+' ['+self.input2+"] fertilizer",
              u'volume', u'kilogram', self.input1+' ['+self.input2+"] fertilizer", uncert_fact)


def replacement_value(self):
    """

    A function find the substitution value of the organic fertilizer to replace
    mineral fertilizers.

    """
    N_inp = self.input3[1][0].N
    P = self.input3[1][1].P2O5 / 2.29
    K = self.input3[1][1].K2O / 1.20

    if self.input5 == 'Straw':
        N = N_inp *0.30 * (0.69/0.392)
        mass = sum([N, P, K])

        return pd.DataFrame([mass, N, P, K],
                            ['mass', 'N', 'P', 'K'], ['Mineral']).T

    if self.input5 == 'ldMixture':
        N = N_inp*0.75*0.38*0.30*(0.69/0.392) + N_inp*(1-0.38)*0.75
        mass = sum([N, P, K])

        return pd.DataFrame([mass, N, P, K],
                            ['mass', 'N', 'P', 'K'], ['Mineral']).T

    elif 'Biochar' in self.input5:
        N = -0.0
        mass = sum([N, P, K])

        return pd.DataFrame([mass, N, P, K],
                            ['mass', 'N', 'P', 'K'], ['Mineral']).T

    elif self.input5 == 'Solids_combusted':
        if self.input1 == 'sdManure' or self.input1 == 'ldManure':
            N = N_inp*0.85 * 1.11
        else:
            N = N_inp*0.85
        mass = sum([N, P, K])

        return pd.DataFrame([mass, N, P, K],
                            ['mass', 'N', 'P', 'K'], ['Mineral']).T
```

```
        elif self.input5 == 'Solids_to_field':
            if self.input1 == 'sdManure' or self.input1 == 'ldManure':
                N = N_inp*0.75 * 1.11
            else:
                N = N_inp*0.75
            mass = sum([N, P, K])

            return pd.DataFrame([mass, N, P, K],
                                ['mass', 'N', 'P', 'K'], ['Mineral']).T
        else:
            print('ERROR IN INPUT TO ORGANIC FERTILIZER INPUT 3 !!!')
            sys.exit()


    def get_lcia(self, input1, input2):
        """

        A function that returns the LCIA results of all associated with all unit processes and
        elementary flows.

        """
        method = input1
        if input2 == 'simple':
            lci = self.get_lci()

            return calcLCA_uniProc(method, lci)

        elif input2 =='full':
            LCI_1 = self.unit_process()*self.input3[0]
            LCI_2 = self.elementary_flow()*self.input3[0]

            return calcLCA_tot(method, LCI_1.T.sum(), LCI_2.T.sum())

    def lci_to_latex(self, filename1, filename2, yes_no):
        """

        A function that returns the LCI data in a LaTex table.

        """
        activity5 = self.get_lci()
        unip_n, unip_u, unip_v, unip_sd = [], [], [], []
        for exc in activity5.index[0].technosphere():
            unip_n.append(exc.input['name'])
            unip_u.append(exc.input['unit'])
            unip_v.append(eng_str(exc.amount*self.input3[0], 3))
            unip_sd.append(eng_str(exc.uncertainty['scale']*self.input3[0], 3))
        unip_table = pd.DataFrame([unip_u, unip_v, unip_sd], ['Unit', 'Amount', 'Standard deviation'], unip_n).T

        if yes_no == 'yes':
            unip_table.to_latex(filename1)
        else:
            pass

        elem_n, elem_u, elem_v, elem_sd = [], [], [], []
        for exc in activity5.index[0].biosphere():
            elem_n.append(exc.input['name']+' to '+exc.input['categories'][0])
            elem_u.append(exc.input['unit'])
            elem_v.append(eng_str(exc.amount*self.input3[0], 3))
            elem_sd.append(eng_str(exc.uncertainty['scale']*self.input3[0], 3))
        elem_table = pd.DataFrame([elem_u, elem_v, elem_sd], ['Unit', 'Amount', 'Standard deviation'], elem_n).T

        if yes_no == 'yes':
            elem_table.to_latex(filename2)
        else:
            pass
        return unip_table, elem_table


class Biochar:
    """

    A class that builds organic fertilizer LCI dataset based biomass composition.
    ** This includes all manure sourced inputs, straw and biochar.
        1) To establish the unit process of this component,
        2) To establish the chemical composition at the outlet,
        3) Extract the LCI data to use in LCIA.
        4) Update LCI data and assign uncertainties.
        5) Write LCI data to LaTex.

    """

    def __init__(self, input1, input3, input6):
        self.input1 = input1
        self.input3 = deepcopy(input3) #Pandas dataframe, DM, C, N, K, P info.
        self.input6 = input6
```

```
def unit_process(self):
    """

    A function that make the LCI unit process for the organic fertilizer class.

    """

    application = ['market for solid manure loading and spreading, by hydraulic loader and spreader',
            'kilogram', 'GLO']
    activity = technosphereData(application)
    dictStruc = {activity: 1.0}
    unitProcess = pd.DataFrame(dictStruc,
                               index = [self.input1+' application']).T


    return unitProcess


def elementary_flow(self):
    """

    A function that make the LCI elementary flows for the storage tank class.

    """
    rts = pd.read_csv('climate_indicators.csv', index_col=0).sum()
    C_CO2 = float(12.0107)/float(2*15.9994+12.0107)

    N2O = ['Dinitrogen monoxide', 'air', 'non-urban air or from high stacks']
    NH3 = ['Ammonia', 'air', 'non-urban air or from high stacks']
    NOx = ['Nitrogen oxides', 'air', 'non-urban air or from high stacks']
    NO3 = ['Nitrate', 'water', 'ground-']
    N2 = ['Nitrogen', 'air']
    emissions1 = [N2O, NH3, NOx, NO3, N2]


    C_inp = self.input3[1][0].C/self.input3[0]
    N_inp = self.input3[1][0].N/self.input3[0]
    P_inp = (self.input3[1][1].P2O5 / 2.29)/self.input3[0]

    n_index = []
    for i in np.arange(len(emissions1)):
        n_index.append(biosphereData_exact(emissions1[i]))

    CO2 = C_inp*rts['Biochar']*(1.0/C_CO2)
    CO2_seq = C_inp*rts['1 year']*(1.0/C_CO2)

    CO2_emi = ['Carbon dioxide, from soil or biomass stock', 'air',
               'low population density, long-term']
    c_index = biosphereData(CO2_emi)

    Cd = ['Cadmium', 'soil', 'agricultural']
    Cu = ['Copper', 'soil', 'agricultural']
    Zn = ['Zinc', 'soil', 'agricultural']
    Pb = ['Lead', 'soil', 'agricultural']
    Ni = ['Nickel', 'soil', 'agricultural']
    Cr = ['Chromium', 'soil', 'agricultural']
    Hg = ['Mercury', 'soil', 'agricultural']
    hm_emissions1 = [Cd, Cu, Zn, Pb, Ni, Cr, Hg]

    hm_index = []
    for i in np.arange(len(hm_emissions1)):
        hm_index.append(biosphereData(hm_emissions1[i]))

    NO3N =  -0.1*C_inp*0.25*0.5
    N2ON_ind = 0.0075*NO3N
    N2ON = N2ON_ind
    N2O = N2ON*(44.01280/14.0067)
    NO3 = NO3N*(62.0049/14.0067)
    NH3 = 0.0
    NOx = 0.0
    N2 = 0.0


    nitrogenEmission = pd.DataFrame([N2O, NH3, NOx, NO3, N2],
                                    index = [n_index] ,
                                    columns = [self.input1+' field emissions '+self.input6])

    p_nam = 'Phosphorus', 'water', 'surface water'
    p_index = biosphereData_exact(p_nam)
    p_dict = {p_index: P_inp * 0.03}
    phosphorusEmission = pd.DataFrame(pd.Series(p_dict))
    phosphorusEmission.columns = [self.input1+' field emissions '+self.input6]

    heavyM = self.input3[1][2] / self.input3[0]

    heavymetalsEmission = pd.DataFrame([heavyM.Cd, heavyM.Cu, heavyM.Zn,
                                        heavyM.Pb, heavyM.Ni, heavyM.Cr,
                                        heavyM.Hg], index=[hm_index],
```

```
                                    columns = [self.input1+' field emissions '+self.input6])

    carbonEmission = pd.DataFrame({c_index: CO2-CO2_seq}, [self.input1+' field emissions '+self.input6])

    elementaryFlow = pd.concat([nitrogenEmission, carbonEmission.T,
                                phosphorusEmission, heavymetalsEmission], axis=0)

    return elementaryFlow


def get_lci(self):
    """

    A function that returns the LCI dataset of the organic fertilizer class.

    """
    db = Database(self.input1+' ['+self.input6+"] fertilizer")

    if db.load() == {}:
        LCI_1 = self.unit_process(); LCI_1.columns = [self.input1+' ['+self.input6+"] fertilizer"]
        LCI_2 = self.elementary_flow(); LCI_2.columns = [self.input1+' ['+self.input6+"] fertilizer"]
        lci_write([LCI_1, LCI_2], self.input1+' ['+self.input6+"] fertilizer",
                  u'volume', u'kilogram', self.input1+' ['+self.input6+"] fertilizer")
        db = Database(self.input1+' ['+self.input6+"] fertilizer")
        IP0 = db.query(NF(self.input1+' ['+self.input6+"] fertilizer"))
        activity = db.get(next(iter(IP0.keys()))[1])
        uniProc = pd.Series({activity:self.input3[0]})
    else:
        IP0 = db.query(NF(self.input1+' ['+self.input6+"] fertilizer"))
        activity = db.get(next(iter(IP0.keys()))[1])
        uniProc = pd.Series({activity:self.input3[0]})

    return uniProc


def update_database(self):
    """

    A function that updates the database built by the organic fertilizer class and
    assigns uncertainty factors.

    """

    uncert_int = pd.read_excel('uncertainty_agriculture_new.xlsx')
    uncert_fact_uni = [uncert_int['sd']['Working material']]
    uncert_fact_ele = [uncert_int['sd']['N2O'], uncert_int['sd']['NH3'],
                       uncert_int['sd']['NOX'], uncert_int['sd']['NO3'],
                       uncert_int['sd']['N2'], uncert_int['sd']['CO2'],
                       uncert_int['sd']['P'], uncert_int['sd']['Cd'],
                       uncert_int['sd']['Cu'], uncert_int['sd']['Zn'],
                       uncert_int['sd']['Pd'], uncert_int['sd']['Ni'],
                       uncert_int['sd']['Cr'], uncert_int['sd']['Hg']]
    uncert_fact = [uncert_fact_uni, uncert_fact_ele]

    LCI_1 = self.unit_process(); LCI_1.columns = [self.input1+' ['+self.input6+"] fertilizer"]
    LCI_2 = self.elementary_flow(); LCI_2.columns = [self.input1+' ['+self.input6+"] fertilizer"]
    lci_write_uncert([LCI_1, LCI_2], self.input1+' ['+self.input6+"] fertilizer",
              u'volume', u'kilogram', self.input1+' ['+self.input6+"] fertilizer", uncert_fact)


def replacement_value(self):
    """

    A function find the substitution value of the organic fertilizer to replace
    mineral fertilizers.

    """
    P = self.input3[1][1].P2O5 / 2.29
    K = self.input3[1][1].K2O / 1.20

    N = -0.0
    mass = sum([N, P, K])

    return pd.DataFrame([mass, N, P, K],
                        ['mass', 'N', 'P', 'K'], ['Mineral']).T


def get_lcia(self, input1, input2):
    """

    A function that returns the LCIA results of all associated with all unit processes and
    elementary flows.

    """
    method = input1
    if input2 == 'simple':
        lci = self.get_lci()
```

```
            return calcLCA_uniProc(method, lci)

        elif input2 =='full':
            LCI_1 = self.unit_process()*self.input3[0]
            LCI_2 = self.elementary_flow()*self.input3[0]

            return calcLCA_tot(method, LCI_1.T.sum(), LCI_2.T.sum())

    def lci_to_latex(self, filename1, filename2, yes_no):
        """

        A function that returns the LCI data in a LaTex table.

        """
        activity5 = self.get_lci()
        unip_n, unip_u, unip_v, unip_sd = [], [], [], []
        for exc in activity5.index[0].technosphere():
            unip_n.append(exc.input['name'])
            unip_u.append(exc.input['unit'])
            unip_v.append(eng_str(exc.amount*self.input3[0], 3))
            unip_sd.append(eng_str(exc.uncertainty['scale']*self.input3[0], 3))
        unip_table = pd.DataFrame([unip_u, unip_v, unip_sd], ['Unit', 'Amount', 'Standard deviation'], unip_n).T

        if yes_no == 'yes':
            unip_table.to_latex(filename1)
        else:
            pass

        elem_n, elem_u, elem_v, elem_sd = [], [], [], []
        for exc in activity5.index[0].biosphere():
            elem_n.append(exc.input['name']+' to '+exc.input['categories'][0])
            elem_u.append(exc.input['unit'])
            elem_v.append(eng_str(exc.amount*self.input3[0], 3))
            elem_sd.append(eng_str(exc.uncertainty['scale']*self.input3[0], 3))
        elem_table = pd.DataFrame([elem_u, elem_v, elem_sd], ['Unit', 'Amount', 'Standard deviation'], elem_n).T

        if yes_no == 'yes':
            elem_table.to_latex(filename2)
        else:
            pass
        return unip_table, elem_table


class MineralFertilizer:
    """

    A class that builds mineral fertilizer (replaced) LCI dataset substitution
    value of the organic fertilizer.
        1) To establish the unit process of this component,
        2) To establish the chemical composition at the outlet,
        3) Extract the LCI data to use in LCIA.
        4) Update LCI data and assign uncertainties.
        5) Write LCI data to LaTex.

    """

    def __init__(self, input1, input2, input3):
        self.input1 = input1 #String statement, source resource type (e.g. 'rawManure').
        self.input2 = input2 #String statement, source separator type (e.g. 'decanter').
        self.input3 = deepcopy(input3) #Pandas dataframe, DM, C, N, K, P info.

    def unit_process(self):
        """

        A function that make the LCI unit process for the organic fertilizer class.

        """

        defaultN = 156
        defaultP = 22
        defaultK = 72
        passes_per_kg = 3.83/(sum([defaultN, defaultP, defaultK]))

        mass_inp = deepcopy(self.input3.mass[0])
        N_inp = deepcopy(self.input3.N[0]) / mass_inp
        P_inp = deepcopy(self.input3.P[0]) / mass_inp
        K_inp = deepcopy(self.input3.K[0]) / mass_inp

        if self.input1 == 'straw':
            baling = ['market for baling', 'unit', 'GLO']
            loading = ['market for bale loading', 'unit', 'GLO']
            application = ['market for fertilising, by broadcaster', 'hectare', 'GLO']
            Nfert = ['market for nitrogen fertiliser, as N',
                    'kilogram', 'GLO']
            Pfert = ['market for phosphate fertiliser, as P2O5',
                    'kilogram', 'GLO']
```

```
        Kfert = ['market for potassium fertiliser, as K2O',
                 'kilogram', 'GLO']
        processes = [baling, loading, application, Nfert, Pfert, Kfert]

        activities = []
        for i in np.arange(len(processes)):
            activities.append(technosphereData_exact(processes[i]))

        unitProcess = pd.DataFrame([0.00144, 0.00625, passes_per_kg, N_inp, P_inp, K_inp],
                                   index = [activities] ,
                                   columns = [self.input1+' fertilizers, -mineral'])
    else:
        application = ['market for fertilising, by broadcaster', #Put in broadcaster
                'hectare', 'GLO']
        Nfert = ['market for nitrogen fertiliser, as N',
                 'kilogram', 'GLO']
        Pfert = ['market for phosphate fertiliser, as P2O5',
                 'kilogram', 'GLO']
        Kfert = ['market for potassium fertiliser, as K2O',
                 'kilogram', 'GLO']
        processes = [application, Nfert, Pfert, Kfert]

        activities = []
        for i in np.arange(len(processes)):
            activities.append(technosphereData_exact(processes[i]))

        unitProcess = pd.DataFrame([passes_per_kg, N_inp, P_inp, K_inp],
                                   index = [activities] ,
                                   columns = [self.input1+' fertilizers, -mineral'])
    return unitProcess


def elementary_flow(self):
    """

    A function that make the LCI elementary flows for the storage tank class.
    ** This functino also returns the value of the biomass at outlet.

    """
    mass_inp = deepcopy(self.input3.mass[0])
    N_inp = deepcopy(self.input3.N[0]) / mass_inp
    P_inp = deepcopy(self.input3.P[0]) / mass_inp
    K_inp = deepcopy(self.input3.K[0]) / mass_inp

    N2O = ['Dinitrogen monoxide', 'air', 'non-urban air or from high stacks']
    NH3 = ['Ammonia', 'air', 'non-urban air or from high stacks']
    NOx = ['Nitrogen oxides', 'air', 'non-urban air or from high stacks']
    NO3 = ['Nitrate', 'water', 'ground-']
    N2 = ['Nitrogen', 'air']
    emissions1 = [N2O, NH3, NOx, NO3, N2]

    n_index = []
    for i in np.arange(len(emissions1)):
        n_index.append(biosphereData_exact(emissions1[i]))

    Cd = ['Cadmium', 'soil', 'agricultural']
    Cu = ['Copper', 'soil', 'agricultural']
    Zn = ['Zinc', 'soil', 'agricultural']
    Pb = ['Lead', 'soil', 'agricultural']
    Ni = ['Nickel', 'soil', 'agricultural']
    Cr = ['Chromium', 'soil', 'agricultural']
    Hg = ['Mercury', 'soil', 'agricultural']
    hm_emissions1 = [Cd, Cu, Zn, Pb, Ni, Cr, Hg]

    hm_index = []
    for i in np.arange(len(hm_emissions1)):
        hm_index.append(biosphereData(hm_emissions1[i]))

    default_N = 156 #Nitrogen fertilizer per hectare
    NH4N = N_inp*0.79
    N2ON_dir = N_inp*0.01
    NH3N= NH4N*0.138 #For whole crop rotation.
    NOxN = 0.1*N2ON_dir
    N2N = 4.5*N2ON_dir

    NO3N =  21.37*(N_inp/default_N)+(0.0037*(765.0/(12.0*1.7))*
              (N_inp-N_inp*0.392))+ \
              (N_inp - NOxN - NH3N - N2ON_dir - N2N -
               N_inp*0.392)*0.5
    N2ON_ind = 0.01*(NH3N+NOxN)+0.0075*NO3N
    N2ON = N2ON_dir + N2ON_ind

    N2O = N2ON*(44.01280/14.0067)
    NO3 = NO3N*(62.0049/14.0067)
    NH3 = NH3N*(17.03052/14.0067)
    NOx = NOxN*(30.00610/14.0067)
    N2 = N2N
```

```
        nitrogenEmission = pd.DataFrame([N2O, NH3, NOx, NO3, N2],
                                        index = [n_index] ,
                                        columns = [self.input1+' field emissions, -mineral'])

        p_nam = 'Phosphorus', 'water', 'surface water'
        p_index = biosphereData_exact(p_nam)
        p_dict = {p_index:P_inp * 0.03}
        phosphorusEmission = pd.DataFrame(pd.Series(p_dict))
        phosphorusEmission.columns = [self.input1+' field emissions, -mineral']

        heavy_N = hm_nitrogen('mass', N_inp)
        heavy_P = hm_phosphorus('mass', P_inp)
        heavy_K = hm_potassium('mass', K_inp)
        heavy = heavy_N + heavy_P + heavy_K

        heavymetalsEmission = pd.DataFrame(list(heavy.values), index=[hm_index],
                                           columns = [self.input1+' field emissions, -mineral'])

        elementaryFlow = pd.DataFrame(pd.concat([nitrogenEmission, phosphorusEmission,
                                    heavymetalsEmission], axis=0).T.sum())
        elementaryFlow.columns=[self.input1+' field emissions, -mineral']

        return elementaryFlow


    def get_lci(self):
        """

        A function that returns the LCI dataset of the storage tank class.

        """
        mass_inp = self.input3.mass[0]
        db = Database(self.input1+' ['+self.input2+'] fertilizer, -mineral')
        if db.load() == {}:

            LCI_1 = self.unit_process(); LCI_1.columns = [self.input1+' ['+self.input2+'] fertilizer, -mineral']
            LCI_2 = self.elementary_flow(); LCI_2.columns = [self.input1+' ['+self.input2+'] fertilizer, -mineral']
            print(LCI_1, 'LCI_1')
            lci_write([LCI_1, LCI_2], self.input1+' ['+self.input2+'] fertilizer, -mineral',
                      u'volume', u'kilogram', "Mineral fertilizer, "+self.input1)
            db = Database(self.input1+' ['+self.input2+'] fertilizer, -mineral')
            IP0 = db.query(NF(self.input1+' ['+self.input2+'] fertilizer, -mineral'))
            activity = db.get(next(iter(IP0.keys()))[1])
            uniProc = pd.Series({activity:-mass_inp})
        else:
            IP0 = db.query(NF(self.input1+' ['+self.input2+'] fertilizer, -mineral'))
            activity = db.get(next(iter(IP0.keys()))[1])
            uniProc = pd.Series({activity:-mass_inp})

        return uniProc


    def update_database(self):
        """

        A function that updates the database built by the mineral fertilizer (replaced) class and
        assigns uncertainty factors.

        """
        if self.input1 == 'straw':
            uncert_int = pd.read_excel('uncertainty_agriculture_new.xlsx')
            uncert_fact_uni = [uncert_int['sd']['Working material'], uncert_int['sd']['Working material'],
                               uncert_int['sd']['Working material2'], uncert_int['sd']['Working material2'],
                               uncert_int['sd']['Working material2'], uncert_int['sd']['Working material2']]

            uncert_fact_ele = [uncert_int['sd']['N2O'], uncert_int['sd']['NH3'],
                               uncert_int['sd']['NOX'], uncert_int['sd']['NO3'],
                               uncert_int['sd']['N2'],
                               uncert_int['sd']['P'], uncert_int['sd']['Cd'],
                               uncert_int['sd']['Cu'], uncert_int['sd']['Zn'],
                               uncert_int['sd']['Pd'], uncert_int['sd']['Ni'],
                               uncert_int['sd']['Cr'], uncert_int['sd']['Hg']]
            uncert_fact = [uncert_fact_uni, uncert_fact_ele]

        else:
            uncert_int = pd.read_excel('uncertainty_agriculture_new.xlsx')
            uncert_fact_uni = [uncert_int['sd']['Working material2'], uncert_int['sd']['Working material2'],
                               uncert_int['sd']['Working material2'], uncert_int['sd']['Working material2']]
            uncert_fact_ele = [uncert_int['sd']['N2O'], uncert_int['sd']['NH3'],
                               uncert_int['sd']['NOX'], uncert_int['sd']['NO3'],
                               uncert_int['sd']['N2'],
                               uncert_int['sd']['P'], uncert_int['sd']['Cd'],
                               uncert_int['sd']['Cu'], uncert_int['sd']['Zn'],
                               uncert_int['sd']['Pd'], uncert_int['sd']['Ni'],
                               uncert_int['sd']['Cr'], uncert_int['sd']['Hg']]
            uncert_fact = [uncert_fact_uni, uncert_fact_ele]

        LCI_1 = self.unit_process(); LCI_1.columns = [self.input1+' ['+self.input2+'] fertilizer, -mineral']
```

```
    LCI_2 = self.elementary_flow(); LCI_2.columns = [self.input1+' ['+self.input2+'] fertilizer, -mineral']
    lci_write_uncert([LCI_1, LCI_2], self.input1+' ['+self.input2+'] fertilizer, -mineral',
              u'volume', u'kilogram', "Mineral fertilizer, "+self.input1, uncert_fact)


def get_lcia(self, input1, input2):
    """

    A function that returns the LCIA results of all associated with all unit processes and
    elementary flows.

    """
    method = input1
    if input2 == 'simple':
        lci = self.get_lci()

        return calcLCA_uniProc(method, lci)

    elif input2 =='full':
        LCI_1 = self.unit_process()*self.input3.mass[0]
        LCI_2 = self.elementary_flow()*self.input3.mass[0]

        return calcLCA_tot(method, LCI_1.T.sum(), LCI_2.T.sum())


def lci_to_latex(self, filename1, filename2, yes_no):
    """

    A function that returns the LCI data in a LaTex table.

    """
    activity5 = self.get_lci()
    unip_n, unip_u, unip_v, unip_sd = [], [], [], []
    for exc in activity5.index[0].technosphere():
        unip_n.append(exc.input['name'])
        unip_u.append(exc.input['unit'])
        unip_v.append(eng_str(exc.amount*-self.input3.mass[0], 3))
        unip_sd.append(eng_str(exc.uncertainty['scale']*-self.input3.mass[0], 3))
    unip_table = pd.DataFrame([unip_u, unip_v, unip_sd], ['Unit', 'Amount', 'Standard deviation'], unip_n).T

    if yes_no == 'yes':
        unip_table.to_latex(filename1)
    else:
        pass

    elem_n, elem_u, elem_v, elem_sd = [], [], [], []
    for exc in activity5.index[0].biosphere():
        elem_n.append(exc.input['name']+' to '+exc.input['categories'][0])
        elem_u.append(exc.input['unit'])
        elem_v.append(eng_str(exc.amount*-self.input3.mass[0], 3))
        elem_sd.append(eng_str(exc.uncertainty['scale']*-self.input3.mass[0], 3))
    elem_table = pd.DataFrame([elem_u, elem_v, elem_sd], ['Unit', 'Amount', 'Standard deviation'], elem_n).T

    if yes_no == 'no':
        elem_table.to_latex(filename2)
    else:
        pass
    return unip_table, elem_table
```

III. Bridge to Other Software

Here the Python code made to bridge between the Dynamic Network Analysis (DNA) software is presented, along with the code made to bridge to the the C-TOOL software.

```
import os, glob
import shutil
import pandas as pd
import numpy as np
from copy import deepcopy
from resources import HHV, CP
import time

"""

A script that contains the Python to DNA bridge.

** Functions within this script:
    * Write the input to DNA based on chemical composition.
    * Asks DNA to simulate the thermal power plant based on inputs.
    * Asks DNA to simulate the biogas engine based on inputs.

"""

def DNA_input(elements):
    """

    A function that takes the chemimcal composition of the input flow to the thermal power plant
    and returns the input text required by DNA.

    """
    elements = deepcopy(elements)
    mass = elements[0]
    DM_tot = mass-elements[1][0].M

    C = np.round(elements[1][0].C/DM_tot,4)
    H = np.round(elements[1][0].H/DM_tot,4)
    O = np.round(elements[1][0].O/DM_tot,4)
    N = np.round(elements[1][0].N/DM_tot,4)
    S = np.round(elements[1][0].S/DM_tot,4)
    ASH = np.round(elements[1][0].A/DM_tot,4)

    ult = [C, O, H, N, S, ASH]
    HHV_dna = HHV(C, O, H, N, S, ASH)
    CP_bio = CP(15)
    MOI = elements[1][0].M / mass

    while np.round(sum(ult),4) < 1.0 or np.round(sum(ult),4) > 1.0:
        ult[1] = 1-ult[0]-ult[2]-ult[3]-ult[4]-ult[5]
        ult = np.round(ult,4)

    DNA_script = 'solid '+'sol'+' C '+str(ult[0])+' O '+str(ult[1])+' H '+str(ult[2])+' \n'\
    +'+ N '+str(ult[3])+' S '+str(ult[4])+' ASH '+str(ult[5])+'\n + HHV '+str(HHV_dna)+' CP '\
    +str(CP_bio)+' \n' \
    'addco m MIX 99 '+str(MOI)+' m MIX 98 '+str(1-MOI)

    return DNA_script


def pyroneer(resource, parameter1, parameter2, parameter3, parameter4, parameter5, parameter6):
    """

    A function that connects with DNA and askes it to simulate the thermal power plant.
    Along with post processing, returning the properties at each state of the power plant.

    """
    newpath = r'C:\\DNA\\hafthor\\case1'
    if not os.path.exists(newpath): os.makedirs(newpath)

    SRCfile = 'C:\\DNA\\simul\\hello\\hello.dna'
    TRGTfile = 'C:\\DNA\\hafthor\\cases\\' \
               'dryer_pyroneer_str.dna'
    UPDfile = 'C:\\DNA\\hafthor\\cases\\' \
               'dryer_pyroneer_str.upd'
    if os.path.exists(TRGTfile):
        os.remove(TRGTfile)

    if os.path.exists(UPDfile):
        os.remove(UPDfile)

    shutil.copyfile(SRCfile, TRGTfile)

    pyroneer = 'C:\\DNA\\hafthor\\Source\\' \
               'dryer_pyroneer_str.dna'

    f = open(TRGTfile, 'w')
    f.write(resource)
    f.write(parameter1)
    f.write(parameter2)
    f.write(parameter3)
    f.write(parameter4)
    f.write(parameter5)
    f.write(parameter6)
```

```
    f.write(open(pyroneer).read())
    f.close()

    while os.path.exists(UPDfile) == False:
        os.system("C:\\DNA\\bin\\dna.exe "+TRGTfile)
        for filename in glob.glob("C:/Users/LOCALA~1/AppData/Local/Temp/gfortrantmp*"):
            os.remove(filename)

    while os.path.exists(UPDfile) == False:
        os.system("C:\\DNA\\bin\\dna.exe "+TRGTfile)

    IDfile = 'C:\\DNA\\hafthor\\cases\\' \
             'dryer_pyroneer_str.id'
    copy = 'C:\\DNA\\hafthor\\cases\\COPY.id'
    if os.path.exists(copy):
        os.remove(copy)

    # Mark all relevant results to generate output
    f = open(IDfile, 'r+').read()
    m = f.replace('*','').replace('RUN NUMBER','RUN NUMBER *') \
        .replace('50','1000')
    fo = open(copy, 'w')
    fo.write(m)
    fo.close()

    to_skip = ["P", "PARAM", "ZA"]
    out_handle = open(IDfile, 'w')
    with open(copy, 'r') as handle:
        for line in handle:
            if set(line.split(' ')).intersection(to_skip):
                continue
            out_handle.write(line)
    out_handle.close()

    # Run the .id file with prepare.exe to generate result tables
    os.system("C:\\DNA\\bin\\prepare.exe C:\\DNA\\hafthor\\cases\\dryer_pyroneer_str")

    f00_file = 'C:\\DNA\\hafthor\\cases\\' \
               'dryer_pyroneer_str.f00'
    data = pd.read_table(f00_file, sep='\s+', header=None, skiprows=[0])
    values = data[3:].astype(float)
    cols = data[0:3].fillna('')

    columns = []
    for i in np.arange(len(cols.T)):
        columns.append(str(cols.values[0][i] + ' '
                           + str(cols.values[1][i] + ' '
                                 + str(cols.values[2][i]))))
    dna_data = pd.DataFrame(np.array(values), columns=columns)
    return dna_data


def biogas_engine(resource, parameter, num):
    """

    A function that connects with DNA and askes it to simulate the biogas engine.
    Along with post processing, returning the properties at input and output.

    """
    SRCfile = 'C:\\DNA\\simul\\hello\\hello.dna'
    TRGTfile = 'C:\\DNA\\hafthor\\biogas_engine' \
               '\\biogas_engine.dna'
    UPDfile = 'C:\\DNA\\hafthor\\biogas_engine' \
               '\\biogas_engine.upd'
    if os.path.exists(TRGTfile):
        os.remove(TRGTfile)
    if os.path.exists(UPDfile):
        os.remove(UPDfile)
    shutil.copyfile(SRCfile, TRGTfile)

    pyroneer = 'C:\\DNA\\hafthor\\Source' \
               '\\biogas_engine.dna'

    f = open(TRGTfile, 'w')
    f.write(resource)
    f.write(parameter)
    f.write(open(pyroneer).read())
    f.close()

    while os.path.exists(UPDfile) == False:
        os.system("C:\\DNA\\bin\\dna.exe "+TRGTfile)
        for filename in glob.glob("C:/Users/LOCALA~1/AppData/Local/Temp/gfortrantmp*"):
            os.remove(filename)

    # Copy the resulting .id file to a temporary file
    IDfile = 'C:\\DNA\\hafthor\\' \
             'biogas_engine\\biogas_engine.id'
    copy = 'C:\\DNA\\hafthor\\biogas_engine' \
```

```
        '\\COPY.id'
if os.path.exists(copy):
    os.remove(copy)

# Mark all relevant results to generate output
f = open(IDfile, 'r+').read()
m = f.replace('*','').replace('RUN NUMBER','RUN NUMBER *') \
    .replace('50','1000')#.replace('LHV','=') # stop marking at ZA
fo = open(copy, 'w')
fo.write(m)
fo.close()

to_skip = ["P", "PARAM", "ZA"]
out_handle = open(IDfile, 'w')
with open(copy, 'r') as handle:
    for line in handle:
        if set(line.split(' ')).intersection(to_skip):
            continue
        out_handle.write(line)
out_handle.close()

# Run the .id file with prepare.exe to generate result tables
os.system('C:\\DNA\\bin\\prepare.exe C:\\DNA\\hafthor\\\\biogas_engine\\biogas_engine')
f00_file = 'C:\\DNA\\hafthor\\biogas_engine\\biogas_engine.f00'

# Make a array of the parameters in the result tables
data = pd.read_table(f00_file, sep='\s+', header=None, skiprows=[0])
values = data[3:].astype(float)

cols = data[0:3].fillna('')
columns = []
for i in np.arange(len(cols.T)):
    columns.append(str(cols.values[0][i] + ' '
                       + str(cols.values[1][i] + ' '
                             + str(cols.values[2][i]))))
dna_data = pd.DataFrame(np.array(values), columns=columns)

return dna_data
```

```
import numpy as np
import pandas as pd
import os

"""

A script that contains the Python to C-TOOL bridge.

** Functions within this script:
    * Simulate the impulse response function.
    * Simulate the carbon decay in soil.
        ** For straw, manure and biochar
    * Simulate biochar decay in soil with varied parameters.

"""

def IRF(j):
    """

    A function that simulates the impulse response function.

    """
    result = 0.217 + 0.186 * np.exp(-(j+1)/1.186) + 0.338 * \
    np.exp(-(j+1)/18.51) + 0.259 * np.exp(-(j+1)/172.9)
    return result


def REF_plant(C):
    """

    A function that connects with C-TOOL and askes it to simulate straw decay in soil.
    Along with post processing, returning the emission profile.

    """
    fo = open('C:\\Users\\localadmin\\C-TOOL\\CN-SIM\\hafthor\\meaninp_fym1.dat', 'w')
    fo.write('8 1 PLANT '+str(C/1000)+' 1'); fo.close()

    os.system('C:\\Users\\localadmin\\C-TOOL\\ctool.exe C:\\Users\\localadmin\\C-TOOL\\CN-SIM\\')
    a = pd.read_table('C://Users//localadmin//C-TOOL//CN-SIM//hafthor//results.txt')
    x = a.values.T[3]*a.values.T[4]
    jnum = len(x)
    m = np.arange(1,jnum, 1)
    yy = [x[0]]; mm = [1]
    for j in m-1:
        yy.append(x[j+1]-x[j])
    for j in m:
        mm.append(0.217 + 0.186 * np.exp(-(j+1)/1.186) + 0.338 * \
        np.exp(-(j+1)/18.51) + 0.259 * np.exp(-(j+1)/172.9))
    nn = yy/yy[0]

    return nn


def REF_manure(C):
    """

    A function that connects with C-TOOL and askes it to simulate manure decay in soil.
    Along with post processing, returning the emission profile.

    """
    fo = open('C:\\Users\\localadmin\\C-TOOL\\CN-SIM\\hafthor\\meaninp_fym1.dat', 'w')
    fo.write('8 1 FYM '+str(C/1000)+' 1'); fo.close()

    os.system('C:\\Users\\localadmin\\C-TOOL\\ctool.exe C:\\Users\\localadmin\\C-TOOL\\CN-SIM\\')
    a = pd.read_table('C://Users//localadmin//C-TOOL//CN-SIM//hafthor//results.txt')
    x = a.values.T[3]*a.values.T[4]
    jnum = len(x)
    m = np.arange(1,jnum, 1)
    yy = [x[0]]; mm = [1]
    for j in m-1:
        yy.append(x[j+1]-x[j])
    for j in m:
        mm.append(0.217 + 0.186 * np.exp(-(j+1)/1.186) + 0.338 * \
        np.exp(-(j+1)/18.51) + 0.259 * np.exp(-(j+1)/172.9))
    nn = yy/yy[0]

    return nn


def REF_ash(C):
    """

    A function that connects with C-TOOL and askes it to simulate biochar decay in soil.
    Along with post processing, returning the emission profile.

    """
    fo = open('C:\\Users\\localadmin\\C-TOOL\\CN-SIM\\hafthor\\meaninp_fym1.dat', 'w')
    fo.write('8 1 ASH '+str(C/1000)+' 1'); fo.close()
```

```
    os.system('C:\\Users\\localadmin\\C-TOOL\\ctool.exe C:\\Users\\localadmin\\C-TOOL\\CN-SIM\\')
    a = pd.read_table('C://Users//localadmin//C-TOOL//CN-SIM//hafthor//results.txt')
    x = a.values.T[3]*a.values.T[4]
    jnum = len(x)
    m = np.arange(1,jnum, 1)
    yy = [x[0]]; mm = [1]
    for j in m-1:
        yy.append(x[j+1]-x[j])
    for j in m:
        mm.append(0.217 + 0.186 * np.exp(-(j+1)/1.186) + 0.338 * \
        np.exp(-(j+1)/18.51) + 0.259 * np.exp(-(j+1)/172.9))
    nn = yy/yy[0]

    return nn


def REF_ash_sense(C,aa,cc):
    """

    A function that connects with C-TOOL and askes it to simulate straw decay in soil.
    ** Using different alpha and beta ratios **
    Along with post processing, returning the emission profile.

    """
    bb = (1-aa) * cc
    dd = 1-aa-bb
    print(aa, 'aa!!!')
    print(bb, 'bb!!!')
    print(dd, 'dd!!!')
    fo = open('C:\\Users\\localadmin\\C-TOOL\\CN-SIM\\hafthor\\meaninp_fym1.dat', 'w')
    fo.write('8 1 ASH '+str(C/1000)+' 1'); fo.close()

    fz = open('C://Users//localadmin//C-TOOL//CN-SIM//addtypes.dat', 'w')
    fz.write('\
    [OrganicProduct(0)]\
    \nName              PLANT\
    \nPool(0)           AOM1\
    \nFraction(0)       0.45\
    \nDecayRate(0)      0.122\
    \nPool(1)           AOM2\
    \nFraction(1)       0.55\
    \nDecayRate(1)      1.22\
    \n\
    \n[OrganicProduct(1)]\
    \nName              FYM\
    \nPool(0)           AOM1\
    \nFraction(0)       0.297\
    \nDecayRate(0)      0.091\
    \nPool(1)           AOM2\
    \nFraction(1)       0.500\
    \nDecayRate(1)      1.22\
    \nPool(2)           NOM\
    \nFraction(2)       0.203\
    \n\
    \n[OrganicProduct(2)]\
    \nName              ASH\
    \nPool(0)           NOM\
    \nFraction(0)       '+str(bb)+'\
    \nDecayRate(0)      0.122\
    \nPool(1)           IOM\
    \nFraction(1)       '+str(aa)+'\
    \nDecayRate(1)      0.1\
    \nPool(2)           AOM1\
    \nFraction(2)       '+str(dd)+'\
    \nDecayRate(2)      1.22\
    \n[end]'); fz.close()
    os.system('C:\\Users\\localadmin\\C-TOOL\\ctool.exe C:\\Users\\localadmin\\C-TOOL\CN-SIM\\')
    a = pd.read_table('C://Users//localadmin//C-TOOL//CN-SIM//hafthor//results.txt')
    x = a.values.T[3]*a.values.T[4]
    jnum = len(x)
    m = np.arange(1,jnum, 1)
    yy = [x[0]]; mm = [1]
    for j in m-1:
        yy.append(x[j+1]-x[j])
    for j in m:
        mm.append(0.217 + 0.186 * np.exp(-(j+1)/1.186) + 0.338 * \
        np.exp(-(j+1)/18.51) + 0.259 * np.exp(-(j+1)/172.9))
    nn = yy/yy[0]

    return nn
```

IV. Utility Functions

The utility functions made to facility the computational code above are presented here.

```
import pandas as pd
import numpy as np
from brightway2 import *
from bw2data.query import NF, UF, LF, CF, NF_exact
from stats_arrays import NormalUncertainty
from math import log10, floor
import decimal

"""

A script that contains utility functions.

** Functions within this script:
    * Search for LCI data within the Ecoinvent database
    * Write a new LCI database based on specific inputs.
        * With and without uncertainty.
    * Various functions that calculates the LCIA based on inputs.
        * For only elementary flows.
        * For only unit processes.
        * For the whole LCI data.

"""

def technosphereData(inp):
    """

    Search for LCI data within the Ecoinvent database

    """
    ei = Database("ecoinvent 3.3 cutoff")
    IP1 = ei.query(NF(inp[0]), UF(inp[1]), LF(inp[2]))
    activity = ei.get(next(iter(IP1.keys()))[1])
    return activity


def biosphereData(inp):
    """

    Search for LCI data within the biosphere database

    """
    bs = Database("biosphere3")
    if len(inp) == 2:
        IP2 = bs.query(NF(inp[0]), CF(inp[1]))
    elif len(inp) == 3:
        IP2 = bs.query(NF(inp[0]), CF(inp[1]), CF(inp[2]))
    else:
        print('Err in inp')
    exchanges = bs.get(next(iter(IP2.keys()))[1])
    return exchanges


def biosphereData_exact(inp):
    """

    Search for LCI data within the Ecoinvent database

    """
    bs = Database("biosphere3")
    if len(inp) == 2:
        IP2 = bs.query(NF_exact(inp[0]), CF(inp[1]))
    elif len(inp) == 3:
        IP2 = bs.query(NF_exact(inp[0]), CF(inp[1]), CF(inp[2]))
    else:
        print('Err in inp')
    exchanges = bs.get(next(iter(IP2.keys()))[1])
    return exchanges


def lci_write_uncert(data, database, reference, unit, lci_ref, uncert):
    """

    Write a new LCI database based on specific inputs, with uncertainty.

    """
    exchanges = []
    for i in np.arange(len(data[0].index)):
        exchanges.append({"amount":float(data[0].values[i]),
                          "input":data[0].index[i].key,
                          "type":"technosphere",
                          "name":data[0].index[i]['name'],
                          "uncertainty_type":NormalUncertainty.id,
                          "loc":float(data[0].values[i]),
                          "scale":float(data[0].values[i])*uncert[0][i]})
    if len(data) < 2:
        pass
    else:
        exchangesBio = []
```

```
        for i in np.arange(len(data[1].index)):
            exchangesBio.append({"amount":float(data[1].values[i]),
                                 "input":data[1].index[i].key,
                                 "type":"biosphere",
                                 "name":data[1].index[i]['name'],
                                 "uncertainty_type":NormalUncertainty.id,
                                 "loc":float(data[1].values[i]),
                                 "scale":float(data[1].values[i])*uncert[1][i]})
        exchanges.extend(exchangesBio)

    example_data = {
        (database, lci_ref): {
            "name": data[0].columns[0],
            "exchanges": exchanges,
            u'reference product': reference, u'unit': unit}}


    db = Database(database)

    if database not in databases:
        db.register()

    db.write(example_data)


def lci_write(data, database, reference, unit, lci_ref):
    """

    Write a new LCI database based on specific inputs without uncertainty.

    """
    exchanges = []
    for i in np.arange(len(data[0].index)):
        exchanges.append({"amount":float(data[0].values[i]),
                          "input":data[0].index[i].key,
                          "type":"technosphere",
                          "name":data[0].index[i]['name']})
    if len(data) < 2:
        pass
    else:
        exchangesBio = []
        for i in np.arange(len(data[1].index)):
            exchangesBio.append({"amount":float(data[1].values[i]),
                                 "input":data[1].index[i].key,
                                 "type":"biosphere",
                                 "name":data[1].index[i]['name']})
        exchanges.extend(exchangesBio)

    example_data = {
        (database, lci_ref): {
            "name": data[0].columns[0],
            "exchanges": exchanges,
            u'reference product': reference, u'unit': unit}}

    db = Database(database)

    if database not in databases:
        db.register()

    db.write(example_data)


def elemental_flow(method, category1, category2, emission, value):
    """

    Functions that calculates the LCIA based on elementary flows inputs.

    """
    eb = Database("biosphere3")
    if category2 == 0:
        IP = eb.query(NF_exact(emission), CF(category1))
    else:
        IP = eb.query(NF(emission), CF(category1), CF(category2))

    m = Method(method)
    mm = m.load()
    mm = np.array(mm).T
    df = pd.DataFrame(mm[1:]).T
    df.index = mm[0]
    index = list(IP.keys())[0][1]
    result = []
    for i in np.arange(len(df.index)):
        if str(index) in df.index[i][1]:
            return float(df.values[i]) * value
        else:
            result = 0
    return result
```

```
def calcLCA_uniProc(method, LCI_1):
    """

    Functions that calculates the LCIA based on unit process inputs.

    """
    funcUnit1_new = LCI_1.to_dict()
    index1 = list(funcUnit1_new)

    dict1 = {}
    for i in np.arange(len(funcUnit1_new)):
        lca = LCA({index1[i]:funcUnit1_new[index1[i]]}, method)
        lca.lci()
        lca.lcia()
        dict1.update({index1[i]['name']:lca.score})

    LCIA_1 = pd.DataFrame(dict1, index = [method[1]])

    return LCIA_1


def calcLCA_tot(method, LCI_1, LCI_2):
    """

    Functions that calculates the LCIA based on full LCI data inputs.

    """
    funcUnit1_new = LCI_1.to_dict()
    funcUnit2_new = LCI_2.to_dict()

    index1 = list(funcUnit1_new)
    index2 = list(funcUnit2_new)

    dict1 = {}
    if len(funcUnit1_new) == 1.0:
        lca = LCA({index1[0]:funcUnit1_new[index1[0]]}, method)
        lca.lci()
        lca.lcia()
        dict1.update({index1[0]['name']:lca.score})

    else:
        for i in np.arange(len(funcUnit1_new)):
            lca = LCA({index1[i]:funcUnit1_new[index1[i]]}, method)
            lca.lci()
            lca.lcia()
            dict1.update({index1[i]['name']:lca.score})

    LCIA_1 = pd.DataFrame(dict1, index = [method[1]])

    dict2 = {}
    for i in np.arange(len(funcUnit2_new)):
        category1 = index2[i]['categories'][0]
        emission = index2[i]['name']
        value = funcUnit2_new[index2[i]]
        if len(index2[i]['categories']) > 1:
            category2 = index2[i]['categories'][1]
            emi_value = elemental_flow(method, category1, category2, emission, value)
            dict2.update({index2[i]['name']:emi_value})
        else:
            dict2.update({index2[i]:elemental_flow(method, category1, 0, emission, value)})

    LCIA_2 = pd.DataFrame(dict2, index = [method[1]])
    LCIA_2 = LCIA_2.T[LCIA_2.T[LCIA_2.T.columns[0]] != 0]
    LCIA = pd.concat([LCIA_1.T, LCIA_2], axis=1).fillna(0.0).T.sum()

    return LCIA


def calcLCA_elem(method, LCI_2):
    """

    Functions that calculates the LCIA based on elementary flows inputs.

    """
    funcUnit2_new = LCI_2.to_dict()

    index2 = list(funcUnit2_new)

    dict2 = {}
    for i in np.arange(len(funcUnit2_new)):
        category1 = index2[i]['categories'][0]
        emission = index2[i]['name']
        value = funcUnit2_new[index2[i]]
        if len(index2[i]['categories']) > 1:
            category2 = index2[i]['categories'][1]
            dict2.update({index2[i]['name']:elemental_flow(method, category1, category2, emission, value)})
        else:
```

```
        dict2.update({index2[i]:elemental_flow(method, category1, 0, emission, value)})
LCIA_2 = pd.DataFrame(dict2, index = [method[1]])
return LCIA_2
```

DTU Mechanical Engineering
Section of Thermal Energy
Technical University of Denmark

Nils Koppels Allé, Bld. 403
DK-2800 Kgs. Lyngby
Denmark
Phone (+45) 4525 4131
Fax (+45) 4588 4325
www.mek.dtu.dk
ISBN: 978-87-7475-497-8

DCAMM
Danish Center for Applied Mathematics and Mechanics

Nils Koppels Allé, Bld. 404
DK-2800 Kgs. Lyngby
Denmark
Phone (+45) 4525 4250
Fax (+45) 4593 1475
www.dcamm.dk
ISSN: 0903-1685